UNIVERSITY OF CALIFORNIA, SAN DIEGO

Laboratory investigations into factors controlling the heterogeneous reactivity of sea spray aerosols

A dissertation submitted in partial satisfaction of the requirements for the degree of Doctor of Philosophy

in

Chemistry

by

Christopher Lee

Committee in charge:

Professor Kimberly A. Prather, Chair
Professor Rommie E. Amaro
Professor Farooq Azam
Professor Timothy H. Bertram
Professor Judy Kim

2017

The Dissertation of Christopher Lee is approved, and is acceptable in quality and form for publication on microfilm and electronically:

_____

_____

_____

_____

_____

Chair

University of California, San Diego

2017

DEDICATION

To my family,

thank you for your unconditional love, sacrifices,

and for always believing in me.

EPIGRAPH

"Try not to become a man of success,

but rather try to become a man of value."

Albert Einstein

TABLE OF CONTENTS

LIST OF ABBREVIATIONS AND SYMBOLS

AFM	atomic force microscope
ATOFMS	aerosol time-of-flight mass spectrometer
APS	aerodynamic particle sizer
ART-2a	adaptive resonance theory, version 2a
BBY	Bodega Bay, California
CCN	cloud condensation nuclei
Chl-a	chlorophyll-a
D_a	aerodynamic diameter
D_{gn}	geometric mean diameter
D_m	mobility diameter
DOC	dissolved organic carbon
DOM	dissolved organic matter
D_p	physical diameter
D_{va}	vacuum aerodynamic diameter
EEM	excitation-emission matrix
FDOM	fluorescent dissolved organic matter
FePhosOrg	iron phosphate-rich organic
HRMS	high-resolution mass spectrometry
IMPACTS	Investigation into Marine PArticle Chemistry and Transfer Science 2014
IN	ice nuclei
LPS	lipopolysaccharide
MART	Marine Aerosol Reference Tank
miniMART	miniature Marine Aerosol Reference Tank

MODIS	Moderate Resolution Imaging Spectroradiometer
MOUDI	micro orifice uniform deposit impactor
OC	organic carbon
PAR	photosynthetically active radiation
POC	particulate organic carbon
POM	particulate organic matter
PSL	polystyrene latex (microspheres)
ppb	parts-per-billion
RH	relative humidity
SCCOOS	Southern California Coastal Ocean Observing System
SEM	scanning electron microscope
SLPM	standard liters per minute
SMPS	scanning mobility particle sizer
SS	sea salt
SSA	sea spray aerosols
SS-OC	sea salt-organic carbon
SSML	sea surface microlayer
SW	seawater
TOC	total organic carbon
VOC	volatile organic compound

LIST OF FIGURES

LIST OF TABLES

ACKNOWLEDGEMENTS

First and foremost, I would like to thank my advisor, Prof. Kimberly Prather. This dissertation in its entirety would not be possible without the guidance, vision, and training gained through Kim. As I reflect back on the years of training, the two main things that I learned that will stay with me as I continue on my career are: the importance of thinking about the big picture and the ability to communicate efficiently to a broad range of audiences, from the general public to scientific professionals. I enjoyed her dedication and enthusiasm when it comes to our line of work and has certainly influenced me to become who I am now. I am grateful for all her guidance, words of wisdom, and support in me to achieve my goals over the years.

I would also like to thank my committee members past and present: Prof. Farooq Azam, Prof. Timothy Bertram, Prof. Judy Kim, Prof. Rommie Amaro, and Prof. Joshua Figueroa. Each member of my committee has dedicated time to help me further my graduate career through providing valuable feedback on my research during the departmental and qualifying exams as well as offering advice and works of encouragement throughout the years. While I've had the opportunity to interact with some members more than others, they all have had an impact on my education. My graduate career wouldn't be possible without the help of our hard-working administrative assistants over the years. I would like to thank Paula Schachter, Carmen Alfaro, Krista Garcia, and Monica Castrejón, who are truly invaluable members of the group.

My interest in atmospheric chemistry began when I was working as a research intern at Korea Research Institute of Standards and Science under Dr. Jin-Seog Kim in the Atmospheric Environment Monitoring Center during my junior year of college. It was an eye-opening experience, as I had very limited knowledge on the application of chemistry prior to this internship. The bright and calming personality of Dr. Deullae Min who I worked with day after day deeply resonated with me and really set the tone as I continued on with my own career in

science. I would never have gotten to this point without the internship experience and the people who patiently took the needed time to teach an undergraduate with no research laboratory working experience.

When I was contemplating about graduate school during my last year of college, it was my undergraduate advisor, Prof. Gilbert Nathanson who had the largest influence. I worked in his laboratory for about a year and a half and he was the kindest and most genuine person that I've ever met in college. It was Gil who "casually" suggested that I look at the Prather Research Group and UCSD for graduate school and how the research being done in Kim's group would be a perfect match for my interests. At the time, Gil never hinted that he knew Kim from his earlier days. It was only when I visited UCSD for a visitation weekend that I found out that Gil and Kim had known each other for many years! This gave me more of a confirmation that UCSD and the Prather Research Group was the place for me. While Gil had a tremendous influence on my decision, I could not have made it without Dr. Alexis Johnson and Dr. Logan Dempsey in Nathanson Research Group. They influenced my career choice by helping and advising me in any way possible (even when a snowstorm was hitting Madison) and gave me the perspective of graduate school that I am very grateful for.

Most of the work that I have been involved in during my graduate school was with the Center for Aerosol Impacts on the Chemistry of the Environment (CAICE). When I first came to UCSD, it was during the Center's first intensive measurement campaign in fall of 2011 during its phase I. I participated in the grand experiment consisting of many researchers from all around the world, learning how a large scale experiments are performed and how many moving pieces are involved. Over time with CAICE moving forth in its phase II, I was able to participate in numerous conceptual and forward-thinking discussions that typical graduate students almost never experience. In addition, I was able to co-lead a major experiment campaign (IMPACTS

2014, documented in detail in this dissertation) with now Dr. Camille Sultana that very few young scientists yet along graduate students will have the chance to lead – for which I am grateful. I will remember the Center's training in teaching me to become a problem-solver, innovator, and forward-thinker.

The Center's experimental efforts were perhaps the most challenging I have ever faced. The experiments allowed a very large degree of freedom on which post-docs and graduate students thought about the big picture and designed their own experiments. However, through these processes, many fruitful discussions came about, and we learned to become a team player, working toward a common goal. As I move on, I will remember interacting with Dr. Luis Cuadra-Rodriguez, who always approached me in a friendly way to check in on me, and Dr. Tim Guasco whom I've shared my first office in the Prather Group (a.k.a. back storage/printer room) and kept things lively. Dr. Defeng Zhao and I worked with Dr. Michael Tauber's Raman spectroscopy setup and I remember sneaking under the black curtain to prevent background light from interfering with the measurements and realized how blockbuster science can be. Dr. Jess Axson took me under her wing when she arrived and really mentored me, having many hours of discussion on how to carefully design an experiment and carry them through. Dr. Jamie Schiffer provided a completely new set of knowledge to my research projects, and made sure that I remained positive throughout the last year as I was finishing up my graduate career. Prof. Vicki Grassian, Prof. Tim Bertram, Prof. Chris Cappa, Prof. Gil Nathanson, Prof. Betsy Stone, Prof. Andy Ault, Dr. Skip Pomeroy, Dr. Paul DeMott, Dr. Christina McCluskey, Dr. Tom Hill, Dr. Richard Cochran, Dr. Grant Deane, Dr. Dale Stokes, and Odin all played a significant role with the CAICE experiments and provided immense amount of support. Dr. Xiaofei Wang will forever be remembered as the Home Depot bucket lover, with message of "Let's Do This."

I must thank the past and present members of the Prather Group. Although not a student, Joe Mayer made everything and anything that we imagined possible. His humor, expertise, and dedication made all the situations when broken things needed a fix, bearable. Dr. Jessie Creamean worked with me during my first year even as she was writing her own dissertation, so the project we were both involved could move forward without delay. Dr. Doug Collins really taught me to be a critical thinker and a leader in the group, who I tried to emulate. Dr. Jack Cahill taught me everything I know about fixing the ATOFMS and other instruments, but most importantly how to keep humor and morale up during times when things don't work out the way you think it will. Dr. Kaitlyn Suski, while I didn't have the opportunity to work closely with her, her dedication to science really shined through. Dr. Olivia Ryder has been the go-to source of information regarding flow tubes and heterogeneous chemistry – one of the main focuses of this dissertation, and kept me thinking positive with her personality. Dr. Camille Sultana, joining the group at the same time, TA-ing the same Chem 6A and 100B classes together, co-leading number of lengthy experiments including IMPACTS 2014, spending many nights in the lab working on fixing ATOFMS ahead of major experiments, is the person that I have the longest history with in the group and her leadership skills and ability to critically analyze situations and problems has certainly rubbed off on me to become a better person. Matt Ruppel and Dr. Steve Schill were always smiling and I remember spending many nights working in the lab with them to make sure that we could get a phytoplankton bloom to happen in the MART. Mitch Santander, who shared an office with me since he join the group until my last year or so of graduate school, humored me with his love for penguins and supported me in various ways including editing and reviewing of number of documents and emails. Hash Al-Mashat and I took a road trip to Pasco, WA in a slightly beat-up U-Haul box truck carrying Shirley for a field study aircraft install and is one of the most memorable experience of my graduate carrier as we tried to strategically stop at interesting towns to make things livelier. Gavin Cornwell and I shared a very cramped space for

few months during IMPACTS and really grew on each other; I know he will be a great leader in the group. Matt Pendergraft and Charlotte Beall both have huge dedication to their research that I look forward to seeing it grow in the future. Jon Sauer, having so much knowledge in his head, I look forward to seeing his research grow in the future. There were two Kathryns that happened to be in the lab around the same time: Kathryn Moore was always visually active, where Kathryn Mayer was calmer; but both showed tremendous passion which I admire. While slightly new to the group, Brock Mitts displays potential to be a great leader of the group in the future. Mallory Picket, Josh Cox, and Robin Richardson, our group's undergraduate researchers in the past, all showed their passionate interest in science and I know they will do great things.

Other Prather Group members who I did not have a chance to work closely include: Dr. Su, Prof. Cassie Gaston, Dr. Alberto Cazorla, Dr. Lindsay Hatch, Dr. Melanie Zauscher, Liz Fitzgerald, Dr. Andy Martin, Dr. Louise Kristensen, Kara Voss, Nicole Campbell, Dolan Lucero, and Natasha Gunawan. Although not a Prather Group member, Dr. Carlos Valle-Diaz has been a wonderful collaborator as he and I worked on PRADACS project. It was a pleasure to get to know them and I wish them all the best in the future.

Lastly, but certainly not the least, I would like to thank my family. When I reflect to think when my life took a turning point, it was when my parents, Gyu-Hwan Lee and Hye-Jung Kim, decided to move our family to Madison, Wisconsin, from South Korea in the summer of 1999. At first, I had no idea what this meant to our family being so young. Now I realize the sacrifices they had to make for my brother and me when we came overseas. Due to circumstances, I moved between Madison and South Korea a few times before finally landing in San Diego, but my parents did everything they could do for me every step of the way. My father is also received his doctoral degree in Chemistry and currently a Professor. He has always been a role model for me, and I wish to continue on with my career with the same level of professional character that he has

demonstrated over the decades, and his love and dedication to his family. I am forever grateful for them and hope to repay them after finishing my degree with this dissertation.

One of the more recent intercontinental moves was when I moved in with my brother, Ed, for college. We had our challenges living together as both hot headed young adults since we had been living in different places and countries for about 5 years. I truly think that the wonderful relationship we have now could not have been possible without the help of my now sister-in-law, Mayu Fujikawa, who kept the two boys in check for 4 years. Ed and I always joked that she was practicing her training on us (she got her doctoral degree in Rehabilitation Psychology). I'm glad and thankful to have both Ed and Mayu by my side, supporting me through all the years.

My wife and best friend, Hye-Gyeong Lee, who I met during my earlier times in graduate school, is easily the biggest reason that I am here right now. Hye-Gyeong set me straight when I was struggling and got me on back on track. While we were on a long-distance relationship for 2 years before asking her to marry me and join me in San Diego, she continued to make sure that I was putting in the best effort in whatever I was doing day after day. We always joke that our long-distance allowed both of us to focus on our work, but I know that supporting each other close to 6,000 miles apart could not have been easy. I am truly appreciative of her and her support, and for always having the patience and ability to make me feel better.

To everyone thanked in this dissertation as well as other friends and family members who I couldn't all include here without writing a full autobiography, I would like to say: I am so thankful and I truly could not have done it without them.

Chapter 2 is reproduced with permission from the American Chemical Society: Lee, C., Sultana, C.M., Collins, D.B., Santander, M.V., Axson, J.L., Malfatti, F., Cornwell, G.C., Grandquist, J.R., Deane, G.B., Stokes, M.D., Azam, F., Grassian V.H., Prather, K.A. Advancing

Model Systems for Fundamental Laboratory Studies of Sea Spray Aerosol using the Microbial Loop, Journal of Physical Chemistry, A, 119 (33), 8860-8870, 2015. The dissertation author was the primary investigator and author of this paper.

Chapter 3 is in preparation: Michaud, J.M.,* Ryder, O.S.,* Sauer, J.S.,* Lee, C.,* Burkart, M.D., Prather K.A. Enzymatic Processing by Lipase in Seawater Determines Sea Spray Aerosol Composition. The dissertation author was the co-primary investigator and co-author of this paper. Authors with * contributed equally. J.M.M., O.S.R., J.S.S., C.L., and K.A.P. designed the experiment, C.L. performed single particle mass spectrometry measurements, J.S.S. performed high resolution mass spectrometry measurements, and J.M.M. performed enzyme assay measurements.

Chapter 4 is in preparation: Lee, C., Ryder, O.S., Michaud, J.M., Sauer, J.S., Burkart, M.D., Prather, K.A. The Effect of Lipase on Sea Spray Aerosol Mixing State and the Impact on Nitric Acid Heterogeneous Reactivity. The dissertation author was the primary investigator and author of this paper. C.L., O.S.R., and K.A.P. designed the experiment, C.L. performed single particle mass spectrometry measurements, C.L. and O.S.R. performed atomic force microscopy measurements.

Chapter 5 has been submitted to ACS Central Science: Malfatti, F.,* Lee, C.,* Tinta, T., Ryder, O.S., Schiffer, J.M., Pendergraft, M.A., Celussi, M., Zhou, Y., Sultana, C.M., Rotter, A., Axson, J.L., Collins, D.B., Santander, M.V., Anides M., A.L., Aluwihare, L.I., Riemer, N., Azam, F., Prather, K.A. Sea Spray Aerosols: Tiny Biochemical Reactors in the Atmosphere. The dissertation author was the co-primary investigator and co-author of this paper. Authors with * contributed equally. F.M., C.L., F.A., and K.A.P. designed the experiment, F.M., T.T., Z.Y., M.A.P. A.M.A. performed enzyme activity measurements, C.L. performed single particle mass

spectrometry measurements, N.R. performed coagulation simulations, and J.M.S. performed molecular dynamic simulations. All other coauthors participated in the experiment.

Chapter 6 is in preparation: Lee, C., Schiffer, J.M., Grassian, V.H., Prather K.A. Calcium-Driven Lipopolysaccharide Aggregation in Sea Spray Aerosol Composition and Nitric Acid Heterogeneous Reactivity. The dissertation author was the primary investigator and author of this paper. C.L., J.M.S., V.H.G., and K.A.P designed the experiment, C.L. performed LPS aggregation and single particle mass spectrometry measurements, and J.M.S. performed molecular dynamics simulations.

VITA

2011	Bachelor of Science, Chemistry, University of Wisconsin-Madison
2011-2012	Teaching Assistant, Department of Chemistry and Biochemistry, University of California, San Diego
2011-2017	Research Assistant, University of California, San Diego
2013	Master of Science, Chemistry, University of California, San Diego
2017	Doctor of Philosophy, Chemistry, University of California, San Diego

PUBLICATIONS

Lee, C., Ryder, O.S., Michaud, J.M., Sauer, J.S., Burkart, M.D., Prather, K.A. The Effect of Lipase on Sea Spray Aerosol Mixing State and the Impact on Nitric Acid Heterogeneous Reactivity, in preparation.

Lee, C., Schiffer, J.M., Grassian, V.H., Prather K.A. Calcium-Driven Lipopolysaccharide Aggregation in Sea Spray Aerosol Composition and Nitric Acid Heterogeneous Reactivity, in preparation.

Michaud, J.M.,* Ryder, O.S.,* Sauer, J.S.,* **Lee, C.,*** Burkart, M.D., Prather K.A. Enzymatic Processing by Lipase in Seawater Impacts Sea Spray Aerosol Composition, in preparation.

Valle-Diaz, C.J., **Lee, C.,** Cuadra-Rodriguez, L.A., Roberts, G.C., Prather, K.A., Mayol-Bracero, O.L. Mixing State and Hygroscopic Properties of Long-Range Transported African Dust at a Caribbean Tropical Montane Cloud Forest. in preparation.

Deane, G.B., Cochran, R.E., Jayarathne, T.J., Stokes, M.D., Forestieri, S.D., Sultana, C.M., **Lee, C.,** Morris, H.S., Ray, K.K., Lee, H.D., Tivanski, A.V., Bertram, T.H., Prather, K.A., Grassian, V.H., Cappa, C.D., Stone, E.A. A Mechanistic Model for the Size-Dependent Transfer of Organic Matter to Sea Spray Aerosol, in preparation.

Malfatti, F.,* **Lee, C.,*** Tinta, T., Ryder, O.S., Schiffer, J.M., Pendergraft, M.A., Celussi, M., Zhou, Y., Sultana, C.M., Rotter, A., Axson, J.L., Collins, D.B., Santander, M.V., Anides M., A.L., Aluwihare, L.I., Riemer, N., Azam, F., Prather, K.A. Sea Spray Aerosols: Tiny Biochemical Reactors in the Atmosphere, *ACS Central Science*, in review 2017.

Santander, M.V., Schiffer, J.M., **Lee, C.,** Axson, J.L., Tauber, M.J., Prather, K.A. Factors Controlling Transfer of Biologically-Derived Organic Species from Seawater to Sea Spray Aerosols, *Scientific Reports,* in review 2017.

Michaud, J.M., Thompson, L.R., Kaul, D., Espinoza, J.L., Richter, R.A., Xu, Z.Z., **Lee, C.,** Pham, K.M., Beall, C.M., Malfatti, F., Azam, F., Knight, R., Burkart, M.D., Dupont, C.L., Prather, K.A. Selective Transfer of Bacteria and Viruses from the Ocean to the Atmosphere. *Nature,* in review 2017.

Cochran, R.E., Laskina, O., Trueblood, J.V., Estillore, A.D., Morris, H.S., Jayarathne, T., Sultana, C.M., **Lee, C.,** Lin, P., Laskin, J., Laskin, A., Dowling, J.A., Qin, Z., Cappa, C.D., Bertram, T.H., Tivanski, A.V., Stone, E.A., Prather, K.A., Grassian, V.H. Molecular Diversity of Individual Sea Spray Aerosol Particles: Influence of Ocean Biology on Particle Composition and Hygroscopicity. *Chem, 2* (5), 655-667, 2017.

McCluskey, C.S., Hill, T.C.J., Malfatti, F., Sultana, C.M., **Lee, C.,** Santander, M.V., Beall, C.M., Moore, K.A., Cornwell, G.C., Collins, D.B., Prather, K.A., Jayarathne, T., Stone, E.A., Azam, F., Kreidenweis, S.M., DeMott, P.J. A Dynamic Link between Ice Nucleating Particles Released in Nascent Sea Spray Aerosol and Oceanic Biological Activity during Two Mesocosm Experiments. *Journal of Atmospheric Science, 74,* 151-166, 2017.

Pham D.Q., O'brien, R.E., Fraund M., Bonanno, D., Laskina, O., Beall, C., Moore, K.A., Forestieri, S., Wang, S., **Lee, C.,** Sultana, C.M., Grassian, V.H., Cappa, C.D., Prather, K.A., Moffet, R.C. Biological Impacts on Carbon Speciation and Morphology of Sea Spray Aerosol. *ACS Earth and Space Chemistry, 10,* 2017.

Cochran, R.E., Laskina, O., Jayarathne, T., Laskin, A., Laskin, J., Lin, P., Sultana, C.M., **Lee, C.,** Moore, K.A., Cappa, C.D., Bertram, T.H., Prather, K.A., Grassian, V.H., Stone, E.A. Analysis of Organic Anionic Surfactants in Fine and Coarse Fractions of Freshly Emitted Sea Spray Aerosol, *Environmental Science &Technology, 50* (5), 2477-2486, 2016.

Collins, D.B., Bertram, T.H., Sultana, C.M., **Lee, C.,** Axson, J.L., Prather, K.A. Phytoplankton blooms weakly influence the cloud forming ability of sea spray aerosol, *Geophysical Research Letters,43* (18), 9975-9983, 2016.

DeMott, P.J., Hill, T.C.J., McCluskey, C.S., Prather, K.A., Collins, D.B., Sullivan, R.C., Ruppel, M.J., Mason, R.H., Irish, V.E., Lee, T., Hwang, C.Y., Rhee, T.S., Snider, J.R., McMeeking, G.R., Dhaniyala, S., Lewis, E.R., Wentzell, J.J.B., Abbatt, J.P.D., **Lee, C.,** Sultana, C.M., Ault, A.P., Axson, J.L., Martinez, M.D., Venero, I., Santos-Figueroa, G., Stokes, M.D., Deane, G.B., Mayol-Bracero, O.L., Grassian, V.H., Bertram, T.H., Bertram, A.K., Moffett, B.F., Franc, G.D. Sea Spray Aerosol as a Unique Source of Ice Nucleating Particles, *Proceedings of the National Academy of Sciences USA, 113* (21), 5797-5803, 2016.

Forestieri, S.D., Cornwell, G.C., Helgestad, T.M., Moore, K.A., **Lee, C.,** Novak, G.A., Sultana, C.M., Wang, X., Bertram, T.H., Prather, K.A., Cappa, C.D. Linking Variations in Sea Spray Aerosol Particle Hygroscopicity to Composition During Two Microcosm Experiments, *Atmospheric Chemistry and Physics,16,* 9003-9018, 2016.

Jayarathne, T., Sultana, C.M., **Lee, C.,** Malfatti, F., Cox, J.L., Pendergraft, M.A., Moore, K.A., Azam, F., Tivanski, A.V., Cappa, C.D., Bertram, T.H., Grassian, V.H., Prather, K.A., Stone, E.A. Enrichment of Saccharides and Divalent Cations in Sea Spray Aerosol

During Two Phytoplankton Blooms, *Environmental Science & Technology, 50* (21), 11511-11520, 2016.

Trueblood, J.V., Estillore, A.D., **Lee, C.,** Dowling, J.A., Prather, K.A., Grassian, V.H. Heterogeneous Chemistry of Lipopolysaccharides with Gas-Phase Nitric Acid: Reactive Sites and Reaction Pathways, *Journal of Physical Chemistry, A, 120* (32), 6444-6450, 2016.

Lee, C., Sultana, C.M., Collins, D.B., Santander, M.V., Axson, J.L., Malfatti, F., Cornwell, G.C., Grandquist, J.R., Deane, G.B., Stokes, M.D., Azam, F., Grassian V.H., Prather, K.A. Advancing Model Systems for Fundamental Laboratory Studies of Sea Spray Aerosol using the Microbial Loop, *Journal of Physical Chemistry, A, 119* (33), 8860-8870, 2015.

Schill, S.R., Collins, D.B., **Lee, C.,** Morris, H.S., Novak, G.A., Prather, K.A., Quinn, P.K., Sultana, C.M., Tivanski, A.V., Zimmermann, K., Cappa, C.D., Bertram, T.H. The Impact of Aerosol Particle Mixing State on the Hygroscopicity of Sea Spray Aerosol, *ACS Central Science, 1* (3), 132-141, 2015.

Wang, X.*, Sultana, C.M.*, Trueblood, J., Hill, T.C.J., Malfatti, F., **Lee, C.,** Laskina, O., Moore, K.A., Beall, C.M., McCluskey, C.S., Cornwell, G.C., Zhou, Y., Cox, J.L., Pendergraft, M.A., Santander, M.V., Bertram, T.H., Cappa, C.D., Azam, F., DeMott, P.J., Grassian, V.H., Prather, K.A. Microbial Control of Sea Spray Aerosol Composition: A Tale of Two Blooms, *ACS Central Science, 1* (3), 124-131 2015.

Creamean, J.M., **Lee, C.,** Hill, T.C.J., Ault, A.P., DeMott, P.J., White, A.B., Ralph, F.M., Prather, K.A. Chemical properties of insoluble precipitation residue particles, *Journal of Aerosol Science, 76,* 13-27, 2014.

Min, D., Lee, J.B., **Lee, C.,** Lee, D.S., Kim, J.S. Estimation of Mass Discrimination Factor for a Wide Range of *m/z* by Argon Artificial Isotope Mixtures and NF_3 Gas, *Bull. Korean Chem. Soc., 35* (8), 2403-2409, 2014.

Ryder, O.S., Ault, A.P., Cahill, J.F., Guasco, T.L., Riedel, T.P., Cuadra-Rodriguez, L.A., Gaston, C.J., Fitzgerald, E., **Lee, C.,** Prather, K.A., Bertram, T.H. On the Role of Particle Inorganic Mixing State in the Reactive Uptake of N_2O_5 to Ambient Aerosol Particles, *Environmental Science & Technology, 48* (3), 1618-1627, 2014.

* Authors contributed equally

FIELDS OF STUDY

Major Field of Study: Chemistry

Studies in Atmospheric and Analytical Chemistry

Professor Kimberly A. Prather

ABSTRACT OF THE DISSERTATION

Laboratory investigations into factors controlling the heterogeneous reactivity of sea spray aerosols

by

Christopher Lee

Doctor of Philosophy in Chemistry

University of California, San Diego, 2017

Professor Kimberly A. Prather, Chair

Aerosols impact climate directly by scattering and absorbing solar radiation or indirectly by influencing cloud properties and lifetime. Additionally, aerosols represent one of the most abundant surfaces available for heterogeneous reactions. Further, as aerosols react and age in the atmosphere, their interaction with solar radiation and water uptake can change. Sea spray aerosols (SSA) constitute one of the most abundant natural aerosols in the atmosphere. Understanding how oceanic biological processes affect SSA composition and heterogeneous chemistry remains an active area of research. To study SSA heterogeneous reaction processes, fundamental laboratory studies must be able to reproduce the full chemical complexity of SSA. In this dissertation, we discuss a novel approach to studying SSA chemistry in the laboratory. This approach entails inducing phytoplankton blooms in a laboratory microcosm experiment to study the impacts of natural microbial processes on the chemical composition of seawater and SSA. From these studies, the role of heterotrophic bacteria and their associated enzymes on the chemical composition of SSA are revealed. This dissertation investigates the impact of enzymes, active in both the seawater as well as in SSA, on aerosol physicochemical properties, including nitric acid heterogeneous reactivity that is important for global nitrogen cycle. Not only can enzymes affect the physicochemical properties of SSA, but they can transform the chemistry of the atmosphere upon coagulation with pre-existing ambient particles. Further, we discovered the roles of monovalent versus divalent cations in the morphology and heterogeneous reactivity lipopolysaccharide-containing SSA. The results uncover the bacterial produced chemicals, including hydrolytic enzymes and lipopolysaccharides, in controlling SSA composition and heterogeneous reactivity in the atmosphere.

1 A Brief Introduction to Heterogeneous Chemistry of Sea Spray Aerosols

The tropospheric atmosphere is comprised of two main classes of components: particles and gases. Aerosols are solid or liquid particles suspended in a gas and are a ubiquitous component of everyday life [*Seinfeld and Pandis, 2016*], profoundly influencing air pollution, visibility, human health, and global climate [*Pope and Dockery, 2006*; *Pöschl, 2005*; *Seinfeld and Pandis, 2016*]. More specifically, aerosols impact climate in two ways: 1) *via* direct scattering and absorption of radiation (Section 1.2.1) and 2) influence cloud lifetime and precipitation by acting as a cloud condensation nuclei (CCN) and ice nuclei (IN). Aerosols serve as CCN by providing a surface upon which water vapor can condense to form a cloud droplet [*Haywood and Boucher, 2000*; *Seinfeld and Pandis, 2016*] (Section 1.2.2). Aerosols can also serve as IN by catalyzing the freezing of water vapor and super-cooled cloud droplets that produce ice crystals, which could otherwise not form at mixed phase cloud temperature ranges of ~-38 ^{o}C to 0 ^{o}C [*Isono et al., 1959*]. Aerosols vary considerably in terms of their source, size (0.001-10 μm), and composition, which change their effects on climate [*Pöschl, 2005*]. Throughout the lifetime of aerosols, they can undergo atmospheric processing, including coagulation, adsorption and desorption of water, and reaction with gas-phase molecules all of which can alter aerosol chemical composition [*Seinfeld and Pandis, 2016*]. The latter process is referred to as heterogeneous chemistry (or reaction), and is one of the main foci of this dissertation.

Heterogeneous and multiphase reactions are chemical reactions that occur between species of different phases, i.e. gas-phase molecules with an aerosol particle [*Finlayson-Pitts and Pitts, 1999*]. In this context, heterogeneous chemistry is constrained to particle surface reactions, whereas multiphase chemistry takes place in the bulk of the liquid medium [*Ravishankara et al., 1997*]. For simplicity, in this dissertation, heterogeneous and multiphase chemistry will be referred to as heterogeneous chemistry. In addition to such reactions depleting the reactive gas-

phase species from the atmosphere [*Ravishankara et al., 1997*] affecting their global budget [*Rossi et al., 2003*], a change in aerosol chemical composition also occurs, and can further impact aerosol climate properties. There are several factors that influence the reactions occurring between gas-phase molecules and aerosol particles including but not limited to: particle size, aerosol surface composition, and gas-phase reactivity [*Abbatt et al., 2012*; *Finlayson-Pitts, 2009*]. Examples of gas-phase reactants that react with tropospheric aerosols are: N_2O_5, HO_2, HNO_3, O_3, OH, and Cl radicals [*Abbatt et al., 2012*]. Here we will focus on heterogeneous reaction that takes place between gas-phase nitric acid (HNO_3) and reactive surface available in the marine environment, such as sea spray aerosols (SSA).

Section 1.1 will discuss the aerosol impacts on the environment, and Section 1.2 will discuss the sources of atmospheric aerosols. Moving forward, Section 1.3 will discuss the link between the ocean at the atmosphere, and Section 1.4 will detail the importance of investigating the heterogeneous reactions of realistic SSA, with Section 1.5 detailing the methods of SSA generation in the laboratory and the analytical technique used in this dissertation. Section 1.6 will outline the outstanding questions that this dissertation will address, and Section 1.7 will conclude this chapter summarizing the goals set forward.

1.1 Environmental Impacts of Atmospheric Aerosols

1.1.1 Aerosol Health Effects

The large variance in size and composition of aerosols leads to not only adverse effects on air quality, but on health as well [*Hidy et al., 1975*; *Pope and Dockery, 2006*]. Adverse health effects from aerosol exposure can range from allergies and asthma [*Dockery et al., 1996*], cardiovascular and pulmonary diseases [*Anderson, 2012; Burnett et al., 2014; Latzin et al., 2009*], mental health [*Oudin et al., 2016*], dermatology [*Drakaki et al., 2014*], reproductive health [*Sram,*

1999], to even serious as increased mortality where it is estimated that air pollution contributes to 5.5 million premature deaths globally [*Anderson, 2012; Brauer et al., 2016; Fann et al., 2012; McNeill, 2017*]. While advancements have been made in improving the understanding of aerosol impacts on human health and implementing government regulations such as the 1970 Clean Air Act and the subsequent National Ambient Air Quality Standards (NAAQS), more work aimed at both studying and setting limits on emissions and air pollution are needed [*Anderson, 2012; Pope and Dockery, 2006*; *Vedal, 1997*]. The physiological mechanisms of aerosol impacts on health are just beginning to be understood [*McNeill, 2017*], and one area that warrants further investigation is in clarifying the relationship between PM and disease, such as cerebrovascular disease on an individual level [*Anderson, 2012*]. Further research is still needed to fully understand how PM affects human health, such as elucidating the actual composition of the harmful particulates as well as the impact from prolonged exposure [*Anderson 2012; Brook et al., 2010*].

1.1.2 Aerosol Direct Effect

The aerosol direct effect can be described as scattering and absorption by aerosol particles of solar radiation. Size and refractive index are two factors that can impact the scattering efficiency of aerosols, where the scattering efficiency increases as a function of aerosol diameter [*Seinfeld and Pandis, 2016*]. Ambient relative humidity has a large influence on the scattering efficiency, as aerosol size can change based on particle hygroscopicity and the amount of water in the atmosphere [*Zieger et al., 2013*]. On the other hand, composition plays the dominant role in absorption by aerosols [*Andreae and Gelencsér, 2006*]. In certain cases, total light absorption of aerosols can even be enhanced when there is a weakly absorbing coating on the surface of a combustion-derived black carbon particle [*Moffet and Prather, 2009*]. Therefore, the direct effect described here demonstrates how atmospheric aerosols can have a cooling (*via* scattering light) or warming (*via* absorbing light) effect on the global climate system [*Stocker et al., 2013*].

1.1.3 Aerosol Indirect Effect

The aerosol indirect effect relates to aerosol influence on cloud properties by their ability serve as a surface for water condensation (cloud condensation nuclei, or CCN), which can lead to cloud droplet formation [*Lohmann and Feichter, 2005*], or catalyze freezing of water vapor and super-cooled cloud droplets to produce ice crystals (ice nuclei, or IN). The largest uncertainty in global radiative forcing is attributed to the indirect effect [*Stocker et al., 2013*], where both the size and chemical composition of aerosols influence their role as CCN [*McFiggans et al., 2006*]. Aerosols greater than 0.2 μm in diameter are automatically efficient CCN based on their size, but for the smaller particles, chemical composition control whether the aerosol will efficiently seed a cloud [*Petters and Kreidenweis, 2007*]. Adding more aerosols to an existing cloud redistributes the available water among more CCN, but leads to a decrease in their average droplet size. As a result, clouds with now greater cloud droplet number concentration have higher albedo [*Twomey, 1977*] and a longer lifetime [*Albrecht, 1989*], resulting in suppressed or delayed onset of precipitation [*Rosenfeld, 2000*] and affecting the water cycle by impacting the location and the intensity of the precipitation [*Andreae et al., 2004*]. Additionally, resulting effects from greater cloud droplets will decrease the overall solar radiation flux at the Earth's surface, the aerosol indirect effect is critically important to the radiation balance in the atmosphere yet remains a significant challenge to understand on a global scale due to heterogeneity of the aerosol composition in the atmosphere.

IN can strongly influence ice crystal concentrations in clouds even in small concentrations [*DeMott et al., 2010*]. Aerosols that serve as an efficient IN are typically more insoluble, such as dust particles and biological material, including those originating from the ocean [*Christner et al., 2008; DeMott et al., 2003; Despres et al., 2012; McCluskey et al., 2017; Wiacek et al., 2010*]. While the concentration can be small, it is estimated that over 50% of global

precipitation is initiated in the ice phase [*Lau and Wu, 2003*]. However, the overall effects of IN on precipitation processes are poorly understood [*Dymarska et al., 2006*] and often conflicting effects of CCN and IN demonstrate the need for improving our understanding of aerosols and their source.

1.2 Sources of Atmospheric Aerosols

Aerosols originate from a number of natural and anthropogenic sources and can be categorized as either primary or secondary aerosols. Primary aerosols are those directly emitted, while secondary aerosols are formed/transformed in the atmosphere through chemical reactions and condensation of gas-phase species. Common anthropogenic primary aerosol sources include incomplete combustion, metal working, and meat cooking [*Pöschl, 2005*; *Prather et al., 2008*]. However, the global aerosol mass burden is mainly comprised of naturally produced dust particles and sea spray aerosols [*Andreae and Rosenfeld, 2008; Textor et al., 2006; Pöschl, 2005*; *Seinfeld and Pandis, 2016*], where dust particles are lofted into the air in arid terrestrial regions [*Ginoux et al., 2012*] and sea spray aerosols (SSA) are produced at the ocean surface [*De Leeuw et al., 2011*; *Lewis and Schwartz, 2004*]. Due to their significance, dust and SSA can be critically important to the global climate [*Textor et al., 2006*].

Secondary aerosols are produced by chemical reactions between gas-phase molecules that result in products that lead to condensation of gas-phase species . The atmosphere is an oxidizing environment, and thus both organic and inorganic species can be involved in forming secondary aerosols [*Kroll and Seinfeld, 2008*; *Seinfeld and Pandis, 2016*]. Volatile organic compounds (VOCs) can be oxidized by reactive species such as O_3 and OH radical to form secondary organic aerosols (SOA) [*Kroll and Seinfeld, 2008*]. Over the ocean, dimethylsulfide (DMS), a volatile metabolite produced by marine microbiome [*Groene, 1995; Nguyen et al., 1988*], can oxidize and

form sulfate aerosols [*Barnes et al., 2006; Charlson et al., 1987; Woodhouse et al., 2013*]. The vast numbers of reaction pathways and sources that can lead to the production of secondary aerosols demonstrate that there is great potential for the secondary aerosols to influence global climate [*Andreae and Rosenfeld, 2008*; *Meskhidze et al., 2011*].

1.3 The Link between the Ocean and the Atmosphere

Oceans cover a vast majority of the Earth's surface (approximately 71%), [*Lewis and Schwartz, 2004*]. SSA is one of the highest aerosol fluxes of any source on Earth [*Andreae and Rosenfeld, 2008*; *De Leeuw et al., 2011*]. SSA are of special interest, having been studied for decades, due to their complex mixture as both inorganic and organic in composition, as well as ranging in size from the Aiken mode (nanometer range) to very large sizes in the coarse mode (micrometer range) larger than few micrometers [*Lewis and Schwartz, 2004*; *Prather et al., 2013*].

The organic matter enriched in SSA is associated with marine biological activity [*O'Dowd et al., 2004*], where organic molecules concentrated at the sea surface microlayer, the upper 1-1000 µm of the ocean, are ejected into the atmosphere through bubble bursting [*Aller et al., 2005*; *Blanchard and Syzdek, 1972*; *Cunliffe et al., 2013*; *Lewis and Schwartz, 2004*]. This association between SSA organic enrichment and marine biological activity was further supported by seasonal-scale measurements and parameterized model simulations [*Tsigaridis et al., 2013*]. However, the correlation between SSA organic enrichment and satellite-retrieved chlorophyll-a (chl-a), a phytoplankton biomass marker used to track the level of biological activity in the surface ocean, showed a time lag of about 1 week between chl-a and SSA organic enrichment [*Rinaldi et al., 2013*]. In addition, recent shipboard measurements showed no difference in organic enrichment of sub-100 nm nascent SSA between oligotrophic and eutrophic regions [*Quinn et al., 2014*]. These apparent discrepancies in demonstrate the need for a

laboratory method that will allow examination of the relationship between marine microbiology and the SSA physicochemical properties. This advancement will allow for better constraint of the atmospheric impact of SSA, their ability to undergo atmospheric processing including heterogeneous reactivity, and their interaction with light.

1.4 Heterogeneous Reactions of Sea Spray Aerosols

Reactive gas-phase species such as nitrogen oxides (NO_x = NO + NO_2) and SO_2 present in the atmosphere can oxidize to form HNO_3 and H_2SO_4, respectively. These species can further interact with aerosols, changing their physicochemical properties [*Ault et al., 2013a*; *Finlayson-Pitts and Pitts, 1999*]. As the surface of SSA constitute one of the largest surfaces in the tropospheric atmosphere, it is critical to understand heterogeneous reactions between SSA and HNO_3 in order to accurately predict impacts of SSA in climate models [*Abbatt et al., 2012*; *Rossi, 2003*] and to understand the global nitrogen cycle [*Pryor et al., 2000*]. Previous studies focused on understanding SSA heterogeneous reaction mechanisms used sodium chloride surfaces as a proxy [*Brink, 1998*; *Finlayson-Pitts and Pitts, 1999; Kolb et al., 2010*; *Pryor and Sørensen, 2000*]. The reaction is shown in Reaction 1.1.

$$NaCl\ (aq, s) + HNO_3\ (g) \rightarrow NaNO_3\ (aq, s) + HCl\ (g) \qquad (R1.1)$$

To understand the role that organic coatings have on R1.1, common organic surfactant proxies have been studied as model systems, including sodium dodecyl sulfate [*Abbatt et al., 2012*; *Donaldson and Vaida, 2006*], alkyl self-assembled monolayers [*Moussa et al., 2012; Nishino et al., 2014*], and fatty acids [*Stemmler et al., 2008*]. Additional studies have added

chemical complexity to the system by incorporating magnesium chloride [*De Haan and Finlayson-Pitts, 1997*; *Liu et al., 2007*], where the reaction is shown in Reaction 1.2.

$$MgCl_2\ (aq, s) + 2HNO_3\ (g) \rightarrow Mg(NO_3)_2\ (aq, s) + 2HCl\ (g) \qquad (R1.2)$$

However, while studies using simple inorganic salts such as NaCl and $MgCl_2$ provided important information on fundamental mechanisms of heterogeneous reactions, a disconnect exists between field observations and laboratory results, stemming from the use of simple systems that fail to properly replicate the composition and associated behavior of SSA [*Abbatt et al., 2012; Ault et al., 2014; Bertram et al., 2009; Kolb et al., 2010; Laskin et al., 2013; Liu et al., 2007*]. Recently, nascent SSA, produced from natural seawater using an ocean-atmosphere facility [*Prather et al., 2013*], were reacted with HNO_3. The results demonstrated that the chemical heterogeneity of SSA leads to a large range in particle reactivity [*Ault et al., 2013a; Ault et al., 2014*]. Moreover, in a similar laboratory study using a realistic SSA generator, organic surfactants (sterol, galactose, lipopolysaccharide, albumin protein, and 1,2-dipalmitoyl-*sn*-glycero-3-phosphate monosodium salt (DPPA)) used to mimic a phytoplankton bloom did not inhibit SSA reactive uptake of N_2O_5, another important reactive gas in the nitrogen cycle [*Ryder et al., 2015*]. This result is in contrast to measurements of reactive uptake of N_2O_5 to ambient marine aerosol, which show suppressed reactivity in comparison. These discrepancies demonstrate the need for laboratory systems that capture and replicate the naturally occurring biological processes to explore fundamental physical chemistry reaction studies such as HNO_3 heterogeneous reactions in the laboratory. In addition to the need of the laboratory system for generating complex SSA, analytical techniques that are able to probe the chemical composition of individual SSA are needed to elucidate the aforementioned complexity. Such techniques are described below.

1.5 Probing the Chemistry of Sea Spray Aerosols in the Laboratory

Establishing a laboratory system to determine the correlation between marine biological activity and SSA organic enrichment that will impact SSA heterogeneous reactivity requires three major steps: 1) replicating the biological drivers of nascent SSA in a laboratory setting, 2) generation of realistic SSA through wave-breaking physical mechanisms, and 3) characterization of single particle composition using single particle mass spectrometry. Each of these three steps is described in Section 1.5.1-1.5.3 below.

1.5.1 Tuning Biological Drivers of SSA Chemistry in the Laboratory Studies

Studying SSA within a laboratory setting has provided unique insights into the chemistry of SSA that was previously not possible with field studies. Aerosols are ubiquitous in the atmosphere and can have lifetimes of seconds to weeks [*Lewis and Schwartz, 2004; Raes et al., 2000; Seinfeld and Pandis, 2016; Williams et al., 2002*]. Thus, it is difficult to isolate pure, nascent SSA from ambient aerosols to study their physicochemical properties, even over remote oceans [*Quinn et al., 2015*]. To study the relationship between ocean biology and the physicochemical properties of SSA in the absence of background aerosols, phytoplankton growths were optimized to recapitulate microbial loop processes common in marine environments [*Pomeroy et al., 2007*]. These growths allow for the production of more realistic SSA, composed of biogenically-derived chemical species in the laboratory and will be discussed further in Section 1.5.2, and Chapter 2.

1.5.2 Simulating Wave-Breaking in Laboratory Settings – Physical Drivers of SSA Chemistry

Bubble size distributions of breaking waves are crucial for accurately producing both the size distribution and chemical composition of SSA [*Collins et al., 2014*; *De Leeuw et al., 2011*;

Lewis and Schwartz, 2004]. An ocean-atmosphere facility that went through robust testing to replicate SSA physicochemical properties [*Ault et al., 2013b*; *Collins et al., 2014; Prather et al., 2013*] was utilized to generate realistic SSA in the laboratory [*Prather et al., 2013*] by using breaking waves to reproduce the bubble size distributions of waves measured in the open ocean [*Deane and Stokes, 2002*]. This study further allowed for the development of two small-scale SSA generators: the Marine Aerosol Reference Tank (MART) [*Stokes et al., 2013*] and miniature Marine Aerosol Reference Tank (miniMART) [*Stokes et al., 2016*]. The ocean-atmosphere facility, MART, and miniMART (Figure 1.1) all generate SSA through replicating the bubble size distributions produced when real ocean waves break [*Deane and Stokes, 2002*; *Stokes et al., 2013*, *2016*]. The difference between the systems is the physical mechanism producing the bubbles. For the ocean-atmosphere facility, this is achieved using a paddle-generated breaking wave action, while a plunging waterfall *via* water circulation pump is used in the MART, and a plunging waterfall *via* rotating wheel for the miniMART. The headspaces of all three systems are continuously purged with filtered clean air, thus ensuring studies of isolated nascent SSA.

1.5.3 Illuminating the Chemical Composition of SSA at Single Particle Resolution with Mass Spectrometry

Previously, aerosol chemical composition studies traditionally relied on sampling techniques involving collecting large number of particles onto a filter prior to analysis, which can introduce artifacts [*Chen, 1955; McMurry, 2000; Sullivan and Prather, 2005*]. While these bulk collection methods are still utilized for many types of offline detailed analysis [*Pratt and Prather, 2012*a], they do not provide key information on the chemical differences different individual particles (i.e. chemical mixing state). Nascent SSA size distributions peak at approximately 150 nm with a clear size dependent difference in the SSA chemical composition. Submicron particles (<1 µm in diameter) are enriched in organics, while larger supermicron particles (>1 µm in diameter) contain more salts [*Prather et al., 2013*]. Thus, when SSA is sampled onto a filter, the

mass is dominated by larger particles [*Seinfeld and Pandis, 2016*] which have a pronounced influence on the measured chemistry. Furthermore, particles ranging from 0.5 to 2.5 µm in diameter will readily undergo heterogeneous reactions due to their dominant surface area-to-volume [*Ault et al., 2014*]. Therefore, if all SSA were sampled onto a filter, the individual particle characteristics will be averaged out, thus providing no information on the range of particle composition [*McMurry, 2000*]. Chemical analysis of single aerosol particles allows for direct characterization of chemical composition of individual SSA, which can be used to assess how composition can further impact their heterogeneous reactivity [*Pratt and Prather, 2012b*].

Single particle mass spectrometry has become a dominant techniques used to perform on-line chemical analysis of individual particles [*Pratt and Prather, 2012*b; *Suess and Prather, 1999*]. One such instrument to perform these measurements, the aerosol time-of-flight mass spectrometer (ATOFMS) was the central instrument utilized in this dissertation [*Gard et al., 1997*; *Prather et al., 1994*]. It allows for the simultaneous measurement of both positive and negative ion mass spectra of size-resolved individual aerosols. The portable nature of the ATOFMS [*Gard et al., 1997*] and the different variants to measure aerosols of different size ranges [*Gard et al., 1997*; *Su et al., 2004*] as well as optical properties [*Moffet and Prather, 2005*] of aerosols make the ATOFMS a powerful technique for individual aerosols. Moreover, ATOFMS used in parallel with spectromicroscopic techniques [*Ault et al., 2013b*; *Ault et al., 2014*; *Collins et al., 2014*; *Prather et al., 2013*] and other aerosol chemical composition measurements [*Wang et al., 2015*] can reveal unique insight into SSA physicochemical properties and the resulting heterogeneous reaction behavior.

Details of the ATOFMS instrument design and operating principles are covered in the literature [*Gard et al., 1997*; *Prather et al., 1994*; *Pratt et al., 2009*; *Su et al., 2004*], and thus only a brief description will be provided here. Particles between 0.2 and 3.0 µm vacuum

aerodynamic diameter, D_{va}, are drawn through a nozzle inlet and accelerated through two stages of differential pumping, where each particle reaches a size-dependent terminal velocity. Particles pass through two orthogonally positioned diode-pumped solid state continuous wave lasers (532 nm, 50 mW). The transit time of the particle between the two lasers is used to determine particle velocity. The D_{va} is calculated for each particle using a calibration curve generated using polystyrene latex spheres of known diameter and density. The velocity is also used to trigger a pulsed, Q-switched Nd:YAG laser at 266 nm (8 ns pulse width, 700 μm spot size, ~10^7 W cm^{-2}) which desorbs and ionizes each particle. Both the positive and negative ion mass spectra of each individual particle were acquired using a dual polarity reflectron time-of-flight mass spectrometer with microchannel plate detectors.

Importantly for the studies in this dissertation, the positive ion mass spectrum typically indicates the particle source, whereas the negative ion mass spectrum usually contains information on the chemical aging history of the aerosol particle. For example, a sea spray particle contains ion markers such as Na^+, K^+, Na_2Cl^+, and Cl^-. When this particle undergoes heterogeneous reaction with reactive nitrogen species such as HNO_3, Cl^- is replaced by NO_2^- and NO_3^- ion markers [*Ault et al., 2013a; Ault et al., 2014*; *Gard et al., 1998*]. The presence of NO_2^- and NO_3^- in the particle mass spectrum informs that the sampled particle has aged.

1.6 Elucidating the Factors Governing Sea Spray Aerosol Heterogeneous Reactivity

As discussed in detail in Sections 1.3 and 1.4, a disconnect exists between laboratory studies of SSA heterogeneous reactions and field observations where the results using model surfactant molecules do not necessarily capture the behavior seen in ambient particles [*Abbatt et al., 2012; Ryder et al., 2015*]. It is expected, that as different classes of organics are created by marine microorganisms in the seawater, that the SSA heterogeneous reactivity will change [*Ryder*

et al., 2015]. Such changes to the organic composition of seawater can be caused during phytoplankton blooms, where enzymes, special proteins secreted by heterotrophic bacteria in the ocean, target specific substrate organic molecules and degrade them into smaller molecules for assimilation [*Azam and Malfatti, 2007*; *Bar-Even et al., 2011*; *Riemann et al., 2000*]. As enzymes have recently been suggested to affect SSA chemical composition [*Wang et al., 2015*], it is critical to investigate their specific impact in controlling SSA physicochemical properties and the resulting influence on heterogeneous reactivity, which has never been studied before.

In addition to enzymes from marine bacteria, bacteria can also influence the reactivity of the SSA directly due to the presence of molecules such as lipopolysaccharides that make up their cell walls. These molecules have been shown to undergo heterogeneous reactions in the atmosphere with reactive nitrogen species [*Ryder et al., 2015; Trueblood et al., 2016*]. To improve our understanding of SSA physicochemical composition, this dissertation addresses the following questions:

1. Can we replicate the biological complexity over a range of conditions in a laboratory setting to generate realistic SSA for fundamental physical chemistry studies of SSA?
2. How does seawater lipase transform the organic content of lipid-rich seawater? Can seawater lipase control SSA composition?
3. How do different organic surfactant mixtures affect SSA heterogeneous reactivity? How is SSA heterogeneous reactivity impacted by lipase-induced changes to organic species in seawater?
4. Do all enzymes produced from biological activity in seawater become transferred and remain active in SSA? Can these enzyme-containing SSA particles coagulate with other particles in the atmosphere to transform their composition and properties?

5. How do cation interactions with lipopolysaccharides impact the heterogeneous reactivity of SSA?

1.7 Synopsis and Goals of the Dissertation

The goal of this dissertation is to investigate the impact of organic mixtures produced by the marine microbial loop on SSA physicochemical properties in an isolated, controlled laboratory setting. Induced naturally occurring processes such as phytoplankton blooms as well as isolated marine-derived organic molecules and enzymes were used in a complimentary manner to assess the impact on SSA. Chapter 2 discusses the method development of growing phytoplankton blooms in a MART system and using the microbial loop to control the chemistry of organics in SSA. Changes in marine microbiology and the resulting physicochemical changes across bulk seawater, SSML, and SSA post-phytoplankton bloom are reported. Observed thickening of the SSA organic coating post-phytoplankton bloom demonstrates implications for SSA reactivity. Chapter 3 discusses a laboratory study using a miniMART to investigate the impact of lipase transformation of organics in seawater and the resulting changes to SSA composition. Chapter 4 extends the study of lipase transformation of simple and complex organics in seawater and presents the evolution of SSA chemical composition and the subsequent impact on SSA heterogeneous reactivity. Chapter 5 focuses on characterizing SSA enzyme hydrolytic activity over the course of induced phytoplankton microcosm experiments performed using the MART. It further discusses how single SSA particles containing enzymes can act as tiny biochemical reactors in the atmosphere. Using a model organic substrate and enzyme pair, it is further demonstrated that the active enzymes in SSA can impact physicochemical properties and heterogeneous reactivity of SSA. Atmospheric implications of this newly discovered reaction pathway are shown using computational simulations. To explain the results observed during large scale induced phytoplankton blooms, Chapter 6 discusses the role that cations present in seawater

and SSA (i.e. sodium, calcium) have on the physicochemical properties of lipopolysaccharide-containing aerosols. Experimental measurement and computational modeling were used in a complimentary manner to probe and explain the impact that lipopolysaccharide aggregation has on heterogeneous reactivity of SSA.

1.8 Acknowledgments

Olivia S. Ryder and Jamie M. Schiffer are acknowledged for assisting in the editing of this chapter.

1.9 Figures

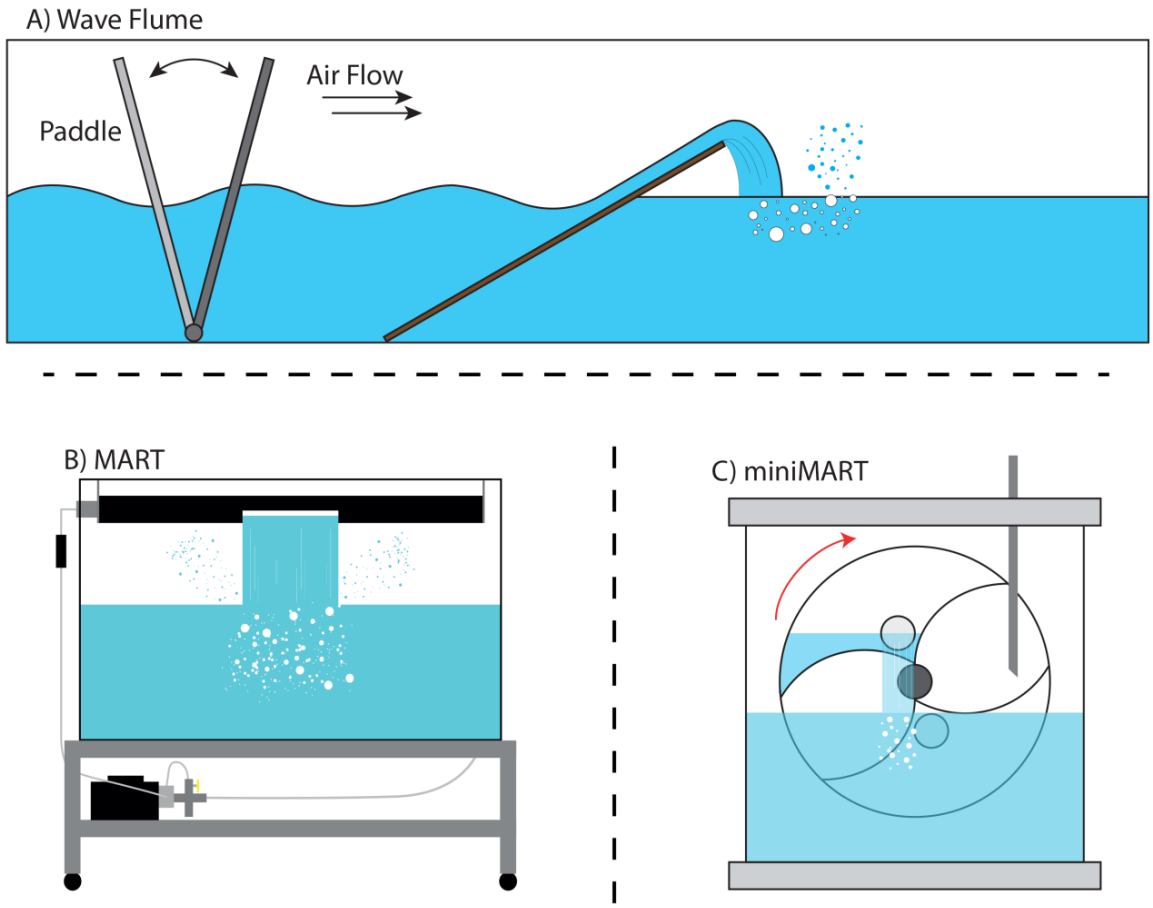

Figure 1.1. Sea spray aerosol generation methods. A) ocean-atmosphere facility generates SSA through paddle-generated breaking waves; B) Marine Aerosol Reference Tank (MART) generates SSA through a plunging water fall by circulating water using a pump; C) miniature Marine Aerosol Reference Tank (miniMART) generates SSA through plunging water using a rotating wheel.

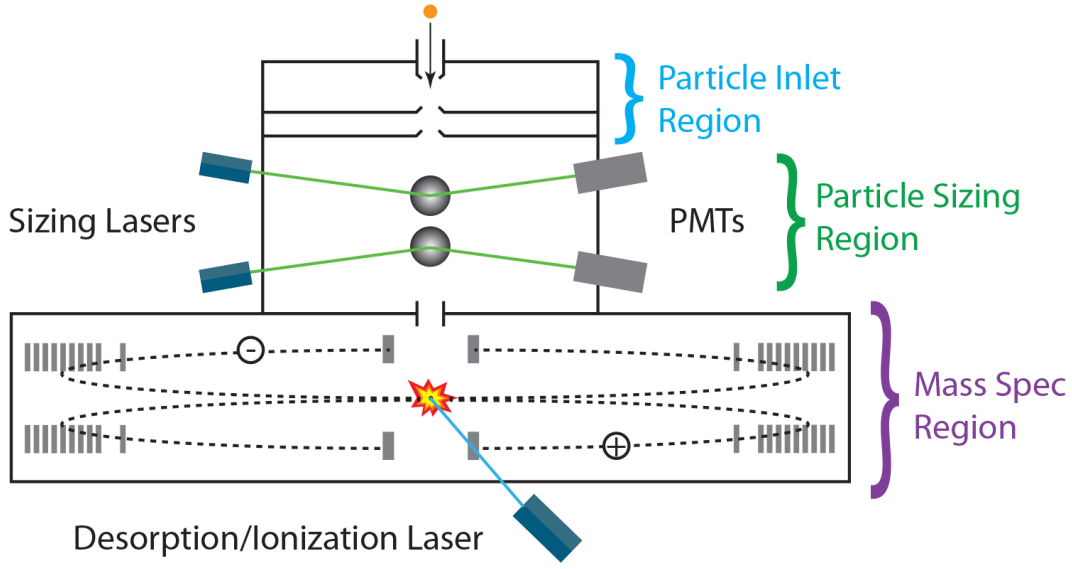

Figure 1.2. Schematic of the standard nozzle inlet ATOFMS adapted from Gard et al., 1997. PMT: photomultiplier tube.

1.10 References

Abbatt, J. P. D., A. K. Y. Lee, and J. A. Thornton, Quantifying trace gas uptake to tropospheric aerosol: recent advances and remaining challenges, Chemical Society Reviews, 41 (19), 6555, 2012.

Albrecht, B. A., Aerosols, cloud microphysics, and fractional cloudiness, Science, 245 (4923), 1277–1230, 1989.

Aller, J. Y., M. R. Kuznetsova, C. J. Jahns, and P. F. Kemp, The sea surface microlayer as a source of viral and bacterial enrichment in marine aerosols, Journal of Aerosol Science, 36 (5–6), 801–812, 2005.

Anderson, J. O., Clearing the air: A review of the effects of particulate matter air pollution on human health, Journal of Medical Toxicology, 8 (2), 166-175, 2012.

Andreae, M. O., D. Rosenfeld, P. Artaxo, A. A. Costa, G. P. Frank, K. M. Longo, and M. A. F. Silva-Dias, Smoking rain clouds over the Amazon, Science, 303 (5662), 1337-1342, 2004.

Andreae, M. O., and A. Gelencsér, Black carbon or brown cabon? The nature of light-absorbing carbonaceous aerosols, Atmospheric Chemistry & Physics, 6 (10), 3131–3148, 2006.

Andreae, M. O., and D. Rosenfeld, Aerosol-cloud-precipitation interactions. Part 1. The nature and sources of cloud-active aerosols, Earth-Science Reviews, 89 (1–2), 13–41, 2008.

Ault, A. P., T. L. Guasco, O. S. Ryder, J. Baltrusaitis, L. A. Cuadra-Rodriguez, D. B. Collins, M. J. Ruppel, T. H. Bertram, K. A. Prather, and V. H. Grassian, Inside versus outside: Ion redistribution in nitric acid reacted sea spray aerosol particles as determined by single particle analysis, Journal of the American Chemical Society, 135 (39), 14528–14531, 2013.

Ault, A. P., R. C. Moffet, J. Baltrusaitis, D. B. Collins, M. J. Ruppel, L. A. Cuadra-rodriguez, D. Zhao, T. L. Guasco, C. J. Ebben, F. M. Geiger, T. H. Bertram, K. A. Prather, and V. H. Grassian, Size-dependent changes in sea spray aerosol composition and properties with different seawater conditions, Environ. Sci. Technol., 47, 5603–5612, 2013.

Ault, A. P., T. L. Guasco, J. Baltrusaitis, O. S. Ryder, J. V. Trueblood, D. B. Collins, M. J. Ruppel, L. A. Cuadra-Rodriguez, K. A. Prather, and V. H. Grassian, Heterogeneous reactivity of nitric acid with nascent sea spray aerosol: Large differences observed between and within individual particles, Journal of Physical Chemistry Letters, 5 (15), 2493–2500, 2014.

Azam, F., and F. Malfatti, Microbial structuring of marine ecosystems., Nature Reviews. Microbiology, 5 (10), 782–791, 2007.

Bar-Even, A., E. Noor, Y. Savir, W. Liebermeister, D. Davidi, D. S. Tawfik, and R. Milo, The moderately efficient enzyme: Evolutionary and physicochemical trends shaping enzyme parameters, Biochemistry, 50 (21), 4402–4410, 2011.

Barnes, I., J. Hjorth, and N. Mihalopoulos, Dimethyl sulfide and dimethyl sulfoxide and their oxidation in the atmosphere, Chemical Reviews, 106 (3), 940-975, 2006.

Bertram, T. H., J. A. Thornton, T. P. Riedel, A. M. Middlebrook, R. Bahreini, T. S. Bates, P. K. Quinn, and D. J. Coffman, Direct observations of N_2O_5 reactivity on ambient aerosol particles, Geophysical Research Letters, 36 (L19803), 2009.

Blanchard, D. C., and L. D. Syzdek, Concentration of bacteria in jet drops from bursting bubbles, Journal of Geophysical Research, 77 (27), 5087, 1972.

Brauer, M. G. Freedman, J. Frostad, A. van Donkelaar, and R. V. Martin, Ambient air pollution exposure estimation for the global burden of disease 2013, Environmental Science and Technology, 50 (1), 79-88, 2016

Brink, H. M. Ten, Reactive uptake of HNO_3 and H_2SO_4 in sea-salt (NaCl) particles, Journal of Aerosol Science, 29 (1–2), 57–64, 1998.

Brook, R. D., S. Rajagopalan, C. A. Pope, J. R. Brook, A. Bhatnagar, A. V. Diez-Roux, F. Holguin, Y. Hong, R. V. Luepker, M. A. Mittleman, A. Peters, D. Siscovick, S. C. Smith, L. Whitsel, and J. D. Kaufman, Particulate matter air pollution and cardiovascular disease: An update to the scientific statement from the American Heart Association, Circulation, 2010.

Burnett, R. T., C. Arden Pope, M. Ezzati, C. Olives, S. S. Lim, S. Mehta, H. H. Shin, G. Singh, B. Hubbell, M. Brauer, H. R. Anderson, K. R. Smith, J. R. Balmes, N. G. Bruce, H. Kan, F. Laden, A. Pruss-Ustun, M. C. Turner, S. M. Gapstur, W. R. Diver, and A. Cohen, An integrated risk function for estimating the global burden of disease attributable to ambient fine particulate matter exposure, Environmental Health Perspectives, 122 (5), 397-403, 2014.

Charlson, R. J., J. E. Lovelock, M. O. Andreae, and S. G. Warren, Oceanic phytoplankton, atmospheric sulphur, cloud albedo and climate, Nature, 326 (6114), 655–661, 1987.

Chen, C. Y., Filtration of aerosols by fibrous media, Chemical Reviews, 55 (3), 595-623, 1955.

Christner, B. C., C. E. Morris, C. M. Foreman, R. M. Cai, and D. C. Sands, Ubiquity of biological ice nucleators in snowfall, Science 219 (5867), 1214-1214, 2008.

Collins, D. B., D. F. Zhao, M. J. Ruppel, O. Laskina, J. R. Grandquist, R. L. Modini, M. D. Stokes, L. M. Russell, T. H. Bertram, V. H. Grassian, G. B. Deane, and K. A. Prather, Direct aerosol chemical composition measurements to evaluate the physicochemical differences between controlled sea spray aerosol generation schemes, Atmospheric Measurement Techniques, 7 (11), 3667–3683, 2014.

Cunliffe, M., A. Engel, S. Frka, B. Gašparović, C. Guitart, J. C. Murrell, M. Salter, C. Stolle, R. Upstill-Goddard, and O. Wurl, Sea surface microlayers: A unified physicochemical and biological perspective of the air-ocean interface, Progress in Oceanography, 109, 104–116, 2013.

Deane, G. B., and M. D. Stokes, Scale dependence of bubble creation mechanisms in breaking waves, Nature, 418 (6900), 839–844, 2002.

De Haan, D. O., and B. J. Finlayson-Pitts, Knudsen cell studies of the reaction of gaseous nitric acid with synthetic sea salt at 298 K, The Journal of Physical Chemistry A, 101 (51), 9993–9999, 1997.

De Leeuw, G., E. L. Andreas, M. D. Anguelova, C. W. Fairall, R. Ernie, C. O. Dowd, M. Schulz, and S. E. Schwartz, Production flux of sea-spray aerosol, Reviews of Geophysics, 80 (2010), 1–39, 2011.

DeMott, P. J., K. Sassen, M. R. Poellot, D. Baumgardner, D. C. Rogers, S. D. Brooks, A. J. Prenni, and S. M. Kreidenweis, African dust aerosols as atmospheric ice nuclei, Geophysical Research Letters, 30 (14), 2003.

DeMott, P. J., A. J. Prenni, X. Liu, S. M. Kreidenweis, M. D. Petters, C. H. Twohy, M. S. Richardson, T. Eidhammer, and D. C. Rogers, Predicting global atmospheric nuclei distributions and their impacts on climate, Proceedings of the National Academy of Sciences of the United States of America, 107 (25), 11217-11222, 2010.

Despres, V. R., J. A. Huffman, S. M. Burrows, C. Hoose, A. S. Safatov, G. Buryak, J. Frohlich-Nowoisky, W. Elbert, M. O. Andreae, U. Poschl, and R. Jaenicke, Primary biological

aerosol particles in the atmosphere: A review, Tellus Series B-Chemical and Physical Meteorology, 64 (015598), 2012.

Dockery, D. W., J. Cunningham, A. L. Damokosh, L. M. Neas, J. D. Spengler, P. Koutrakis, J. H. Ware, M. Raizenne, and F. E. Speizer, Health effects of acid aerosols on North American children: Respiratory symptoms, Environmental Health Perspectives, 104 (5), 500–505, 1996.

Donaldson, D. J., and V. Vaida, The influence of organic films at the air-aqueous boundary on atmospheric processes, Chemical Reviews, 106 (4), 1445–1461, 2006.

Drakaki, E., C. Dessinioti, and C. V. Antoniou, Air pollution and the skin, Frontiers in Environmental Science, 2-11, 2014.

Dymarska, M., B. J. Murray, L. M. Sun, M. L. Eastwood, D. A. Knopf, and A. K. Bertram, Deposition ice nucleation on soot at temperatures relevant for the lower troposphere, Journal of Geophysical Research: Atmospheres, 111 (D4), 2006.

Fann, N. A. D. Lamson, S. C. Anenberg, K. Wesson, D. Risley, B. J. Hubbell, Estimating the national public health burden associated with exposure to ambient $PM_{2.5}$ and ozone, Risk Analysis, 32 (1), 81-95, 2012.

Finlayson-Pitts, B. J., Reactions at surfaces in the atmosphere: integration of experiments and theory as necessary (but not necessarily sufficient) for predicting the physical chemistry of aerosols, Physical Chemistry Chemical Physics : PCCP, 11 (36), 7759, 2009.

Finlayson-Pitts, B. J., and J. N. Pitts, Chemistry of the upper and lower atmosphere: Theory, experiments, and applications, 1999.

Gard, E. E., J. E. Mayer, B. D. Morrical, T. Dienes, D. P. Fergenson, and K. A. Prather, Real-time analysis of individual atmospheric aerosol particles: Design and performance of a portable ATOFMS, Analytical Chemistry, 69 (20), 4083–4091, 1997.

Gard, E. E., M. J. Kleeman, D. S. Gross, L. S. Hughes, J. O. Allen, B. D. Morrical, D. P. Fergenson, T. Dienes, M. E. Galli, R. J. Johnson, G. R. Cass, and K. A. Prather, Direct observation of heterogeneous chemistry in the atmosphere, Science, 279 (5354), 1184–1187, 1998.

Ginoux, P., J. M. Prospero, T. E. Gill, N. C. Hsu, and M. Zhao, Global-scale attribution of anthropogenic and natural dust sources and their emission rates based on MODIS Deep Blue aerosol products, Reviews of Geophysics, 2012.

Groene, T., Biogenic production and consumption of dimethylsulfide (DMS) and dimethylsulfoniopropionate (DMSP) in the marine epipelagic zone: A review, Journal of Marine Systems, 6, 191-209, 1995.

Haywood, J., and O. Boucher, Estimates of the direct and indirect radiative forcing due to tropospheric aerosols: A review, Reviews of Geophysics, 2000.

Hidy, G. M., B. R. Appel, R. J. Charlson, W. E. Clark, S. K. Friedlander, D. H. Hutchison, T. B. Smith, J. Suder, J. J. Wesolowski, and K. T. Whitby, Summary of the California aerosol characterization experiment, Journal of the Air Pollution Control Association, 25 (11), 1106–1114, 1975.

Isono, K., M. Komabayasi, and A. Ono, The nature and origin of ice nuclei in the atmosphere, Journal of the Meteorological Society of Japan, 37, 211-233, 1959.

Kolb, C. E., R. A. Cox, J. P. D. Abbatt, M. Ammann, E. J. Davis, D. J. Donaldson, B. C. Garrett, C. George, P. T. Griffiths, D. R. Hanson, M. Kulmala, G. McFiggans, U. Pöschl, I. Riipinen, M. J. Rossi, Y. Rudich, P. E. Wagner, P. M. Winkler, D. R. Worsnop, and C. D. O'Dowd, An overview of current issues in the uptake of atmospheric trace gases by aerosols and clouds, Atmospheric Chemistry and Physics, 10 (21), 10561–10605, 2010.

Kroll, J. H., and J. H. Seinfeld, Chemistry of secondary organic aerosol: Formation and evolution of low-volatility organics in the atmosphere, Atmospheric Environment, 2008.

Laskin, J., A. Laskin, and S. A. Nizkorodov, New mass spectrometry techniques for studying physical chemistry of atmospheric heterogeneous processes, International Review in Physical Chemistry, 32, 128-170, 2013.

Latzin, P., M. Röösli, A. Huss, C. E. Kuehni, and U. Frey, Air pollution during pregnancy and lung function in newborns: A birth cohort study, European Respiratory Journal, 33 (3), 594–603, 2009.

Lau, K. M., and H. T. Wu, Warm rain processes over tropical oceans and climate implications, Geophysical Research Letters, 30 (24), 2003.

Lewis, E. R., and S. E. Schwartz, Sea salt aerosol production: Mechanisms, methods, measurements and models, Geophysical Monograph Series, 152, 413, 2004.

Liu, Y., J. P. Cain, H. Wang, and A. Laskin, Kinetic study of heterogeneous reaction of deliquesced NaCl particles with gaseous HNO_3 using particle-on-substrate stagnation flow reactor approach, Journal of Physical Chemistry A, 111 (40), 10026–10043, 2007.

Lohmann, U., and J. Feichter, Global indirect aerosol effects: A review, Atmospheric Chemistry and Physics, 5, 715–737, 2005.

McCluskey, C. S., T. C. J. Hill, F. Malfatti, C. M. Sultana, C. Lee, M. V. Santander, C. M. Beall, K. A. Moore, G. C. Cornwell, D. B. Collins, K. A. Prather, T. Jayarathne, E. A. Stone, F. Azam, S. M. Kreidenweis, and P. J. DeMott, A dynamic link between ice nucleating particles released in nascent sea spray aerosol and oceanic biological activity during two mesocosm experiments, Jounal of the Atmospheric Sciences, 74, 151-166, 2017.

McFiggans, G., P. Artaxo, U. Baltensperger, H. Coe, M. C. Facchini, G. Feingold, S. Fuzzi, M. Gysel, A. Laaksonen, U. Lohmann, T. F. Mentel, D. M. Murphy, C. D. O'Dowd, J. R. Snider, and E. Weingartner, The effect of physical and chemical aerosol properties on warm cloud droplet activation, Atmospheric Chemistry and Physics, 6, 2593–2649, 2006.

McMurry, P. H., A review of atmospheric aerosol measurements, Atmospheric Environment, 34(12-14), 1959-1999, 2000.

Meskhidze, N., J. Xu, B. Gantt, Y. Zhang, a. Nenes, S. J. Ghan, X. Liu, R. Easter, and R. Zaveri, Global distribution and climate forcing of marine organic aerosol: 1. Model improvements and evaluation, Atmospheric Chemistry and Physics, 11 (22), 11689–11705, 2011.

Moffet, R. C., and K. A. Prather, Extending ATOFMS measurements to include refractive index and density, Analytical Chemistry, 77 (20), 6535–6541, 2005.

Moffet, R. C., and K. A. Prather, In-situ measurements of the mixing state and optical properties of soot with implications for radiative forcing estimates., Proceedings of the National Academy of Sciences of the United States of America, 106 (29), 11872–11877, 2009.

Moussa, S. G., A. C. Stern, J. D. Raff, C. W. Dilbeck, D. J. Tobias and B. J. Finlayson-Pitts, Experimental and theoretical studies of the interaction of gas phase nitric acid and water with a self-assembled monolayer, Physical Chemistry Chemical Physics, 15 (2), 2012.

Nguyen, B. C., S. Belviso, N. Mihalopoulos, J. Gostan, and P. Nival, Dimethyl sulfide production during natural phytoplanktonic blooms, Marine Chemistry, 24 (2), 133–141, 1988.

Nishino, N. S. A. Hollingsworth, A. C. Stern, M. Roeselova, D. J. Tobias, and B. J. Finlayson-Pitts, Interactions of gaseous HNO_3 and water with individual and mixed alkyl self-assembled monolayers at room temperature, Physical Chemistry Chemical Physics, 16 (6), 2358–67, 2014.

O'Dowd, C. D., M. C. Facchini, F. Cavalli, D. Ceburnis, M. Mircea, S. Decesari, S. Fuzzi, Y. J. Yoon, and J.-P. Putaud, Biogenically driven organic contribution to marine aerosol, Nature, 431 (7009), 676–680, 2004.

Oudin, A., L. Braback, D. O. Astrom, M. Stromgren, and B. Forsberg, Association between neighbourhood air pollution concentrations and dispensed mediation for psychiatric disorders in a large longtitudinal cohort of Swedish children and adolescents, BMJ Open, 6, 1-12, 2016.

Petters, M. D., and S. M. Kreidenweis, A single parameter representation of hygroscopic growth and cloud condensation ucleus activity, Atmospheric Chemistry and Physics, 7 (8), 1961-1971, 2007.

Pomeroy, L. R., P. J. I. Williams, F. Azam, and J. E. Hobbie, The microbial loop, Oceanography, 20 (2), 28–33, 2007.

Pope, C. A., and D. W. Dockery, Health effects of fine particulate air pollution: Lines that connect, Journal of the Air & Waste Management Association, 56 (6), 709–742, 2006.

Pöschl, U., Atmospheric aerosols: Composition, transformation, climate and health effects, Angewandte Chemie - International Edition, 44 (46), 7520–7540, 2005.

Prather, K. A., C. D. Hatch, and V. H. Grassian, Analysis of atmospheric aerosols., Annual Review of Analytical Chemistry (Palo Alto, Calif.), 1, 485–514, 2008.

Prather, K. A., T. Nordmeyer, and K. Salt, Real-time characterization of individual aerosol particles using time-of-flight mass spectrometry, Analytical Chemistry, 66 (9), 1403–1407, 1994.

Prather, K. A., T. H. Bertram, V. H. Grassian, G. B. Deane, M. D. Stokes, P. J. Demott, L. I. Aluwihare, B. P. Palenik, F. Azam, J. H. Seinfeld, R. C. Moffet, M. J. Molina, C. D. Cappa, F. M. Geiger, G. C. Roberts, L. M. Russell, A. P. Ault, J. Baltrusaitis, D. B. Collins, C. E. Corrigan, L. A. Cuadra-Rodriguez, C. J. Ebben, S. D. Forestieri, T. L. Guasco, S. P. Hersey, M. J. Kim, W. F. Lambert, R. L. Modini, W. Mui, B. E. Pedler, M. J. Ruppel, O. S. Ryder, N. G. Schoepp, R. C. Sullivan, and D. Zhao, Bringing the ocean into the laboratory to probe the chemical complexity of sea spray aerosol., Proceedings of the National Academy of Sciences of the United States of America, 110 (19), 7550–5, 2013.

Pratt, K. A., and K. A. Prather, Mass spectrometry of atmospheric aerosols-Recent developments and applications. Part I: Off-line mass spectrometry techniques, Mass Spectrometry Reviews, 2012.

Pratt, K. A., and K. A. Prather, Mass spectrometry of atmospheric aerosols-Recent developments and applications. Part II: On-line mass spectrometry techniques, Mass Spectrometry Reviews, 2012.

Pratt, K. A., J. E. Mayer, J. C. Holecek, R. C. Moffet, R. O. Sanchez, T. P. Rebotier, H. Furutani, M. Gonin, K. Fuhrer, Y. Su, S. Guazzotti, K. A. Prather, X. K. Fuhrer, and X. Y. Su, Development and characterization of an aircraft aerosol time-of-flight mass spectrometer, Analytical Chemistry, 81 (5), 1792–1800, 2009.

Pryor, S. C., and L. L. Sørensen, Nitric acid–sea salt reactions: Implications for nitrogen deposition to water surfaces, Journal of Applied Meteorology, 39 (5), 725–731, 2000.

Quinn, P. K., D. B. Collins, V. H. Grassian, K. A. Prather, and T. S. Bates, Chemistry and related properties of freshly emitted sea spray aerosol, Chemical Reviews, 115, 4383–4399, 2015.

Quinn, P. K., T. S. Bates, K. S. Schulz, D. J. Coffman, A. A. Frossard, L. M. Russell, W. C. Keene, and D. J. Kieber, Contribution of sea surface carbon pool to organic matter enrichment in sea spray aerosol, Nature Geoscience, 7 (3), 228–232, 2014.

Raes, F., R. Van Dingenen, E. Vignati, J. Wilson, J. P. Putaud, J. H. Seinfeld, and P. Adams. Formation and cycling of aerosols in the global troposphere, Atmospheric Environment, 34, 4215-4240, 2000.

Ravishankara, A. R., Heterogeneous and multiphase chemistry in the troposphere, 276 (5315), 1058-1065, 1997.

Riemann, L., G. F. Steward, and F. Azam, Dynamics of bacterial community composition and activity during a mesocosm diatom bloom, Applied and Environmental Microbiology, 66 (2), 578–587, 2000.

Rinaldi, M., S. Fuzzi, S. Decesari, S. Marullo, R. Santoleri, A. Provenzale, J. Von Hardenberg, D. Ceburnis, A. Vaishya, C. D. O'Dowd, and M. C. Facchini, Is chlorophyll-a the best surrogate for organic matter enrichment in submicron primary marine aerosol?, Journal of Geophysical Research: Atmospheres, 118 (10), 4964–4973, 2013.

Rosenfeld, D., Suppression of rain and snow by urban and industrial air pollution, Science, 287 (5459), 1793-1796, 2000.

Rossi, M. J., Heterogeneous reactions on salts, Chemical Reviews, 103 (12), 4823–4882, 2003.

Ryder, O. S., N. R. Campbell, H. Morris, S. Forestieri, M. J. Ruppel, C. Cappa, A. Tivanski, K. Prather, and T. H. Bertram, Role of organic coatings in regulating N_2O_5 reactive uptake to sea spray aerosol, Journal of Physical Chemistry A, 119 (48), 11683–11692, 2015.

Seinfeld, J. H., and S. N. Pandis, Atmospheric chemistry and physics: From air pollution to climate change (Vol. 3rd), 2016.

Sram, R., Impact of air pollution on reproductive health, Environmental Health Perspectives 107 (11), A542-543, 1999.

Stemmler K., A. Vlasenko, C. Guimbaud, and M. Ammann, The effect of fatty acid surfactants on the uptake of nitric acid to deliquesced NaCl aerosol, Atmospheric Chemistry and Physics, 8, 5127–5141, 2008.

Stocker, T. F., Q. Dahe, G.-K. Plattner, L. V. Alexander, S. K. Allen, N. L. Bindoff, F.-M. Bréon, J. A. Church, U. Cubash, S. Emori, P. Forster, P. Friedlingstein, L. D. Talley, D. G. Vaughan, and S.-P. Xie, Technical summary, Climate Change 2013: The physical science basis. Contribution of working group I to the fifth assessment report of the Intergovernmental Panel on Climate Change, 33–115, 2013.

Stokes, M. D., G. B. Deane, D. B. Collins, C. D. Cappa, T. H. Bertram, A. Dommer, S. Schill, S. Forestieri, and M. Survilo, A miniature Marine Aerosol Reference Tank (miniMART) as a compact breaking wave analogue, Atmospheric Measurement Techniques, 9, 4257–4267, 2016.

Stokes, M. D., G. B. Deane, K. Prather, T. H. Bertram, M. J. Ruppel, O. S. Ryder, J. M. Brady, and D. Zhao, A Marine Aerosol Reference Tank system as a breaking wave analogue for the production of foam and sea-spray aerosols, Atmospheric Measurement Techniques, 6 (4), 1085–1094, 2013.

Su, Y., M. F. Sipin, H. Furutani, and K. A. Prather, Development and characterization of an aerosol time-of-flight mass spectrometer with increased detection efficiency, Analytical Chemistry, 76 (3), 712–719, 2004.

Suess, D. T., and K. A. Prather, Mass spectrometry of aerosols, Chemical Reviews, 99 (10), 3007–36, 1999.

Sullivan, R. C., and K. A. Prather, Recent advances in our understanding of atmospheric chemistry and climate made possible by on-line aerosol analysis instrumentation, Analytical Chemistry, 77, 3861-3885, 2005.

Textor C., M. Schulz, S. Guibert, S. Kinne, Y. Balkanski, S. Bauer, T. Bernsten, T. Berglen, O. Boucher, M. Chin, F. Dentener, T. Diehl, R. Easter, H. Feichter, D. Fillmore, S. Ghan, P. Ginoux, S. Gong, A. Grini, J. Hendricks, L. Horowitz, P. Huang, I. Isaksen, I. Iversen, S. Kloster, D. Koch, A. Kirkenvag, J. E. Kristjansson, M. Krol, A. Lauer, J. F. Lamarque, X. Liu, V. Montanaro, G. Myhre, J. Penner, G. Pitari, S. Reddy, O. Seland, P. Stier, T. Takemura, and X. Tie, Analysis and quantification of diversities of aerosol life cycles within AeroCom, Atmospheric Chemistry and Physics, 6, 1777-1813, 2006.

Trueblood, J. V., A. D. Estillore, C. Lee, J. A. Dowling, K. A. Prather, and V. H. Grassian, Heterogeneous chemistry of lipopolysaccharides with gas-phase nitric acid: Reactive sites and reaction pathways, Journal of Physical Chemistry A, 120 (32), 6444–6450, 2016.

Tsigaridis, K., D. Koch, and S. Menon, Uncertainties and importance of sea spray composition on aerosol direct and indirect effects, Journal of Geophysical Research: Atmospheres, 118 (1), 220–235, 2013.

Twomey, S., The Influence of pollution on the shortwave albedo of clouds, Journal of the Atmospheric Sciences, 34 (7), 1149–1152, 1977.

Vedal, S., Ambient particles and health: Lines that divide, Journal of the Air and Waste Management Association, 47 (5), 551–581, 1997.

Wang, X., C. M. Sultana, J. Trueblood, T. C. J. Hill, F. Malfatti, C. Lee, O. Laskina, K. A. Moore, C. M. Beall, C. S. McCluskey, G. C. Cornwell, Y. Zhou, J. L. Cox, M. A. Pendergraft, M. V. Santander, T. H. Bertram, C. D. Cappa, F. Azam, P. J. DeMott, V. H. Grassian, and K. A. Prather, Microbial control of sea spray aerosol composition: A tale of two blooms, ACS Central Science, 1 (3), 124–131, 2015.

Wiacek, A., T. Peter, and U. Lohmann, The potential influence of Asian and African mineral dust on ice, mixed-phase and liquid water clouds, Atmospheric Chemistry and Physics, 10 (18), 8649-8667, 2010.

Williams, J., M. de Reus, R. Krejci, H. Fischer, and J. Strom, Application of the variability-size relationship to atmospheric aerosol studies: Estimating aerosol lifetimes and ages. Atmospheric Chemistry and Physics, 2, 133-145, 2002.

Woodhouse, M. T., G. W. Mann, K. S. Carslaw, and O. Boucher, Sensitivity of cloud condensation nuclei to regional changes in dimethyl-sulphide emissions, Atmospheric Chemistry and Physics, 13 (5), 2723-2733, 2013.

Zieger, P., R. Fierz-Schmidhauser, E. Weingartner, and U. Baltensperger, Effects of relative humidity on aerosol light scattering: Results from different European sites, Atmospheric Chemistry and Physics, 13 (21), 10609–10631, 2013.

2 Advancing Model Systems for Fundamental Laboratory Studies of Sea Spray Aerosol Using the Microbial Loop

2.1 Synopsis

Sea spray aerosol (SSA) particles represent one of the most abundant surfaces available for heterogeneous reactions to occur upon and thus profoundly alter the composition of the troposphere. In an effort to better understand tropospheric heterogeneous reaction processes, fundamental laboratory studies must be able to accurately reproduce the chemical complexity of SSA. Here we describe a new approach that uses microbial processes to control the composition of seawater and SSA particle composition. By inducing a phytoplankton bloom, we are able to create dynamic ecosystem interactions between marine microorganisms, which serve to alter the organic mixtures present in seawater. Using this controlled approach, changes in seawater composition become reflected in the chemical composition of SSA particles 4 to 10 d after the peak in chlorophyll-a (Chl-a). This approach for producing and varying the chemical complexity of a dominant tropospheric aerosol provides the foundation for further investigations of the physical and chemical properties of realistic SSA particles under controlled conditions.

2.2 Introduction

Seminal studies by Professor Mario J. Molina and co-workers demonstrated the profound influence heterogeneous reactions can have on the composition of the stratosphere. These studies provided an exemplary example of how laboratory studies of fundamental physical chemistry can play an essential role in explaining atmospheric observations [*Abbatt and Molina, 1993*; *Molina and Rowland, 1974*; *Prenni and Tolbert, 2001*], ultimately providing solutions to complex environmental problems. Laboratory studies simulated the composition of stratospheric aerosol particles comprised of ice, nitric acid, and ammonium sulfate [*Abbatt and Molina, 1992*; *Tolbert*

et al., 1987]. The studies, which elucidated the detailed mechanisms involving surface adsorption and chemistry [*Prenni and Tolbert, 2001*], led to the understanding of their climatic effects and lifetime in the stratosphere [*Deshler, 2008*].

Compared to stratospheric aerosols, tropospheric aerosols are chemically far more complex. They originate from a wide range of natural and anthropogenic sources, can be comprised of multiple phases, and contain thousands of compounds, including complex mixtures of organic and inorganic species [*Lewis and Schwartz, 2004*; *Prather et al., 2008*]. Sea spray aerosol (SSA) particles are generated at the ocean surface by breaking waves and bursting of whitecap foam bubbles [*Blanchard and Woodcock, 1957*; *De Leeuw et al., 2011*; *Lewis and Schwartz, 2004*] and constitute one of the most abundant aerosol particle types in the atmosphere [*Lewis and Schwartz, 2004*; *Prather et al., 2008*; *Tsigaridis et al., 2013*]. Previous studies have suggested that the organic fraction of SSA in the marine boundary layer increases during periods of high biological activity in the ocean [*O'Dowd et al., 2004*]. Understanding the factors controlling these changes is important as inclusion of organic material in SSA particles has been shown to influence water uptake [*Cruz and Pandis, 2000*; *Saxena and Hildemann, 1995*], heterogeneous nucleation of ice [*Cziczo et al., 2004*; *Möhler et al., 2008*], and chemical reactivity with important atmospheric trace gases [*McNeill et al., 2006*; *Ryder et al., 2014*].

The initial studies by Molina and co-workers on stratospheric aerosol particles demonstrated how controlled fundamental studies were essential for understanding and solving large-scale atmospheric phenomena [*Bogdan and Molina, 2010*; *Molina et al., 1996*; *Salcedo et al., 2000, 2001*]. Since these early studies, fundamental physical chemistry investigations have probed tropospheric SSA particles [*McNeill et al., 2006*; *You et al., 2014*] using model SSA systems comprised of sodium chloride mixed with organic species such as sodium dodecyl sulfate [*Abbatt et al., 2012*; *Finlayson-Pitts, 2009*; *Krueger et al., 2003*]. While studies using model

systems have provided critical insights into the behavior of mixtures of organic and inorganic species, they cannot be used to explain reactions that occur on chemically complex naturally produced SSA particles. Accurately replicating tropospheric aerosols so that laboratory study results can be used to explain atmospheric observations represent an enormous challenge as the interfacial properties and overall chemical composition of SSA particles depend in a poorly understood way on seawater composition and sea spray production mechanisms [*Collins et al., 2014*; *Prather et al., 2013*].

Breaking waves lead to a unique production mechanism that ultimately produces SSA particles [*Prather et al., 2013*; *Stokes et al., 2013*]. Efforts have been made to replicate the same physical mechanisms for SSA particle production in the laboratory through the development of the Marine Aerosol Reference Tank (MART), a portable system with ability to produce a similar set of bubble sizes to breaking waves that are critical to replicating the size distribution and chemical mixing state of SSA generated by wave breaking [*Collins et al., 2014*; *Stokes et al., 2013*]. While previous studies have investigated the effect serial additions of representative microorganism cultures and organic molecules to seawater has on SSA chemical and physical properties [*Ault et al., 2013b*; *Collins et al., 2014*; *Prather et al., 2013*], it is impossible to replicate the full complexity of the myriad of organic molecules present in ambient seawater using this method. The novelty of this study involves developing a protocol for reproducing the natural chemical complexity inherent to biologically active regions of the oceans by utilizing phytoplankton blooms to induce a change in the seawater composition and the resulting SSA. The interactions between phytoplankton, bacteria, and viruses present in the seawater produce a complex mixture of organic molecules that closely represent surface ocean biochemical conditions.

This study illustrates how one can use microbial processes to produce a chemically complex suite of organic compounds such as those produced in the ocean [*Azam et al., 1983*, *1994*; *Azam and Malfatti, 2007*; *Pomeroy et al., 2007*; *Teeling et al., 2012*] for more realistic studies of isolated SSA physical and chemical properties. Figure 2.1A shows an idealized scheme of the dynamic of marine microorganisms within a phytoplankton bloom microcosm experiment. Phytoplankton reduce CO_2 and represent a source of dissolved organic carbon (DOC) in the seawater. This organic matter is further transformed and processed by interactions with marine microorganisms such as heterotrophic bacteria [*Azam et al., 1994*; *Azam and Malfatti, 2007*; *D. Hessen and Tranvik, 1998*; *Pomeroy et al., 2007*]. The natural synthesis and subsequent chemical processing of organic compounds by marine microorganisms allows the complexity of ocean chemistry to be replicated in a manner that mimics naturally occurring ocean processes that ultimately influence the composition of ejected SSA particles, affecting water uptake and reactivity. Fundamental studies of the physicochemical properties of SSA particles can then be performed in a controlled environment on aerosol particles that closely resemble those produced in the natural environment [*Collins et al., 2014*].

2.3 Experimental Methods

2.3.1 Marine Aerosol Reference Tank Photobioreactor Configuration

High-definition fluorescent tubes (Full Spectrum Solutions, model 205457) with a blackbody radiation temperature of 5700 K, to closely mimic the radiation profile of the sun, were mounted to the MART to irradiate the seawater and stimulate the growth of marine phytoplankton (Figure 2.8). These lights were positioned to generated ~70 $\mu E\ m^{-2}\ s^{-1}$ photosynthetically active radiation (PAR; Apogee Instruments, MQ-200) measured at ~15 cm below the surface of the seawater in the MART. Summer noon surface PAR levels have been

reported from satellite observations to be from ~1000 to 1500 µE m^{-2} s^{-1} regularly between 40° N and 40° S [*Bouvet et al., 2002*], whereas the much lower experimental irradiance condition used in this study simulates the radiation flux density typically used in the growth of phytoplankton cultures [*Brown and Richardson, 1968*; *Sorokin and Krauss, 1958*]. Constant PAR illumination at the level used in this study allowed steady and controlled growth of phytoplankton in the MART.

Natural seawater collected at the end of Scripps Pier (La Jolla, CA; 32° 52′ 00″ N, 117° 15′ 21″ W; 275 m offshore) was filtered using 50 µm Nitex mesh (Sefar Nitex 03-100/32) and added to the MART (ocean conditions at the time of seawater sampling listed in Table 2.1). After a 24 h temperature adjustment period, phytoplankton growth was stimulated by adding diatom growth medium commonly known as Guillard's f medium (ProLine Aquatic Ecosystems) diluted by a factor of 2 (f/2) or by a factor of 20 (f/20) including Na_2SiO_3 (full list of components and concentrations listed in Table 2.2) [*Guillard, 1975*; *Guillard and Ryther, 1962*]. The biological community and the chemical composition of the collected seawater were not controlled or adjusted prior to the addition of diatom growth medium with the exception of filtering large phytoplankton predators known as grazers using the Nitex mesh filter [*Azam and Malfatti, 2007*; *Pomeroy et al., 2007*]; thus, the starting conditions are referred to as "unconstrained." A bubbler system of Tygon tubing and glass weights was then placed on the bottom of the MART to produce gentle mixing and aeration until *in vivo* chlorophyll-a (Chl-a) concentrations reached ~12 mg m^{-3}.

The threshold of 12 mg m^{-3} was chosen to be the time to begin using the SSA particle production mechanism as studies found that the water recirculation system used to produce the plunging waterfall could inhibit the phytoplankton growth. This was attributed to the lysing of phytoplankton cells by the high shear force of the mechanical pump used to circulate the seawater through the plunging waterfall aerosol generation apparatus. Once the Chl-a concentration

reached the threshold, the bubbler system was removed and SSA particle generation was started through pulsed plunging waterfall technique with 4 s waterfall duty cycle [*Stokes et al., 2013*]. SSA particles were generated and analyzed during 2 h periods followed by 2 h with no particle generation or mixing. This "2 h on, 2 h off" protocol was implemented as a compromise to allow the biological processes in the seawater to thrive while providing enough SSA particles to sample. Operating the mechanical pump for SSA particle generation past this threshold for 2 h did not affect Chl-a concentrations. The Chl-a concentration continued to increase for several (2−4) days after particle generation resumed, thus suggesting that even with the mechanical pump, some phytoplankton populations were still able to bloom. A total of six MART microcosm experiments were conducted in this study to explore the variability due to the lack of chemical/biological constraint on the initial seawater sample; full details can be found in Supporting Information.

2.3.2 Chemical and Biological Measurements of Seawater

Subsurface bulk seawater was collected through a stainless steel valve mounted ~20 cm below the surface of the seawater on the tank. To sample the sea surface microlayer (SSML), the glass plate method was utilized as this technique allowed efficient collection of the large volume needed for microscopic analysis from the upper 100 μm of the sea surface [*Cunliffe et al., 2013*]. Aerosol impingers (Chemglass, CG-1820, 0.2 μm D_p lower cutoff) were used to collect SSA particles for quantification of ejected marine microorganisms and chemical characterization of aerosolized organic matter by fluorescence spectroscopic methods. Throughout the course of the microcosm experiment, daily measurements of the bulk DOC concentration and *in vivo* Chl-a fluorescence were made. *In vivo* Chl-a fluorescence, measured by a commercial portable fluorimeter (Aquafluor, Turner Designs), was used to track phytoplankton biomass. For determination of DOC concentrations, a metric used to quantify dissolved organic matter (DOM), bulk seawater was passed through a 0.7 μm filter (Whatman GF/F, Z242489) and immediately

acidified with two drops of trace metal-free 12 N HCl to approximately a pH of 2. The sample was then analyzed using the high-temperature combustion method (Shimadzu Scientific Instruments, TOC-V CSN) [*Álvarez-Salgado and Miller, 1998*]. The same filtering process was performed to filter the seawater for fluorescence excitation− emission matrix (EEM) spectroscopy (Horiba Scientific, Aqualog) to characterize and obtain relative concentration of fluorescent organic compounds. Optical counts of marine bacteria and viruses in the bulk, SSML, and impinged SSA particles in sterile seawater were performed using epifluorescence microscopy (Olympus, IX71) with SYBR Green-I nucleic acid gel stain (Life Technologies, S-7563) where bacteria and viruses were discriminated based on their size [*Noble and Fuhrman, 1998*].

2.3.3 Chemical Measurements of Sea Spray Aerosol Particles

Under the typical operating conditions for this study, the headspace of the MART during SSA particle generation had a relative humidity (RH) greater than 90% (Vaisala, HMP110) with a residence time less than 15 min at an air flow rate of 6 SLPM. The relatively short residence time led to sampling primary SSA particles [*Abbatt et al., 2012*], as secondary (gas-particle) chemistry processes such as secondary aerosol formation are slower than the average lifetime in the headspace [*Fry et al., 2014*; *Osto et al., 2009*]. The size-resolved chemical compositions of individual SSA particles ranging from 0.2 to 3.0 μm in vacuum aerodynamic diameter (D_{va}) were measured in real time using an aerosol time-of-flight mass spectrometer (ATOFMS). More detailed information on this analytical technique can be found elsewhere [*Gard et al., 1997*], and in Section 1.5.3. Data were imported into MATLAB (The Math Works, Inc.) with software toolkit YAADA (www.yaada.org) for further data analysis.

MART-generated SSA particles were collected for further offline analysis of physical and chemical composition using a Micro Orifice Uniform Deposit Impactor (MOUDI, MSP Corp. model 100-NR, 10 stages) and aerosol impingers. The MOUDI allows size-fractionated particle

samples to be collected. SSA particles (aerodynamic diameter range from 0.56 to 1.0 μm) collected on Si wafer substrates (Ted Pella Inc., 16008) mounted in the MOUDI on stage 6 (aerodynamic diameter range of 0.56-1.0 μm) were analyzed using scanning electron microscopy (SEM; Hitachi S-4800, 5 kV accelerating voltage, 15 μA, 10× magnification). Aerosol impingers filled with ultrapure water were used to collect SSA particles for further analysis through fluorescence EEM spectroscopy.

2.4 Results and Discussion

2.4.1 Validation of Marine Aerosol Reference Tank and Ambient Measurements

Comparison of the laboratory approach in this study to ambient measurements served as a test of how closely laboratory-generated SSA resembled atmospheric aerosols. The chemical compositions of particles generated from the MART microcosm experiments were compared to ambient data collected at Bodega Bay, CA (Bodega Marine Laboratory, 38° 18′ 13″ N, 123° 03′ 52″ W). A period during which clean marine air arrived at the coastal sampling site from the oceanic northwestern sector with minimal contributions from anthropogenic sources verified by particle chemical analysis by ATOFMS (March 17, 2015, 10:00 to 21:00; wind from 313° ± 6°, 12.3 ± 1.7 m s^{-1}) was used for comparison with SSA particles generated from natural seawater in a MART prior to addition of any nutrients. The surface ocean surrounding Bodega Bay had elevated biological activity during the time of sampling (~2 mg m^{-3} in Chl-a concentration observed from MODIS, Figure 2.9). Ambient particles were sampled in real time and were chemically classified based on their dual-polarity mass spectra using criteria previously established [*Prather et al., 2013*] and described below. MART tank D was chosen for this intercomparison due to the similarity of Chl-a concentrations (~2 mg m^{-3}) with those during the study at Bodega Bay.

Real-time measurements of single SSA particle chemical composition using ATOFMS have revealed a number of particle types enriched in organic components [*Gaston et al., 2011*; *Guasco et al., 2014*; *Prather et al., 2013*]. Figure 2.10 shows the representative mass spectra of three distinct types of SSA particles observed in these experiments. Three main classifications of SSA particles were determined: sea salt (SS), sea salt mixed with organic carbon (SS-OC), and a biological type consisting of Mg^{2+} coupled with organic-nitrogen species (Biological), consistent with the SSA types reported previously [*Gaston et al., 2011*; *Prather et al., 2013*]. The SS type consists of particles containing dominant ion markers for sodium and chloride ($^{23}Na^+$ and $^{35,37}Cl^-$) with sodium chloride ion clusters observed at $^{81,83}Na_2Cl^+$ and $^{93,95,97}NaCl_2^-$ and a minor signal from $^{24}Mg^+$ and $^{39}K^+$. The SS-OC type closely resembled the signature of the SS type but with elevated signal from $^{24}Mg^+$, $^{39}K^+$, $^{26}CN^-$, and $^{42}CNO^-$ with a minor contribution from $^{79}PO_3^-$. Biological-type spectra were dominated by $^{24}Mg^+$ ion signal with contributions from $^{39}K^+$, $^{129,131,133}MgCl_3^-$, $^{35,37}Cl^-$, $^{26}CN^-$, $^{42}CNO^-$ and $^{79}PO_3^-$. A detailed analysis of the SS-OC and biological particle types, abundances, and association with the composition of the seawater will be described in a separate manuscript.

During the clean marine period, a small fraction (~11%) of the particles sampled at Bodega Bay showed signs of atmospheric chemical processing due to the presence of nitrate ion markers ($^{46}NO_2^-$, $^{62}NO_3^-$) [*Gard et al., 1998*], where during other periods, fractions of atmospherically aged particles ranged from 20 to 80%. The fractions of SS-OC and Biological particles compared to SS from the clean marine period ambient measurements were similar to those produced in the MART experiments for the size range measured by the ATOFMS (0.2 to 3.0 μm D_{va}). The ambient particle fraction of both laboratory and field studies examining marine systems show a large SS dominance, followed by Biological and SS-OC-type particles (Figure 2.2). The variations can be attributed to the difference in ocean conditions and organic

concentrations in the bulk seawater and the SSML, as the organic enrichment in SSA particles depends on the state of biological cycle as discussed below. Despite differences in seawater conditions, the MART microcosm showed remarkable similarity in particle types and mixing state to those observed in ambient air at a coastal site during onshore flow. SSA particles greater than 1 μm in diameter (D_p) are sensitive to secondary processing such as heterogeneous chemistry due to large surface area to unit volume available [*Abbatt et al., 2012*; *Kolb et al., 2010*].

As ATOFMS is sensitive in distinguishing the extent of atmospheric processing in the size that would have the significant impact (1-3 μm D_p), the generation of SSA from natural unconstrained seawater using a realistic particle production mechanism in the isolated MART system overall replicates primary SSA particles observed in the atmosphere. Isolating natural SSA produced using the proper physical and biological mechanisms will allow controlled laboratory studies of the heterogeneous reaction of natural sea spray particles without competing effects from anthropogenic sources.

2.4.2 Simulating the Biological Chemical Engine in the Marine Aerosol Reference Tank

Six phytoplankton microcosm experiments were conducted to determine the reproducibility and natural variability in the seawater and SSA composition using this approach. Despite the unconstrained starting conditions of each experiment, *in vivo* Chl-a measurements showed that the phytoplankton blooms had similar temporal behavior. Figure 2.11 shows a compilation of Chl-a concentration measurements normalized to each respective maximum Chl-a concentration. In these microcosm experiments, peak Chl-a concentrations ranging from 25 to 59 mg m^{-3} were achieved using f/2 and f/20 nutrient concentrations, thus providing a range of Chl-a concentrations for the systematic study of seawater bio-geochemistry on SSA (Figure 2.11). Typical phytoplankton blooms in the oceans have been observed from ~1 to 70 mg m^{-3} Chl-a

[*Cloern, 1996*; "NASA Earth Observations Chlorophyll Concentration (Aqua/Modis)," *2014*, "National Oceanic and Atmospheric Administration, U.S.D.o.C. Ocean," *2014*; *Sullivan et al., 1993*; *Yoder et al., 1993*]. Although the observed peak Chl-a concentrations from the microcosms were within the range of observed oceanic phytoplankton blooms ["NASA Earth Observations Chlorophyll Concentration (Aqua/Modis)," *2014*], having this higher level of biological activity will lead to larger more easily measured changes in SSA composition. Overall, studies on SSA produced from MART microcosms will be useful for understanding how changes in SSA composition affects SSA particle properties such as water uptake and heterogeneous chemistry ["NASA Earth Observations Chlorophyll Concentration (Aqua/Modis)," *2014*].

Phytoplankton bloom microcosms generated in the MART showed similar trends in behavior with blooms starting within 5 d, peaking within 7 to 11 d, and senescence occurring within 12 to 15 d after media addition (Figure 2.3). The differences in bloom peak behaviors are likely due to differences in growth rates of different phytoplankton species [*Gilstad and Sakshaug, 1990*; *Mura and Agusti, 1996*; *Tang, 1995*]. The range of biological conditions provides the opportunity to probe how changes in the chemical composition of seawater lead to changes in SSA composition, reactivity, and climate properties. These results will inform the assumptions required by global climate models regarding the size and single particle mixing state of nascent SSA particles [*De Leeuw et al., 2011*; *Prather et al., 2013*]. In these microcosm experiments, the growth and subsequent death of the phytoplankton population resulted in changes in the concentration (Figure 2.4) and chemical composition (Figure 2.5A-C) of DOM. This change in the DOM content of seawater induced by the phytoplankton bloom created an environment that sustained the growth of marine bacteria and viruses occurring with or after the phytoplankton peak (Figures 2.1B and 2.6). Figure 2.1B provides an example of one microcosm experiment illustrating the dynamic nature of the three classes of marine microbes, consistent with prior

marine microbiological studies [*Azam et al., 1994*; *Azam and Malfatti, 2007*; *Pomeroy et al., 2007*]. The high concentrations of bacteria and marine viruses further alter the chemical composition of the natural organic matter through enzymatic, metabolic, and infectious processes [*Azam and Malfatti, 2007*; *Hans Peter Grossart et al., 2006*; *Grossart and Ploug, 2001*; *Pomeroy et al., 2007*; *Smith et al., 1992, 1995*]. Deviating from the conventional method of adding known compounds to synthesize a complex chemical system, the method described in this study, utilizing marine microbiology to induce realistic chemical changes in the seawater, can lead toward a better understanding of the properties and reactivity of realistic atmosphere SSA particles.

The abundances of bacteria and viruses showed distinct temporal trends in the bulk, SSML, and SSA compartments (Figure 2.6). The abundances of bacteria ($\sim 1 \times 10^{9}$ L^{-1}) and viruses ($\sim 1 \times 10^{10}$ L^{-1}) were comparable to the ranges observed in the ocean before the phytoplankton bloom [*Azam and Malfatti, 2007*] as ambient seawater used to begin the microcosms, and the abundances of bacteria ($\sim 1 \times 10^{9}$ to 1×10^{10} L^{-1}) and viruses ($\sim 1 \times 10^{10}$ to 1×10^{11} L^{-1}) observed throughout the microcosm were also comparable to the abundances observed during oceanic bloom conditions ($\sim 1 \times 10^{10}$ L^{-1} and $\sim 1 \times 10^{11}$ to 1×10^{12} L^{-1}) [*Bird and Kalff, 1984*; *Riemann et al., 2000*; *Suttle, 2005*]. Transfer of microbial species from the seawater to the aerosol phase has been previously quantified in the field [*Aller et al., 2005*; *Dueker and O'Mullan, 2014*] and is of great interest to the community as biological particles can lead to heterogeneous nucleation of ice crystals in the atmosphere [*Aller et al., 2005*; *Burrows et al., 2013*; *Després et al., 2012*; *Schnell and Vali, 1976*; *Vali et al., 1976*; *Wolber, 1993*] and influence cloud properties [*Sun and Ariya, 2006*]. Detailed investigations into the source and nature of ice nucleating particles by quantifying the transfer and abundance of microorganisms in bulk seawater, SSML,

and SSA particles during changing seawater biological and chemical concentrations and compositions from microcosms will be presented in future publications.

2.4.3 Effect in Chemical Complexity of Seawater from Phytoplankton Blooms

Scheme 2.1 shows how phytoplankton, heterotrophic bacteria, and viruses contribute to and process the organics in the DOC pool of the ocean. The typical DOC concentration in the euphotic zone of the ocean is ~80 μM C [*Aristegui, 2002*; *DeLong, 2006*; *McCarthy, 1998*] with some observations as high as 250 μM in actively blooming regions [*Kirchman et al., 1995*; *Norrman et al., 1995*]. The maximum DOC concentration observed in MART microcosms with f/20 and f/2 nutrient concentration were ~185 μM C and 325 μM C, respectively (Figure 2.4). Note that elevated DOC concentrations immediately after nutrient addition prior to phytoplankton bloom in each experiment is an artifact of the addition of growth media, which contain ~12 μM of organic material ($Na_2EDTA \cdot 2H_2O$, vitamins B1, B12, and H, listed in Table 2.2) for MART microcosms with f/2 concentration of media. The DOC concentrations up to 325 μM C are above observed oceanic surface seawater conditions (typically 80 μM C) [*Aristegui, 2002*; *DeLong, 2006*; *McCarthy, 1998*]. The majority of the increase in the DOC concentration (175-200 μM C) is due to the media addition, where control studies of the SSA chemical composition using ATOFMS revealed small fraction (~10%) of particles indicative of media appearing post addition and were not included in the analysis. Thus, despite the initial increase in DOC concentration that remained elevated during the microcosms with high concentration of media, the change observed in the chemistry of the SSA particles reflects the changes in the seawater from microorganisms process. Primary production of organics by photosynthetic organisms caused the concentration of DOC to increase by ~40-80 μM C reaching maxima during or after the bloom of phytoplankton (Figure 2.4), with the eventual decrease observed in the f/20 microcosm experiments likely a result of heterotrophic bacterial assimilation and degradation, along with flocculation and

sedimentation. Larger increases in DOC concentration were observed for the microcosms initiated with higher nutrient concentrations due to the greater abundance of the phytoplankton.

To characterize the evolution of DOM over the course of the microcosm due to the marine microbiology, fluorescence EEM measurements of the bulk seawater were performed. The fluorescent regions indicative of humic-like (excitation/ emission ranges: 360/445-460 nm, 260/425-475 nm, and 320/400-420 nm) and protein-like (excitation/emission ranges: 275/300 and 340 nm) organic material [*Coble, 1996*] increased as the phytoplankton bloom progressed, divided into three time periods: before the growth of phytoplankton (pre-peak), during the bloom (peak), and after phytoplankton senescence (post-peak; Figure 2.5A-C). Most of the sources of fluorescent dissolved organic matter (FDOM) in marine systems are assumed to be derived from biological processes [*Jaffé et al., 2008*; *Maie et al., 2006*] such as byproducts of bacterial metabolism [*Nieto-Cid et al., 2006*; *Shimotori et al., 2010*; *Yamashita and Tanoue, 2008*]. This assumption correlates well with the EEM results detailed above. The fluorescent species detected in the bulk seawater were concentrated in the SSML (Figure 2.5D and E) likely through scavenging of surface active compounds by bubbles rising through the water column [*Blanchard, 1975*; *Keene et al., 2007*]. The bulk seawater has been observed in the literature to contain organic compounds such as carbohydrates, lipopolysaccharides, proteins, and lipids [*Aller et al., 2005*; *Carlson, 1983*; *D. Hessen and Tranvik, 1998*]. The scavenging by bubbles likely led to enrichment of these organics at the SSML [*Aller et al., 2005*; *Carlson, 1983*; *Cunliffe et al., 2011*; *D. Hessen and Tranvik, 1998*] and thus in SSA particles [*Collins et al., 2014*; *Lewis and Schwartz, 2004*; *Prather et al., 2013*] in the microcosm experiments. The isolated enclosed nature of the MART system and the plunging waterfall mechanism renews the surface between plunging waterfalls and mixes the seawater very well. However, in the enclosed area of the surface seawater in the MART, surface active compounds could build to higher concentrations than in the

open ocean and thus have more pronounced changes in SSA physical and chemical composition than would occur in under similar biological conditions in the marine environment. However, while the high phytoplankton density reliably obtained in the microcosm experiments led to greater concentrations of oceanic relevant organic content than typical marine bloom conditions [*Vali et al., 1976*; *Wolber, 1993*], the microcosms provided easily measurable links between seawater biological activity and SSA composition. In future studies, microcosms with more oceanic relevant level of biological activity that mimic the ocean will be examined.

2.4.4 Changes in Chemical Composition of Sea Spray Aerosol over the Microcosm

The chemical composition of SSA particles sampled using ATOFMS were divided into three time periods discussed previously for a typical microcosm experiment (Tank E from Figure 2.3, for example). Period 1 corresponds to ATOFMS measurements from the pre-peak (day 0) conditions. Periods 2 and 3 average ATOFMS measurements corresponding to the phytoplankton bloom peak (days 9-12) and post-peak (13-22), respectively. Inorganic particles become enriched with biogenically derived organics over the course of the microcosm, which can be traced by ion markers such as $^{26}CN^-$, $^{42}CNO^-$, $^{43}CHNO^+/C_3H_2O^+$, and $^{77}C_6H_5$+. The top panel of Figure 2.7 shows relative intensities of organic ion markers to total ion intensities in the inorganic salt particles from the three designated periods, illustrating the significant organic enrichment observed after the peak of phytoplankton. Increases in the intensities of organic markers were coincident with an increase of seawater DOC concentration as the microcosm experiment progressed. While a previous study has observed a time lag between Chl-a concentrations from satellite measurements and organic matter enrichment in ambient marine aerosol [*Rinaldi et al., 2013*], this study illustrates that the increases in the organic enrichment of SSA particles started to occur during the phytoplankton bloom (period 2) and become most significant after the peak in phytoplankton (period 3; Figure 2.7). The relationship between the dynamics of organic species in seawater and SSA mixing state will be discussed in future publications.

In addition to online measurements of SSA composition, off-line SEM measurements were performed of SSA particles with aerodynamic diameters between 0.56 and 1.0 μm collected using a MOUDI sampler. Prior to the phytoplankton bloom (pre-peak, period 1 in Figure 2.7), SSA particles with a strong sodium chloride signal measured by ATOFMS showed small intensities of biogenically derived organic markers. Corresponding microscopy measurements show that the morphology of the SSA particles in this size range were cubic, indicative of salt particles with low organic and water content (Figure 2.7A). As the bloom progressed to the peak (peak, period 2 in Figure 2.7), the intensities of organic markers in spectra from SSA started to increase, and a residue around the cubic salts started to appear, which has been previously observed to be organic in nature (Figure 2.7B and C) [*Ault et al., 2013b*; *Prather et al., 2013*]. During phytoplankton senescence (post-peak, period 3 in Figure 2.7), the organic residue around the salt core became one of the dominant features in the microscopic analysis of SSA particles, corresponding to a significant increase in the intensities of the organic markers in the ATOFMS generated spectra. These results demonstrate that the approach described herein is capable of producing the chemical complexity of SSA particles whose composition varies in response to microcosm conditions. By varying microcosm conditions, it is possible to perform fundamental molecular-level studies of the heterogeneous reactivity of trace gases with aerosol particles [*McNeill et al., 2006*; *You et al., 2014*]. By utilizing an aerosol flow tube reactor, the reactivity of SSA particles mixed with the complex combination of organic species produced by the microcosms will be compared to typical surfactant mimics such as sodium dodecyl sulfate [*Abbatt et al., 2012*; *Finlayson-Pitts, 2009*; *Krueger et al., 2003*] in future publications.

Spectroscopic measurements of organic material in the bulk, SSML, and SSA particles were made to examine the selective partitioning of organic material (i.e., humic and protein-like substances) from the bulk seawater to the SSML and subsequent organic enrichment in SSA

particles. EEM spectroscopic measurements of the bulk seawater, SSML, and the SSA particles post-peak of the phytoplankton bloom (Figure 2.5D-F, respectively) show that the organic species synthesized in the water such as protein-like substances are enriched at the SSML as well as the SSA particles. A more detailed examination of the temporal trends and the transfer of the organic species will be presented in the future.

The microcosm studies showed a clear lag between Chl-a and organic enrichment in SSA particles, peaking after the phytoplankton (period 3). The overall trend of the organic enrichment of SSA particles occurring after the peak in phytoplankton proves that the biological processes must be considered to understand the organic enrichment in the SSA. This demonstrates the ability to recreate the complex biological conditions observed in the real world in a lab setting. The ability to replicate the chemical and biological complexity of seawater in the isolated laboratory setting will allow for more detailed physicochemical investigations of the mechanism by which organic material is enriched in SSA particles, which can further guide future marine field studies and global models.

To probe the heterogeneous reactivities of SSA particles with gas-phase pollutants such as nitric acid [*Ault et al., 2013a; Ault et al., 2014*], it is crucial to simulate the surface composition of such particles in the laboratory. The interfacial composition strongly depends on properly producing the seawater biological processes as well as physical production mechanisms as demonstrated in this study. The most critical step involves producing the proper bubble size distributions as these will selectively scavenge organic species from the water column [*Blanchard, 1975*] and ultimately break at the sea surface, producing a very specific surface composition, which will control particle reactivity.

2.5 Conclusions

Here we describe a method for producing realistic SSA particles in the laboratory through the natural synthesis and subsequent chemical processing of organic compounds by marine microorganisms. This study demonstrates that the particles generated in the MART are similar to ambient particles measured during onshore flow at a coastal sampling site in the size range sampled by ATOFMS (0.2 to 3.0 μm).

Adapting a MART system as a photobioreactor allows one to form a vast array of organic species such as those occurring in the ocean to study the influence on SSA physicochemical properties. With unconstrained starting conditions, the temporal behavior of the experiments showed a reasonable level of variability with blooms starting within 5 d, peaking within 7-11 d, and becoming senescent within 12-15 d of media addition. The variance in the peaks in Chl-a concentrations that serve as a metric for phytoplankton biomass are likely due to different growth rates of phytoplankton species and nutrient concentrations. Quantitative measurements of cell counts using epifluorescence microscopy throughout the microcosm illustrate that the concentrations of heterotrophic bacteria and viruses are dynamic, increasing after the peak of phytoplankton in the bulk, SSML, and aerosol phase with distinct temporal behavior in the three compartments. EEM spectroscopic measurements during the period of phytoplankton senescence in a microcosm showed that the SSA organic composition was similar to the SSML, which was enriched in biological material, that is, protein-like substances, relative to the concentrations in the bulk. It is crucial to further understand the partitioning and transfer of biogenic particles and organic matter to the atmosphere as they modify physicochemical processes of SSA such as heterogeneous reactivity and affect climate-relevant processes such as ice nucleation and cloud formation.

The overall concentration and spectroscopic analysis of the DOC present in bulk seawater illustrate that the seawater became more chemically complex as the humic and protein-like species in FDOM and the DOC concentrations increased over the course of the microcosm experiments. The increase in FDOM and the overall DOC concentration in seawater are in good agreement with the assumption that the source of these organics are from biological processes. As the microcosm progressed, the SSA particles became enriched with organic species as observed from the increase in intensities of biogenically derived organic markers in ATOFMS measurements. In addition to the organic enrichment observed through mass spectrometry, the amount of residue indicative of organic material around the inorganic core of SSA particles increased as the bloom progressed. Specifically, the time lag in which the SSA particles showed a maximum in organic enrichment was observed to be between 4 and 10 d (between periods 2 and 3). The impact of this enrichment on particle properties and heterogeneous reactivity will be shown in future publications.

The approach developed in this study provides for more detailed physicochemical investigations of the mechanisms by which the chemical composition of SSA properties becomes changed above the surface of the ocean. Further, this new approach replicates the chemical complexity of SSA particles, producing a representative blend of inorganic and organic molecules in the particles that will control interfacial processes such as heterogeneous chemical reactions, water uptake, light scattering, and cloud properties of SSA.

2.6 Acknowledgements

The authors would like to thank R. Pomeroy, T. Bertram, O. Laskina, and all the collaborators involved. The authors would also like to acknowledge Bodega Marine Reserve, University of California Davis and UC Natural Reserve System. This study was funded by the

Center for Aerosol Impacts on Climate and Environment (CAICE), an NSF Center for Chemical Innovation (CHE-1305427) and through support from an endowment for the Distinguished Chair in Atmospheric Chemistry at the Univ. of California, San Diego.

Chapter 2 is reproduced with permission from the American Chemical Society: Lee, C., Sultana, C.M., Collins, D.B., Santander, M.V., Axson, J.L., Malfatti, F., Cornwell, G.C., Grandquist, J.R., Deane, G.B., Stokes, M.D., Azam, F., Grassian V.H., Prather, K.A. Advancing Model Systems for Fundamental Laboratory Studies of Sea Spray Aerosol using the Microbial Loop, Journal of Physical Chemistry, A, 119 (33), 8860-8870, 2015. The dissertation author was the primary investigator and author of this paper.

2.7 Figures

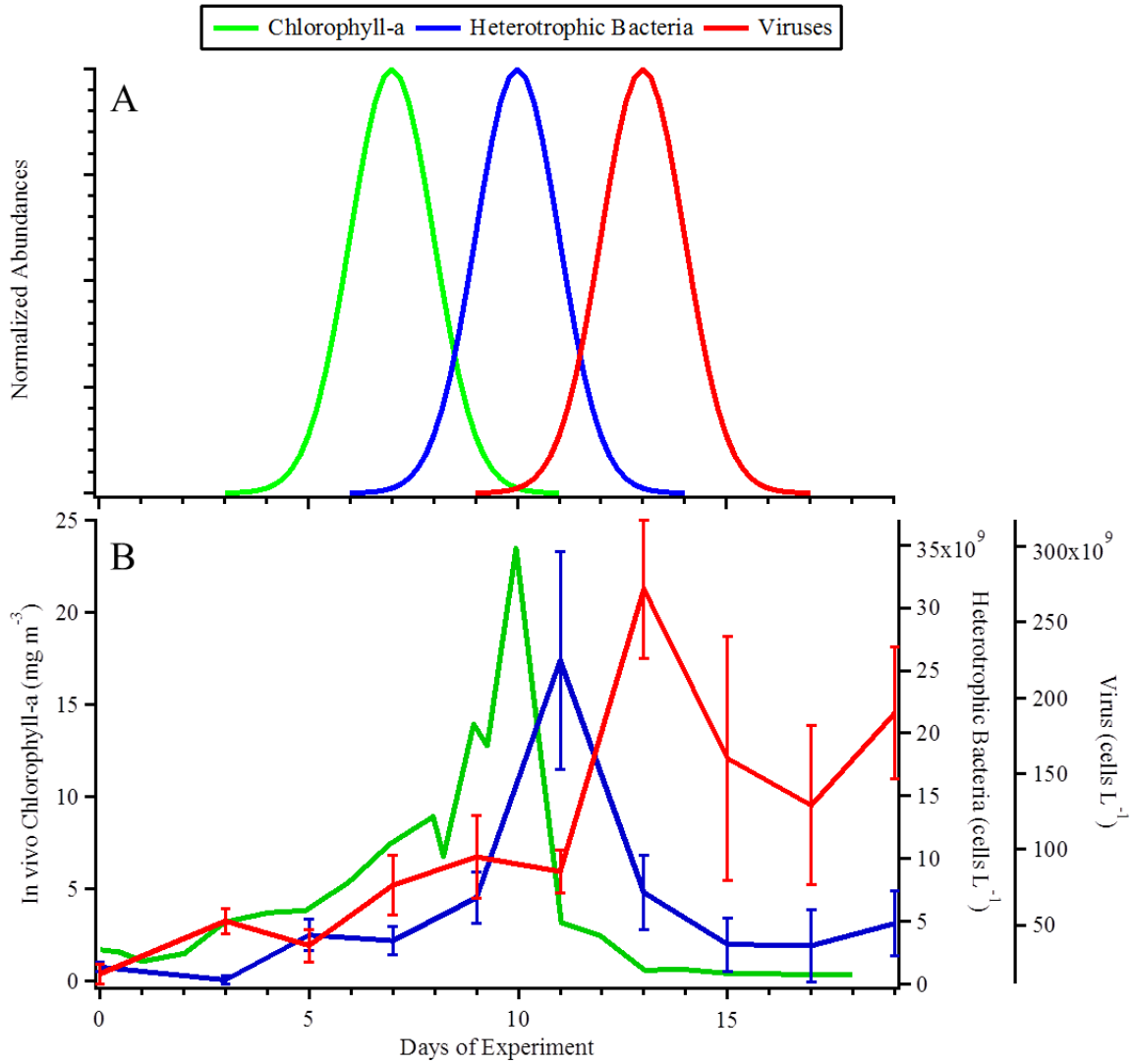

Figure 2.1. Evolution of phytoplankton as chlorophyll-a, heterotrophic bacteria, and virus concentrations for an idealized microcosm (panel A) vs data (panel B) from a representative experiment (data from Tank B).

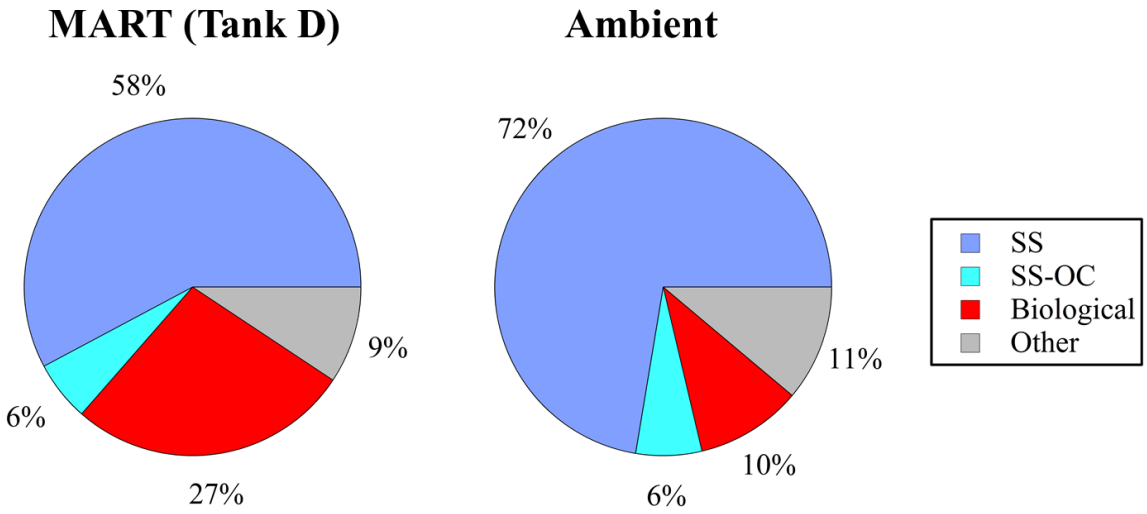

Figure 2.2. Comparison of particle-type fractions observed in a MART microcosm (left) and ambient marine aerosols during a clean atmospheric period at Bodega Bay, CA. MART measurements were made prior to media addition. On the basis of individual particle composition, particles are categorized into sea salt (SS), sea salt-organic carbon (SS-OC), biological, and other.

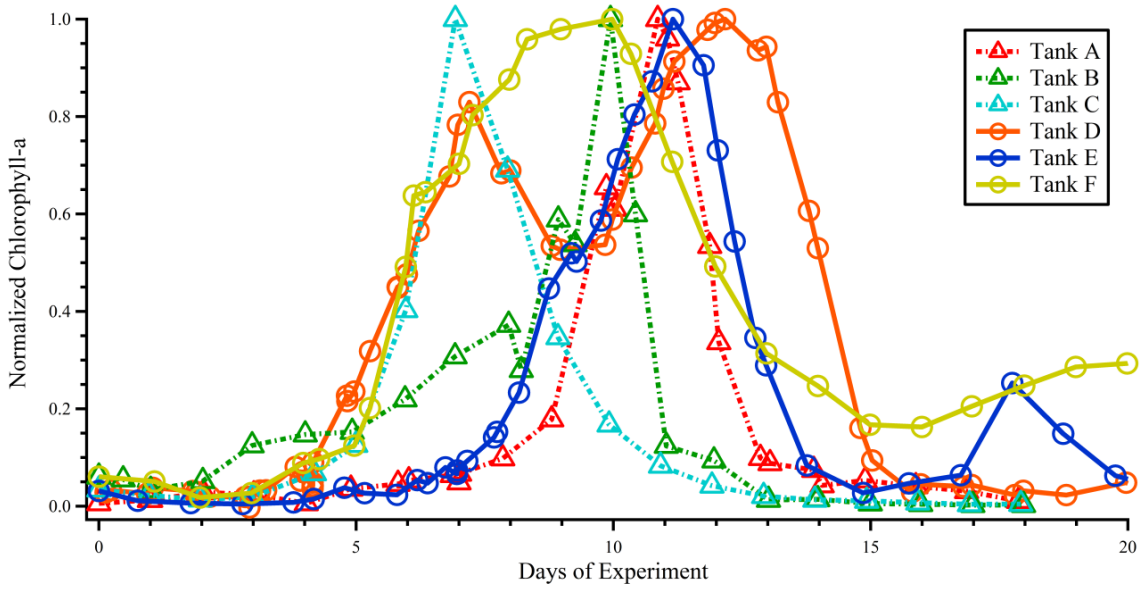

Figure 2.3. Compilation of normalized chlorophyll-a concentrations for the MART microcosm experiments. Despite starting with natural seawater, progression of chlorophyll-a, an indicator of phytoplankton biomass, behaves similarly. Dashed lines with ∆ markers and solid lines with ○ markers denote tanks with lower and higher concentration of nutrients added, respectively.

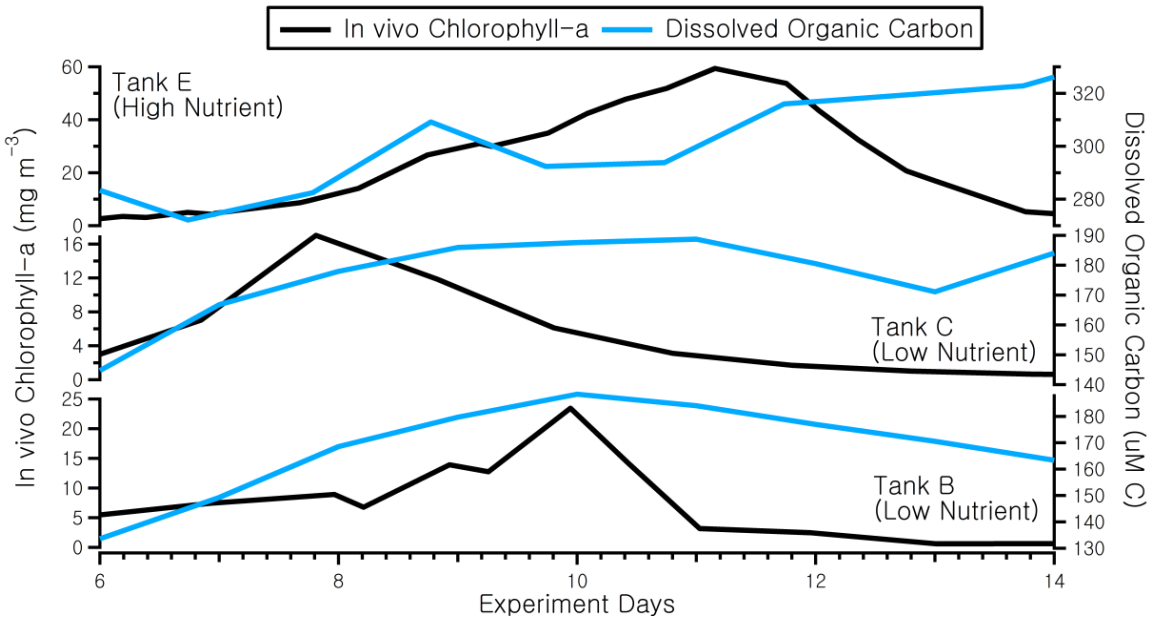

Figure 2.4. Changes in concentration of DOC over the course of a microcosm experiment with a high concentration of media added (f/2) (Tank E, upper), and a low concentration of media added (f/20) (Tank C and B, center and lower, respectively).

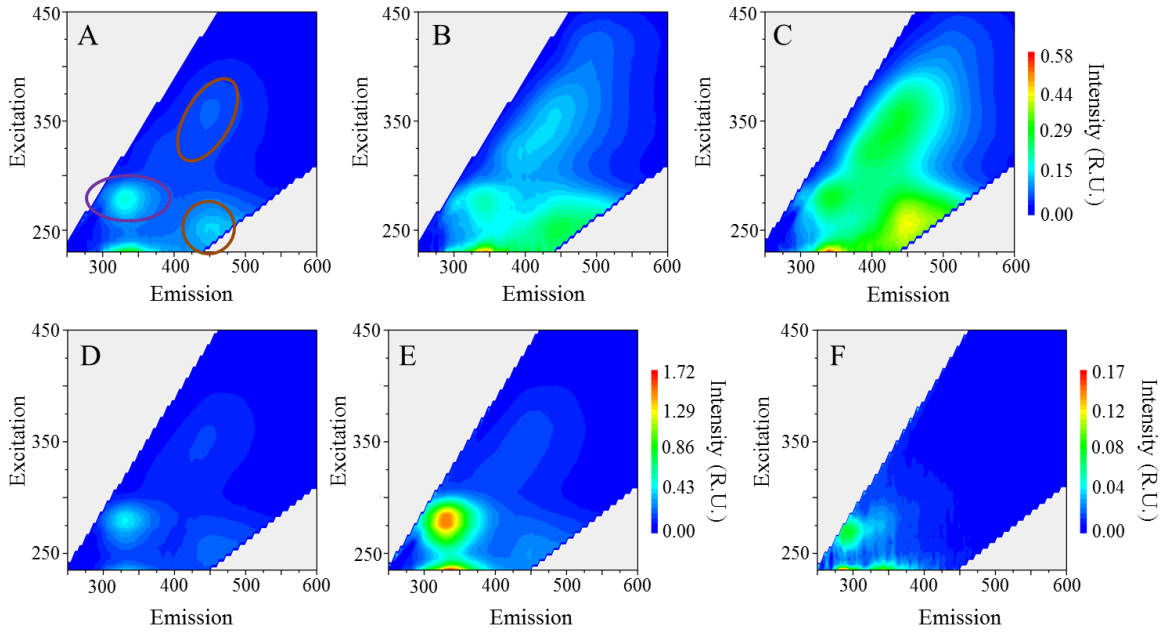

Figure 2.5. EEM spectroscopic measurement of bulk seawater at prebloom (panel A, Day 4), bloom peak (panel B, Day 11), and post-peak (panel C, Day 22) of chlorophyll-a for Tank E. Panels D, E, and F show the EEM measurements of bulk seawater, SSML, and aerosol phase post-peak (Day 22) for Tank E. EEMs in panel C and D are of the same sample, but on different scales to highlight the enhancement in panel E from D. Humic-like substances are present at excitation/emission ranges of 360/445−460 nm, 260/425−475 nm, and 320/400−420 nm (shown in brown circles in panel A). Protein-like substances are present at 275/340 nm and 275/300 nm (region shown in purple circle in panel A).

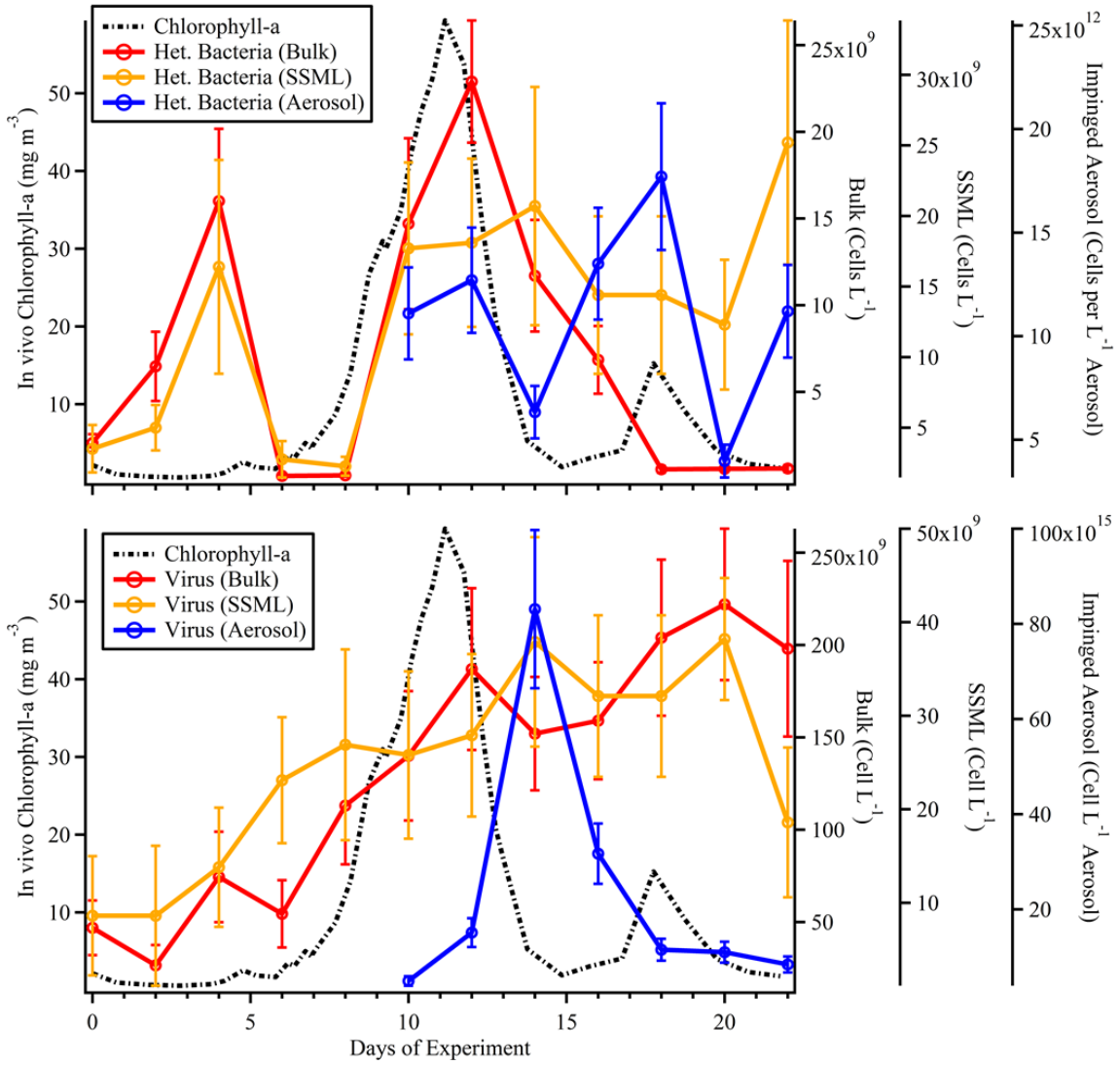

Figure 2.6. Epifluorescence microscopy counts of heterotrophic bacteria (upper) and virus (lower) in the bulk (red), SSML (orange), and aerosols (blue) from an example microcosm experiment (Tank E).

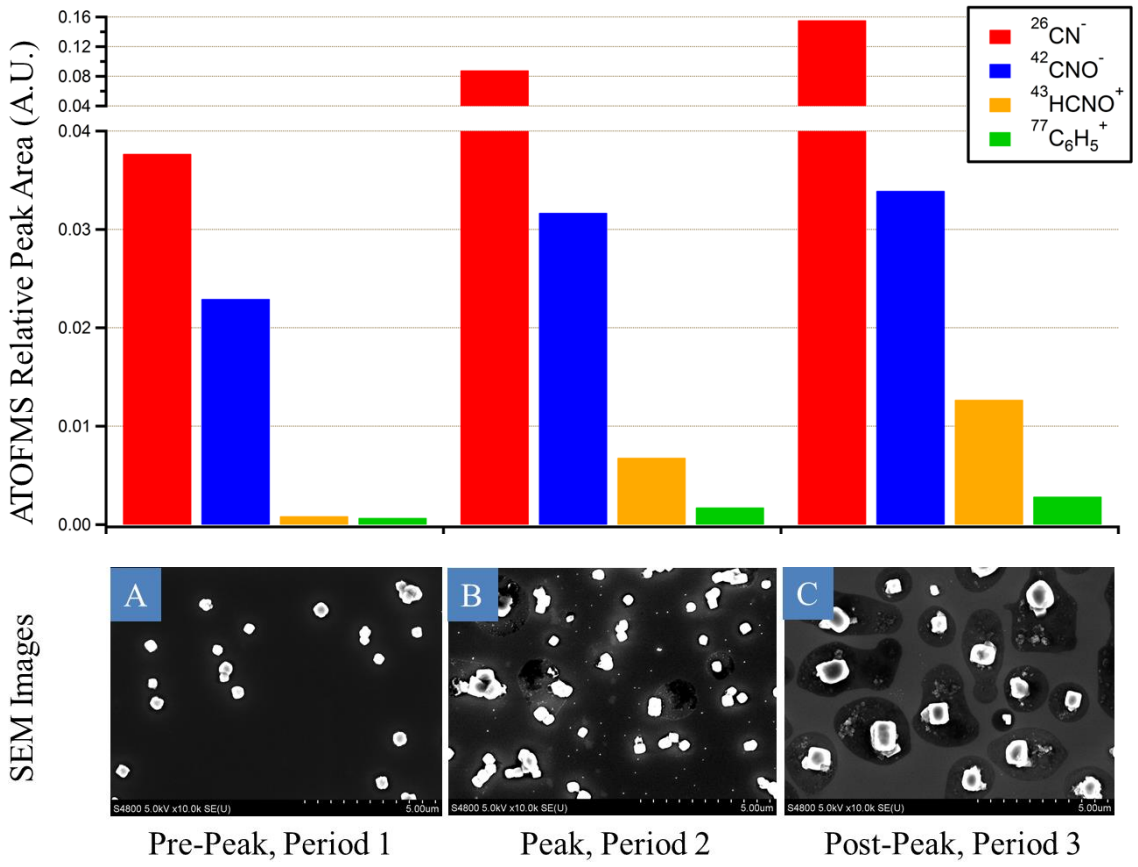

Figure 2.7. (upper) Average ATOFMS relative peak area to total area intensities of select organic ion markers in inorganic salt particles from the phytoplankton bloom during the pre-peak (growth, day 0, period 1), peak (days 9−12, period 2), and post-peak (death, days 13−22, period 3) periods of the Tank E microcosm. (lower) SEM images of SSA particles (0.56 to 1.0 μm aerodynamic diameter) observed for pre-peak (day 0, panel A), peak (day 11, panel B), and post-peak (day 28, panel C) bloom periods.

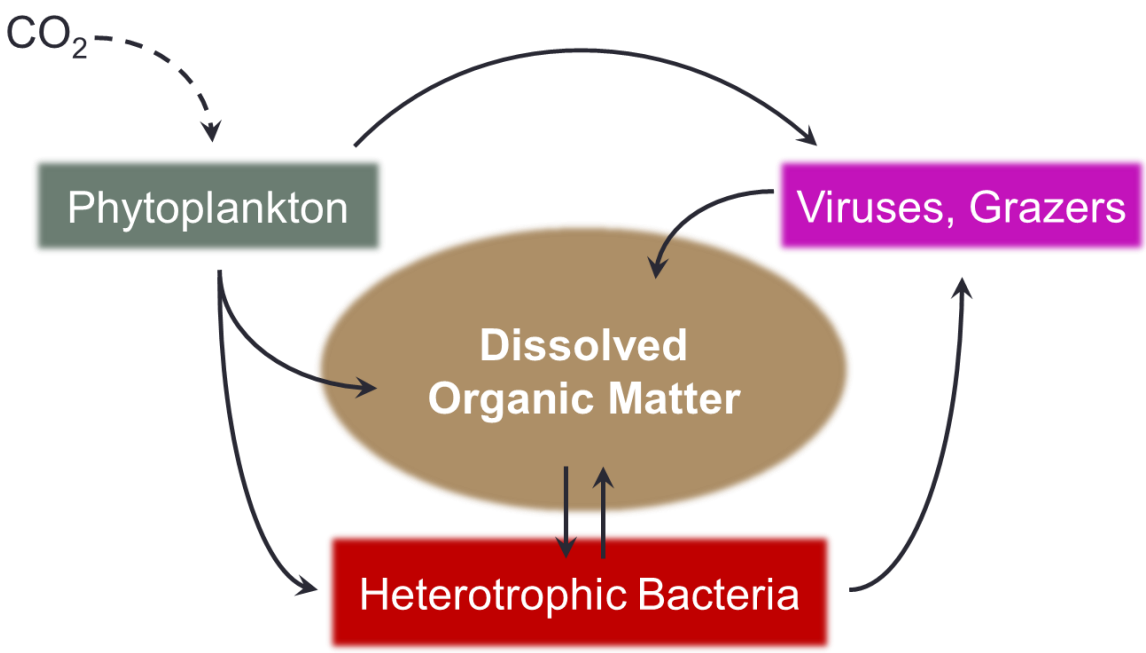

Figure 2.8. Simplified schematic of the microbial loop showing the relationship between marine microorganisms and dissolved organic matter.

2.8 Supporting Information

MART photobioreactor microcosm method

The Southern California Coastal Ocean Observing System (www.sccoos.org), a seawater monitoring system off the coast of southern California, was used to monitor ocean conditions. When ocean condition parameters such as salinity, sea surface temperature, and Chl-a concentration were within the location's monthly mean values, seawater was collected using a cleaned bucket tied to a hoist at the end of Scripps Pier (275 m offshore) located in Scripps Institution of Oceanography, University of California, San Diego. Seawater was filtered using 50 µm Nitex mesh prior to filling the MART. The 50 µm filtration removed any grazers that feed on phytoplankton without altering other microbial species. Fresh seawater was added to a MART

system that had been previously cleaned with ethanol or isopropanol and triple rinsed with deionized water.

Once the MART was filled, control measurements utilizing the freshly collected seawater were performed, after which nutrients were added to the desired concentration. Another set of control measurements were performed immediately after nutrient addition to account for the change in seawater chemical composition due to the growth media. It was found empirically that longer periods of aerosol generation led to insignificant phytoplankton growth, likely due to phytoplankton cell damage in the centrifugal pump used to circulate water through the plunging waterfall aerosol generation apparatus.[1] Phytoplankton growth was initiated by illuminating the nutrient-doped seawater with two full spectrum fluorescent lamps (5700 K blackbody temperature; Full Spectrum Solutions, 205457). During this initial growth period, water was mixed and aerated by gently bubbling the sample by forcing particle-free air at 1 liter per minute through 4-6 Tygon tubes (1/8 inch inside diameter) that were held on the bottom of the MART by glass weights.

Once sufficient phytoplankton cell density was reached, determined empirically to be approximately 12 mg chlorophyll m^{-3}, the bubbler system was removed and the MART was sealed. The headspace of the MART was then purged with particle-free air. With the MART purged of background particles, verified with a Condensation Particle Counter (TSI 3010), the aerosol measurements were performed as described in the methods section. Aerosols were generated with a two hours on, two hours off schedule. During aerosol generation, the waterfall was operated with a 4 seconds on and 4 seconds off duty cycle to simulate the episodic nature of natural breaking waves [*Callaghan et al., 2012*; *Collins et al., 2014*; *Stokes et al., 2013*]. ATOFMS measurements were performed daily until at least one week past the return of Chl-a concentrations to that of the freshly collected seawater, in order to capture chemical changes due

to the biochemical processes associated with marine bacteria and viruses. Each microcosm experiment lasted about 24 to 28 days total.

In vivo Chl-a measurements were made at least once daily, and samples of the bulk seawater for DOC, EEM measurements, and epifluorescence microscopy cell counts were taken once daily. Samples for EEM analysis were analyzed the day of sampling. EEM excitation and emission wavelengths ranged from 235-450 nm and 213-620 nm, respectively. EEM spectra were blank subtracted using ultrapure water. Spectra were also corrected for inner-filter effects and Rayleigh scatter masked (1^{st} and 2^{nd} order). To calibrate the EEM measurements, each spectrum was normalized to the area of the water Raman scatter peak at 350 nm taken daily and are reported in Raman Units (R.U.) [*Lawaetz and Stedmon, 2009*; *Murphy, 2011*]. Bulk seawater samples for epifluorescence microscopy were taken daily, but SSML and SSA particle samples for epifluorescence microscopy were taken every two days. Fluorescence microscopy samples were pipetted into sterile cryogenic vials and preserved with glutaraldehyde (0.05% electron microscopy grade). After an incubation period of 15 minutes at approximately 4 ºC, samples were flash frozen with liquid nitrogen and kept at -80 ºC until analysis.

2.8.1 Supporting Information Figures

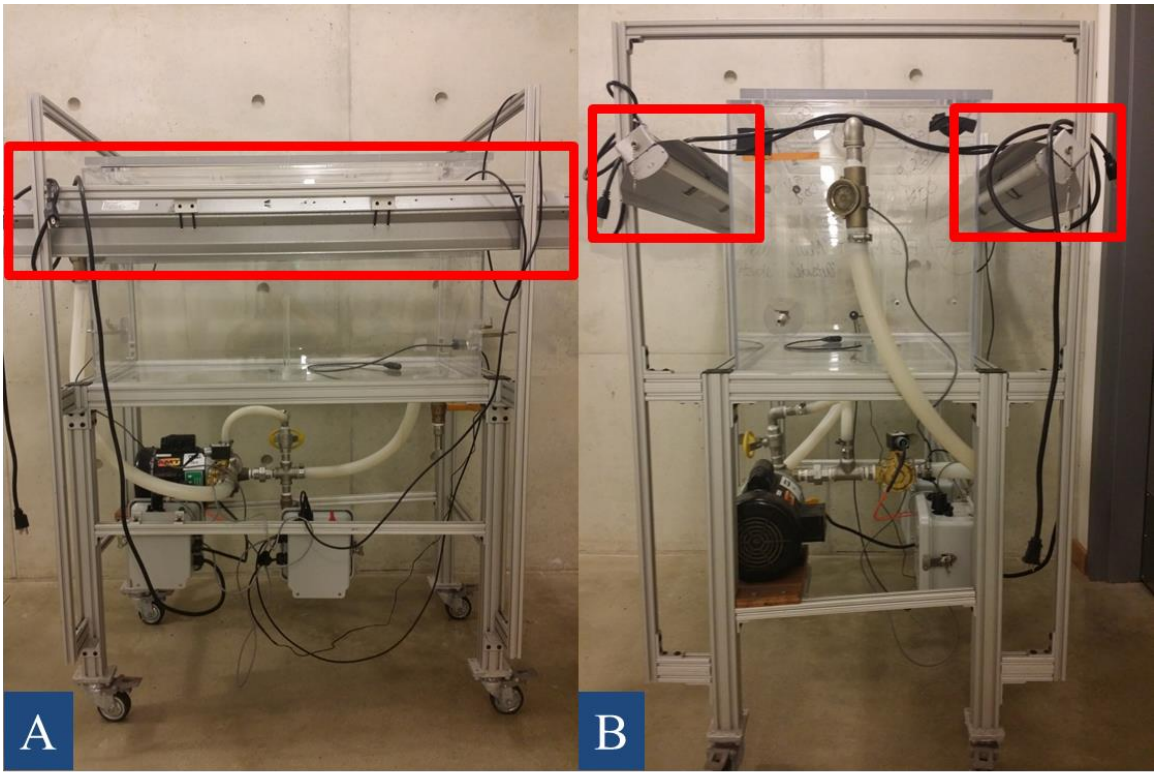

Figure 2.9. Picture of modified MART photobioreactor. Highlighted boxes are two fluorescent glow light fixtures that provide necessary illumination for growth of autotrophic microorganisms. A. front view and B. side view.

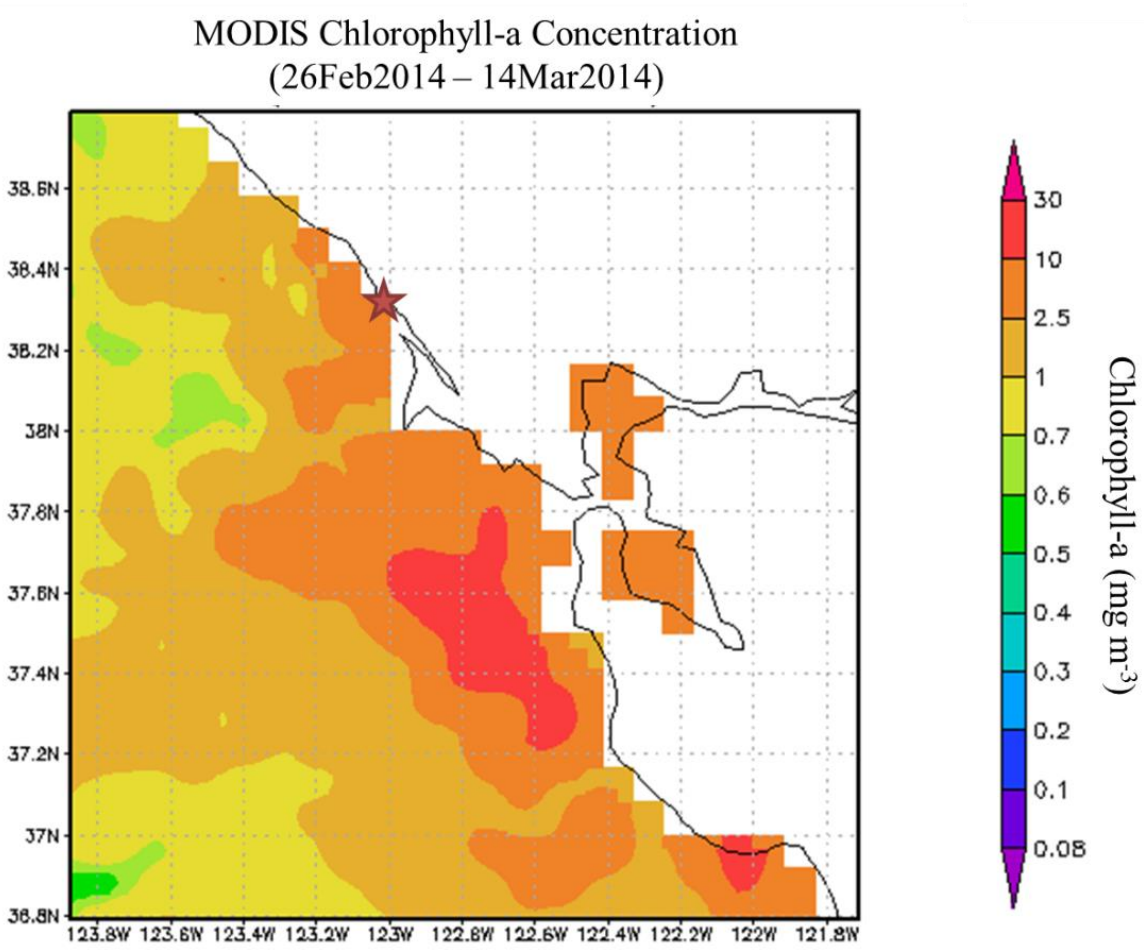

Figure 2.10. Satellite-derived ocean surface chlorophyll-a concentration (MODIS) in the vicinity of Bodega Bay, CA (red star). Chlorophyll-a concentration near the sampling location is ~ 2 mg m^{-3}. Wind direction and velocity measured at the time of sampling (313 ± 6 degrees 12.3 ± 1.7 m s^{-1}) suggest the air sampled is of primarily marine origin.

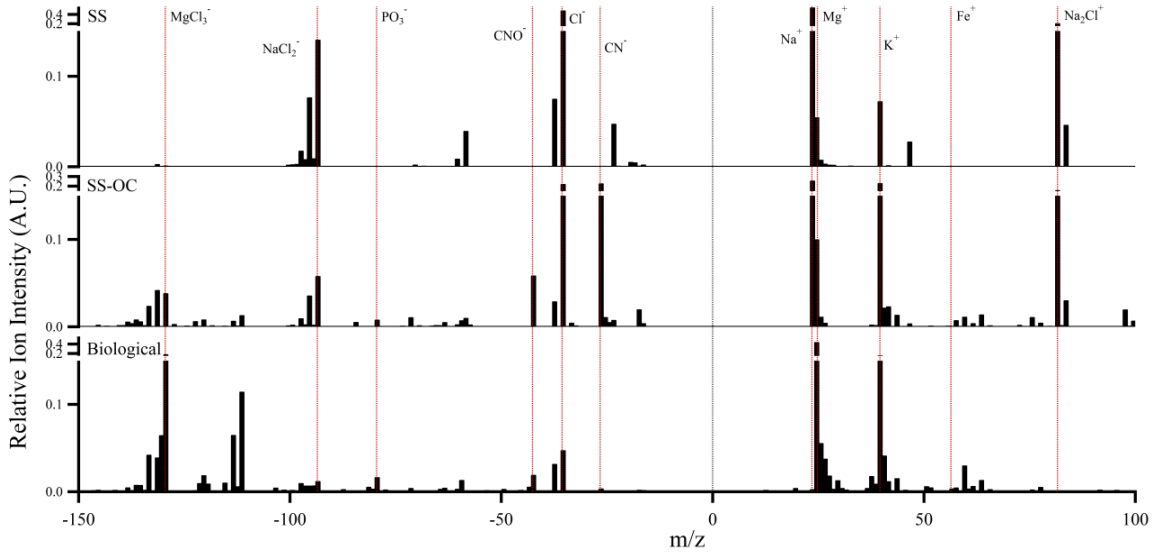

Figure 2.11. Representative dual polarity mass spectra of 3 main particle types from ATOFMS observed in the microcosm experiments. From top to bottom panels, sea salt (SS), sea salt-organic carbon (SS-OC), and Biological type particle spectra are shown respectively.

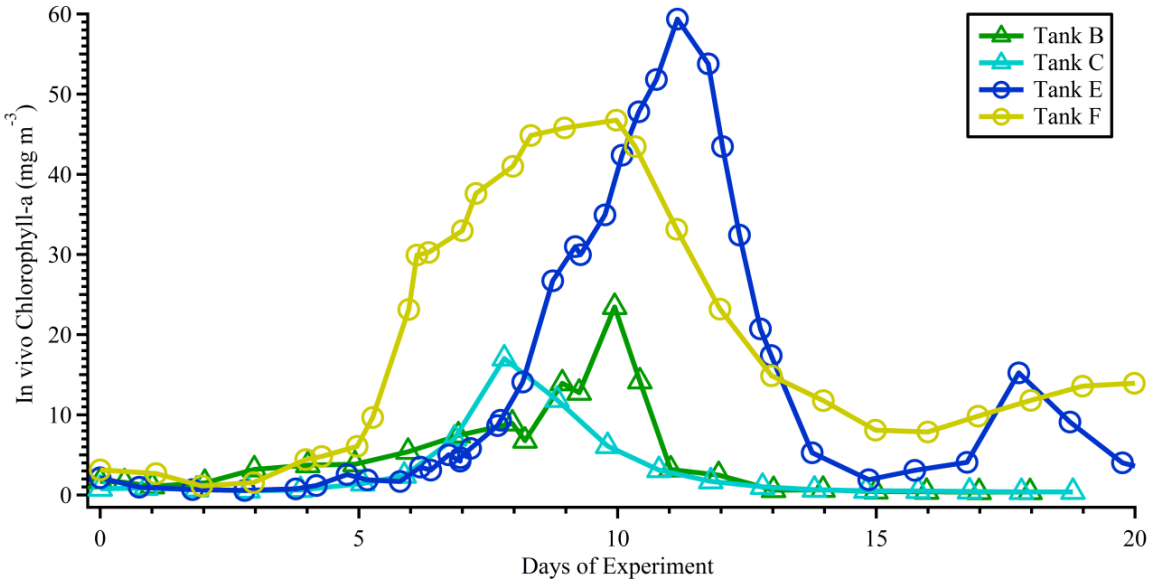

Figure 2.12. Compilation of absolute chlorophyll-a concentrations (mg m^{-3}) for four phytoplankton microcosms in this study (Tanks B, C, E, and F). Data from tanks A and D are not shown as the calibration for the chlorophyll-a concentration calculation during these two microcosms was not reliable. Initial chlorophyll-a concentrations for the two microcosms were provided by SCCOOS (Table 2.1).

2.8.2 Supporting Information Tables

Table 2.1. Select metrics for the chemical conditions of the coastal Pacific Ocean at the time of seawater collection for each experiment. Data from SCCOOS were not available for the 12/1/13 collection (Tank C).

Date	*Chlorophyll-a* ($mg\ m^{-3}$)	*Water Temp.* (^oC)	*Pressure* (*dbar*)	*Salinity* (*PSU*)	*Tank Notation*
7/11/13 12:00	0.837	21.0916	4.132	33.6435	A
9/10/13 18:00	2.029	17.2773	5.542	33.4388	D
11/7/13 15:00	3.709	15.8678	5.171	33.4449	B
12/1/13 12:00	n/a	n/a	n/a	n/a	C
1/5/2014 16:30	1.346	15.0671	5.116	33.5286	E
4/11/2014 12:00	4.491	14.3358	3.508	33.4264	F

Table 2.2. Tabulated concentrations of nutrients in the final volume of seawater for higher concentration (f/2) and lower concentration (f/20) nutrient additions. $Na_2SiO_3 \cdot 9H_2O$ is not part of the ProLine nutrient mix, and was added separately.

	Molar Concentration	
Components	f/2 (M)	f/20 (M)
$NaNO_3$	8.82×10^{-4}	8.82×10^{-5}
$NaH_2PO_4 \cdot H_2O$	3.62×10^{-5}	3.62×10^{-6}
$Na_2SiO_3 \cdot 9H_2O$	1.06×10^{-4}	1.06×10^{-5}
$FeCl_3 \cdot 6H_2O$	1.17×10^{-5}	1.17×10^{-6}
$Na_2EDTA \cdot 2H_2O$	1.17×10^{-5}	1.17×10^{-6}
$CuSO_4 \cdot 5H_2O$	3.93×10^{-8}	3.93×10^{-9}
$Na_2MoO_4 \cdot 2H_2O$	2.60×10^{-8}	2.60×10^{-9}
$ZnSO_4 \cdot 7H_2O$	7.65×10^{-8}	7.65×10^{-9}
$CoCl_2 \cdot 6H_2O$	4.20×10^{-8}	4.20×10^{-9}
$MnCl_2 \cdot 4H_2O$	9.10×10^{-7}	9.10×10^{-8}
Thiamine HCl (vit. B_1)	2.96×10^{-7}	2.96×10^{-8}
Biotin (vit. H)	2.05×10^{-9}	2.05×10^{-10}
Cyanocobalamin (vit. B_{12})	3.69×10^{-10}	3.69×10^{-11}

2.9 References

Abbatt, J. P. D., and M. J. Molina, Heterogeneous interactions of nitryl hypochlorite and hydrogen chloride on nitric acid trihydrate at 202 K, The Journal of Physical Chemistry, 96 (19), 7674–7679, 1992.

Abbatt, J. P. D., and M. J. Molina, Status of stratospheric ozone depletion *Annual review of energy and the environment. Vol. 18*, 1993.

Abbatt, J. P. D., A. K. Y. Lee, and J. A. Thornton, Quantifying trace gas uptake to tropospheric aerosol: recent advances and remaining challenges, Chemical Society Reviews, 41 (19), 6555, 2012.

Aller, J. Y., M. R. Kuznetsova, C. J. Jahns, and P. F. Kemp, The sea surface microlayer as a source of viral and bacterial enrichment in marine aerosols, Journal of Aerosol Science, 36 (5–6), 801–812, 2005.

Á lvarez-Salgado, X. A., and A. E. J. Miller, Simultaneous determination of dissolved organic carbon and total dissolved nitrogen in seawater by high temperature catalytic oxidation: Conditions for precise shipboard measurements, Marine Chemistry, 62 (3–4), 325–333, 1998.

Aristegui, J., Dissolved organic carbon support of respiration in the dark ocean, Science, 298 (5600), 1967–1967, 2002.

Ault, A. P., T. L. Guasco, O. S. Ryder, J. Baltrusaitis, L. A. Cuadra-Rodriguez, D. B. Collins, M. J. Ruppel, T. H. Bertram, K. A. Prather, and V. H. Grassian, Inside versus outside: Ion redistribution in nitric acid reacted sea spray aerosol particles as determined by single particle analysis, Journal of the American Chemical Society, 135 (39), 14528–14531, 2013.

Ault, A. P., R. C. Moffet, J. Baltrusaitis, D. B. Collins, M. J. Ruppel, L. A. Cuadra-Rodriguez, D. Zhao, T. L. Guasco, C. J. Ebben, F. M. Geiger, T. H. Bertram, K. A. Prather, and V. H. Grassian, Size-dependent changes in sea spray aerosol composition and properties with different seawater conditions, Environ. Sci. Technol., 47, 5603–5612, 2013.

Ault, A. P., T. L. Guasco, J. Baltrusaitis, O. S. Ryder, J. V. Trueblood, D. B. Collins, M. J. Ruppel, L. A. Cuadra-Rodriguez, K. A. Prather, and V. H. Grassian, Heterogeneous reactivity of nitric acid with nascent sea spray aerosol: Large differences observed between and within individual particles, Journal of Physical Chemistry Letters, 5 (15), 2493–2500, 2014.

Azam, F., D. C. Smith, G. F. Steward, and Å . Hagström, Bacteria-organic matter coupling and its significance for oceanic carbon cycling, Microbial Ecology, 28 (2), 167–179, 1994.

Azam, F., and F. Malfatti, Microbial structuring of marine ecosystems., Nature Reviews. Microbiology, 5 (10), 782–791, 2007.

Azam, F., T. Fenchel, J. G. Field, J. S. Gray, L. A. Meyer-Reil, and F. Thingstad, The ecological

role of water-column microbes in the sea, Marine Ecology Progress Series, 10, 257–263, 1983.

Bird, D. F., and J. Kalff, Empirical relationships between bacterial abundance and chlorophyll concentration in fresh and marine waters, Canadian Journal of Fisheries and Aquatic Sciences, 41, 1015–1023, 1984.

Blanchard, D. C., Bubble scavenging and water-to-air transfer of organic material in sea, Advances in Chemistry Series, 145, 360–387, 1975.

Blanchard, D. C., and A. H. Woodcock, Bubble formation and modification in the sea and its meteorological significance, Tellus IX, 9 (2), 145–158, 1957.

Bogdan, A., and M. J. Molina, Aqueous aerosol may build up an elevated upper tropospheric ice supersaturation and form mixed-phase particles after freezing, Journal of Physical Chemistry A, 114 (8), 2821–2829, 2010.

Bouvet, M., N. Hoepffner, and M. D. Dowell, Parameterization of a spectral solar irradiance model for the global ocean using multiple satellite sensors, Journal of Geophysical Research-Oceans, 107 (C12), 3215, 2002.

Brown, T. E., and F. L. Richardson, The effect of growth environment on the physiology of alage: Light intensity, Journal of Phycology, 4 (1), 38–54, 1968.

Burrows, S. M., C. Hoose, U. Pöschl, and M. G. Lawrence, Ice nuclei in marine air: Biogenic particles or dust?, Atmospheric Chemistry and Physics, 13 (1), 245–267, 2013.

Callaghan, A. H., G. B. Deane, M. D. Stokes, and B. Ward, Observed variation in the decay time of oceanic whitecap foam, Journal of Geophysical Research: Oceans, 117 (9), 2012.

Carlson, D. J., Dissolved organic materials in surface microlayers - Temporal and spatial variability and relation to sea state, Limnology and Oceanography, 28, 415–431, 1983.

Cloern, J. E., Phytoplankton bloom dynamics in coastal ecosystems: A review with some general lessons from sustained investigation of San Francisco Bay, California, Reviews of Geophysics, 34 (2), 127–168, 1996.

Coble, P. G., Characterization of marine and terrestrial DOM in seawater using excitation-emission matrix spectroscopy, Marine Chemistry, 51 (4), 325–346, 1996.

Collins, D. B., D. F. Zhao, M. J. Ruppel, O. Laskina, J. R. Grandquist, R. L. Modini, M. D. Stokes, L. M. Russell, T. H. Bertram, V. H. Grassian, G. B. Deane, and K. A. Prather, Direct aerosol chemical composition measurements to evaluate the physicochemical differences between controlled sea spray aerosol generation schemes, Atmospheric Measurement Techniques, 7 (11), 3667–3683, 2014.

Cruz, C. N., and S. N. Pandis, Deliquescence and hygroscopic growth of mixed inorganic - Organic atmospheric aerosol, Environmental Science and Technology, 34 (20), 4313–4319, 2000.

Cunliffe, M., R. C. Upstill-Goddard, and J. C. Murrell, Microbiology of aquatic surface microlayers, FEMS Microbiology Reviews, 35 (2), 233–246, 2011.

Cunliffe, M., A. Engel, S. Frka, B. Gašparović, C. Guitart, J. C. Murrell, M. Salter, C. Stolle, R. Upstill-Goddard, and O. Wurl, Sea surface microlayers: A unified physicochemical and biological perspective of the air-ocean interface, Progress in Oceanography, 109, 104–116, 2013.

Cziczo, D. J., P. J. DeMott, S. D. Brooks, A. J. Prenni, D. S. Thomson, D. Baumgardner, J. C. Wilson, S. M. Kreidenweis, and D. M. Murphy, Observations of organic species and atmospheric ice formation, Geophysical Research Letters, 31 (12), 2–5, 2004.

DeLong, E. F., Community genomics among stratified microbial assemblages in the ocean's interior, Science, 311 (5760), 496–503, 2006.

Deshler, T., A review of global stratospheric aerosol: Measurements, importance, life cycle, and local stratospheric aerosol, Atmospheric Research, 90 (2–4), 223–232, 2008.

Després, V. R., J. Alex Huffman, S. M. Burrows, C. Hoose, A. S. Safatov, G. Buryak, J. Fröhlich-Nowoisky, W. Elbert, M. O. Andreae, U. Pöschl, and R. Jaenicke, Primary biological aerosol particles in the atmosphere: A review, Tellus, Series B: Chemical and Physical Meteorology, 2012.

Dueker, M. E., and G. D. O'Mullan, Aeration remediation of a polluted waterway increases near-surface coarse and culturable microbial aerosols, Science of the Total Environment, 478, 184–189, 2014.

Finlayson-Pitts, B. J., Reactions at surfaces in the atmosphere: integration of experiments and theory as necessary (but not necessarily sufficient) for predicting the physical chemistry of aerosols, Physical Chemistry Chemical Physics : PCCP, 11 (36), 7759, 2009.

Fry, J. L., D. C, K. C. Barsanti, J. N. Smith, J. Ortega, P. M. Winkler, M. J. Lawler, S. S. Brown, P. M. Edwards, R. C. Cohen, L. Lee, D. C. Draper, K. C. Barsanti, J. N. Smith, J. Ortega, P. M. Winkler, M. J. Lawler, S. S. Brown, P. M. Edwards, R. C. Cohen, and L. Lee, Secondary organic aerosol formation and organic nitrate yield from NO_3 oxidation of biogenic hydrocarbons, Environmental Science & Technology, 48 (20), 11944–11953, 2014.

Gard, E. E., J. E. Mayer, B. D. Morrical, T. Dienes, D. P. Fergenson, and K. A. Prather, Real-time analysis of individual atmospheric aerosol particles: Design and performance of a portable ATOFMS, Analytical Chemistry, 69 (20), 4083–4091, 1997.

Gard, E. E., M. J. Kleeman, D. S. Gross, L. S. Hughes, J. O. Allen, B. D. Morrical, D. P. Fergenson, T. Dienes, M. E. Galli, R. J. Johnson, G. R. Cass, and K. A. Prather, Direct observation of heterogeneous chemistry in the atmosphere, Science, 279 (5354), 1184–1187, 1998.

Gaston, C. J., H. Furutani, S. A. Guazzotti, K. R. Coffee, T. S. Bates, P. K. Quinn, L. I.

Aluwihare, B. G. Mitchell, and K. A. Prather, Unique ocean-derived particles serve as a proxy for changes in ocean chemistry, Journal of Geophysical Research: Atmospheres, 116 (18), 1–13, 2011.

Gilstad, M., and E. Sakshaug, Growth-rates of 10 diatom species from the Barents Sea at different irradiances and day lengths, Marine Ecology Progress Series, 64, 169–173, 1990.

Grossart, H. P., and H. Ploug, Microbial degradation of organic carbon and nitrogen on diatom aggregates, Limnology and Oceanography, 46 (2), 267–277, 2001.

Grossart, H. P., G. Czub, and M. Simon, Algae-bacteria interactions and their effects on aggregation and organic matter flux in the sea, Environmental Microbiology, 8 (6), 1074–1084, 2006.

Guasco, T. L., L. A. Cuadra-Rodriguez, B. E. Pedler, A. P. Ault, D. B. Collins, D. Zhao, M. J. Kim, M. J. Ruppel, S. C. Wilson, R. S. Pomeroy, V. H. Grassian, F. Azam, T. H. Bertram, and K. A. Prather, Transition metal associations with primary biological particles in sea spray aerosol generated in a wave channel, Environmental Science and Technology, 48 (2), 1324–1333, 2014.

Guillard, R. R. L., Culture of phytoplankton for feeding marine invertebrates, In *Culture of Marine Invertebrate Animals* (pp. 29–60), 1975.

Guillard, R. R. L., and J. H. Ryther, Studies of marine planktonic diatoms: I. Cyclotella nana Hustedt, and Detonula confervacea (Cleve) Gran, Canadian Journal of Microbiology, 8 (2), 229–239, 1962.

Hessen, D., and L. Tranvik, Aquatic humic substances (D. O. Hessen & L. J. Tranvik, Eds.) (Vol. 133). Berlin, Heidelberg: Springer Berlin Heidelberg, 1998.

Jaffé, R., D. McKnight, N. Maie, R. Cory, W. H. McDowell, and J. L. Campbell, Spatial and temporal variations in DOM composition in ecosystems: The importance of long-term monitoring of optical properties, Journal of Geophysical Research: Biogeosciences, 113 (4), 2008.

Keene, W. C., H. Maring, J. R. Maben, D. J. Kieber, A. A. P. Pszenny, E. E. Dahl, M. A. Izaguirre, A. J. Davis, M. S. Long, X. Zhou, L. Smoydzin, and R. Sander, Chemical and physical characteristics of nascent aerosols produced by bursting bubbles at a model air-sea interface, Journal of Geophysical Research Atmospheres, 112 (21), 2007.

Kirchman, D. L., Y. Suzuki, C. Garside, and H. W. Ducklow, High turnover rates of dissolved organic carbon during a spring phytoplankton bloom, Letters to Nature, 1995.

Kolb, C. E., R. A. Cox, J. P. D. Abbatt, M. Ammann, E. J. Davis, D. J. Donaldson, B. C. Garrett, C. George, P. T. Griffiths, D. R. Hanson, M. Kulmala, G. McFiggans, U. Pöschl, I. Riipinen, M. J. Rossi, Y. Rudich, P. E. Wagner, P. M. Winkler, D. R. Worsnop, and C. D. O'Dowd, An overview of current issues in the uptake of atmospheric trace gases by aerosols and clouds, Atmospheric Chemistry and Physics, 10 (21), 10561–10605, 2010.

Krueger, B. J., V. H. Grassian, M. J. Iedema, J. P. Cowin, and A. Laskin, Probing heterogeneous chemistry of individual atmospheric particles using scanning electron microscopy and energy-dispersive X-ray Analysis, Analytical Chemistry, 75 (19), 5170–5179, 2003.

Lawaetz, A. J., and C. A. Stedmon, Fluorescence intensity calibration using the Raman scatter peak of water, Applied Spectroscopy, 63 (8), 936–940, 2009.

De Leeuw, G., E. L. Andreas, M. D. Anguelova, C. W. Fairall, R. Ernie, C. O. Dowd, M. Schulz, and S. E. Schwartz, Production flux of sea-spray aerosol, Reviews of Geophysics, 80 (2010), 1–39, 2011.

Lewis, E. R., and S. E. Schwartz, Sea salt aerosol production: Mechanisms, methods, measurements and models, Geophysical Monograph Series, 152, 413, 2004.

Maie, N., J. N. Boyer, C. Yang, and R. Jaffé, Spatial, geomorphological, and seasonal variability of CDOM in estuaries of the Florida Coastal Everglades, Hydrobiologia, 569 (1), 135–150, 2006.

McCarthy, M. D., Major bacterial contribution to marine dissolved organic nitrogen, Science, 281 (5374), 231–234, 1998.

McNeill, V. F., J. Patterson, G. M. Wolfe, and J. A. Thornton, The effect of varying levels of surfactant on the reactive uptake of N_2O_5 to aqueous aerosol, Atmospheric Chemistry and Physics, 6, 1635-1644, 2006.

Möhler, O., S. Benz, H. Saathoff, M. Schnaiter, R. Wagner, J. Schneider, S. Walter, V. Ebert, and S. Wagner, The effect of organic coating on the heterogeneous ice nucleation efficiency of mineral dust aerosols, Environmental Research Letters, 3 (2), 25007, 2008.

Molina, M. J., L. T. Molina, and C. E. Kolb, Gas-phase and heterogeneous chemical kinetics of the troposphere and stratosphere, Annual Review of Physical Chemistry, 47 (1), 327–367, 1996.

Molina, M. J., and F. S. Rowland, Stratospheric sink for chlorofluoromethanes: chlorine atom-catalysed destruction of ozone, Nature, 249 (5460), 810–812, 1974.

Mura, M. P., and S. Agusti, Growth rates of diatoms from coastal Antarctic waters estimated by in situ dialysis incubation, Marine Ecology Progress Series, 144, 237–245, 1996.

Murphy, K. R., A note on determining the extent of the water Raman peak in fluorescence spectroscopy, Applied Spectroscopy, 65 (2), 233–236, 2011.

NASA Earth observations chlorophyll concentration (Aqua/Modis), 2014. Retrieved September 16, 2014, from http://neo.sci.gsfc.nasa.gov/view.php?datasetId=MY1DMM_%0ACHLORA

National Oceanic and Atmospheric Administration, U.S.D.o.C. Ocean, 2014. Retrieved May 29, 2015, from http://www.noaa.gov/ocean.html

Nieto-Cid, M., X. A. Á lvarez-Salgado, and F. F. Pérez, Microbial and photochemical reactivity of fluorescent dissolved organic matter in a coastal upwelling system, Limnology and Oceanography, 51 (3), 1391–1400, 2006.

Noble, R. T., and J. A. Fuhrman, Use of SYBR Green I for rapid epifluorescence counts of marine viruses and bacteria, Aquatic Microbial Ecology, 14 (2), 113–118, 1998.

Norrman, B., U. L. Zweifel, C. S. Hopkinson, and B. Fry, Production and utilization of dissolved organic-carbon during an experimental diatom bloom, Limnology and Oceanography, 40 (5), 898–907, 1995.

O'Dowd, C. D., M. C. Facchini, F. Cavalli, D. Ceburnis, M. Mircea, S. Decesari, S. Fuzzi, Y. J. Yoon, and J.-P. Putaud, Biogenically driven organic contribution to marine aerosol., Nature, 431 (7009), 676–680, 2004.

Osto, M. D., R. M. Harrison, H. Coe, P. Williams, M. Dall'Osto, R. M. Harrison, H. Coe, P. Williams, M. D. Osto, R. M. Harrison, H. Coe, P. Williams, M. Dall'Osto, R. M. Harrison, H. Coe, P. Williams, M. D. Osto, R. M. Harrison, H. Coe, and P. Williams, Real-time secondary aerosol formation during a fog event in London, Atmospheric Chemistry and Physics, 9 (7), 2459–2469, 2009.

Pomeroy, L. R., P. J. I. Williams, F. Azam, and J. E. Hobbie, The microbial loop, Oceanography, 20 (2), 28–33, 2007.

Prather, K. A., C. D. Hatch, and V. H. Grassian, Analysis of atmospheric aerosols., Annual Review of Analytical Chemistry, 1, 485–514, 2008.

Prather, K. A., T. H. Bertram, V. H. Grassian, G. B. Deane, M. D. Stokes, P. J. Demott, L. I. Aluwihare, B. P. Palenik, F. Azam, J. H. Seinfeld, R. C. Moffet, M. J. Molina, C. D. Cappa, F. M. Geiger, G. C. Roberts, L. M. Russell, A. P. Ault, J. Baltrusaitis, D. B. Collins, C. E. Corrigan, L. A. Cuadra-Rodriguez, C. J. Ebben, S. D. Forestieri, T. L. Guasco, S. P. Hersey, M. J. Kim, W. F. Lambert, R. L. Modini, W. Mui, B. E. Pedler, M. J. Ruppel, O. S. Ryder, N. G. Schoepp, R. C. Sullivan, and D. Zhao, Bringing the ocean into the laboratory to probe the chemical complexity of sea spray aerosol., Proceedings of the National Academy of Sciences of the United States of America, 110 (19), 7550–7555, 2013.

Prenni, A. J., and M. A. Tolbert, Studies of polar stratospheric cloud formation, Accounts of Chemical Research, 34 (7), 545–553, 2001.

Riemann, L., G. F. Steward, and F. Azam, Dynamics of bacterial community composition and activity during a mesocosm diatom bloom dynamics of bacterial community composition and activity during a mesocosm diatom bloom, Applied and Environmental Microbiology, 66 (2), 578–587, 2000.

Rinaldi, M., S. Fuzzi, S. Decesari, S. Marullo, R. Santoleri, A. Provenzale, J. Von Hardenberg, D. Ceburnis, A. Vaishya, C. D. O'Dowd, and M. C. Facchini, Is chlorophyll-a the best surrogate for organic matter enrichment in submicron primary marine aerosol?, Journal of Geophysical Research: Atmospheres, 118 (10), 4964–4973, 2013.

Ryder, O. S., A. P. Ault, J. F. Cahill, T. L. Guasco, T. P. Riedel, L. A. Cuadra-Rodriguez, C. J. Gaston, E. Fitzgerald, C. Lee, K. A. Prather, and T. H. Bertram, On the role of particle inorganic mixing state in the reactive uptake of N_2O_5 to ambient aerosol particles, Environmental Science and Technology, 48 (3), 1618–1627, 2014.

Salcedo, D., L. T. Molina, and M. J. Molina, Nucleation rates of nitric acid dihydrate in 1:2 HNO_3/H_2O solutions at stratospheric temperatures, Geophysical Research Letters, 27 (2), 193–196, 2000.

Salcedo, D., L. T. Molina, and M. J. Molina, Homogeneous freezing of concentrated aqueous nitric acid solutions at polar stratospheric temperatures, Journal of Physical Chemistry A, 105 (9), 1433–1439, 2001.

Saxena, P., and L. M. Hildemann, Organics alter hygroscopic behavior of atmospheric particles, Journal of Geophysical Research, 100 (95), 18755–18770, 1995.

Schnell, R. C., and G. Vali, Biogenic ice nuclei: Part I. Terrestrial and marine Sources, Journal of the Atmospheric Sciences, 1976.

Shimotori, K., Y. Omori, and T. Hama, Bacterial production of marine humic-like fluorescent dissolved organic matter and its biogeochemical importance, Aquatic Microbial Ecology, 58 (1), 55–66, 2010.

Smith, D. C., M. Simon, A. L. Alldredge, and F. Azam, Intense hydrolytic enzyme activity on marine aggregates and implications for rapid particle dissolution, Nature, 359 (6391), 139–142, 1992.

Smith, D. C., G. F. Steward, R. A. Long, and F. Azam, Bacterial mediation of carbon fluxes during a diatom bloom in a mesocosm, Deep Sea Research Part II: Topical Studies in Oceanography, 42 (1), 75–97, 1995.

Sorokin, C., and R. W. Krauss, The effects of light intensity on the growth rates of green algae., Plant Physiologyhysiology, 33 (2), 109–13, 1958.

Stokes, M. D., G. B. Deane, K. Prather, T. H. Bertram, M. J. Ruppel, O. S. Ryder, J. M. Brady, and D. Zhao, A Marine Aerosol Reference Tank system as a breaking wave analogue for the production of foam and sea-spray aerosols, Atmospheric Measurement Techniques, 6 (4), 1085–1094, 2013.

Sullivan, C. W., K. R. Arrigo, C. R. McClain, J. C. Comiso, and J. Firestone, Distributions of phytoplankton blooms in the Southern Ocean, Science, 262 (5141), 1832–1837, 1993.

Sun, J., and P. A. Ariya, Atmospheric organic and bio-aerosols as cloud condensation nuclei (CCN): A review, Atmospheric Environment, 40, 795–820, 2006.

Suttle, C. A., Viruses in the sea, Nature, 437 (7057), 356–361, 2005.

Tang, E. P. Y., The allometry of algal growth rates, Journal of Plankton Research, 17, 1325–

1335, 1995.

Teeling, H., B. M. Fuchs, D. Becher, C. Klockow, A. Gardebrecht, C. M. Bennke, M. Kassabgy, S. Huang, A. J. Mann, J. Waldmann, M. Weber, A. Klindworth, A. Otto, J. Lange, J. Bernhardt, C. Reinsch, M. Hecker, J. Peplies, F. D. Bockelmann, U. Callies, G. Gerdts, A. Wichels, K. H. Wiltshire, F. O. Glockner, T. Schweder, and R. Amann, Substrate-controlled succession of marine bacterioplankton populations induced by a phytoplankton bloom, Science, 336 (6081), 608–611, 2012.

Tolbert, M. A., M. J. Rossi, R. Malhotra, and D. M. Golden, Reaction of chlorine nitrate with hydrogen chloride and water at antarctic stratospheric temperatures., Science, 238 (4831), 1258–60, 1987.

Tsigaridis, K., D. Koch, and S. Menon, Uncertainties and importance of sea spray composition on aerosol direct and indirect effects, Journal of Geophysical Research: Atmospheres, 118 (1), 220–235, 2013.

Vali, G., M. Christensen, R. W. Fresh, E. L. Galyan, L. R. Maki, and R. C. Schnell, Biogenic ice nuclei. Part II: Bacterial sources, Journal of the Atmospheric Sciences, 1976.

Wolber, P. K., Bacterial ice nucleation, Advances in Microbial Physiology, 34 (C), 203–237, 1993.

Yamashita, Y., and E. Tanoue, Production of bio-refractory fluorescent dissolved organic matter in the ocean interior, Nature Geoscience, 1 (9), 579–582, 2008.

Yoder, J. A., C. R. McClain, G. C. Feldman, and W. E. Esaias, Annual cycles of phytoplankton chlorophyll concentrations in the global ocean: A satellite view, Global Biogeochemical Cycles, 7 (1), 181–193, 1993.

You, Y., M. L. Smith, M. Song, S. T. Martin, and A. K. Bertram, Liquid–liquid phase separation in atmospherically relevant particles consisting of organic species and inorganic salts, International Reviews in Physical Chemistry, 33 (1), 43–77, 2014.

3 Enzymatic Processing by Lipase in Seawater Impacts Sea Spray Aerosol Composition

3.1 Synopsis

A 2015 study found that a phytoplankton bloom exhibiting low bacteria counts and low lipase activity resulted in submicron SSA organic enrichment, while a second phytoplankton bloom peak with high bacterial counts and high lipase activity resulted in the loss of SSA organic enrichment. In this study, the specific impact of lipase has on SSA is investigated using a miniature Marine Aerosol Reference Tank and two model organic substrates: 1) triolein and 2) diatom lysate extracted from *Thalisiossira pseudonanna* culture. High resolution mass spectrometry analysis of bulk aerosol and seawater in addition to aerosol time-of-flight mass spectrometry measurements of single particle chemical composition demonstrate for the first time that lipase activity in the seawater can significantly control the SSA chemical composition. Triolein system resulted in lipase-degraded products preferentially ejected in the supermicron SSA fraction found to be more associated with calcium. Building up the chemical complexity of the system, single particle results showed measureable changes in biogenically-derived organic markers that track lipase degradation, further demonstrating the effect of lipase on SSA chemistry. Findings from this study have significant implications for SSA heterogeneous reactivity, morphology, phase state, and cloud forming ability.

3.2 Introduction

The composition of seawater is controlled by enzymatic processes described by the microbial loop [*Arnosti, 2011*; *Azam et al., 1983*; *Fenchel, 2008*; *Pomeroy et al., 2007*]. As sea spray aerosol (SSA) is derived from seawater, its composition is dependent upon the chemical makeup of seawater. However, the link between oceanic enzymatic activity and the composition

of SSA has not been examined. Because the ocean provides a significant portion of atmospheric aerosols [*De Leeuw et al., 2011*; *Liu et al., 2007*; *Struthers et al., 2013*] and the composition of SSA determines its atmospheric properties [*Ault et al., 2014*; *Forestieri et al., 2016*; *Quinn et al., 2015*; *Ryder et al., 2015*], ascertaining processes that affect chemical makeup and atmospheric properties is crucial. While previous studies have used chlorophyll-a (Chl-a) to correlate with SSA organic enrichment [*O'Dowd et al., 2004*; *Quinn et al., 2014*; *Rinaldi et al., 2013*], a recent study demonstrated the potential role of marine bacteria on SSA organic enrichment [*Wang et al., 2015*], shifting the paradigm in elucidating marine biological control over SSA chemical composition.

Marine bacteria cannot utilize macromolecules or detritus larger than 600 Da as they are not able to cross cell walls [*Weiss et al., 1991*]. To break molecules and cells down, bacteria use extracellular enzymes to digest them into smaller molecules which can be consumed [*Arnosti, 2011*; *Weiss et al., 1991*]. By virtue of these degradation processes, bacteria are responsible for the recycling of carbon and degradation of decaying organisms involved in phytoplankton blooms [*Buchan et al., 2014*; *Riemann et al., 2000*]. The specific contribution of microbial processing to biogeochemical cycles and atmospheric carbon are not well understood [*Arndt et al., 2013*; *Azam and Malfatti, 2007*]. However, biomolecules prevalent in phytoplankton and bacteria are often used as model molecules in atmospheric and biogeochemical studies. Enzymatic activity is an ongoing, dominant process and bacterial species possess diverse enzymes of probable varied activity [*Arnosti et al., 2014*; *Buchan et al., 2014*; *Pedler et al., 2014*; *Zimmerman et al., 2013*]. As such, the alterations to model molecules by extracellular enzymes in marine systems need to be both considered and determined to elucidate the biological processes occurring in marine environments.

A study of nutrient-stimulated phytoplankton blooms correlated a loss in SSA submicron organic enrichment to increased seawater lipase activity and heterotrophic bacterial concentrations [*Wang et al., 2015*]. To examine if lipase activity would directly influence SSA composition, we sought to examine resulting changes to SSA composition with seawater lipase addition in simplified model systems. A small volume apparatus that produces SSA in ocean-relevant size distributions, the miniature marine aerosol reference tank (miniMART) [*Stokes et al., 2016*] was selected for controlled studies in seawater. We tested the substrates triolein, a triacylglycerol, and lysate extracted from marine diatom culture, *Thalisiossira pseudonanna*, and observed composition changes by high-resolution mass spectrometry (HRMS) and aerosol time-of-flight mass spectrometry (ATOFMS) [*Pratt and Prather*, *2012*a, *2012*b] to complement detailed offline analysis with chemical information of individual SSA particles.

3.3 Materials and Methods

3.3.1 SSA Generation and Sequential Addition of Reagents

A miniMART was utilized to generate SSA. Details of the operating principle can be found elsewhere [*Stokes et al., 2016*]. In brief, the tank utilizes a rotating water wheel to intermittently produce a plunging waterfall into an approximately 6 L reservoir, producing a bubble size distribution that mimics that of breaking waves [*Deane and Stokes*, *2002*; *Stokes et al., 2016*]. This in turn replicates the size and physicochemical composition of the resulting SSA [*Ault et al., 2013*; *Collins et al., 2014*; *Prather et al., 2013*]. The headspace of the miniMART was constantly purged using particle free air (Sabio Instruments, Model 1001) at 1 standard liters per minute (SLPM) greater than the sampling flow rate of the instruments and apparatus. This overflow of 1 SLPM ensured positive pressurization of the headspace, preventing any accidental

back-sampling of room air. Under normal operation conditions, the headspace had relative humidity (RH) of > 90% (Vaisala, HMP110).

Prior to beginning of the experiments, all surfaces, including the rotating wheel were cleaned using ethanol (90% v/v) and rinsed with ultra-pure water. Seawater used in this study was either 1) natural seawater collected at Scripps Pier (La Jolla, CA; 32° 52' 00" N, 117° 15' 21" W) filtered using a 0.7 µm filter (Whatman GF/F, Z242489) to remove most of the particulate organic matter (POM) and then autoclaved (121 ℃ for 90 min), or 2) synthetic artificial seawater made by dissolving reef salt mix (Brightwell Aquatics, NēoMarine, 35.53 g L^{-1}) in ultra-pure water followed by autoclaving at 121 ℃ for 90 min. Once the measurement techniques (Sections 3.3.4 and 3.3.5) performed the baseline seawater measurements, 500 mg of triolein (Sigma-Aldrich, T7140) was added to the water reservoir. Following measurements under these conditions, 2 mg of lipase (70 U added, Sigma-Aldrich, lipase from *pseudomonas cepacia*, 62309) was added and the measurements were repeated.

To test the diatom lysate in the system, the triolein addition was replaced by the addition of extracted lysate *Thalisiossira pseudonanna* grown in nutrient rich, artificial seawater (ASW) medium, keeping all other experimental procedures the same. The detailed method for ASW medium preparation can be found in Section 4.8.1 and the list of chemicals in the ASW medium can be found in Table 4.1.Further detail on preparation of the lysate can be found in Section 3.3.3.

3.3.2 Enzymatic Activity Assays

To assess lipase acitivity in triolein system, and lipase, protease, phosphatase, or glucosidase enzymatic activity in lysate system to verify the culture itself did not produce any enzymes, assays described by Hoppe were performed [*Hoppe, 1993*]. This methodology uses model substrates attached to a fluorophore: MUF (4-methylumbelliferone, MilliporeSigma M1381) or MCA (4-rnethylcoumarinyl-7-amide, MilliporeSigma A9891). Enzymatic activity was

demonstrated by cleavage of the fluorophore from the attached substrate detectable by fluorescence at λ_{ex} = 360 nm / λ_{em} = 465 nm. An oleate substrate (MUF-oleate, MilliporeSigma 75164) was used to detect lipase activity. A glucose substrate (MUF-β-D-glucopyranoside, MilliporeSigma M3633) was used to detect β- glucosidase activity. A phosphate substrate (MUF-phosphate, MilliporeSigma M8883) was used to detect phosphatase activity. A leucine substrate (L-leucine-MCA, MilliporeSigma L2145) was used to detect protease activity. The activity of the lipase in this seawater systems were confirmed and max turnover of an oleate-fluorophore substrate determined to be between 2 - 27 μM hr^{-1} (Figure 3.8).

3.3.3 Preparation of Diatom Lysate

Cultures of *Thalisiossira pseudonanna* were grown at 18 ℃ in ASW medium [*Darley and Volcani, 1969*] to late exponential phase, ~5 x 10^6 cells mL^{-1}. Cells were harvested via centrifugation and filtration on 3 μm polycarbonate filters (Whatman) to maximize cell recovery. Lysis was performed by triplicate passes through a French press at ~20,000 psi. Lysate was added directly to the miniMART providing ~1 x 10^6 lysed cells mL^{-1}.

3.3.4 Bulk Sea Spray Aerosol Sampling and Analysis by High Resolution Mass Spectrometry

3.3.4.1 Filter Sample Collection and Preparation

MiniMART generated SSA particles were collected onto 0.2 μm PTFE 47 mm filters (Whatman) encased in aluminum or polypropylene filter cartridges. For each sampling period of 13 hours, SSA were collected into two size fractions by splitting the air stream without drying with diffusion driers. The first stream collected the entire aerosol size distribution passed at 1.2 SLPM onto the filter cartridge The second air stream, passed through a cyclone separator (BGI - SCC 0.695) at 1.2 SLPM, to allow for collection of aerosols < 1.0 μm aerodynamic diameter (D_a). After collection, filters were stored in muffled aluminum foil in a -20 ℃ freezer for

subsequent analysis. Filters were subsampled using a clean razor blade to cut out ½ of the filter, with the residual half reserved for repeat analyses. Subsampled filters were extracted by sonication in 1 mL of $CHCl_3$ (Sigma-Aldrich > 99% HPLC) for 30 minutes, the liquid was moved to a separate vial, and extraction was repeated 2 more times. The final 3 mL of $CHCl_3$ was evaporated under a gentle stream of N_2 gas. Extracted organics were re-dissolved in 1 mL of acetonitrile (ACN, Sigma-Aldrich > 99% HPLC) and transferred to autosampler vials for LC/MS.

Liquid samples of diatom lysate (1 mL) were liquid-liquid extracted by 1 mL of $CHCl_3$ after 30 minutes of sonication. The extraction was performed 3 times, with the extracted 3 mL of $CHCl_3$ evaporated under a gentle stream of N_2 gas. Extracted organics were re-suspended in 1mL of ACN and transferred to autosampler vials. Standards of triolein, diolein, and monolein (Sigma-Aldrich > 99% HPLC, D3627, 44893-U, respectively) were solubilized in ACN in combusted glass vials.

3.3.4.2 Orbitrap Ultra High Resolution Mass Spectrometry

Extracted and prepared samples (10 µL) were injected onto a Thermo Scientific (Vanquish) ultra-high pressure liquid chromatograph utilizing an Accucore C18 column 3 × 50 cm, 2.6 µm on an empirically determined gradient elution with solvent A: Acetonitrile with 2.5 mM ammonium acetate (NH_4Ac), solvent B: Isopropanol with 2.5 mM NH_4Ac, and solvent C: H_2O with 2.5 mM NH_4Ac. Details on the gradient profile can be found in Table 3.1. Column eluent was passed into an electrospray ionization mass spectrometer (Orbitrap Elite). Positive mode settings were: electrospray ionization (ESI) voltages of 3.5 kV (+) and 2.6kV (-), ESI temperature of 350 ℃, mass range of 100-1500 Da, and capillary temperature of 350 ℃. Data files produced by the instrument were processed in the Thermo Excalibur data analysis software in which operations such as extracted ion chromatograms and background subtraction were evaluated.

3.3.5 Chemical Composition of Individual Sea Spray Aerosols

ATOFMS was used to elucidate the chemical differences between individual SSA particles. ATOFMS provides real-time measurements of single particle size and chemical composition of aerosol particles between 0.2-3.0 µm vacuum aerodynamic diameter (D_{va}). Detailed instrument design and operating principle can be found elsewhere [*Gard et al., 1997*; *Prather et al., 1994*] and already detailed in Section 1.5.2. Data are imported into MATLAB (The MathWorks, Inc.) with the FATES software toolkit [*Sultana et al., 2017*] for analysis.

In addition to single particle chemical composition measurements, SSA size distributions were monitored to track the changes over the course of the experiment. The sample flow was split after diffusion driers between the ATOFMS, aerodynamic particle sizer (APS, TSI Model 3321, sample flow rate of 1 SLPM) and scanning mobility particle sizer (SMPS, TSI Model 3080, sample/sheathe flow rate of 0.3/3.0 SLPM) (Figure 3.1B). APS and SMPS provided number size distribution of the SSA particles generated from the miniMART in the size ranges of approximately 0.5-20 µm D_a and 13-750 nm mobility diameter (D_m), respectively.

3.4 Results and Discussion

3.4.1 Lipase Degradation of Triolein and the Resulting Changes in SSA Chemistry

Triolein is a triacylglycerol with three oleic acids (C18:1) attached to a glycerol backbone. It was selected as a model lipid due to its similarity to fatty acid-based lipids like triacylglycerols, phospholipids, wax esters, and glycolipids commonly found in marine ecosystems which are predominantly combinations of C16:0, C16:1, C18:0, and C18:1 fatty acids [*Hama, 1999*; *Kattner et al., 1983*; *Parrish, 2013*]. The expected processing of triolein to diolein

and monolein by lipase is shown in Figure 3.7. Lipase from *Pseudomonas cepacia* (MilliporeSigma 62309) was selected due to its bacterial origin and validation against triolein.

Changes in the composition of filter-collected SSA caused by triolein and subsequent lipase additions were observed by high resolution mass spectrometry. Figure 3.2 shows two mass spectra corresponding to aerosols collected after triolein addition (Figure 3.2A) and after lipase addition (Figure 3.2B). In Figure 3.2A, the mass spectrum is dominated by the presence of intact triolein 902.81 m/z $(M+NH_4)^+$ as well as a small contribution from a fragment ion corresponding to loss of an oleic acid from triolein 603.53 m/z (M-OA)+, producing diolein. Differentiation of ionization-induced fragmentation of triolein from enzymatic digestion of triolein was determined by retention time of the ion observed as well as complexation with ammonium present in the eluent. Diolein and monolein were both observed to elute separately than triolein in the chromatographic separation. These ions also appeared as ammonium adducts 638.57 m/z and 374.32 m/z when ionized by electrospray, but not when generated as fragments from triolein. These results are in line with observations in the literature [*Kalo et al., 2006*]. Figure 3.2B qualitatively illustrates the impact of lipase, showing an increase in diolein and monolein observed. Other ions, likely also products of digestion were present in the spectra, however the masses of these ions do not match known fragmentation or degradation products of triolein.

The ion intensities of non-fragment diolein and monolein, obtained from peak area integration, were compared to the intensity of triolein in each filter sample obtained for both the full size distribution and submicron SSA filter samples. In Figure 3.3A, both the ratios of diolein to triolein and monolein to triolein are dominated by the intensity of triolein. This result indicates that, as expected, the majority of the triolein did not undergo significant autohydrolysis in the mini-MART tank before lipase was added. Following the addition of lipase, it is evident that the diolein:triolein and monolein:triolein ratios significantly increase, caused by the digestion of

triolein and the transfer of enzyme products to the aerosol phase in the supermicron mass-dominated regime of the full cut size distribution. For the submicron filter samples (Figure 3.3B), the ratios of enzyme products to substrate did not show a notable change after addition of lipase. We hypothesize that this effect could be caused by the increased solubility of diolein and monolein versus triolein, which would result in a seawater interface composed of primarily triolein with the digestion products more soluble in the bulk. In Cochran et al., 2016, the selectivity of organic molecules for the aerosol phase in submicron film drops was shown to be related to alkanoic acid chain length and their solubility in the bulk phase, with more insoluble material showing higher enrichment factors in the aerosol phase. This effect could also be occurring in the triolein system, with differences in solubility between triolein, diolein, and monolein mediating their transfer to the aerosol phase in a size selective manner.

Complementary single particle chemical information provided by ATOFMS also observed the changes in SSA chemical composition with triolein and lipase additions. Using two organic ion markers ($^{37}C_3H^+$ and $^{43}C_3H_7^+$, see Figure 3.9 for more details), Figure 3.4 shows the change of SSA chemistry in a single particle level. Once triolein is added, a population of SSA particles containing $^{37}C_3H^+$ and $^{43}C_3H_7^+$ with a very small amount of $^{40}Ca^+$ appeared (red circles, Figure 3.4 B and D, respectively). Upon lipase addition to the seawater, the population observed in Figure 3.4 B and D previously disappears, and is replaced with population of SSA particles containing both organic ($^{37}C_3H^+$ and $^{43}C_3H_7^+$) ion markers along with large intensity of $^{40}Ca^+$ (green circles, Figure 3.4 E and F, respectively). In previous studies, fatty and phosphatidic acids have been seen to bond with calcium due to its high binding affinity toward the head group of the acid [*Adams et al., 2016*; *Adams and Allen, 2013*; *Zhang et al., 2016*]. This phenomena can be used to explain the single particle observations in this study, where freed oleic acid from triolein is likely being deprotonated, forming oleate, which can then bond with calcium and produce

population of SSA containing both organic and calcium ion markers. This can have profound implications for surface-sensitive processes such as heterogeneous chemistry [*Abbatt et al., 2012*; *Zahardis and Petrucci, 2007*], and ability to form cloud droplets [*Nguyen et al., 2017*], and will be further explored in future publications.

3.4.2 Lipase Degradation of Diatom Lysate and the Resulting Changes in SSA Chemistry

To assess whether seawater lipase processing would have similar effects in a more complex and relevant system, we sought to mimic the peak of a phytoplankton bloom at the point when phytoplankton death prompts bacterial-mediated degradation. *Thalasssiosira pseudonana,* a marine, centric diatom, was selected as it is well-characterized and has a rich lipid and fatty acid composition [*Hildebrand et al., 2012*], and diatoms are usually a prominent organism type in phytoplankton blooms [*Kooistra et al., 2007*]. Cultured cells were collected and lysed to initiate cell death and added to the miniMART system.

To elucidate the molecular changes that lipase has on diatom lysate, high resolution mass spectrometry was performed. High resolution mass spectrometry of concentrated extracted diatom lysate was performed as the concentration of lysate collected on aerosol filters from the miniMART experiments was found to be near or below the dynamic range of the HRMS system. While the analysis was not of aerosol samples, performing analysis of the concentrated lysate provided the insight into the molecular changes by lipase, and further correlate to the changes observed with ATOFMS. Cellular lysate was found to be composed of a wide variety of triglycerides and fatty acids, with the majority of the instrument intensity originating from a number of unsaturated palmitic acid (16:0-16:4) and tripalmitate species. These results are in general agreement with lipid speciation of *Thalisiossira pseudonanna* performed by others [*Tonon et al., 2002*; *Zendejas et al., 2012*]. In order to better understand the change in lipid

composition of the cellular lysate after the addition of lipase, the following calculation was performed to normalize the intensity of negative-mode palmitic acids to the intensity of the tripalmitate ions observed in the same sample in positive mode.

$$Normalized\ Fatty\ Acid\ Intensity = \frac{Individual\ Palmitic\ Acid\ Intensity}{Summed\ Tripalmitate\ Species\ Intensity} \quad \text{(E3.1)}$$

Figure 3.5 shows the results of this calculation for analyzed samples of diatom lysate before and after addition of lipase. Notably, the ratio of fatty acid intensity significantly increases for all of the fatty acids after the addition of lipase (detailed change of ratios for both triglyceride and fatty acids found in Figures 3.10 and 3.11, respectively). This result confirms the likely transfer of lipase-generated fatty acids to the SSA as cellular lysate is digested by lipase.

In marine relevant diatom lysate system, biogenically-derived organic markers previously observed in the SSA such as $^{26}CN^-$, $^{42}CNO^-$, and $^{79}PO_3^-$ [*Ault et al., 2014*; *Prather et al., 2013*] (Figure 3.9) were monitored over the course of the experiment. Upon lysate addition, the fraction of SSA containing these ion markers within the single particle mass spectrum increased by 4 to 22 folds depending on the ion marker (Figure 3.6). Additionally, the intensity of the ion marker in the single particle mass spectrum also increased, from pre-lysate addition range of 50-1000 A.U. to as high as 5000 A.U. post-addition. SSA particles containing lysate showed both the organic ion markers, as well as cation such as sodium, magnesium, potassium, calcium, and iron [*Groussman et al., 2015*] (Figure 3.9) as the culture was grown in an ASW medium containing trace metals. Upon lipase addition to the seawater, the fraction of SSA particles containing the three biogenically-derived organic markers decreased, yet still remained elevated 2-3 folds greater than the seawater baseline (Figure 3.6). This behavior is generally similar to that of triolein and lipase experiments, as in both systems the organic enrichment detected by ATOFMS

was elevated upon substrate addition, and still remained slightly elevated over the seawater baseline following lipase addition. Observed changes in SSA chemistry in the bulk as well as on the single particle level both demonstrate the influence of lipase on the SSA composition.

3.5 Conclusions

In summary, this study demonstrates for the first time that active lipase in seawater directly controls SSA chemical composition. The results presented herein clearly demonstrate a new relationship between ocean microbiology and SSA composition that had been only suggested in previous study [*Wang et al., 2015*]. Lipase-induced changes have important implications since changes in SSA composition can impact their morphology, phase state [*Qiu and Molinero, 2015*], and ultimately their ability to undergo heterogeneous reactivity [*Abbatt et al., 2012*; *Estillore et al., 2016*; *Rossi, 2003*; *Stemmler et al., 2008*]. Specifically in the context of heterogeneous reactivity, it has been demonstrated that the lengths of the carbon chain and the saturation of the fatty acid molecules on surface of salt particles can control reactive uptake [*Kolb et al., 2010; Stemmler et al., 2008*]. It is not the amount of fatty acid, but the phase state that is critical to reactive uptake, inline with other works that show even sub-monolayer coating of organic films may perturb uptake of gas-phase species to the aqueous surface [*Kolb et al., 2010; Mmeriki et al., 2003; Clifford et al., 2007*]. Overall, this work concludes that bacteria-poor, lipid-rich oceans will generate highly organic submicron particles, while ocean regions with high bacteria and lipid concentrations will give rise to saltier, less organic-enriched particles, due directly to the activity of enzymes in the ocean. The strong link between lipase activity in the ocean and the chemical composition of SSA presented in this work is a significant advancement in our understanding of SSA composition and its direct link to ocean biological conditions, providing a step forward towards improved model predictions of SSA properties.

3.6 Acknowledgements

The authors would like to acknowledge K.A. Moore, K.J. Mayer, and all the collaborators involved. This study was funded by the Center for Aerosol Impacts on Chemistry of the Environment (CAICE), an NSF Center for Chemical Innovation (CHE-1305427).

Chapter 3 is in preparation: Michaud, J.M.,* Ryder, O.S.,* Sauer, J.S.,* Lee, C.,* Burkart, M.D., Prather K.A. Enzymatic Processing by Lipase in Seawater Determines Sea Spray Aerosol Composition. The dissertation author was the co-primary investigator and co-author of this paper. Authors with * contributed equally. J.M.M., O.S.R., J.S.S., C.L., and K.A.P. designed the experiment, C.L. performed single particle mass spectrometry measurements, J.S.S. performed high resolution mass spectrometry measurements, and J.M.M. performed enzyme assay measurements.

3.7 Figures

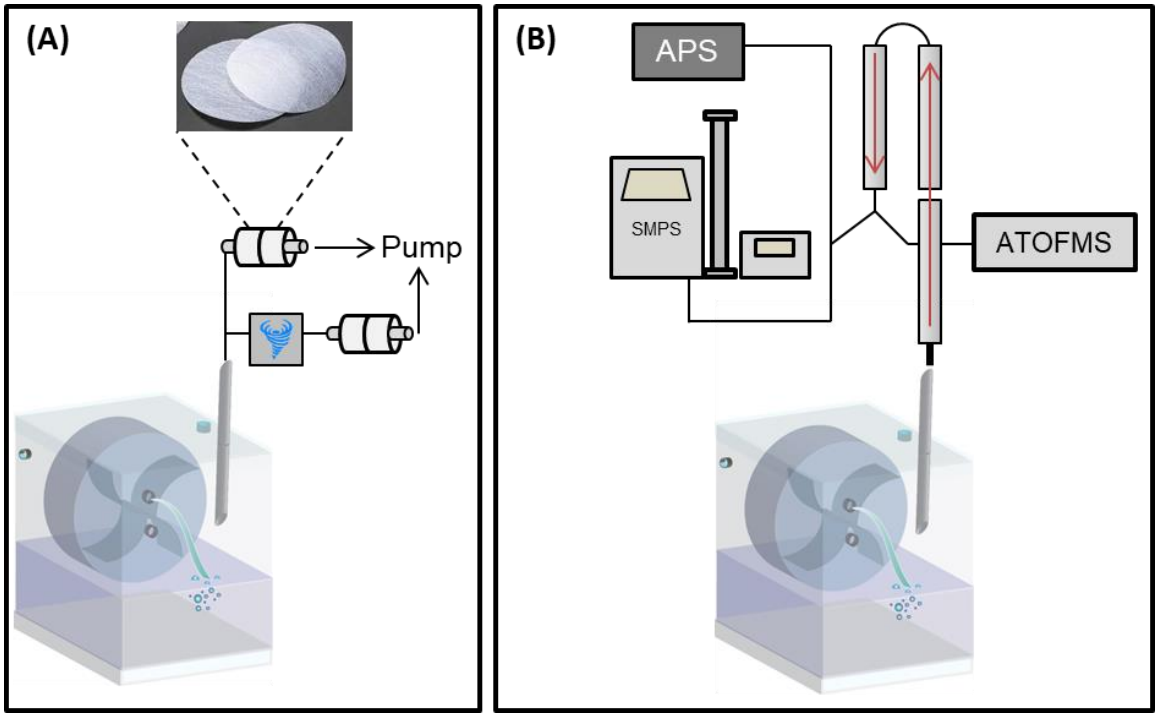

Figure 3.1. Schematic of experimental methodology. (A) Filter collection of entire SSA and size cut SSA using an aerosol cyclone (transmission of SSA < 1 µm D_a at 1.2 SLPM) and (B) Sampling of online instruments (ATOFMS: aerosol time-of-flight mass spectrometer; APS: aerodynamic particle sizer; SMPS: scanning mobility particle sizer).

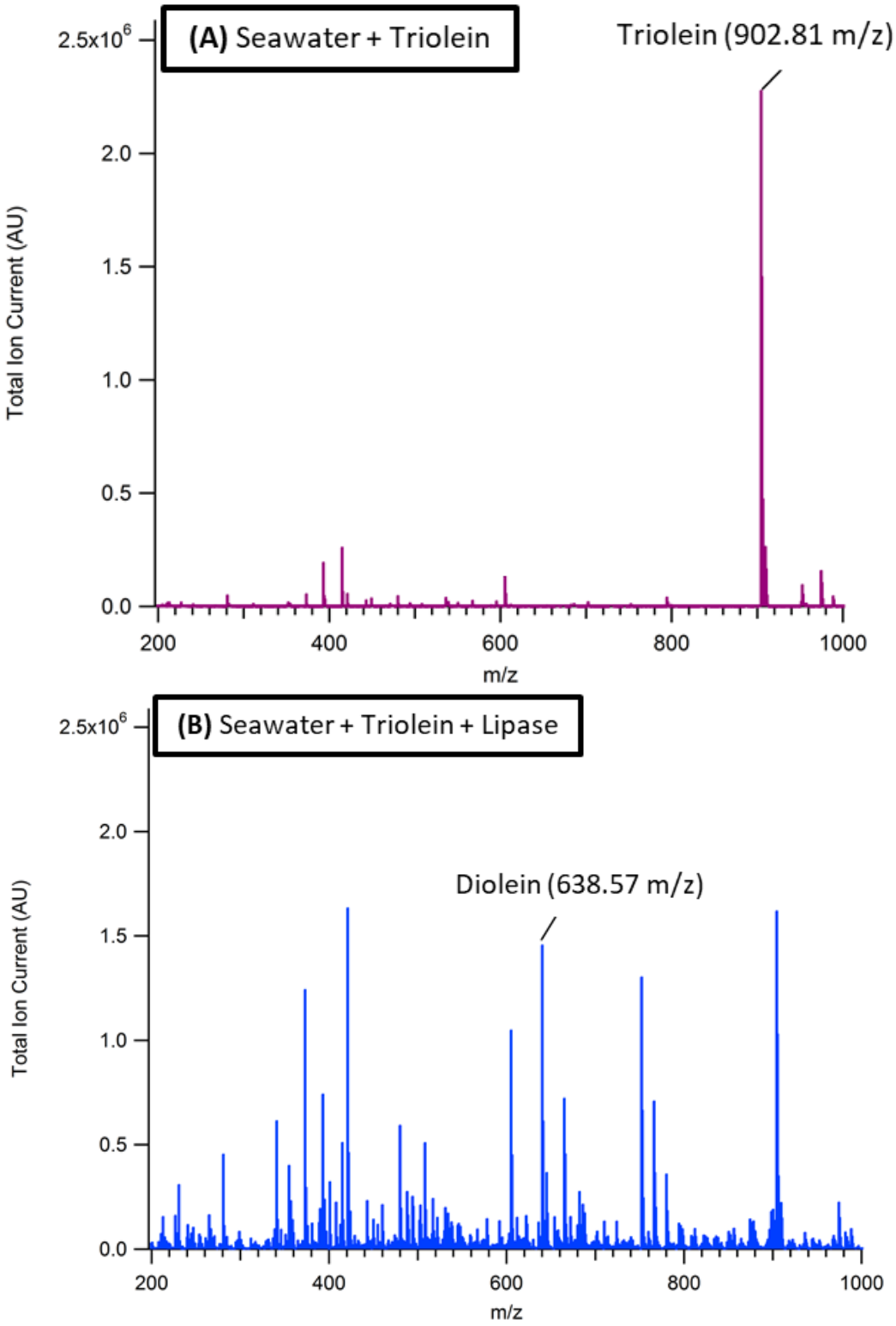

Figure 3.2. High resolution mass spectrum of triolein (A) and diolein from lipase cleavage of triolein (B) identified from complete size distribution aerosol filter sample.

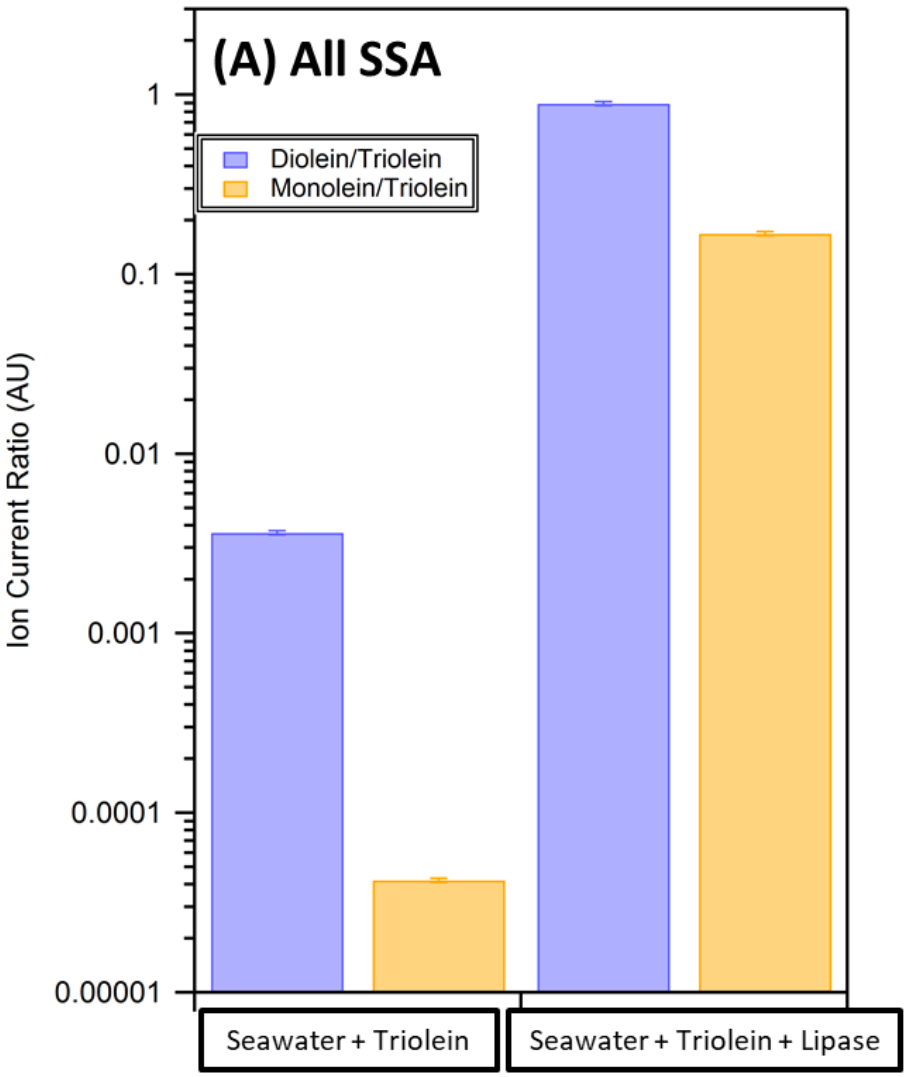

Figure 3.3. Ratio of diolein-to-triolein (blue) and monolein-to-triolein (yellow) observed in the entire SSA population (A) and submicron SSA (B) in seawater + triolein (left) and seawater + triolein + lipase (right).

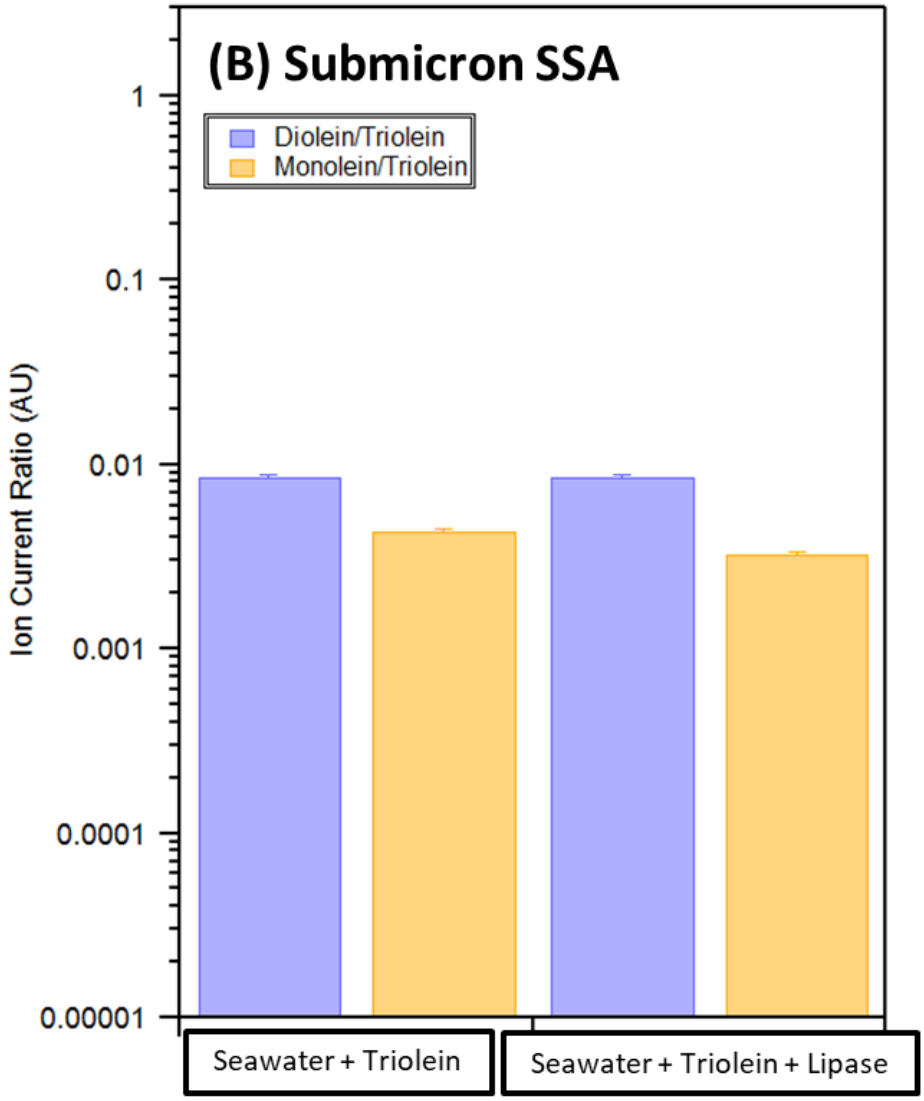

Figure 3.3. Ratio of diolein-to-triolein (blue) and monolein-to-triolein (yellow) continued.

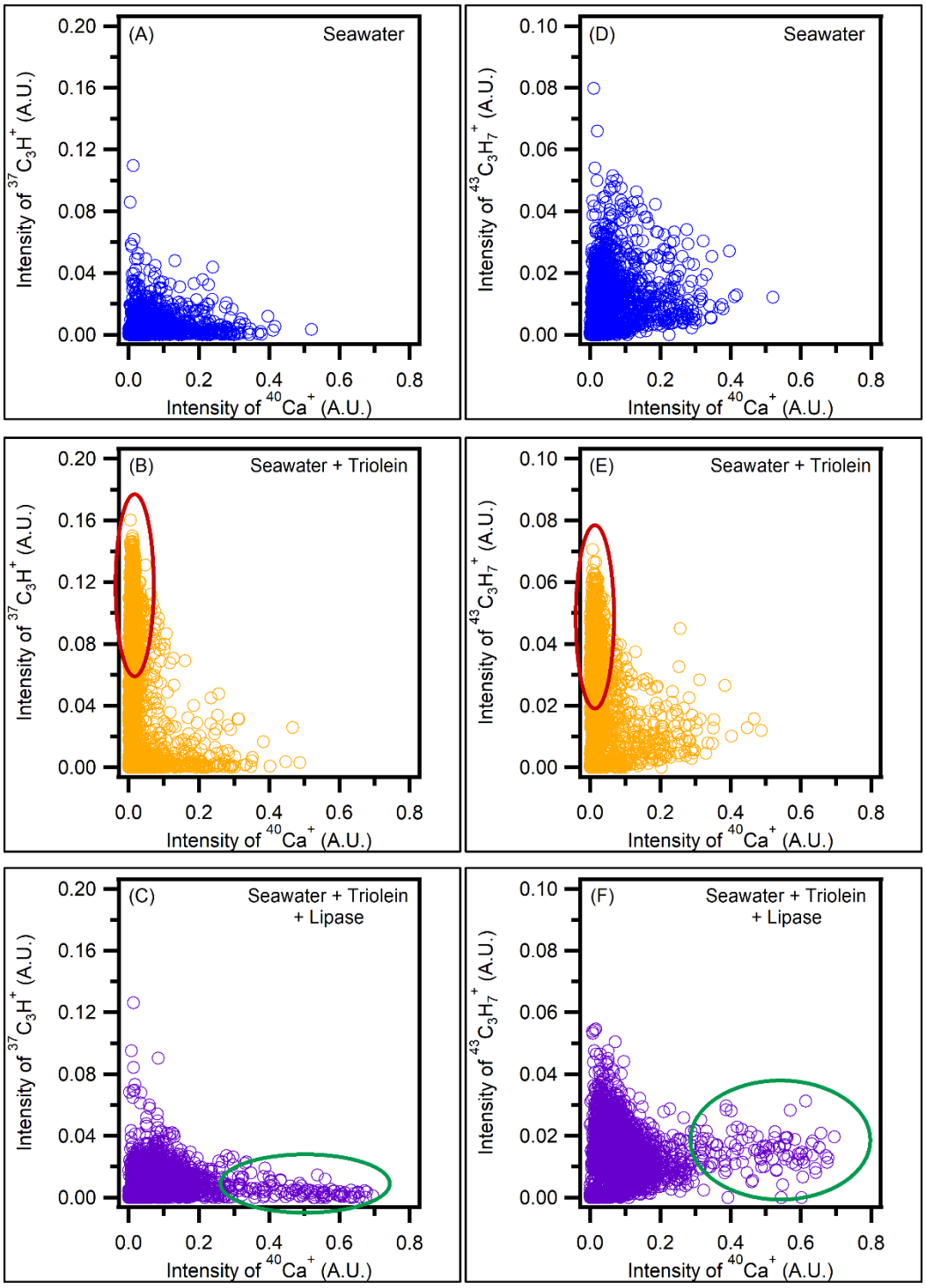

Figure 3.4. Intensity of $^{37}C_3H^+$ and $^{43}C_3H_7^+$ vs Intensity of $^{40}Ca^+$ plots for seawater background (A,D), seawater + triolein (B,E), and seawater + triolein + lipase (C,F), respectively. Red circles highlight the organic-enriched SSA due from triolein addition. Green circles highlight the emergence of particles with organic-enriched, high intensity of $^{40}Ca^+$ containing particles from the lipase cleavage of triolein.

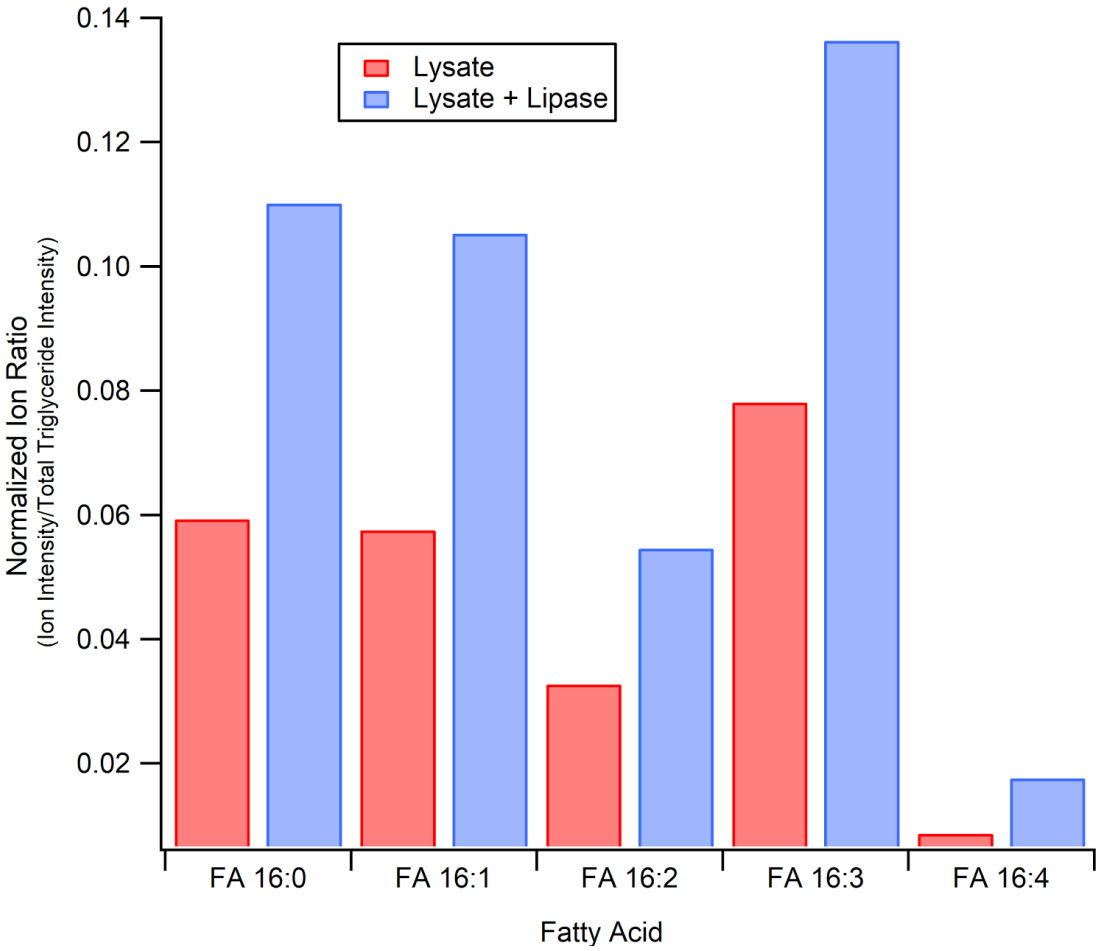

Figure 3.5. High resolution mass spectrometry derived normalized ion ratios for fatty acids identified in diatom seawater + lysate (red) and seawater + lysate + lipase (blue)

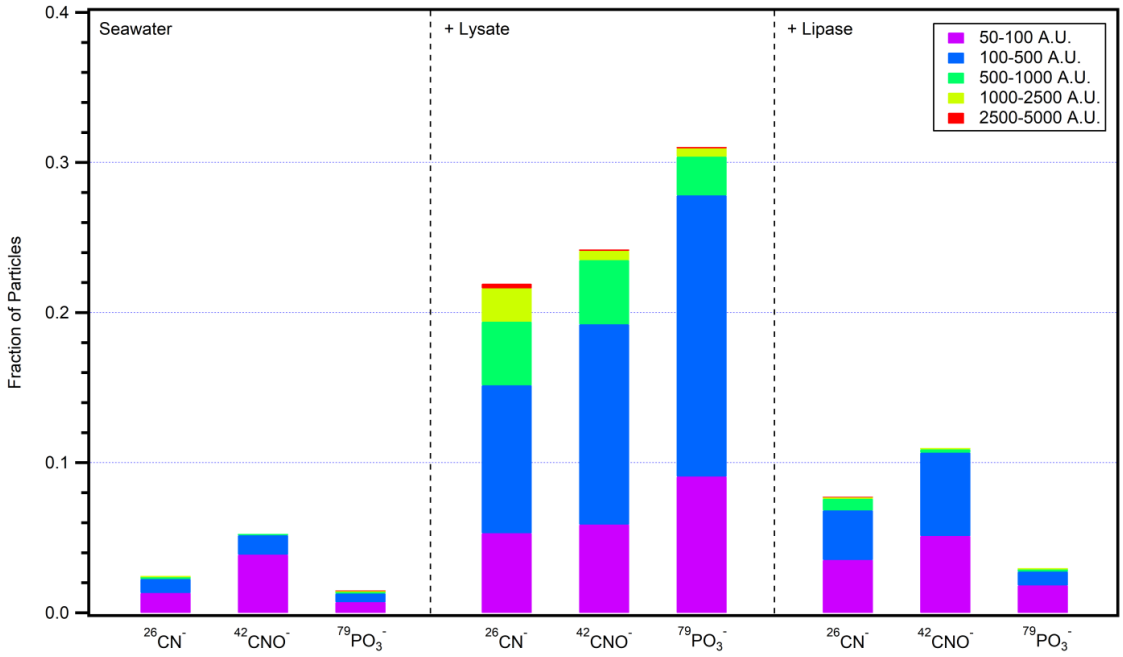

Figure 3.6. Color stack figure of particles containing $^{26}CN^-$, $^{42}CNO^-$, and $^{79}PO_3^-$ ion markers for seawater (left), seawater + lysate (center), and seawater + lysate + lipase (right). Y-axis represents the fraction of particles containing the ion marker and the color represents the intensity of the peak present in the mass spectrum.

3.8 Supporting Information

Additional information regarding the preparation of artificial seawater (ASW) medium and the control experiments demonstrating that the changes observed were not artifacts of the experimental setup can be found in Section 4.8. Chapter 4 extends the results shown in Chapter 3, thus share many of the details regarding the experimental setup.

3.8.1 Supporting Information Figures

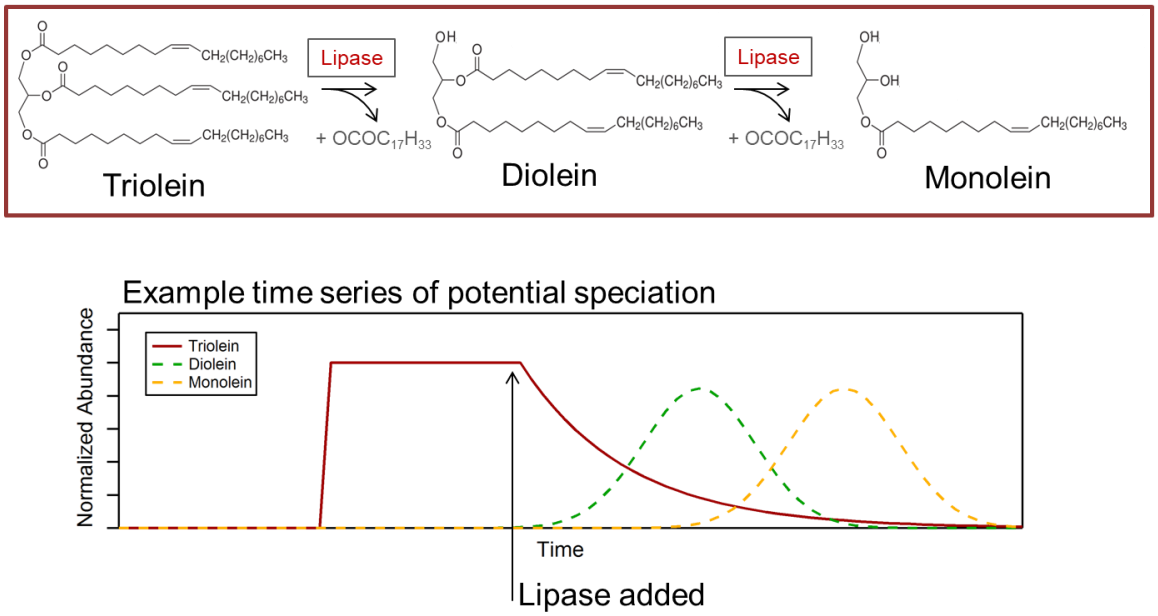

Figure 3.7. Schematic of example experiment progression. Upon lipase addition, the triolein will release oleic acid to form diolein and monolein with its potential abundance with respect to time.

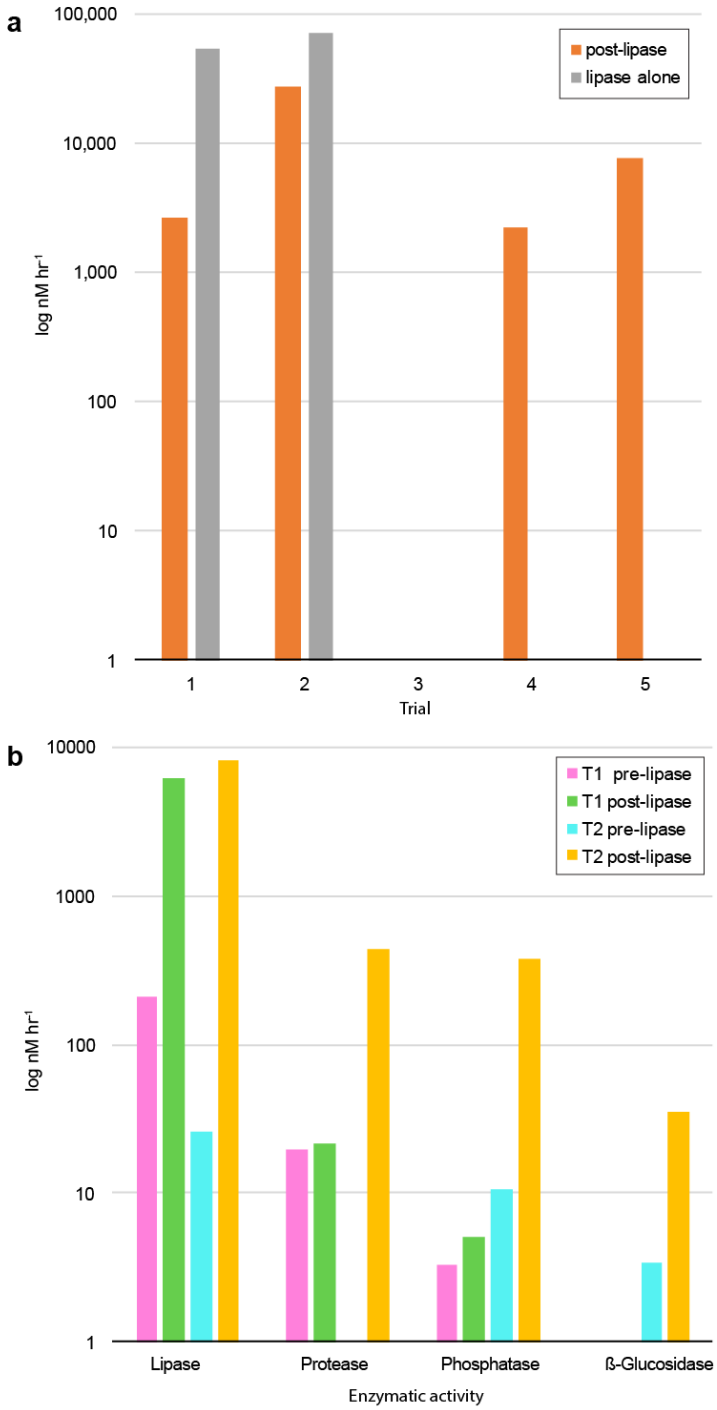

Figure 3.8 Results of enzyme assays across experiments. (a) Lipase activity by cleavage of MUF-oleate substrate across triolein runs. The activity post-lipase addition (orange) is shown and enzyme solution activity (gray) is shown for trials 1-3. Trial 3 utilized heat-killed enzyme sample and measurements verified a loss of activity. (b) Lipase (MUF-oleate), protease (MCA-Leucine), phosphatase (MUF-phosphate), and glucosidase (MUF glucose) activity are shown for *T. pseudonana* (diatom) lysate and lipase treated lysate in seawater studies. Two separate lysate experiment trials (T1, T2) are shown pre- and post- lipase addition.

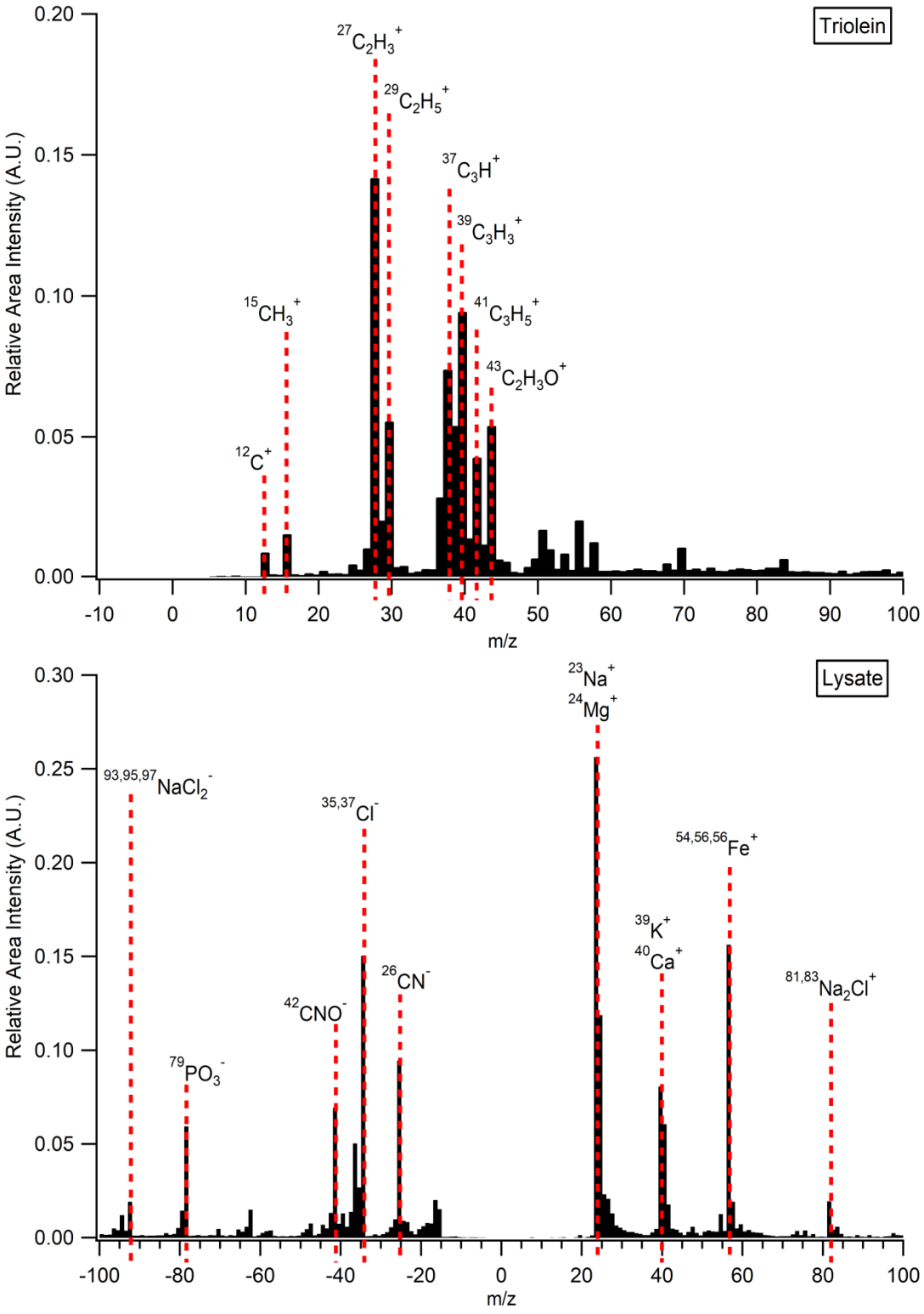

Figure 3.9. Averaged ATOFMS mass spectra of organic-enriched SSA upon triolein addition (TOP) and lysate (BOTTOM).

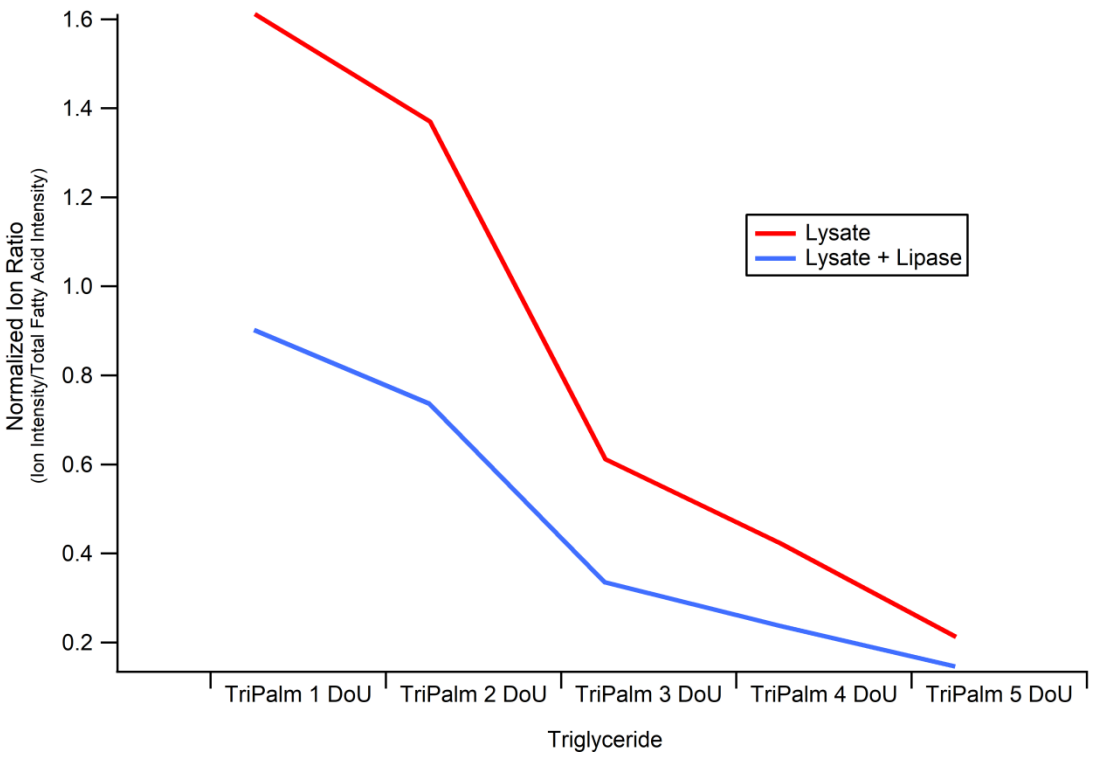

Figure 3.10. High resolution mass spectrometry derived normalized ion intensities for triglycerides for diatom lysate (blue) and lysate + lipase (red). TriPalm represents tripalmitate, and DoU stands for degrees of unsaturation. Levels of tripalmitates are decreased upon lipase addition.

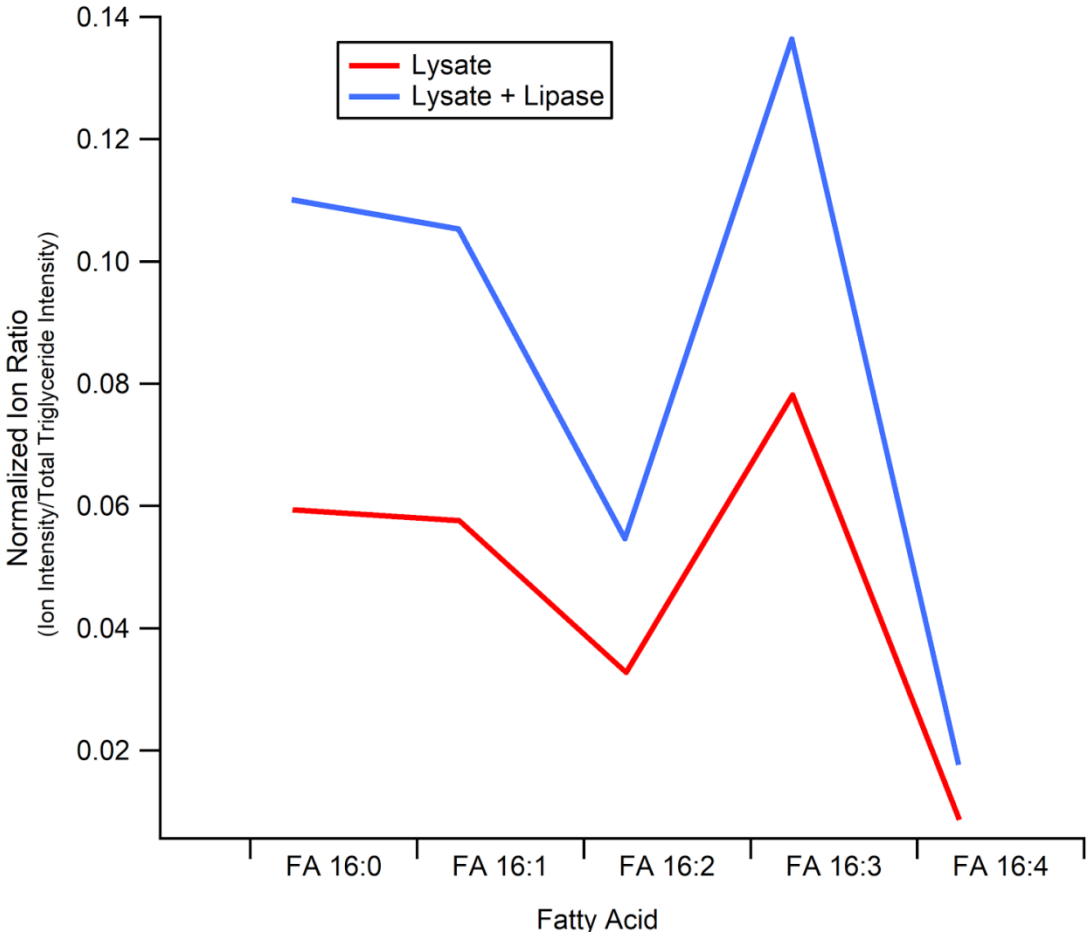

Figure 3.11. High resolution mass spectrometry derived normalized ion intensities for fatty acids (FA) for diatom lysate (red) and lysate + lipase (blue). Levels of fatty acids are increased upon lipase addition.

3.8.2 Supporting Information Tables

Table 3.1. Detailed high performance liquid chromatography gradient profile utilized for Orbitrap high resolution mass spectrometry.

Time (min)	% A	% B	% C
0.00	10.0	0.0	90.0
2.50	10.0	0.0	90.0
4.00	50.0	50.0	0.0
7.50	50.0	50.0	0.0
10.00	0.0	100.0	0.0
14.00	0.0	100.0	0.0
15.00	50.0	50.0	0.0
17.00	50.0	50.0	0.0
18.00	10.0	0.0	90.0
22.00	10.0	0.0	90.0

*Total flow remained at 0.500 L/min for entirety of run

3.9 References

Abbatt, J. P. D., A. K. Y. Lee, and J. A. Thornton, Quantifying trace gas uptake to tropospheric aerosol: recent advances and remaining challenges, Chemical Society Reviews, 41 (19), 6555, 2012.

Adams, E. M., and H. C. Allen, Palmitic acid on salt subphases and in mixed monolayers of cerebrosides: Application to atmospheric aerosol chemistry, Atmosphere, 4 (4), 315–336, 2013.

Adams, E. M., C. B. Casper, and H. C. Allen, Effect of cation enrichment on dipalmitoylphosphatidylcholine (DPPC) monolayers at the air-water interface, Journal of Colloid and Interface Science, 478, 353–364, 2016.

Arndt, S., B. B. Jørgensen, D. E. LaRowe, J. J. Middelburg, R. D. Pancost, and P. Regnier, Quantifying the degradation of organic matter in marine sediments: A review and synthesis, Earth-Science Reviews, 2013.

Arnosti, C., Microbial Extracellular Enzymes and the Marine Carbon Cycle, Annual Review of Marine Science, 3 (1), 401–425, 2011.

Arnosti, C., S. Durkin, and W. H. Jeffrey, Patterns of extracellular enzyme activities among pelagic marine microbial communities: Implications for cycling of dissolved organic carbon, Aquatic Microbial Ecology, 38 (2), 135–145, 2005.

Arnosti, C., C. Bell, D. L. Moorhead, R. L. Sinsabaugh, A. D. Steen, M. Stromberger, M. Wallenstein, and M. N. Weintraub, Extracellular enzymes in terrestrial, freshwater, and marine environments: Perspectives on system variability and common research needs, Biogeochemistry, 2014.

Ault, A. P., R. C. Moffet, J. Baltrusaitis, D. B. Collins, M. J. Ruppel, L. A. Cuadra-Rodriguez, D. Zhao, T. L. Guasco, C. J. Ebben, F. M. Geiger, T. H. Bertram, K. A. Prather, and V. H. Grassian, Size-dependent changes in sea spray aerosol composition and properties with different seawater conditions, Environ. Sci. Technol., 47, 5603–5612, 2013.

Ault, A. P., T. L. Guasco, J. Baltrusaitis, O. S. Ryder, J. V. Trueblood, D. B. Collins, M. J. Ruppel, L. A. Cuadra-Rodriguez, K. A. Prather, and V. H. Grassian, Heterogeneous reactivity of nitric acid with nascent sea spray aerosol: Large differences observed between and within individual particles, Journal of Physical Chemistry Letters, 5 (15), 2493–2500, 2014.

Azam, F., and F. Malfatti, Microbial structuring of marine ecosystems., Nature Reviews. Microbiology, 5 (10), 782–791, 2007.

Azam, F., T. Fenchel, J. G. Field, J. S. Gray, L. A. Meyer-Reil, and F. Thingstad, The ecological role of water-column microbes in the sea, Marine Ecology Progress Series, 10, 257–263, 1983.

Buchan, A., G. R. LeCleir, C. A. Gulvik, and J. M. González, Master recyclers: Features and functions of bacteria associated with phytoplankton blooms, Nature Reviews Microbiology, 12 (10), 686–698, 2014.

Clifford, D. T. Bartesis-Rausch, and D. J. Donaldson, Suppression of aqueous surface hydrolysis by monolayers of short chain organic amphiphiles, Physical Chemistry Chemical Physics, 9, 1362-1369, 2007.

Cochran, R. E., O. Laskina, T. Jayarathne, A. Laskin, J. Laskin, P. Lin, C. M. Sultana, C. Lee, K. A. Moore, C. D. Cappa, T. H. Bertram, K. A. Prather, V. H. Grassian, and E. A. Stone, Analysis of organic anionic surfactants in fine (PM2.5) and coarse (PM10) fractions of freshly emitted sea spray aerosol, Environmental Science & Technology, 50 (5), 2477–2486, 2016.

Collins, D. B., D. F. Zhao, M. J. Ruppel, O. Laskina, J. R. Grandquist, R. L. Modini, M. D. Stokes, L. M. Russell, T. H. Bertram, V. H. Grassian, G. B. Deane, and K. A. Prather, Direct aerosol chemical composition measurements to evaluate the physicochemical differences between controlled sea spray aerosol generation schemes, Atmospheric

Measurement Techniques, 7 (11), 3667–3683, 2014.

Darley, W. M., and B. E. Volcani, Role of silicon in diatom metabolism: A silicon requirement for deoxyribonucleic acid synthesis in the diatom Cylindrotheca fusiformis Reimann and Lewin, Experimental Cell Research, 58 (2–3), 334–342, 1969.

Deane, G. B., and M. D. Stokes, Scale dependence of bubble creation mechanisms in breaking waves, Nature, 418 (6900), 839–844, 2002.

Estillore, A., J. Tureblood, and V. H. Grassian, Atmospheric chemistry of bioaerosols: Heterogeneous and multiphase reactions with atmospheric oxidants and other trace gases, Chem. Sci., 7 (11), 6604–6616, 2016.

Fenchel, T., The microbial loop - 25 years later, Journal of Experimental Marine Biology and Ecology, 366 (1–2), 99–103, 2008.

Forestieri, S. D., G. C. Cornwell, T. M. Helgestad, K. A. Moore, C. Lee, G. A. Novak, C. M. Sultana, X. Wang, T. H. Bertram, K. A. Prather, and C. D. Cappa, Linking variations in sea spray aerosol particle hygroscopicity to composition during two microcosm experiments, Atmospheric Chemistry and Physics, 16, 9003-9018, 2016.

Gard, E. E., J. E. Mayer, B. D. Morrical, T. Dienes, D. P. Fergenson, and K. A. Prather, Real-time analysis of individual atmospheric aerosol particles: Design and performance of a portable ATOFMS, Analytical Chemistry, 69 (20), 4083–4091, 1997.

Groussman, R. D., M. S. Parker, and E. V. Armbrust, Diversity and evolutionary history of iron metabolism genes in diatoms, PLoS ONE, 10 (6), 1–25, 2015.

Hama, T., Fatty acid composition of particulate matter and photosynthetic products in subarctic and subtropical Pacific, Journal of Plankton Research, 21 (7), 1355–1372, 1999.

Hildebrand, M., A. K. Davis, S. R. Smith, J. C. Traller, and R. Abbriano, The place of diatoms in the biofuels industry, Biofuels, 3 (2), 221–240, 2012.

Hoppe, H.-G., Use of fluorogenic model substrates for extracellular enzyme activity (EEA) measurement of bacteria, Handbook of Methods in Aquatic Microbial Ecology, 423–431, 1993.

Kalo, P. J., V. Ollilainen, J. M. Rocha, and F. X. Malcata, Identification of molecular species of simple lipids by normal phase liquid chromatography-positive electrospray tandem mass spectrometry, and application of developed methods in comprehensive analysis of low erucic acid rapeseed oil lipids, International Journal of Mass Spectrometry, 254 (1–2), 106–121, 2006.

Kattner, G., G. Gercken, and K. Hammer, Development of lipids during a spring plankton bloom in the northern North Sea, Marine Chemistry, 14, 163–173, 1983.

Kolb, C. E., R. A. Cox, J. P. D. Abbatt, M. Ammann, E. J. Davis, D. J. Donaldson, B. C. Garrett, C. George, P. T. Griffiths, D. R. Hanson, M. Kulmala, G. McFiggans, U. Poschl, I.

Riipinen, M. J. Rossi, Y. Rudich, P. E. Wagner, P. M. Winkler, D. R. Worsnop, and C. D. O'Dowd, An overview of current issues in the uptake of atmospheric trace gases by aerosols and clouds, Atmospheric Chemistry and Physics, 10 (21), 10561-10605, 2010.

Kooistra, W. H. C. F., R. Gersonde, L. K. Medlin, and D. Mann, The origin and evolution of the diatoms: their adaptation to a planktonic existence (P. G. Falkowski & A. H. Knoll, Eds.), *Evolution of planktonic photoautotrophs*. Burlington, MA: Elsevier Academic Press, 2007.

De Leeuw, G., E. L. Andreas, M. D. Anguelova, C. W. Fairall, R. Ernie, C. O. Dowd, M. Schulz, and S. E. Schwartz, Production flux of sea-spray aerosol, Reviews of Geophysics, 80 (2010), 1–39, 2011.

Liu, X., J. E. Penner, B. Das, D. Bergmann, J. M. Rodriguez, S. Strahan, M. Wang, and Y. Feng, Uncertainties in global aerosol simulations: Assessment using three meteorological data sets, Journal of Geophysical Research Atmospheres, 112 (11), 2007.

Mmereki, B. T., S. R. Chaudhuri, and D. J. Donaldson, Enhanced uptake of PAHs by organic-coated aqueous surfaces, Journal of Physical Chemistry A, 107, 2264-2269, 2003.

Nguyen, Q. T., K. H. Kjær, K. I. Kling, and T. Boesen, Impact of fatty acid coating on the CCN activity of sea salt particles, Tellus B: Chemical and Physical Meteorology, 889, 1–15, 2017.

O'Dowd, C. D., M. C. Facchini, F. Cavalli, D. Ceburnis, M. Mircea, S. Decesari, S. Fuzzi, Y. J. Yoon, and J.-P. Putaud, Biogenically driven organic contribution to marine aerosol., Nature, 431 (7009), 676–680, 2004.

Parrish, C. C., Lipids in marine ecosystems, ISRN Oceanography, 2013, 1–16, 2013.

Pedler, B. E., L. I. Aluwihare, and F. Azam, Single bacterial strain capable of significant contribution to carbon cycling in the surface ocean, Proceedings of the National Academy of Sciences of the United States of America, 111 (20), 7202–7207, 2014.

Pomeroy, L. R., P. J. I. Williams, F. Azam, and J. E. Hobbie, The microbial loop, Oceanography, 20 (2), 28–33, 2007.

Prather, K. A., T. Nordmeyer, and K. Salt, Real-time characterization of individual aerosol particles using time-of-flight mass spectrometry, Analytical Chemistry, 66 (9), 1403–1407, 1994.

Prather, K. A., T. H. Bertram, V. H. Grassian, G. B. Deane, M. D. Stokes, P. J. Demott, L. I. Aluwihare, B. P. Palenik, F. Azam, J. H. Seinfeld, R. C. Moffet, M. J. Molina, C. D. Cappa, F. M. Geiger, G. C. Roberts, L. M. Russell, A. P. Ault, J. Baltrusaitis, D. B. Collins, C. E. Corrigan, L. A. Cuadra-Rodriguez, C. J. Ebben, S. D. Forestieri, T. L. Guasco, S. P. Hersey, M. J. Kim, W. F. Lambert, R. L. Modini, W. Mui, B. E. Pedler, M. J. Ruppel, O. S. Ryder, N. G. Schoepp, R. C. Sullivan, and D. Zhao, Bringing the ocean into the laboratory to probe the chemical complexity of sea spray aerosol., Proceedings of the National Academy of Sciences of the United States of America, 110 (19), 7550–5,

2013.

Pratt, K. A., and K. A. Prather, Mass spectrometry of atmospheric aerosols-Recent developments and applications. Part I: Off-line mass spectrometry techniques, Mass Spectrometry Reviews, 2012.

Pratt, K. A., and K. A. Prather, Mass spectrometry of atmospheric aerosols-Recent developments and applications. Part II: On-line mass spectrometry techniques, Mass Spectrometry Reviews, 2012.

Qiu, Y., and V. Molinero, Morphology of liquid–liquid phase separated aerosols, Journal of the American Chemical Society, 2015.

Quinn, P. K., D. B. Collins, V. H. Grassian, K. A. Prather, and T. S. Bates, Chemistry and related properties of freshly emitted sea spray aerosol, Chemical Reviews, 115, 4383–4399, 2015.

Quinn, P. K., T. S. Bates, K. S. Schulz, D. J. Coffman, A. A. Frossard, L. M. Russell, W. C. Keene, and D. J. Kieber, Contribution of sea surface carbon pool to organic matter enrichment in sea spray aerosol, Nature Geoscience, 7 (3), 228–232, 2014.

Riemann, L., G. F. Steward, and F. Azam, Dynamics of bacterial community composition and activity during a mesocosm diatom bloom, Applied and Environmental Microbiology, 66 (2), 578–587, 2000.

Rinaldi, M., S. Fuzzi, S. Decesari, S. Marullo, R. Santoleri, A. Provenzale, J. Von Hardenberg, D. Ceburnis, A. Vaishya, C. D. O'Dowd, and M. C. Facchini, Is chlorophyll-a the best surrogate for organic matter enrichment in submicron primary marine aerosol?, Journal of Geophysical Research: Atmospheres, 118 (10), 4964–4973, 2013.

Rossi, M. J., Heterogeneous reactions on salts, Chemical Reviews, 103 (12), 4823–4882, 2003.

Ryder, O. S., N. R. Campbell, H. Morris, S. Forestieri, M. J. Ruppel, C. Cappa, A. Tivanski, K. Prather, and T. H. Bertram, Role of organic coatings in regulating N_2O_5 reactive uptake to sea spray aerosol, Journal of Physical Chemistry A, 119 (48), 11683–11692, 2015.

Stemmler, K., A. Vlasenko, C. Guimbaud, and M. Ammann, The effect of fatty acid surfactants on the uptake of nitric acid to deliquesced NaCl aerosol, Atmospheric Chemistry and Physics, 8, 5127–5141, 2008.

Stokes, M. D., G. B. Deane, D. B. Collins, C. D. Cappa, T. H. Bertram, A. Dommer, S. Schill, S. Forestieri, and M. Survilo, A miniature Marine Aerosol Reference Tank (miniMART) as a compact breaking wave analogue, Atmospheric Measurement Techniques, 9, 4257–4267, 2016.

Struthers, H., A. M. L. Ekman, P. Glantz, T. Iversen, a. Kirkevåg, O. Seland, E. M. Mårtensson, K. Noone, and E. D. Nilsson, Climate-induced changes in sea salt aerosol number emissions: 1870 to 2100, Journal of Geophysical Research: Atmospheres, 118 (2), 670–682, 2013.

Sultana, C. M., G. C. Cornwell, P. Rodriguez, and K. A. Prather, FATES: A flexible analysis toolkit for the exploration of single-particle mass spectrometer data, Atmospheric Measurement Techniques, 10 (4), 1323–1334, 2017.

Tonon, T., D. Harvey, T. R. Larson, and I. A. Graham, Long chain polyunsaturated fatty acid production and partitioning to triacylglycerols in four microalgae, Phytochemistry, 61 (1), 15–24, 2002.

Wang, X., C. M. Sultana, J. Trueblood, T. C. J. Hill, F. Malfatti, C. Lee, O. Laskina, K. A. Moore, C. M. Beall, C. S. McCluskey, G. C. Cornwell, Y. Zhou, J. L. Cox, M. A. Pendergraft, M. V. Santander, T. H. Bertram, C. D. Cappa, F. Azam, P. J. DeMott, V. H. Grassian, and K. A. Prather, Microbial control of sea spray aerosol composition: A tale of two blooms, ACS Central Science, 1 (3), 124–131, 2015.

Weiss, M. S., U. Abele, J. Weckesser, W. Welte, E. Schiltz, and G. E. Schulz, Molecular architecture and electrostatic properties of a bacterial porin, Science, 254 (5038), 1627–1630, 1991.

Zahardis, J., and G. A. Petrucci, The oleic acid-ozone heterogeneous reaction system: products, kinetics, secondary chemistry, and atmospheric implications of a model system – a review, Atmospheric Chemistry and Physics, 7, 1237–1274, 2007.

Zendejas, F. J., P. I. Benke, P. D. Lane, B. A. Simmons, and T. W. Lane, Characterization of the acylglycerols and resulting biodiesel derived from vegetable oil and microalgae (Thalassiosira pseudonana and Phaeodactylum tricornutum), Biotechnology and Bioengineering, 109 (5), 1146–1154, 2012.

Zhang, T., M. G. Cathcart, A. S. Vidalis, and H. C. Allen, Cation effects on phosphatidic acid monolayers at various pH conditions, Chemistry and Physics of Lipids, 200, 24–31, 2016.

Zimmerman, A. E., A. C. Martiny, and S. D. Allison, Microdiversity of extracellular enzyme genes among sequenced prokaryotic genomes, The ISME Journal, 7 (6), 1187–1199, 2013.

4 The Effect of Lipase on Sea Spray Aerosol Mixing State and the Impact on Nitric Acid Heterogeneous Reactivity

4.1 Synopsis

Lipase activity in seawater impacts the organic composition of SSA. However, the question remains concerning how these enzymatically-induced changes can impact the atmospheric properties of SSA, such as their ability to react with gases. Previous heterogeneous reactivity studies of realistic individual SSA produced from an ocean-atmosphere facility exhibited large differences in reactivity. It is thus crucial to understand the underlying role that enzymes have on SSA reactivity to be able to reconcile the large reactivity range observed in previous laboratory studies and ambient measurements. In this study, the impact of bacterial enzymes on SSA is measured with respect to its influence on HNO_3 heterogeneous reactivity. Specifically, this is investigated using the extracellular enzyme lipase and two separate model organic substrate systems, triolein and marine phytoplankton cellular lysate from *Thalisiossira pseudonanna*. Prior to enzyme addition, triolein-enriched SSA showed a decrease in the fraction of SSA population reacted as compared to background seawater (from 0.52 to 0.29), indicating that addition of triolein inhibited HNO_3 reaction. However, in the case of cellular lysate, organic-enriched SSA showed an increase in the fraction of reacted particles (from 0.63 to 0.80). This is likely due to the presence of phospholipids, previously found in the lysate of *Thalisiossira pseudonanna* culture, providing an additional reaction pathway for HNO_3 at the surface of the SSA. Upon enzyme addition, lipase degradation of the substrate molecules brought the fractions of reacted particles in both systems closer to pre-organic added background (reacted fraction for Triolein: 0.50 and Lysate: 0.76), demonstrating that lipase can directly control the composition and heterogeneous reactivity of SSA. This work also provides further insight into the previously

unidentified link between marine enzymes used by microorganisms and the behavior of SSA in the atmosphere.

4.2 Introduction

Sea spray aerosols (SSA) represent a significant fraction of tropospheric aerosol particles [*Grythe et al., 2014*; *De Leeuw et al., 2011*; *Lewis and Schwartz, 2004*]. While SSA play a crucial role in the atmosphere by interacting directly with solar radiation [*Murphy et al., 1998*] and indirectly by affecting cloud properties [*Partanen et al., 2014*], our current understanding of SSA effects on climate still contain large uncertainties [*Carslaw et al., 2013*; *De Leeuw et al., 2011*], much larger than those associated with greenhouse gases [*IPCC, 2014*]. Therefore, closer examination of SSA and the biogeochemical factors that affect its physicochemical nature is warranted, as these changes in SSA chemistry are important as organic components of SSA has been shown to influence their climate properties such as water uptake [*Cruz and Pandis, 2000*; *Saxena and Hildemann, 1995*], heterogeneous nucleation of ice [*Cziczo et al., 2004*; *Möhler et al., 2008*], and chemical reactivity with atmospherically important trace gases [*McNeill et al., 2006*; *Ryder et al., 2014*].

Freshly emitted SSA contain both inorganic and organic material, depending on the biogeochemical state of the ocean [*O'Dowd et al., 2004*]. A wide array of organic matter are synthesized and altered by the microbiology present in the ocean [*Azam and Malfatti, 2007*; *Pomeroy et al., 2007*], and certain lower solubility organic matter ejected during the breaking of the waves [*De Leeuw et al., 2011*; *Lewis and Schwartz, 2004*] can strongly affect the climate-relevant properties of the resultant SSA [*Cochran et al., 2017*; *Quinn et al., 2015*]. Studies that link the organic content of SSA with remotely sensed surface ocean biomarkers, such as chlorophyll-a (Chl-a) concentration that represents phytoplankton biomass, have been

inconclusive [*McClain, 2009*; *O'Dowd et al., 2004*; *Quinn et al., 2014*; *Rinaldi et al., 2013*]. Recent work by Wang and Sultana et al. 2015 suggests a mechanistic framework based on laboratory mesocosm studies where the microbial degradation processes in the ocean and the SSA organic enrichment are coupled. Therefore, in an effort to elucidate the role of biological processes on SSA chemical composition, systematic laboratory studies are required to explore the effect from individual steps in biological processing, such as heterotrophic bacterial enzyme degradation of organic molecules [*Azam and Malfatti, 2007*].

Specifically, in the study by Wang and Sultana et al., the breakdown of aliphatic organic matter by lipase was suggested to be a key factor in controlling the size specific organic enrichment of SSA [*Wang et al., 2015*]. One of the ways marine bacteria hydrolyze polymers and particles is *via* use of extracellular enzymes [*Azam and Malfatti, 2007*; *Gupta et al., 2004*]. These transform organic matter produced during phytoplankton primary production into a form that is digestible by heterotrophic bacterial species [*Azam and Malfatti, 2007*; *Ducklow, 1999*; *Gupta et al., 2004*; *Martinez et al., 1996*]. If these enzymes are directly ejected into SSA, they can continue to alter SSA physicochemical properties in the atmosphere (Chapter 5) [*Reis et al., 2009*].

This work provides direct evidence concerning the effect of seawater enzymatic activity on the chemical composition and heterogeneous reactivity of SSA in the atmosphere. Two model organic molecule systems were chosen to be investigated in this study: triolein and cellular lysate from marine phytoplankton culture. Triolein is a good candidate to monitor the impact on SSA physicochemical properties for the following reasons: 1) triolein is an proxy triglyceride produced by marine phytoplankton [*Yu et al., 2009*] and 2) enzymatic degradation of triolein by lipase is well documented [*Gupta et al., 2004*; *Hoppe and Theimer, 1996*; *Lee et al., 1998*; *Salentinig et al., 2010*; *Schotz and Grove, 1970*]. To better represent ocean organic complexity, cellular lysate (herein referred to as lysate) containing a myriad of different organic molecules extracted from

the culture of lipid-rich marine phytoplankton *Thalisiossira pseudonanna*, was used as the second model system. Example lipase degradation schemes for triolein and two organic molecules previously identified in *Thalisiossira pseudonanna* [*Suzumura, 2005*; *Vieler et al., 2007*; *Yu et al., 2009*] are shown in Figure 4.1. Herein we describe model experiments that show how lipase activity in seawater affects SSA chemical composition and reactivity when relevant lipids such as triolein or marine phytoplankton lysate are present in the seawater.

4.3 Materials and Methods

4.3.1 SSA Generation and Sequential Additions to Seawater

A miniature-marine aerosol reference tank (miniMART) was recently developed as a compact breaking wave analogue and was used for these studies [*Stokes et al., 2016*]. Further detail can be found elsewhere [*Stokes et al., 2016*], but in brief, the tank utilizes a rotating water wheel to produce an intermittently plunging water jet into an approximately 6 L reservoir. The plunging jet action results in a bubble plume and whitecap that are similar to that of the original marine aerosol reference tank (MART) [*Stokes et al., 2013, 2016*], and thus to breaking waves [*Stokes et al., 2013*]. The smaller reservoir allows for gentler condition and smaller, better controllable amounts prepared of triolein, lysate, and lipase. All surfaces of the miniMART were cleaned by wiping with ethanol (90% v/v) and Kimwipes, and multiple rinses of ultra-pure water in between experiments. For this study, seawater was prepared through either of the following methods: 1) filtering natural seawater collected at Scripps Pier (La Jolla, CA; 32º 52' 00'' N, 117º 15' 21'' W, approx. 1 µm sand filtered) using 0.7 µm filter (Whatman GF/F, Z242489) to remove most of the particulate organic matter (POM) then autoclaved (121 ºC; 90 min) to stop the growth of microbiology that are smaller than the filter cut-size that have passed through [*Verdugo et al.*,

2004], or 2) synthesizing artificial seawater by dissolving reef salt mix (Brightwell Aquatics, NēoMarine, 35.53 g L^{-1}) in ultra-pure water followed by autoclaving the seawater.

Approximately 6 L of the prepared seawater was put in the miniMART reservoir, and the headspace purged with particle-free zero air (Sabio Instruments, Model 1001). The flow rate of the particle free air was always greater by 1 SLPM than the flow pulled by the instrument to ensure positive pressurization of the miniMART headspace, preventing accidental back-sampling of room air. Under typical operating conditions during SSA generation, the minimart headspace had relative humidity (RH) >90% (Vaisala, HMP110).

Due to the low concentration of particles generated from the miniMART (90 cm^{-3}) [*Stokes et al., 2016*], sampling of unreacted SSA occurred on the first day of an addition, followed by sampling of the flow tube reacted SSA the following day in order to sample a statistically significant number of particles under both conditions. Further details regarding instrumentation are discussed below. Control experiments performed confirmed the stability of the seawater and SSA chemical properties to verify that the seawater and SSA chemical and physical properties observed on the second day were not artifacts of the sampling protocol. After two days of measurements on the seawater background, 500 mg of triolein (Sigma-Aldrich, T7140) was added and measured for two days, followed lastly by the addition of 2 mg of lipase (Sigma-Aldrich, lipase from *pseudomonas cepacia,* 62309) for another two days of measurement, alternating between unreacted and reacted SSA measurements respectively. In the cellular lysate experiment, 500 mg of lysate was obtained through French-pressing of a culture of *Thalisiossira pseudonanna* grown in an artificial seawater (ASW) medium (recipe in 4.8). The extracted lysate was then added in place of triolein, keeping all other experimental procedures the same. Additional control experiments performed verified the changes observed in this sequential addition experiment were due to actual biochemical changes occurring in the seawater.

4.3.2 Sampling of Nascent SSA

For online measurement of the chemical composition and size distribution of unreacted SSA, miniMART generated aerosol were dried using three diffusion driers reducing the RH to <10%. The sample flow was then split between aerodynamic particle sizer (APS, TSI Model 3321), and aerosol time-of-flight mass spectrometer (ATOFMS) (Figure 4.2). The APS provided size distributions of SSA particles generated from the miniMART in the size ranges of 0.5-20 µm D_a (aerodynamic diameter), where the ATOFMS provided real-time measurement of single particle size and chemical composition of SSA between 0.2 to 3.0 µm D_{va} (vacuum aerodynamic diameter) [*Gard et al., 1997*].

More detailed information concerning the ATOFMS can be found elsewhere [*Gard et al., 1997*] and in Section 1.5.3. Data are imported into MATLAB (The Math-Works, Inc.) with software toolkit FATES [*Sultana et al., 2017*] for further data analysis and particle types were determined using ART-2a clustering algorithm [*Song et al., 1999*]. Uncertainty in the reported fractions of particles was calculated using equations (4.1) and (4.2), where F is fraction, x is the number of particles containing select ion marker, N is total number of particles, and SE stands for standard error of 1σ.

$$\mathrm{F} = \frac{x}{N} \tag{E4.1}$$

$$\mathrm{SE} = \sqrt{\frac{F(1-F)}{N}} \tag{E4.2}$$

MiniMART generated SSA were collected for further offline analysis using a micro orifice uniform deposit impactor (MOUDI, MSP Corp. model 100-NR, 10 stages) (Figure 4.2). The MOUDI allows aerodynamic size-fractionated particle samples to be collected. SSA particles between the size ranges of 0.56 and 1.0 µm were collected on Si wafer substrates (Ted Pella Inc.,

16008) mounted on MOUDI stage 6, and were analyzed using atomic force microscope (Bruker Dimension Icon and Dimension Fast Scan Atomic Force Microscopes running in scanasyst air mode) for investigation of particle morphology.

4.3.3 Sampling of Reacted SSA using Aerosol Reaction Flow Tube

To probe the reactivity of the SSA over the course of the experiment, an aerosol reaction flow tube setup was utilized. The sample flow containing SSA generated from the miniMART was split prior to the diffusion driers (Figure 4.2). The portion that did not flow through the diffusion driers was directed into the flow tube (Figure 4.2) for reaction with HNO_3 gas. Detailed experimental setup of the flow tube can be found in 5.8.5. In brief, HNO_3 permeation tube (Kin-Tek, HRT-010.00-2022/60) was heated to 30 ℃ and used as a constant source of reactant gas. The residence time of the flow tube was 1.8 min, the concentration of HNO_3 at the top of the flow tube was approximately 10 ppb and the flow tube relative humidity was 50 ± 2%. These operational reaction parameters were chosen to mimic typical conditions in an urban coastal region such as Los Angeles, CA [*Solomon et al., 1992*]. As reacted SSA exited the flow tube, the flow was split between a RH and temperature probe and a second set of diffusion driers leading to the ATOFMS.

4.4 Results and Discussion

4.4.1 Changes in Particle Size Distributions

The sequential addition of triolein and lipase to the bulk seawater led to drastic changes in the APS observed particle number size distribution (Figure 4.3). Figure 4.3B shows a significant increase in the smaller, submicron particles (<1 µm) after triolein is added, in agreement with previous observations that show submicron particle numbers increase during periods of high biological activity, indicative of organic enrichment in the seawater [*Gantt and*

Meskhidze, 2013; *Hoffman and Duce, 1974*; *O'Dowd et al., 2004*]. Similar increase in the submicron particle concentration was observed when lysate was added to the seawater (Figure 4.3E). However, in addition to the increase of mode 1 (peak at 0.85 µm D_a) observed with the triolein experiment, mode 2 (peak at 2.19 µm D_a) also increased when lysate was added (peak fitting results found in Figure 4.7; increase/decrease of mode is with respect to the other mode). The difference between the triolein and lysate results is also observed in the analysis of size-resolved particle types detected by ATOFMS (Figure 4.8 and 4.9). These results show that in the triolein experiment the fraction of organic carbon (OC) particle type indicative of triolein was skewed to smaller particle sizes. However the size of iron phosphate-rich organic (FePhosOrg) particle type, indicative of the lysate which contain phospholipids (Figure 4.1) and iron containing ferroproteins [*Geider and Roche, 1994; Groussman et al., 2015; Sunda and Huntsman, 1997*], were skewed to larger sizes. This behavior is likely due to the differences in the hydrophobicity of the organics. Triolein is hydrophobic and would be ejected in film drops to be enriched in submicron SSA [*Lewis and Schwartz, 2004*], whereas the lysate (composed of lipids, phospholipids, proteins, and fatty acids which will be complexed with cations originating from the cell structure [*Brown et al., 1996*; *Suzumura, 2005*]) will be less hydrophobic and would be ejected in jet drops, thus enriched in supermicron SSA (>1 µm) [*Lewis and Schwartz, 2004*].

When the lipase was added to the bulk seawater for the triolein and lysate experiments (Figure 4.3C and F, respectively), number size distributions further transformed, each in a different way. For the triolein experiment, the concentration of very small particles (<0.7 µm D_a) decreased, while mode 1 further increased (Figure 4.3C). This shift is attributed to break down of the insoluble aliphatic triolein by lipase into more water soluble products with respect to triolein (i.e. monolein and diolein) present in seawater [*Tang et al., 2010*; *Wang et al., 2015*] and thus will be ejected as jet drops. The number size distribution of lysate following the addition of lipase

(Figure 4.3F) lacked the change in the very small sizes (<0.7 µm D_a) observed in the triolein experiment (Figure 4.3C). However, the relative decrease in mode 2 (Figure 4.3E) upon addition of lipase to the lysate system indicates that lipase is digesting organic molecules of lysate to be better transferred in submicron SSA. Molecular analysis of the transformation of organic species in the lysate will be presented in future publications. The difference observed between the triolein and lysate SSA size distributions illustrates how critical the chemical composition and properties of organics in seawater and the air-sea interface impact their transfer to SSA.

4.4.2 Evolution of Particle Types Detected by Single Particle Mass Spectrometry

The sequential addition of the triolein/lysate and lipase can significantly impact the SSA physicochemical properties. To understand the types of particles produced throughout the course of the two separate sequential addition experiments, single particle clustering analysis of the ATOFMS detected particles was performed. Single particle clustering analysis revealed 4 particle types similar to what has been observed in the past [*Prather et al., 2013*]: sea salt (SS), sea salt mixed with organic carbon (SS-OC), OC, and FePhosOrg (Figure 4.8). It should be noted that recent study has demonstrated that the particle types such as SS and SS-OC are not two distinct particle types, but rather a continuum of particles with differences in the organic coating where the similarity threshold set in the clustering algorithm separated to two types based on the mass spectral signal of organic species [*Sultana et al., 2017*]. However, with the constant clustering threshold applied throughout the data analysis of this study, the trends in the evolution of particle types still provide meaningful insight on the changes in SSA chemistry.

Monitoring the evolution of particle types over the course of the sequential experiments provided direct evidence of how enzymes control SSA chemistry. As is expected, the addition of triolein or lysate to the seawater led to a significant increase in the OC (Figure 4.4A) or FePhosOrg (Figure 4.4B) particle fractions, respectively. Upon the addition of lipase to seawater,

OC or FePhosOrg fractions showed immediate decrease during the 1st hour post-addition, referred to as the "mixing" period. The levels of OC or FePhosOrg fractions in the respective experiments continued to decrease post-lipase addition as observed in Lipase Day 1 and 3 periods. During this time, the fraction of SS-OC increased, taking the place of OC or FePhosOrg, likely attributed to the products from the enzymatic degradation bonding with the cations present in the seawater. Ultimately, the ATOFMS-detected proportion of SSA particle types 3 days after the lipase addition very closely resembled proportions observed in the initial condition of the seawater prior to organic enrichment, demonstrating the significant impact enzymes have on the SSA chemical composition.

Given that the physicochemical properties can influence secondary atmospheric processing of SSA [*Abbatt et al., 2012*; *Cochran et al., 2017*; *Quinn et al., 2015*], the SSA physicochemical change due to the enzyme degradation processes was further investigated by performing AFM measurements and depth profiling data analysis of the ATOFMS detected particles [*Cahill et al., 2015*; *Sultana et al., 2017*; *Zelenyuk et al., 2008*]. When triolein/lysate was added to the system, the cubic salt structure changed to more oil slick-like form (Figure 4.5A, B). While a small core indicative of salt is observed within the particles, the presence of thick organic coating is likely leading to incomplete desorption/ionization of the particles to be categorized as OC. After lipase was added to the system to degrade triolein/lysate, the SSA morphology changed and exhibited a core-shell morphology with organic coating as observed in the past with organic enrichment (Figure 4.5C) [*Ault et al., 2010*; *O'Dowd et al., 2004*; *Sultana et al., 2017*]. Furthermore, depth profiling results (Figure 4.5, bottom) of such particles showed divalent cations such as calcium with signatures of organic species were present at the shell surface. This finding corroborates the trends observed in the particles types in Figure 4.4, where the particles

containing divalent cation-bound fatty acids from lipid degradation increase and replace the OC or the FePhosOrg particle types.

4.4.3 Impact of Lipase on SSA Heterogeneous Reactivity

The physicochemical changes occurring at the SSA interface can have profound implications on the heterogeneous reaction of particles in the atmosphere [*Abbatt et al., 2012*; *Ault et al., 2014*; *Cochran et al., 2017*; *Rossi, 2003*]. Reaction between SSA and HNO_3 has traditionally been viewed as involving inorganic salts, where organic coatings present on the surface act to inhibit reactive uptake [*Abbatt et al., 2012*; *Ault et al., 2014*; *Rossi, 2003*]. Recent studies have illustrated that bioorganic molecules present in SSA can undergo direct acid-base reaction with gaseous nitric acid in the atmosphere, shifting the paradigm from purely inorganic reactions to more complex reactions involving inorganic and organic species [*Cochran et al., 2017*; *Trueblood et al., 2016*]. This paradigm shift warranted further investigations of the role biological processes such as enzymatic degradation processes have on the heterogeneous reactivity of SSA and investigated in this study.

In the sequential addition experiments, addition of triolein or lysate to seawater produced SSA that exhibited very different heterogeneous reactivity. The ATOFMS can easily distinguish between unreacted and reacted SSA due to the presence of nitrate ion markers ($^{46}NO_2^-/^{62}NO_3^-$, >1% relative area intensity threshold) in the reacted SSA particle mass spectra [*Ault et al., 2013, Ault et al., 2014*; *Gard et al., 1998*]. The addition of triolein resulted in a decrease in the reacted SSA fraction (0.52 to 0.29), while the addition of lysate led to an increase in the reacted SSA fraction (0.63 to 0.80) (Figure 4.6). As observed in Figure 4.4 and 4.5B, in the case of triolein, the particles contain a small salty core and a very thick organic coating, which is inhibiting reactive uptake of HNO_3. In addition, C8 and C18 alkyl self-assembled monolayers have been shown to sequester HNO_3 due to the pockets present in their irregular mixtures of chains preventing HNO_3

reactive dissociation [*Nishino et al., 2014*] which could potential occur with triolein. However in the lysate addition case, the presence of marine relevant organic molecules from the phytoplankton cell structure that contain potential acid-base reaction sites previously suggested [*Trueblood et al., 2016*] (such as the phospholipids in Figure 4.1 at the SSA-air interface) are likely leading to additional reactive sites for HNO_3. Figure 4.10 demonstrates that the lysate can undergo reaction and result in increased uptake observed in Figure 4.6.

When lipase was added to the triolein and lysate systems, respectively, the fraction of the reacted particles in the triolein experiment returned to same level as the background measurement (prior to triolein addition, 0.50). Enzymatic degradation of triolein to fatty acids did not inhibit reactive uptake of HNO_3, consistent with previous observation that unsaturated oleic acid on NaCl surface at monolayer quantities had no detectable effect on the HNO_3 uptake [*Stemmler et al., 2008*]. It was concluded that the unsaturation in the oleic acid prevented efficient surface packing of the molecule to inhibit reactive uptake [*Stemmler et al., 2008*]. It was further concluded that the structures of the monolayer formed determined the resistance to HNO_3 uptake.

However, the fraction of reacted SSA for the lipase added lysate system decreased slightly, yet did not return to the background (pre-lysate addition) and remained elevated at 0.76. This suggests that the lipase degraded products were still readily reacting with HNO_3 at the surface of the particle. Lysate contains a myriad of organic molecules, including lipids, phospholipids, and proteins [*Yu et al., 2009*]. It is hypothesized that either 1) phospholipid backbone with fatty acids removed by lipase is undergoing reaction with HNO_3, or 2) proteins, which lipase cannot degrade due to its specificity toward lipids, can undergo reaction with HNO_3 [*Franze et al., 2005*]. Molecular understanding of the organic species in the lysate system pre- and post-lipase addition will further provide insight into the validity of these hypotheses.

However, in both of the substrate systems, lipase-induced chemical changes directly impact the SSA physicochemical properties including heterogeneous reactivity.

4.5 Conclusions

To accurately understand the impact of lipase on the heterogeneous reactivity of realistic SSA, two substrate systems. triolein and diatom lysate, were investigated in this study. While the single particle unreacted composition for the two systems exhibited similar trends following substrate and enzyme addition, the heterogeneous reactivity behavior of these particles showed a significant difference. Addition of triolein led to an inhibited reactive uptake of HNO_3, whereas addition of lysate increased the reactivity of the particles. Furthermore, lipase degradation of triolein and led to SSA reactivity behavior similar to that of the background measurement pre-substrate addition for triolein, while lipase degradation of lysate showed decrease in reactivity but stayed elevated, likely due to presence of phospholipid backbone and proteins at the surface for HNO_3 to react with. This direct comparison of simple and complex model systems demonstrate the need for caution in performing investigations of SSA properties using simple organic surfactants, as their properties may not be sufficient in replicating the important characteristics of realistic SSA. This study demonstrates seawater lipase impact on SSA heterogeneous reactivity for the first time, and shed light into the underlying microbiological role on SSA reactivity to reconcile the large reactivity range observed in previous laboratory studies and ambient measurements.

4.6 Acknowledgements

The authors would like to acknowledge K.A. Moore, K.J. Mayer, and all the collaborators involved. This study was funded by the Center for Aerosol Impacts on Chemistry of the Environment (CAICE), an NSF Center for Chemical Innovation (CHE-1305427).

Chapter 4 is in preparation: Lee, C., Ryder, O.S., Michaud, J.M., Sauer, J.S., Burkart, M.D., Prather, K.A. The Effect of Lipase on Sea Spray Aerosol Mixing State and the Impact on Nitric Acid Heterogeneous Reactivity. The dissertation author was the primary investigator and author of this paper. C.L., O.S.R., and K.A.P. designed the experiment, C.L. performed single particle mass spectrometry measurements, C.L. and O.S.R. performed atomic force microscopy measurements.

4.7 Figures

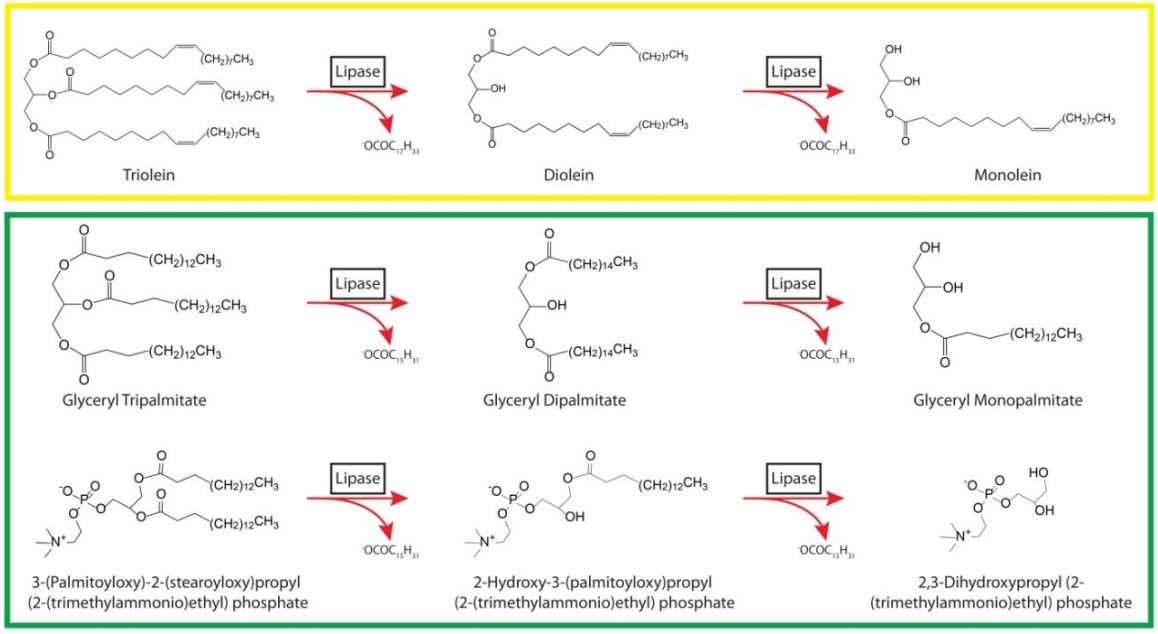

Figure 4.1. Schematic showing reactant and product molecules from lipase degradation of lipids in the sequential addition experiments: triolein (yellow) and previously identified lipid and phospholipid molecules from *Thalisiossira pseudonanna* [*Suzumura, 2005*; *Vieler et al., 2007*; *Yu et al., 2009*] (green).

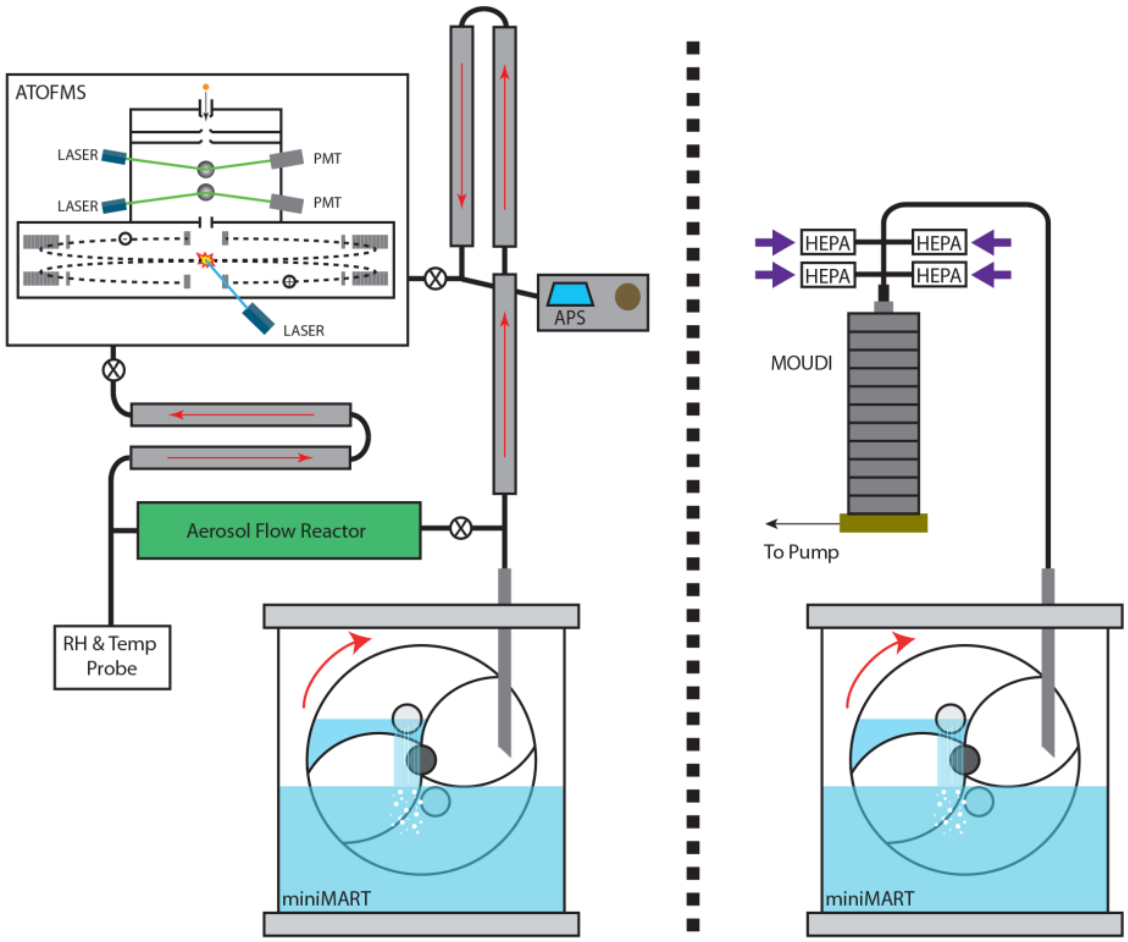

Figure 4.2. Experimental setup with online instrumentation (aerosol time-of-flight mass spectrometer, ATOFMS, aerodynamic particle sizer, APS) and aerosol flow tube (LEFT) and offline impaction collector (RIGHT)

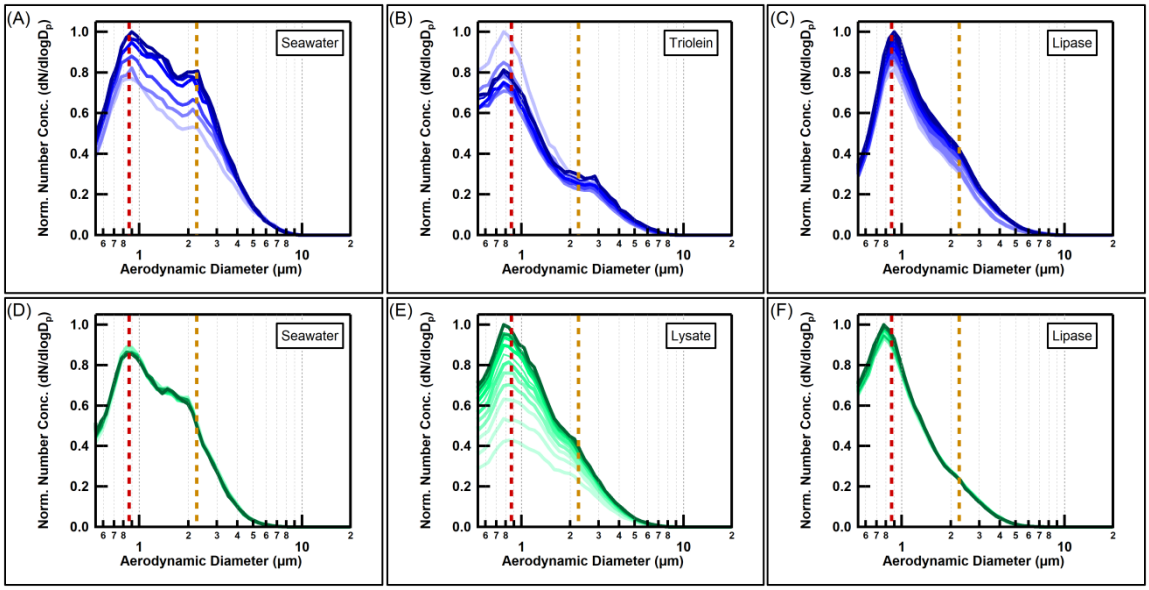

Figure 4.3. Normalized aerodynamic particle size distribution of SSA generated with seawater, organic substrate addition, and lipase addition for triolein (A-C) and lysate (D-F) experiment. Light to darker traces indicate the hourly averages since the starting of the measurement for the given period. Dashed lines (red and orange) represent modes 1 and 2 from the multi-peak fitting results, respectively.

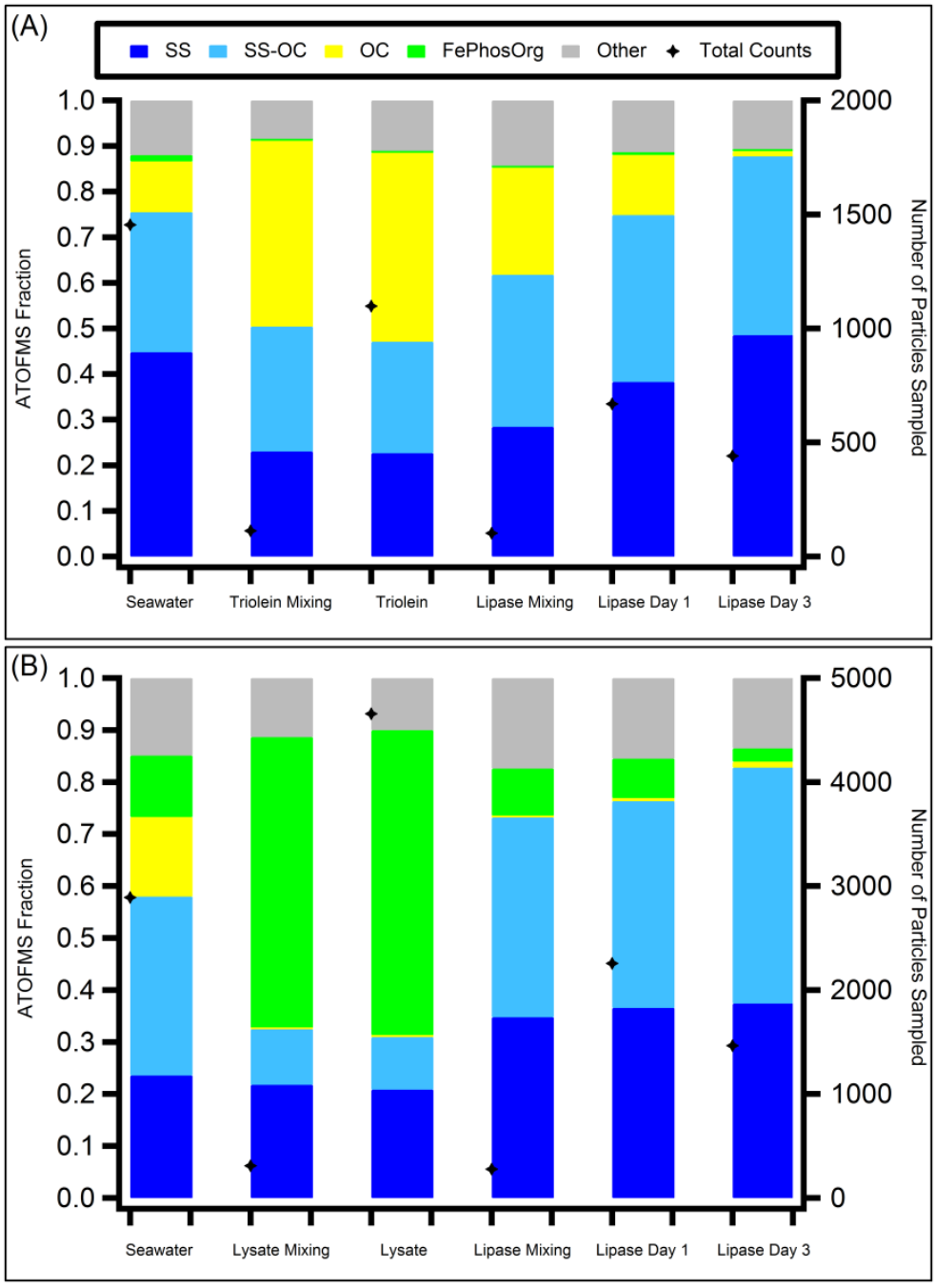

Figure 4.4. Fractions of particle types detected by ATOFMS at each step of the sequential addition experiment for (A) triolein and (B) marine phytoplankton cellular lysate as the added organic substrate. “Mixing” label denotes the first 1 h after the addition of the organic substrate or lipase. Number of particles sampled denotes the total number of particles sampled for given period.

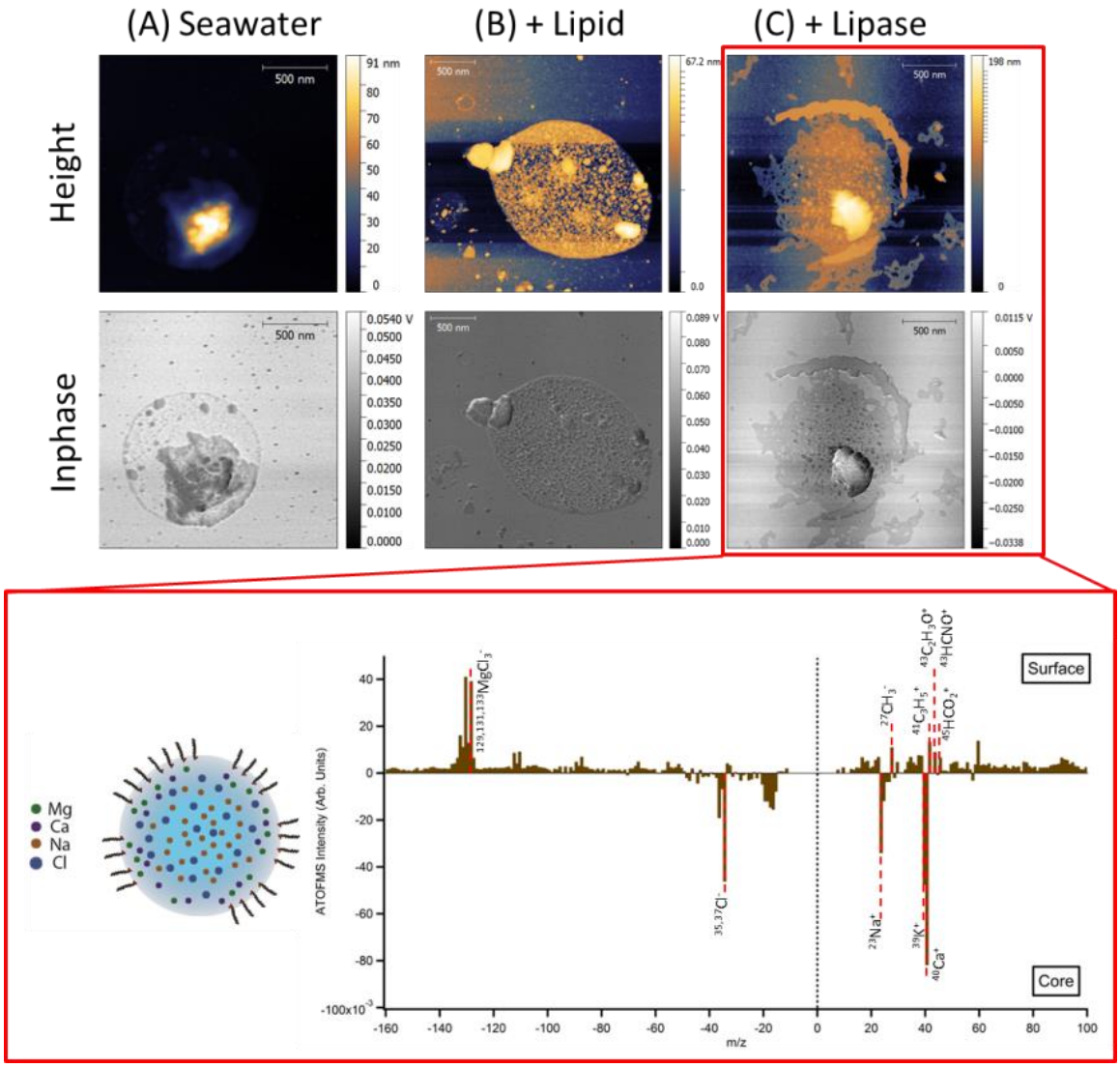

Figure 4.5. (TOP) Atomic force microscopy image of impactor sampled particles throughout the different conditions of sequential addition experiment: (A) seawater, (B) lipid added to seawater, (C) lipase added to lipid containing seawater. (BOTTOM) Subtraction spectra showing surface versus core enhanced ion markers for SS-OC particle type.

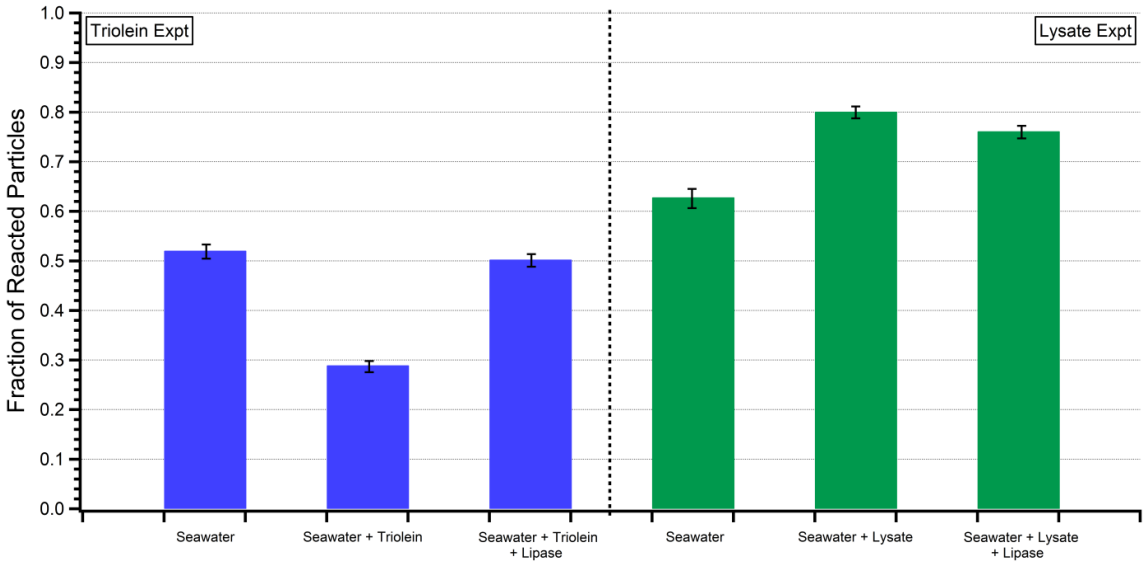

Figure 4.6. Fraction of reacted particles for triolein (blue) and lysate (green) sequential addition experiment. Error bars represent 2σ for 95% confidence limit.

4.8 Supporting Information

4.8.1 Preparation of Artificial Seawater Medium for Growth of *Thalisiossira pseudonanna* culture

Culture of *Thalisiossira pseudonanna* was grown in a mix of artificial seawater (ASW) medium that is an average of the recipes found in National Center for Marine Algae and Microbiota's ASM and ESAW media (https://ncma.bigelow.org/algal-recipes, accessed July 14, 2013), and Canadian Center for the Culture of Microorganisms' ESAW medium (www3.botany.ubc.ca/cccm/NEPCC/esaw.html, accessed July 14, 2013). List of compounds in the ASW medium can be found in Table 4.1. All glassware use in the preparation of the medium were sterilized prior to use by autoclaving at 121 ℃ for 90 min.

4.8.2 Control Experiments

In addition to the experiments detailed in main text, further control experiments were performed to verify the changes observed were not an artifact of additions. These control experiments were nascent and flow tube reacted measurements of seawater spiked with 2 mg of lipase, seawater spiked with triolein and inactive, heat-treated lipase. Size resolved chemical composition measurements with the ATOFMS revealed that chemical composition and the heterogeneous reactivity toward HNO_3 for seawater spiked with 2 mg of lipase closely resembled seawater only condition, and seawater spiked with triolein and inactive lipase resembled seawater spiked with triolein condition. Additionally, closer look at the ATOFMS sampled particles' size distributions at each condition (Figure 4.11) confidently demonstrate that the changes in the particle types observed are result of the changes in the SSA chemical composition and not from the additions and the changes in particle size distribution from the additions.

On days of flow tube measurement, HNO_3 permeation tube was loaded into temperature controlled chamber for at least 30 min. After 30 min, sodium chloride solution (Sigma Aldrich, concentration of 0.1 g NaCl / 100 mL H_2O) was atomized using a collison nebulizer [*May, 1973*] with particle free air at 1.5 SLPM and sampled with the flow tube connected to ATOFMS as shown in Figure 4.7. Calculated chloride displacement ratio after minimum sampling time of 30 min was used as a metric to evaluate fluctuations in the reaction flow tube. Calculation of the chloride displacement ratio (CDR) [*Ault et al., 2014*] can be found in equation (4.3). The calculated ratio under normal operating condition of the flow tube was approximately 0.37 ± 0.02. If the ratio was outside this average, then either 1) HNO_3 permeation tube needed more time to equilibrate or 2) walls of the flow tube had built up too much HNO_3 and needed to be rinsed and reset. At end of each flow tube measurement, the HNO_3 permeation tube was removed from the

chamber and the flow tube walls were rinsed with ultrapure water and purged with N_2 to dry overnight.

$$\mathrm{CDR} = {}^{35}Cl^{-} \Big/ \left({}^{35}Cl^{-} + {}^{46}NO_2{}^{-} + {}^{62}NO_3{}^{-}\right) \quad \text{(E4.3)}$$

4.8.3 Supporting Information Figures

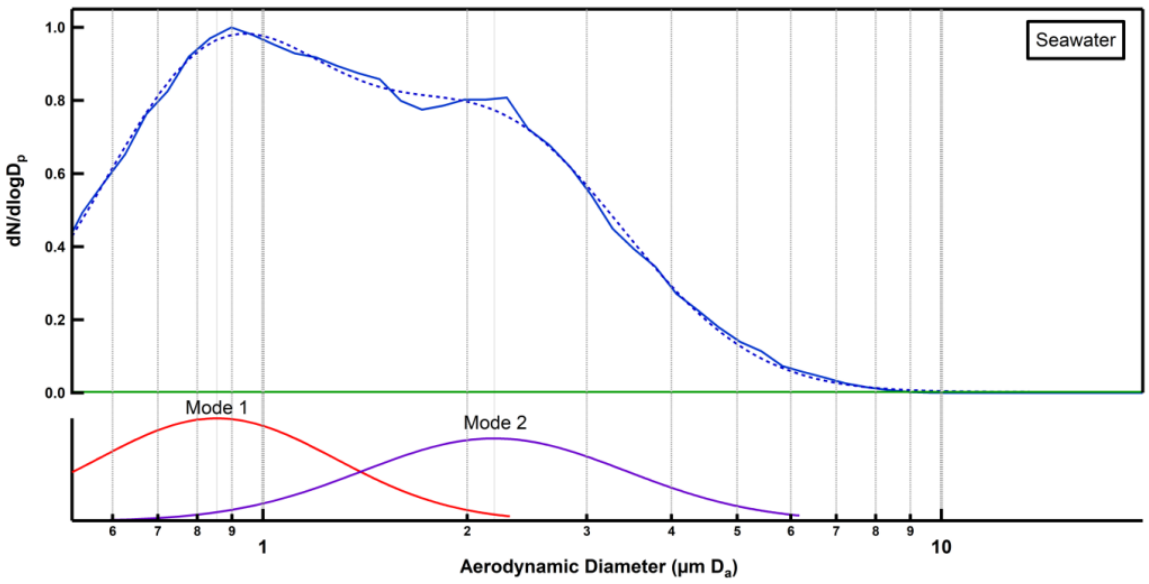

Figure 4.7. Multi-peak fitting results of APS seawater number size distribution. Peak of the two modes are at 0.85 and 2.19 µm D_a, respectively.

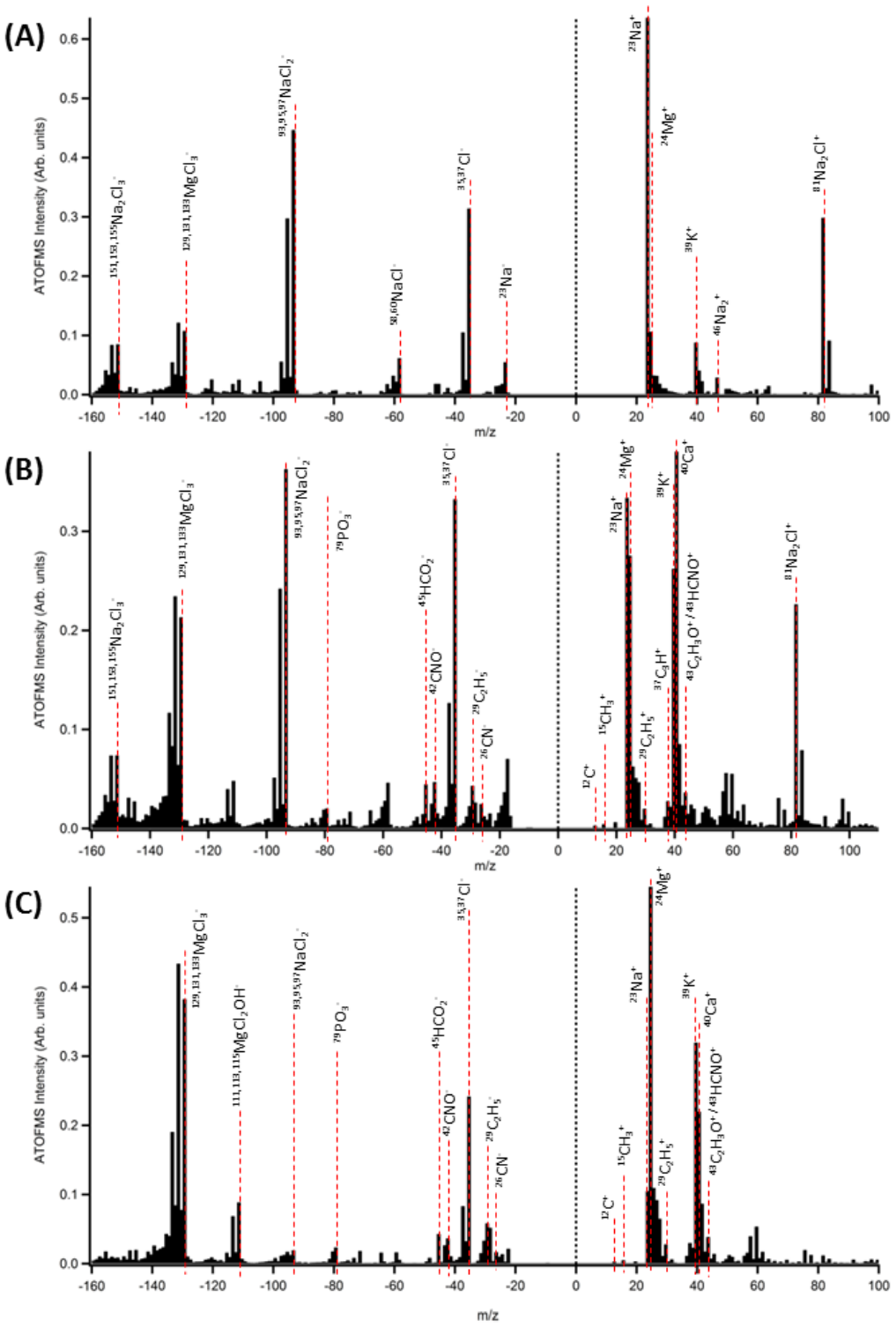

Figure 4.8. Representative averaged mass spectra for different particle types observed by ATOFMS. SS: Sea salt (A), SS-OC: sea salt – organic carbon (B and C), OC: organic carbon (D), and FePhosOrg: iron phosphate-rich organics (E).

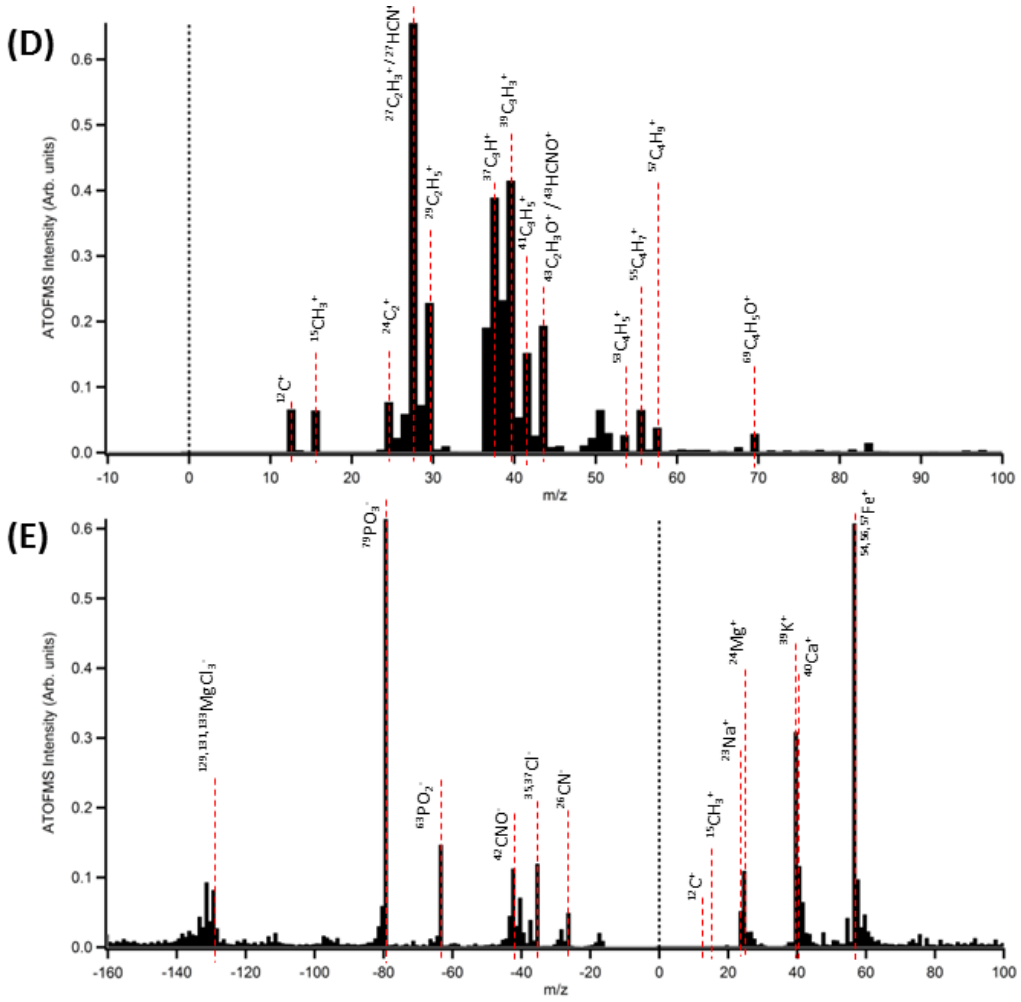

Figure 4.8. Representative averaged mass spectra for different particle types observed by ATOFMS continued.

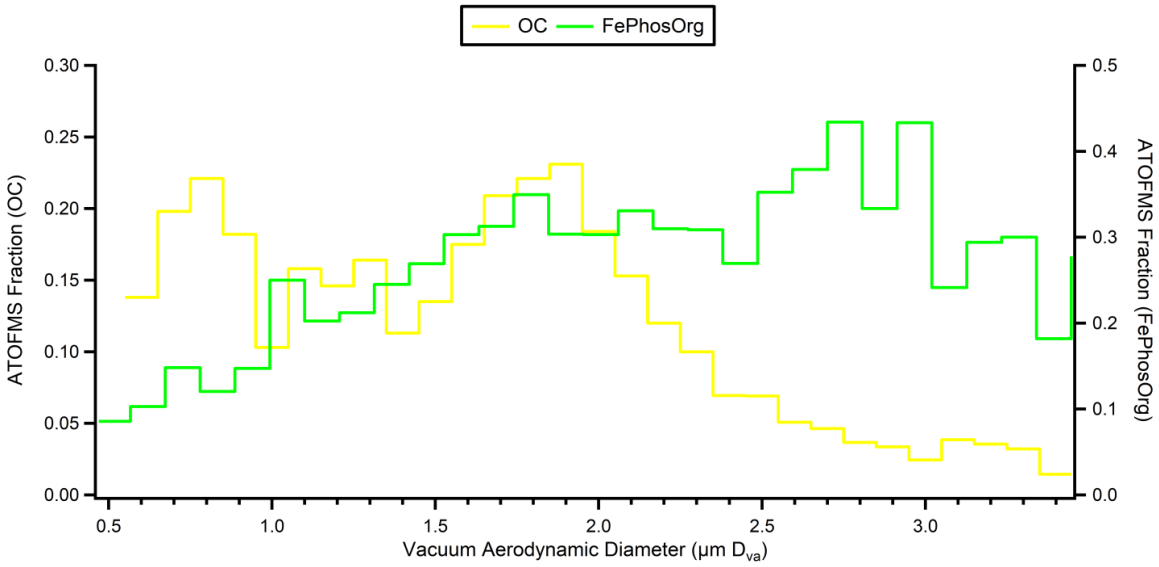

Figure 4.9. ATOFMS size distributions for organic carbon (OC, yellow) and iron phosphate-rich organic (FePhosOrg, green) types.

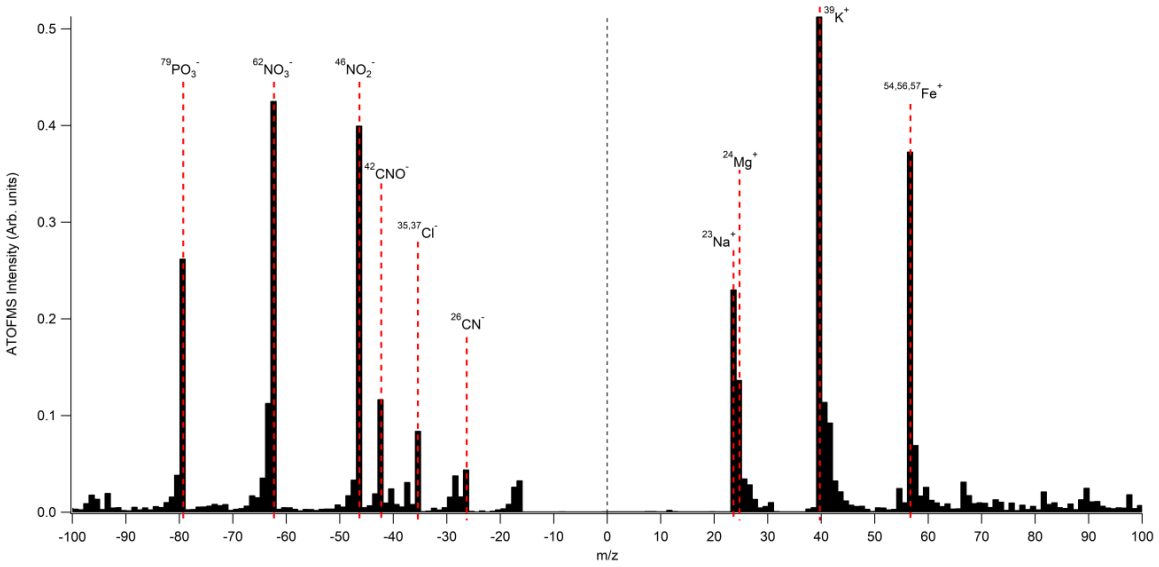

Figure 4.10. ATOFMS observed representative averaged mass spectra of reacted iron phosphate-rich organic (FePhosOrg) particle type. Strong presence of $^{46}NO_2^-$ and $^{62}NO_3^-$ demonstrates that the FePhosOrg particles have undergone reaction with HNO_3.

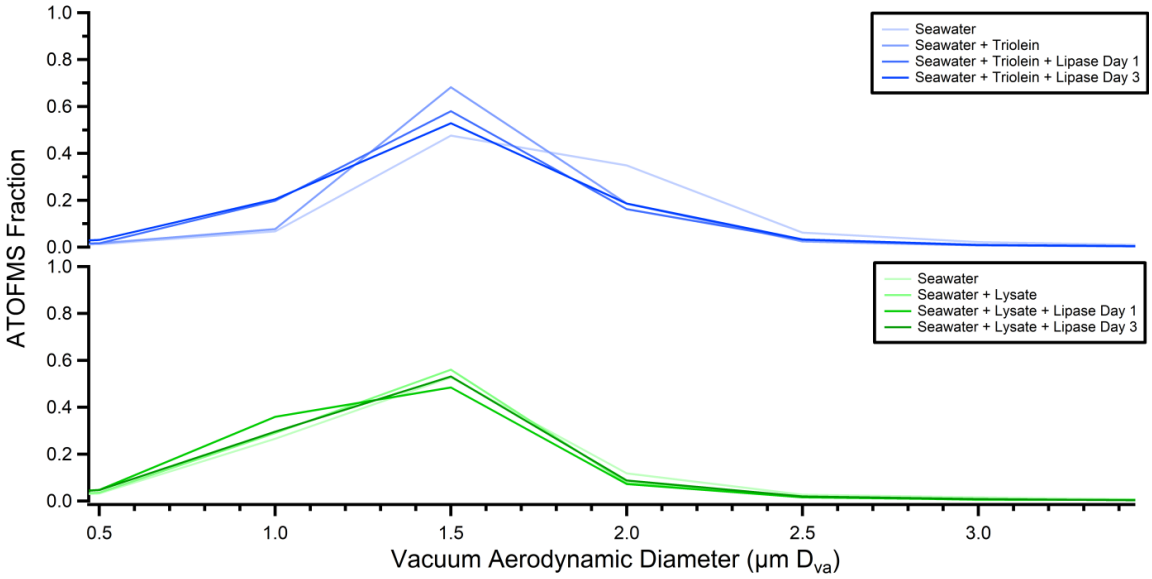

Figure 4.11. Normalized size distribution of ATOFMS sampled particles at each conditions of sequential addition experiments.

4.8.4 Supporting Information Tables

Table 4.1. List of compounds and concentrations used to make ASW medium. Further detailed information can be found in the recipes provided by National Center for Marine Algae and Microbiota and Canadian Center for the Culture of Microorganisms

	g/L
NaCl	22.200
$CaCl_2 \cdot 2H_2O$	1.397
$MgCl_2 \cdot 6H_2O$	9.031
Na_2SO_4	3.167
KCl	0.768
NaH_2PO_4	0.024
$NaNO_3$	0.255
Tricine	2.688
	mL/L
Trace Elements Stock Solution	1.0
CoB Stock Solution	1.0
1M $Na_2SiO_3 \cdot 9H_2O$	0.4
Vitamin Stock Solution	1.0

4.9 References

Abbatt, J. P. D., A. K. Y. Lee, and J. A. Thornton, Quantifying trace gas uptake to tropospheric aerosol: recent advances and remaining challenges, Chemical Society Reviews, 41 (19), 6555, 2012.

Ault, A. P., T. L. Guasco, O. S. Ryder, J. Baltrusaitis, L. A. Cuadra-Rodriguez, D. B. Collins, M. J. Ruppel, T. H. Bertram, K. A. Prather, and V. H. Grassian, Inside versus outside: Ion redistribution in nitric acid reacted sea spray aerosol particles as determined by single particle analysis, Journal of the American Chemical Society, 135 (39), 14528–14531, 2013.

Ault, A. P., T. L. Guasco, J. Baltrusaitis, O. S. Ryder, J. V. Trueblood, D. B. Collins, M. J. Ruppel, L. A. Cuadra-Rodriguez, K. A. Prather, and V. H. Grassian, Heterogeneous reactivity of nitric acid with nascent sea spray aerosol: Large differences observed between and within individual particles, Journal of Physical Chemistry Letters, 5 (15), 2493–2500, 2014.

Ault, A. P., C. J. Gaston, Y. Wang, G. Dominguez, M. H. Thiemens, and K. A. Prather, Characterization of the single particle mixing state of individual ship plume events measured at the port of Los Angeles, Environmental Science and Technology, 44 (6), 1954–1961, 2010.

Azam, F., and F. Malfatti, Microbial structuring of marine ecosystems., Nature Reviews. Microbiology, 5 (10), 782–791, 2007.

Brown, M. R., G. A. Dunstan, S. J. Torrcd, and K. A. Mzller, Effects of harvest stage and light on the biochemical composition of the diatom Thalassiosira Pseudonana, J. Phycol., 32, 64–73, 1996.

Cahill, J. F., H. Fei, S. M. Cohen, and K. A. Prather, Characterization of core–shell MOF particles by depth profiling experiments using on-line single particle mass spectrometry, Analyst, 140 (5), 1510–1515, 2015.

Carslaw, K. S., L. A. Lee, C. L. Reddington, K. J. Pringle, A. Rap, P. M. Forster, G. W. Mann, D. V Spracklen, M. T. Woodhouse, L. A. Regayre, and J. R. Pierce, Large contribution of natural aerosols to uncertainty in indirect forcing., Nature, 503 (7474), 67–71, 2013.

Cochran, R. E., O. S. Ryder, V. H. Grassian, and K. A. Prather, Sea spray aerosol: The chemical link between the oceans, atmosphere, and climate, Accounts of Chemical Research, 50 (3), 599–604, 2017.

Cruz, C. N., and S. N. Pandis, Deliquescence and hygroscopic growth of mixed inorganic - Organic atmospheric aerosol, Environmental Science and Technology, 34 (20), 4313–4319, 2000.

Cziczo, D. J., P. J. DeMott, S. D. Brooks, A. J. Prenni, D. S. Thomson, D. Baumgardner, J. C. Wilson, S. M. Kreidenweis, and D. M. Murphy, Observations of organic species and atmospheric ice formation, Geophysical Research Letters, 31 (12), 2–5, 2004.

Ducklow, H. W., Minireview: The bacterial content of the oceanic euphotic zone, FEMS Microbiology-Ecology, 30, 1–10, 1999.

Franze, T., M. G. Weller, R. Niessner, and U. Pöschl, Protein nitration by polluted air, Environmental Science and Technology, 39 (6), 1673–1678, 2005.

Gantt, B., and N. Meskhidze, The physical and chemical characteristics of marine primary organic aerosol: A review, Atmospheric Chemistry and Physics, 13 (8), 3979–3996, 2013.

Gard, E. E., J. E. Mayer, B. D. Morrical, T. Dienes, D. P. Fergenson, and K. A. Prather, Real-time analysis of individual atmospheric aerosol particles: Design and performance of a portable ATOFMS, Analytical Chemistry, 69 (20), 4083–4091, 1997.

Gard, E. E., M. J. Kleeman, D. S. Gross, L. S. Hughes, J. O. Allen, B. D. Morrical, D. P. Fergenson, T. Dienes, M. E. Galli, R. J. Johnson, G. R. Cass, and K. A. Prather, Direct

Observation of Heterogeneous Chemistry in the Atmosphere, Science, 279 (5354), 1184–1187, 1998.

Geider, R. J., and J. La Roche, The role of iron in phytoplankton photosynthesis, and the potential for iron-limitation of primary productivity in the sea, Photosynthesis Research, 39 (3), 275–301, 1994.

Groussman, R. D., M. S. Parker, and E. V. Armbrust, Diversity and evolutionary history of iron metabolism genes in diatoms. PLoS One, 10, 1-25, 2015

Grythe, H., J. Ström, R. Krejci, P. Quinn, and A. Stohl, A review of sea-spray aerosol source functions using a large global set of sea salt aerosol concentration measurements, Atmospheric Chemistry and Physics, 14 (3), 1277–1297, 2014.

Gupta, R., N. Gupta, and P. Rathi, Bacterial lipases: An overview of production, purification and biochemical properties, Applied Microbiology and Biotechnology, 64 (6), 763–781, 2004.

Hoffman, E. J., and R. A. Duce, The organic carbon content of marine aerosols collected on Bermuda, Journal of Geophysical Research, 79 (30), 4474–4477, 1974.

Hoppe, A., and R. R. Theimer, Titrimetric test for lipase activity using stabilized triolein emulsions, Phytochemistry, 42 (4), 973–978, 1996.

IPCC, Climate Change 2014: Synthesis Report. Contribution of working groups I, II and III to the fifth assessment report of the Intergovernmental Panel on Climate Change, 2014.

Lee, Y.-H., T.-K. Kim, H.-D. Shin, and D.-C. Park, Enzymatic hydrolysis of hydrophobic triolein by lipase in a mono-phase reaction system containing cyclodextrin; Reaction characteristics, Biotechnology and Bioprocess Engineering, 3 (2), 103–108, 1998.

De Leeuw, G., E. L. Andreas, M. D. Anguelova, C. W. Fairall, R. Ernie, C. O. Dowd, M. Schulz, and S. E. Schwartz, Production flux of sea-spray aerosol, Reviews of Geophysics, 80 (2010), 1–39, 2011.

Lewis, E. R., and S. E. Schwartz, Sea salt aerosol production: Mechanisms, methods, measurements and models, Geophysical Monograph Series, 152, 413, 2004.

Martinez, J., D. C. Smith, G. F. Steward, and F. Azam, Variability in ectohydrolytic enzyme activities of pelagic marine bacteria and its significance for substrate processing in the sea, Aquatic Microbial Ecology, 10 (3), 223–230, 1996.

May, K. R., The collison nebulizer: Description, performance and application, Journal of Aerosol Science, 4 (3), 235–243, 1973.

McClain, C. R., A decade of satellite ocean color observations., Annual Review of Marine Science, 1, 19–42, 2009.

McNeill, V. F., J. Patterson, G. M. Wolfe, and J. A. Thornton, The effect of varying levels of

surfactant on the reactive uptake of N2O5 to aqueous aerosol, Atmospheric Chemistry and Physics Discussions, 6 (1), 17–43, 2006.

Möhler, O., S. Benz, H. Saathoff, M. Schnaiter, R. Wagner, J. Schneider, S. Walter, V. Ebert, and S. Wagner, The effect of organic coating on the heterogeneous ice nucleation efficiency of mineral dust aerosols, Environmental Research Letters, 3 (2), 25007, 2008.

Murphy, D. M., J. R. Anderson, P. K. Quinn, L. M. McInnes, F. J. Brechtel, S. M. Kreidenweis, A. M. Middlebrook, M. Posfai, D. S. Thomson, and P. R. Buseck, Influence of sea-salt on aerosol radiative properties in the Southern Ocean marine boundary layer, Nature, 392 (6671), 62–65, 1998.

Nishino, N. S. A. Hollingsworth, A. C. Stern, M. Roeselova, D. J. Tobias, and B. J. Finlayson-Pitts, Interactions of gaseous HNO_3 and water with individual and mixed alkyl self-assembled monolayers at room temperature, Physical Chemistry Chemical Physics, 16 (6), 2358–67, 2014.

O'Dowd, C. D., M. C. Facchini, F. Cavalli, D. Ceburnis, M. Mircea, S. Decesari, S. Fuzzi, Y. J. Yoon, and J.-P. Putaud, Biogenically driven organic contribution to marine aerosol., Nature, 431 (7009), 676–680, 2004.

Partanen, A.-I., E. M. Dunne, T. Bergman, A. Laakso, H. Kokkola, J. Ovadnevaite, L. Sogacheva, D. Baisnee, J. Sciare, A. Manders, C. O'Dowd, G. De Leeuw, and H. Korhonen, Global modelling of direct and indirect effects of sea spray aerosol using a source function encapsulating wave state, Atmospheric Chemistry and Physics, 14 (21), 11731–11752, 2014.

Pomeroy, L. R., P. J. I. Williams, F. Azam, and J. E. Hobbie, The microbial loop, Oceanography, 20 (2), 28–33, 2007.

Prather, K. A., T. H. Bertram, V. H. Grassian, G. B. Deane, M. D. Stokes, P. J. Demott, L. I. Aluwihare, B. P. Palenik, F. Azam, J. H. Seinfeld, R. C. Moffet, M. J. Molina, C. D. Cappa, F. M. Geiger, G. C. Roberts, L. M. Russell, A. P. Ault, J. Baltrusaitis, D. B. Collins, C. E. Corrigan, L. A. Cuadra-Rodriguez, C. J. Ebben, S. D. Forestieri, T. L. Guasco, S. P. Hersey, M. J. Kim, W. F. Lambert, R. L. Modini, W. Mui, B. E. Pedler, M. J. Ruppel, O. S. Ryder, N. G. Schoepp, R. C. Sullivan, and D. Zhao, Bringing the ocean into the laboratory to probe the chemical complexity of sea spray aerosol., Proceedings of the National Academy of Sciences of the United States of America, 110 (19), 7550–5, 2013.

Quinn, P. K., D. B. Collins, V. H. Grassian, K. A. Prather, and T. S. Bates, Chemistry and related properties of freshly emitted sea spray aerosol, Chemical Reviews, 115, 4383–4399, 2015.

Quinn, P. K., T. S. Bates, K. S. Schulz, D. J. Coffman, A. A. Frossard, L. M. Russell, W. C. Keene, and D. J. Kieber, Contribution of sea surface carbon pool to organic matter enrichment in sea spray aerosol, Nature Geoscience, 7 (3), 228–232, 2014.

Reis, P., K. Holmberg, H. Watzke, M. E. Leser, and R. Miller, Lipases at interfaces: A review,

Advances in Colloid and Interface Science, 147–148 (C), 237–250, 2009.

Rinaldi, M., S. Fuzzi, S. Decesari, S. Marullo, R. Santoleri, A. Provenzale, J. Von Hardenberg, D. Ceburnis, A. Vaishya, C. D. O'Dowd, and M. C. Facchini, Is chlorophyll-a the best surrogate for organic matter enrichment in submicron primary marine aerosol?, Journal of Geophysical Research: Atmospheres, 118 (10), 4964–4973, 2013.

Rossi, M. J., Heterogeneous reactions on salts, Chemical Reviews, 103 (12), 4823–4882, 2003.

Ryder, O. S., A. P. Ault, J. F. Cahill, T. L. Guasco, T. P. Riedel, L. A. Cuadra-Rodriguez, C. J. Gaston, E. Fitzgerald, C. Lee, K. A. Prather, and T. H. Bertram, On the role of particle inorganic mixing state in the reactive uptake of N2O5 to ambient aerosol particles, Environmental Science and Technology, 48 (3), 1618–1627, 2014.

Salentinig, S., L. Sagalowicz, and O. Glatter, Self-assembled structures and pK a value of oleic acid in systems of biological levance, Langmuir, 26 (14), 11670–11679, 2010.

Saxena, P., and L. M. Hildemann, Organics alter hygroscopic behavior of atmospheric particles, Journal of Geophysical Research, 100 (95), 18755–18770, 1995.

Schotz, C., and D. Grove, A rapid assay for lipoprotein lipase, 11, 68–69, 1970.

Solomon, P. A., L. G. Salmon, T. Fall, and G. R. Cass, Spatial and temporal distribution of atmospheric nitric-acid and particulate nitrate concentrations in the Los-Angeles area, Environmental Science and Technology, 26 (8), 1594–1601, 1992.

Song, X. H., P. K. Hopke, D. P. Fergenson, and K. A. Prather, Classification of single particles analyzed by ATOFMS using an artificial neural network, ART-2A, Analytical Chemistry, 71 (4), 860–865, 1999.

Stemmler K., A. Vlasenko, C. Guimbaud, and M. Ammann, The effect of fatty acid surfactants on the uptake of nitric acid to deliquesced NaCl aerosol, Atmospheric Chemistry and Physics, 8, 5127–5141, 2008.

Stokes, M. D., G. B. Deane, D. B. Collins, C. D. Cappa, T. H. Bertram, A. Dommer, S. R. Schill, S. Forestieri, and M. Survilo, A miniature Marine Aerosol Reference Tank (miniMART) as a compact breaking wave analogue, Atmospheric Measurement Techniques Discussions, 9 (May), 1–28, 2016.

Stokes, M. D., G. B. Deane, K. Prather, T. H. Bertram, M. J. Ruppel, O. S. Ryder, J. M. Brady, and D. Zhao, A Marine Aerosol Reference Tank system as a breaking wave analogue for the production of foam and sea-spray aerosols, Atmospheric Measurement Techniques, 6 (4), 1085–1094, 2013.

Sultana, C. M., D. B. Collins, and K. A. Prather, The effect of structural heterogeneity in chemical composition on online single particle mass spectrometry analysis of sea spray aerosol particles, Environmental Science and Technology, 2017.

Sultana, C. M., G. C. Cornwell, P. Rodriguez, and K. A. Prather, FATES: A flexible analysis

toolkit for the exploration of single-particle mass spectrometer data, Atmospheric Measurement Techniques, 10 (4), 1323–1334, 2017.

Sunda, W. G., S. A. Huntsman, Interrelated influence of iron, light and cell size on marine phytoplankton growth, Nature, 390 (6658), 289–393, 1997.

Suzumura, M., Phospholipids in marine environments: A review, Talanta, 66, 422–434, 2005.

Tang, C. Y., Z. Huang, and H. C. Allen, Binding of Mg(2+) and Ca(2+) to palmitic acid and deprotonation of the COOH headgroup studied by vibrational sum frequency generation spectroscopy., The Journal of Physical Chemistry. B, 114 (51), 17068–17076, 2010.

Trueblood, J. V., A. D. Estillore, C. Lee, J. A. Dowling, K. A. Prather, and V. H. Grassian, Heterogeneous chemistry of lipopolysaccharides with gas-phase nitric acid: Reactive sites and reaction pathways, Journal of Physical Chemistry A, 120 (32), 6444–6450, 2016.

Verdugo, P., A. L. Alldredge, F. Azam, D. L. Kirchman, U. Passow, and P. H. Santschi, The oceanic gel phase: A bridge in the DOM-POM continuum, Marine Chemistry, 92 (1–4 SPEC. ISS.), 67–85, 2004.

Vieler, A., C. Wilhelm, R. Goss, R. Süß, and J. Schiller, The lipid composition of the unicellular green alga Chlamydomonas reinhardtii and the diatom Cyclotella meneghiniana investigated by MALDI-TOF MS and TLC, Chemistry and Physics of Lipids, 150 (2), 143–155, 2007.

Wang, X., C. M. Sultana, J. Trueblood, T. C. J. Hill, F. Malfatti, C. Lee, O. Laskina, K. A. Moore, C. M. Beall, C. S. McCluskey, G. C. Cornwell, Y. Zhou, J. L. Cox, M. A. Pendergraft, M. V. Santander, T. H. Bertram, C. D. Cappa, F. Azam, P. J. DeMott, V. H. Grassian, and K. A. Prather, Microbial control of sea spray aerosol composition: A tale of two blooms, ACS Central Science, 1 (3), 124–131, 2015.

Yu, E. T., F. J. Zendejas, P. D. Lane, S. Gaucher, B. A. Simmons, and T. W. Lane, Triacylglycerol accumulation and profiling in the model diatoms Thalassiosira pseudonana and Phaeodactylum tricornutum (Baccilariophyceae) during starvation, Journal of Applied Phycology, 21 (6), 669–681, 2009.

Zelenyuk, A., Y. Juan, S. Chen, R. A. Zaveri, and D. Imre, “Depth-profiling” and quantitative characterization of the size, composition, shape, density, and morphology of fine particles with SPLAT, a single-particle mass spectrometer, Journal of Physical Chemistry A, 112 (4), 669–671, 2008.

5 Sea Spray Aerosols: Tiny Biochemical Reactors in the Atmosphere

5.1 Synopsis

Sea spray aerosols (SSA) produced from the ocean that cover nearly 75% of the Earth's surface profoundly influence clouds, climate, and precipitation processes. SSA contain complex mixtures of sea salt and biological species including proteins, viruses, and bacteria, yet limited understanding exists as to how ocean-derived biological species can influence the atmospheric aerosol composition and climate. Here, diverse active enzymes such as protease, lipase, alkaline phosphatase in freshly produced SSA were detected for the first time in controlled laboratory settings and in coastal ambient air. SSA hydrolases showed variability in hydrolysis rates and associated organic matter degradation patterns. We further studied the potential role of SSA hydrolases in changing the chemical composition of SSA after particle ejection and revealed that enzymes influence the surface composition and heterogeneous reactivity of SSA particles by changing the solubility and surface activity of SSA organic species. Further, simulations suggest that within hours after ejection, nascent enzyme-containing SSA can coagulate with ambient aerosols, which will alter composition, morphology, and reactivity of other particles in the atmosphere. The discovery of active enzymes in SSA and their role in controlling particle chemistry, particle reactivity and particle fate through previously unexplored biotic reaction pathways is of uttermost importance in understanding the functioning of ocean-atmosphere interactions.

5.2 Introduction

Sea spray aerosols (SSA) play a major role in affecting human and ecosystem health [*Pöschl, 2005*; *Stocker et al., 2013*]. SSA influence atmospheric optical properties, the number

and properties of cloud condensation and ice nuclei, and the overall composition of the atmosphere [*Haywood and Boucher, 2000*]. SSA are produced when bubbles burst at the ocean surface [*Lewis and Schwartz, 2004*] and are comprised of mixtures of sea salt and biologically-derived species [*Ault et al., 2013*; *Duce and Hoffman, 1976*], including viable marine bacteria and viruses, gel particles, vesicles, and carbohydrates, proteins, and lipids [*Blanchard and Syzdek, 1972*; *Meskhidze et al., 2013*; *O'Dowd et al., 2015*; *Orellana et al., 2011*; *Patterson et al., 2016*; *Rastelli et al., 2017*]. Interdisciplinary approaches have shown that biological processes can lead to enrichment of organic matter in SSA, which can become transformed by solar radiation [*Gantt and Meskhidze, 2013*], modify their climate-relevant physicochemical properties [*Collins et al., 2013*; *O'Dowd et al., 2015*; *Quinn et al., 2015*; *Wang et al., 2015*] and their heterogeneous chemical reactions by oxidants [*Abbatt et al., 2012*; *Ault et al., 2014*]. Within the atmosphere-ocean interactions biologically mediated framework, here we show a new pathway for how ocean-derived biological species can impact marine aerosols, specifically in the context of catalytic enzyme degradation processes.

The ocean and atmosphere exchange on the order of 10^6 prokaryotes m^{-2} of ocean surface on a daily basis [*Mayol et al., 2014*]. In the upper ocean, bacteria are abundant (10^{12} m^{-3}) and play a major role in controlling the composition, the structure, and the abundance of organic matter. Since bioorganic species occur predominantly in the form of large polymeric molecules or particulate organic matter, a critical biochemical strategy of bacteria is to express multiple cell-surface-bound enzymes that can hydrolyze organic species into forms accessible for cellular uptake [*Hoppe, 1983*; *Martinez et al., 1996*]. Bacterial cell-surface hydrolases are ubiquitously found in upper ocean seawater samples (thus including the surface microlayer) throughout the world's oceans, across wide ranges of temperature and pressure [*Baltar et al., 2010*; *Hoppe, 1983*; *Kuznetsova and Lee, 2001*; *Martinez et al., 1996*]. A recently study have shown that marine bacterial enzymatic action on dissolved organic matter pool (i.e. bacterial lipases on fatty acid)

can control the timing of the release and the type of organics that get transferred in SSA [*Wang et al., 2015*]. Consequently, the interactions between marine bacteria and organic matter pool are fundamental in regulating the functioning of ocean-atmosphere ecosystem. Furthermore, the propensity of specific enzymes to work at chemical and biological interfaces is an important feature that supports the idea of a pivotal role of bacterial enzymes in structuring SSA particles in the atmosphere. Specifically, lipases are active at aqueous/organic interfaces [*Reis et al., 2009*] while other hydrolases, like proteases and phosphatases, have a strong propensity to act at cellular membranes (e.g.: biological interfaces), such as bacterial periplasmic space [*Luo et al., 2009*] and vesicles.

In this study, we hypothesize that when bacteria are ejected into the atmosphere within nascent sea spray aerosol (SSA), their associated enzymes are active and can continue to change the properties of organic matter associated with nascent SSA and the local marine aerosol. This will occur even in the absence of *de novo* hydrolases synthesis post-ejection provided the enzymes are stable and remain active within the SSA microenvironment under typical atmospheric conditions (e.g., temperature, pH, and salinity). The activity and localization of these hydrolases at interfaces have profound implications for the physicochemical properties of nascent SSA and other atmospheric particles with which they coagulate.

5.3 Materials and Methods

5.3.1 Measurements of Enzymatic Activities During the Microcosm Bloom Experiments and at coastal ocean

Surface seawater was collected off the end of the Ellen Browning Scripps Memorial Pier (Scripps Pier), La Jolla, California (32° 52.02’ N, 117° 15.43’ W, USA) with an acid clean

carboy. The seawater was pre-filtered through 50 µm acid-washed Nitex to remove larger herbivores and kept protected from light. Within 1 h, the water was brought into the laboratory and the Marine Aerosol Reference Tank (MART) [*Stokes et al., 2013*] was filled. Three MART experiments were set-up in November 2013 (MART-A), in December 2013 (MART-B), in January 2014 (MART-C, Table 5.1). In August 2016 (14-16), we set up a MART microcosm incubation experiment (MART-E), with post phytoplankton bloom seawater. Nutrients [*Guillard and Ryther, 1962*] as in f/20 (MART-A, -B) and as in f/2 (MART-C) were added to stimulate a phytoplankton bloom under constant light (cool, white light 100 µE m^{-2} s^{-1}, 5700 K). In MART-E, nutrients (f/20) were previously added to an experimental reservoir tank of seawater (~1500 L) that was kept outdoors at environmental temperature and it was irradiated with natural sunlight and diurnal cycle 120 L was taken at phytoplankton senescence to fill MART-E.

In MART-A, -B, -C, a suite of parameters was measured either every day in the bulk water (*in vivo*, not presented in this paper, and extracted chlorophyll-a (Chl-a), and dissolved organic carbon, DOC) or every 2 days (bacteria, viral abundance and ectohydrolytic activities) in the bulk seawater (SW), sea surface microlayer (SSML) and impinged sea spray aerosol (SSA) fractions. Seawater was collected using a lateral port on the MART into a sterilized 50 mL tube and immediately processed. Sea surface microlayer (SSML) was sampled with an acid-washed and precombusted glass plate [*Harvey, George W., Burzell, 2012*]. The glass plate, 45.5 x 33 x 0.6 cm, with an effective sampling area of 33 x 33 cm was dipped 5 times to recover 20 mL equal to 115 µm SSML thickness. 2.5 mL were aliquoted and diluted by a factor of 10 for the determination of bacterial and viral abundances and enzyme assays. SSA were impinged into midget impingers (Chemglass) containing 0.2 µm filtered autoclaved seawater (FASW) at a flow rate of 1 SLPM. Details can be found in Lee et al. 2015(*34*). In MART- E, we sampled SW and SSA as described above to test the "self-contained biochemical reactor" hypothesis.

Marine aerosols were sampled from atop Ellen Browning Scripps Memorial Pier (Scripps Pier), La Jolla, California (32° 52.02’ N, 117° 15.43’ W, USA) to probe for the presence of viable enzymes there (June 8, 9, 10 and July 1, 7, 14 2017). On each day, 2 pre-combusted glass impingers were set out, each pulling 0.75 SLPM (1 SLPM on June 8) and kept protected from direct sunlight to prevent photo-degradation. One impinger sampled ambient aerosol through a stainless steel inlet extending ~0.75 m from the pier. The other impinger served as a field blank by sampling air through a HEPA filter that removed all particles and, thus, all sources of airborne enzymes. Methods of ectohydrolytic activity measurements are discussed in 5.3.4.

5.3.2 Chlorophyll-a and Dissolved Organic Carbon Measurements (DOC)

Extracted Chl-a was determined fluorometrically [*Holm-Hansen et al., 1965*] in duplicates. Samples (100–200 mL) were filtered onto Whatman GF/F filters, extracted in 90% acetone and their fluorescence was measured and corrected for phaeopigments using a Turner Design 700 fluorometer. *In vivo* Chl-a was determined fluorometrically in triplicates using a hand-held fluorometer (Aquafluor, Turner Design).

For the determination of DOC concentrations, seawater was filtered through precombusted (450 ℃ for 6 h) GF/F filters in a precombusted metal-glass filtration tower system with a hand-pump (pressure differential 12.5 cm Hg; during high Chl-a days filters were changed frequently to minimize cell breakage). The filtrate was transferred into precombusted 40-mL glass vials and immediately acidified with two drops of trace metal-free concentrated 12 N HCl (final pH 2). Samples were stored at 4° C in the dark. DOC analyses were conducted as per standard high-temperature combustion procedures on a Shimadzu TOC 5000A [*Álvarez-Salgado and Miller, 1998*; *Cauwet, 1994*].

5.3.3 Bacterial and Viral Abundance in SW, SSML, and SSA Fractions

Seawater samples from the SW, SSML, and SSA fractions were fixed with a 0.2 µm filtered 37% formaldehyde solution (final concentration 2%) and stored at 4 ℃ for 30 min and then filtered onto 0.02 µm Anodisc (Whatman) membrane and stained with SYBR Green I (Thermo Fisher Sci.) following the protocol of Noble and Fuhrman (1998) [*Noble and Fuhrman, 1998*]. For SW and SSML fractions, duplicate filters were analyzed on an Olympus BX71 epifluorescence microscope at 1000 x final magnification with a 480 nm excitation and 520 nm emission filter set. More than 200 cells or viruses were counted in random fields. For the SSA fraction, that was more challenging due to the dim signal, duplicate filters were imaged at Wide-Field Nikon TE2000-U inverted microscope using a Plan Apochromat VC 100x, 1.4 NA oil immersion objective (Nikon Instruments, Japan) and with a CoolSNAP HQ CCD Camera (Photrometric). SYBR Green I filter set was 490 nm excitation and 528 nm emission. The exposure time ranged from 100 ms to 1 s depending on the sample.

5.3.4 Ectohydrolytic Activities in SW, SSML, and SSA Fractions

The bulk ectohydrolytic activities for total, <1 µm (bacterial) and <0.2 µm (dissolved) fractions were measured using fluorogenic substrate analogs at saturating concentrations (20 µM) [*Hoppe, 1983*]. The substrates were purchased from Sigma-Aldrich. Alkaline phosphatase (APase, AP), protease (leucine, P), lipase (oleate, O and stearate, S) and chitinase (NAG) were measured respectively with 4-methyl-umbelliferone-phosphate, L-leucine-7-amino-4-methyl-coumarin, 4-methyl-umbelliferone oleate, 4-methyl-umbelliferone stearate, and 4-methyl-umbelliferone-N-acetyl-β-D-glucosaminide. Fluorescence resulting from enzymatic release of the free fluorophores (4-Methylumbelliferone (MUF) and 7-Amido-4-methylcoumarin (AMC)) was measured by a multimode reader (SpectraMax M3, Molecular Device) on 96-well microtiter plates incubated in the dark at in situ temperature for 1 hr. Fluorescence was measured immediately after adding substrates and again at the end of the incubation [*Danovaro et al.*,

2005], at 355 nm excitation and 460 nm emission. Note that protease mentioned throughout the MART experiments refer to protease-leucine.

Ectohydrolytic activities of the marine aerosols were measured using the above 5 fluorogenic substrate analogs plus 4-methylumbellifreyl butyrate and L-serine-7-amido-4-methylcoumarin hydrochloride (20 µM both) for lipase-butyrate and protease-serine, respectively.

Enzyme activities were measured in concentration of substrate hydrolyzed per unit time of incubation. Replicates for each sample-substrate combination were analyzed in 3-6 wells on the microtiter plate. Standard curves of the free fluorophores AMC and MUF were used to relate fluorescence to free fluorophore concentration. Enzyme activity for aerosol samples is reported as the difference between the sample and a blank generated by sampling particle free air. We tested a range of substrate concentrations (from 20 to 100 µM) over the course of 24 h to determine the saturating concentrations. In MART-C experiment, the seawater sample was filtered onto 1 µm autoclaved polycarbonate filter and then sequentially onto 0.2 µm low-binding protein Acrodisc syringe filter [*Kim et al., 2007*; *Obayashi and Suzuki, 2008*] to determine the bacterial fraction and the dissolved fraction. Protease-leucine activity was measured in SW and SSA before and after adding the protease Pronase E to the SW.

5.3.5 Statistical Analysis for Scaling Enzymatic Hydrolysis Rates

All statistical analyses were done in R programming language (R Core Team 2013; http://www.R-project.org/) using the package »nlme« (Jose Pinheiro, Douglas Bates, Saikat DebRoy, Deepayan Sarkar) and the R Development Core Team (2013) for the Linear and Nonlinear Mixed Effects Models. The hydrolysis rate data were log 10 transformed. The model was set to predict the log 10 hydrolysis rates from the hydrolysis rate of the three fractions (SW, SSML, in comparison to SSA), Chl-a, DOC and the time from the beginning of the experiment. The differences among the three MART experiments were taken as sources of random effects. A

p-value of 0.05 or less was taken as an indicator for a statistically significant relation between the predictor variables and the log 10 hydrolysis rate values.

NMDS analyses: Enzymatic hydrolysis rates were expressed as percentage of the diverse activities per day. The data fed the Non-Metric Multi Dimensional Scaling (NMDS) analysis in Primer 5 (version 5.2.9) [*Clarke and Warwick, 2001*]. A similarity matrix was constructed with the Bray-Curtis similarity coefficient for all pairs of samplings. NMDS plots degradation patterns. Stress level <0.1 or lower indicate a little data distortion.

Please note that DOC, bacteria and virus abundance in SW, SSML and SSA data of MART-C experiments have been previously published in Lee et al., 2015 and can be found in Chapter 2.

5.3.6 Sea Spray Aerosol Production and Sampling

MART is a breaking wave analogue for the production of SSA by pulsed-plunging waterfall [*Lee et al., 2015*; *Stokes et al., 2013*]. The tank headspace was purged with a particle free air (Sabio Instruments) to constantly maintain a positive pressure to minimize room contamination. Analytical instruments can be placed in line using the lateral ports. Water was plunged on the day after the seawater collection day (day 1) and daily plunging was resumed after *in vivo* Chl-a fluorescence showed an exponential. The plunging waterfall had a 2 h duty cycle in order to minimize the shear stress for the phytoplankton. The shear stress is caused by the centrifugal pump that is used to recirculate water in the tank for SSA production. SSA was collected by impinging the air into a 40 mL precombusted glass vial that was filled with 0.2 µm FASW. The impinging method preferentially collects particles >200 nm [*Lee et al., 2015*]. The same batch of FASW was used for the three MART experiments and was stored in the dark at 4° C. New batch of FASW was used solely for the MART-E experiment. The SSA-impinged solution was immediately aliquoted undiluted for bacterial and viral abundance analyses and for

ectohydrolytic activity assays after a 1:1 dilution in FASW (this step was necessary due to the limited sample volume available). Undiluted SSA-impinged solution volumes (10 and 50 µL) were plated on ZoBell medium [*Zobell, 1941*] to estimate the colony forming units (CFU), thus surveying the SSA bacterial viability.

All aerosol measurements were conducted after passing the sample through silica gel diffusion driers to attain a relative humidity of <10%. Number size distributions of SSA particles were measured using a scanning mobility particle sizer (SMPS, TSI 3936, 0.3/3.0 SLPM sample/sheathe flow) for particles with mobility diameters (d_m) between 0.013 and 0.7 µm, and an aerodynamic particle sizer (APS, TSI 3321, 1 SLPM sample flow) for particles with an aerodynamic diameters (d_a) between 0.6 and 20 µm. Size distributions from these two different instruments, with different aerosol size metrics were unified by converting both d_m and d_a to the physical diameter (d_p) [*DeCarlo and Slowik, 2004*], assuming all particles were spherical and had a density (ρ_p) of 1.8 g cm^{-3} [*Zelenyuk et al., 2007*] and a reference density (ρ_0) of 1 g cm^{-3}. It is important to note that SSA particles were dried prior analysis and so the spherical particle assumption may not be accurate in all cases. SSA is an external mixture of particles with different compositions [*Collins et al., 2013*; *Prather et al., 2013*], including size dependent differences in morphology [*Ault et al., 2013*]. Caution is therefore encouraged when making quantitative comparisons between SSA size distributions reported using different methods. Dried SSA particles were also sampled for single particle chemical analysis as detailed below.

5.3.7 MART-E Coagulation and Control Experiments

5.3.7.1 MART-E Coagulation Experiment

In order to test SSA as "self-contained biochemical reactor" hypothesis, in MART-E experiment, we used post-phytoplankton bloom seawater as a source of enzymes and substrates in SSA. First, we generated SSA from the MART which was then, sent through the experimental

setup (Figure 5.4A) without the atomizer as a baseline. Second, in the coagulation experimental part with natural SSA enzymes, a Collison nebulizer (herein referred to as atomizer) [*May, 1973*] was used to generate fine particles from a liquid solution of casein (Sigma-Aldrich C6780) in FASW. Third, 33 mg of the protease Pronase E (Sigma-Aldrich P8811, final concentration of approx. 0.1 units mL^{-1} seawater) was added to the MART to increase the enzyme concentration in SSA and repeated the test. Samples from the bulk seawater and aerosol impingers (1 h sampling, 1 SLPM) were taken for each measurement conditions to measure protease activities in both compartments. Further details on the operation and technique of the impingers can be found in Lee et al. 2015.

The two aerosol sources (natural SSA and atomized casein) were mixed using a mixing tube (3/8 in i.d. x 5 in length conductive tubing, containing inside a spiral wound with 8 in x 0.051 in o.d. of stainless steel wire) based on design reported [*Rodrigue et al., 2007*] prior to a mixing flow tube (10 cm o.d. x 50 cm length, approx. 4 L in volume with 4 min residence time at 1 SLPM) (Figure 5.4B), allowing the air to be well mixed and the aerosol particles to coagulate (Figure 5.4B). For the pristine experiment, no nitric acid was utilized and sampled directly, bypassing the aerosol reaction flow tube. For heterogeneous reactivity studies, the particles post-mixing tube at each step of the experiment were sent through the nitric acid flow tube (Figure 5.4B) at reaction parameters of 25 ± 1 ^{o}C, 50 ± 2% RH, approx. 10 ppb HNO_3 [*Solomon et al., 1992*], and residence time of 1.8 min, then sampled using ATOFMS. For each measurement condition, the particles after the mixing tube were then sampled using an aerosol time-of-flight mass spectrometer (ATOFMS, 1 SLPM) [*Gard et al., 1997*], or through combined sampling by an APS and SMPS (TSI 3938, 0.3/3.0 SLPM sample/sheathe flow) to keep the mixing tube residence time comparable. All particles, pristine as well as reacted, were dried using two diffusion driers (RH <10%) prior to sampling with any of the instruments. Dual polarity mass

spectra of at least 3000 particles >2 µm vacuum aerodynamic diameter, D_{va}, were used for analysis in each of the MART-E measurement conditions, except for SSA reactivity measurement (Fig 3. [1]) with 567 particles above 2 µm D_{va} being analyzed.

More detailed information on ATOFMS can be found elsewhere [*Gard et al., 1997*] and in Section 1.5.3. Data are imported into MATLAB (The Mathworks, Inc) with software toolkit FATES [*Sultana et al., 2017*] for further data analysis. Threshold in determining ion presence in the mass spectra was set at 1% relative peak area intensity. Ion markers used for phosphate-containing and reacted particles were $^{79}PO_3^-$ and $^{46}NO_2^-/^{62}NO_3^-$, respectively. Uncertainty in the reported particle fractions can be calculated using the following equations (E5.1) and (E5.2), where F is fraction, x is the number of particles containing select ion marker, N is total number of particles, and SE stands for standard error of 1σ.

$$F = \frac{x}{N} \quad \text{(E5.1)}$$

$$SE = \sqrt{\frac{F(1-F)}{N}} \quad \text{(E5.2)}$$

5.3.7.2 Control Experiment

Further control experiments were performed to directly obtain chemical signatures of the casein and protease Pronase E degraded casein in FASW. The steps of the control experiments were: 1) FASW sampled as a baseline, 2) casein dissolved in FASW (1 mg mL^{-1} seawater), and 3) Pronase E directly added (0.1 units mL^{-1} seawater) to the casein-containing solution. At each step of the experiment, the solution was atomized and then passed through two diffusion driers (RH <10%) prior to sampling with the ATOFMS.

5.3.8 Molecular Modeling of Enzymes and Peptides

5.3.8.1 Molecular Model of Lipase in SSA mimicking Lipid Monolayer

The structure of lipase was built from PDB 3LIP for the *Pseudomonas cepacia* lipase in open conformation [*Schrag et al., 1997*]. Hydrogens and missing side-chains were added using Maestro's protein preparation wizard ["Schrodinger Release 2015-3: Maestro," *2015*] at pH 8.14. CHARMMGUI [*Jo et al., 2008*] was then used to build the monolayer embedded lipase system.

5.3.8.2 Molecular Models and Bioinformatic Analyses of Casein Peptide Products from Pronase E Degradation

Peptide cleavage products from Pronase E digestion of *casein* were analyzed for their phase behavior as intrinsically disordered peptides with CIDER [*Holehouse et al., 2017*], for their likely solubilities with Innovagen's pepcalc, and for their likely three dimensional structures with Pepfold [*Maupetit et al., 2010*]. The top models from Pepfold were analyzed with APBS electrostatics to visualize the charge distribution on the surface of these folded peptides [*Baker et al., 2001*; *Dolinsky et al., 2004*].

5.3.9 Particle Coagulation Simulations

Particle Brownian coagulation simulations of SSA with background particles were performed, using the stochastic, particle-resolved aerosol model PartMC. Details of the model description can be found elsewhere [*Riemer et al., 2009*], but in brief, the particle-resolved approach allows for the tracking of the full aerosol mixing state as the population is undergoing Brownian coagulation. Two initially externally mixed particle distributions were used as inputs for the simulation, and mixed particles are formed as the particles evolved over the course of the 24 h simulation. One of the input distributions was the dry nascent SSA particle distribution previously reported [*Collins et al., 2013*], where the other, referred to as "background," was adapted from the idealized urban plume distribution reported in Riemer et al., 2009. The

concentrations in the Aitken and accumulation modes of the background aerosol distribution were scaled to three different desired total background concentrations to quantify the formation of mixed particles under different atmospherically relevant conditions. A summary of parameters used for the background distributions can be found in Table 5.2.

5.4 Results and Discussion

We explored the working hypothesis of enzymatically active SSA particles by two strategies: 1) Laboratory controlled seawater microcosm experiments in the MART [*Lee et al., 2015*; *Stokes et al., 2013*] designed for studying the impacts of ocean biology on aerosol chemistry (MART-A, -B, and -C, Table 5.1); 2) Sampling for the presence of active enzymes in coastal marine aerosol thus supporting the finding of enzyme release in our laboratory settings. Then, we validated the hypothesis of biologically mediated chemical changes in nascent SSA and their consequences for particle reactivity by running a focused MART experiment using a substrate and enzyme model system (MART-E, Figure 5.4). Furthermore, we employed a simulation modeling approach to estimate the nascent SSA potential in transforming marine aerosol and other particles via coagulation.

5.4.1 Discovery of Bacterial Hydrolases in Nascent SSA in Microcosm Experiments and in Ambient Coastal Air

In three separate MART microcosm experiments, after nutrient enrichment, diatom-dominated phytoplankton blooms formed and then decayed over a multi-day period (SI description of MART dynamics and Figure 5.5). In seawater, bacteria responded to the phytoplankton bloom by growing at the expenses of newly synthesized organic matter and algal detritus thus expressing specific hydrolases (Figure 5.5). Within these dynamic biological scenarios, we demonstrate for the first time that bacterial hydrolases present in seawater (SW)

and in sea surface microlayer (SSML) (Figure 5.5) are transferred into nascent SSA and retain their activities (Figures 5.1 and 5.7). Over the bloom dynamic, bacteria in SW and in SSML showed heightened protease, lipase (oleate, stearate), alkaline phosphatase, and chitinase activities (Figure 5.6). Thus, suggesting intense microbial remineralization pathways of the organic matter pool present such as lipids, proteins, phosphorus rich- organic molecules and carbohydrates. Enzyme activities in SSML exceeded those in SW up to 7.7-fold. SSA lipase (oleate and stearate), protease, and alkaline phosphatase activities were the highest. MART SSA hydrolases changed over the course of a bloom both in terms of hydrolysis rate magnitude and patterns (Figure 5.7). By normalizing MART SSA rates by the total volume of SSA, they were tens to hundreds of femtomoles h^{-1}, faster than in SW or SSML (~attomoles h^{-1}). We propose that the increased rates of SSA hydrolyses is due to their confinement in a space enriched in organic species but also due the enhanced transfer efficiency of enzymes either cell-surface- bound, vesicle-bound or freely dissolved. Given the short timeframe between SSA sampling and enzymatic assay one can rule out bacterial over expression of SSA hydrolases. Since, it is known that marine bacteria have the potential to express a vast suite of hydrolyses that can also present biphasic kinetics [*Luo et al., 2009; Arrieta et al., 2001; Unanue et al., 1999; Azam et al., 1977*], we envision that different (in structure and in function) hydrolyses could be transferred in nascent SSA over time, thus creating a more complex mosaic of reactivity within each SSA particle. It is important to mention that, in SSA, most of the activity was in the bacterial size fraction cell bound (<1 µm), whereas the dissolved fraction (<0.2 µm) never exceeded 21% of total activity (Table 5.2, in MART-C). This raises more questions than giving answers on the selectivity mechanisms that influence the ejection of a protein (dissolved enzyme) versus a bacteria cell (cell-surface-bound enzymes) in SSA. To strengthen the concept of selectivity mechanisms, that is urgent to investigate in this research line, we cannot find in our dataset a clear linear correlation among enzymatic activities and bacterial abundances in SW and SSML versus SSA.

When comparing the organic matter degradation activities in SW, SSML, and SSA (Figure 5.6F-H), SSA possessed unique enzymatic fingerprints and different hydrolysis rates than those occurring in SW and SSML. We hypothesize that these SSA enzyme qualitatively features are caused first by their synthesis by SW bacteria (secreted from or localized to microbial membranes or in the periplasm) and then ejected into SSA directly as free enzymes, enriched in the SSML, in jet drops, or mixed with active enzymes expressed in SSML bacteria that are ejected as film drops. Nevertheless, the active enzymes present in SSA will cleaved the polymeric structures into monomers that either will be taken up by bacteria or will build up in the recalcitrant organic matter pool. Additionally, the resulting SSA makeup could be modified by cell stress (e.g. strong temperature and UV gradients near the surface), and SW bacterial species-dependent transfer mechanisms.

In ambient coastal air, we detected hydrolytic activities in nascent SSA (Figure 1 and Table 5.3) with rates at the lower end of activities measured in the MART experiments. This is to be expected given the dilution processes of nascent SSA (up to 100X in comparison with the MART system) and additional non-marine sources that occur in ambient air [*Ault et al., 2009*]. The activities in ambient SSA were variable over the course of hours and days, controlled possibly by changes in ocean microbiology, SSA production mechanisms, meteorological conditions, and UV intensity. This demonstrates the relevance, the potential global scale dimension and natural variability of microbial fingerprints in SSA as determined by the biogeochemical state of the ocean (*i.e.* low vs. high biological activity).

5.4.2 Enzyme-Mediated Changes in SSA Chemistry and Reactivity: Model-System Approach

To explore how the measured enzymes change the chemistry at the SSA interface [*Dobson et al., 2000*], we used a protein substrate and enzyme model system (phosphoprotein α-

casein, referred herein as casein, and protease, Pronase E) in a coagulation "SSA mixing" MART setup (MART-E). In this setup, freshly released Pronase E-containing MART SSA was mixed with particles containing casein in an aerosol mixing tube. Using ATOFMS, the changes in SSA composition due to enzymatic degradation are reflected in the percentage of SSA particles containing phosphate throughout the "SSA mixing" experiment in MART-E and control experiments (Figure 5.2). Before enzyme addition, SSA from MART-E lacked significant proteolytic activities (Figure 5.4D), and the percentage of phosphate-containing particles slightly increased upon coagulation with casein (Figure 5.2A, [1]-[2]). When Pronase E was added to SW, SSA proteolytic activity increased (Figure 5.4D) commensurate with a decrease in the percentage of phosphate-containing particles (Figure 5.2A, [3]), as observed in the control (Figure 5.2B). These decreases were likely due to the enzymatic conversion of casein-bound phosphate to an inorganic salt that is soluble within the particle which is not readily ionized and detected by the ATOFMS [*Van Vaeck et al., 1994*a, *1994*b]. These results strongly suggest that SSA enzymes can impact chemistry of pre-existing atmospheric particles *via* degradation of organic species after ejection and coagulation.

Next, to explore how enzymatic reactions in SSA can affect surface properties and the associated reactivity, we studied the heterogeneous reaction of SSA particles with HNO_3 [*Abbatt et al., 2012*], which has important implications for NO_x budgets [*Rossi, 2003*]. Inorganic reactions of SSA particles have been traditionally been a major focus of heterogeneous reaction studies of SSA, however a recent study illustrates biomolecules in SSA can undergo heterogeneous reactions with HNO_3 [*Trueblood et al., 2016*]. To investigate the role of bioorganic molecules and hydrolases on heterogeneous reactivity, SSA particles throughout the coagulation experiment (MART-E) were reacted with HNO_3 at atmospherically relevant conditions using an aerosol reaction flow tube prior to ATOFMS sampling (Figure 5.4B). Reacted particles were easily

distinguished by the dominant presence of $^{46}NO_2^-$ and $^{62}NO_3^-$ in the negative ion mass spectra [*Ault et al., 2014; Gard et al., 1998*].

Casein forms agglomerates on the surface of coagulated SSA which can inhibit uptake of HNO_3 [*Abbatt et al., 2012; Ault et al., 2014*], react with HNO_3 directly [*Franze et al., 2005*], or form islands which expose the bulk of the aerosol, allowing the chloride-nitrate displacement reaction to occur. The percentage of reacted particles shows a decrease between nascent SSA (Figure 5.3, [1]) and casein coagulated SSA (Figure 5.3, [2]). Upon Pronase E transfer from SW to SSA, followed by coagulation with casein particles, the percentage of reacted organic-enriched SSA further decreases (Figure 5.3, [3]). This is likely due to formation of insoluble peptides from digested casein blocking access to the particle surface and inhibiting reactive uptake of HNO_3 [*Abbatt et al., 2012*; *Ault et al., 2014*], as suggested by molecular models and bioinformatic analyses of the peptides which result from Pronase E degradation of casein agglomerates as solubility depends on which organics and ions are present (Figure 5.9B-D). These results demonstrate the ability of enzymes to significantly alter the surface properties and ultimately reactivity of SSA particles (Figure 5.9A, see 5.8.6)

5.4.3 Simulating Coagulation of Nascent SSA and Atmospheric Particles: Implications for Chemistry of the Atmosphere

Finally, the more widespread impact of this newly discovered enzymatic reaction pathway was estimated by examining how rapidly the enzyme-containing SSA particles would mix with background marine particles. A stochastic, particle-resolved aerosol model is used to simulate coagulation timescales under three atmospherically relevant background conditions using a previously reported SSA number distribution [*Collins et al., 2013; Riemer et al., 2009*] (see 5.8.7). After mixing with pre-existing particles in the atmosphere, the model predicts that after only 24 hours up to 18% of the background particles will coagulate with at least one SSA

particle depending on the background particle concentration (Fig. 5.10, top). While this number may seem small, further size-resolved analysis revealed nearly every background particle in the size range important for heterogeneous reactions [*Ault et al., 2014; Finlayson-Pitts and Pitts,* 1999] (>500 nm) have coagulated with at least one SSA after only 24 hours (Fig. 5.10, bottom). These results highlight that hydrolases can significantly impact the composition, reactivity, and properties of a substantial fraction of particles in the marine environment.

5.5 Conclusions

In summary, active marine microbial enzymes are ejected in SSA, an extension of the aerosol bioreactor hypothesis proposed by Dobson et al., 2000. This has a number of important implications as enzyme reactions can: 1) change the composition of SSA and background tropospheric aerosols over time; 2) alter surface properties which in turn impact phase segregation, heterogeneous reactivity, and cloud activation properties; 3) provide a new atmospheric reaction pathway that can be more efficient than heterogeneous reactions, 4) represent a new source for reactions at interfaces which lead to small volatile organic compounds in the atmosphere, and 5) form surface active species, including fatty acids, alcohols, hydrophobic peptides, and lipids which can alter cloud droplet and ice nucleation processes. Importantly, this study provides a previously unidentified link showing how ocean-derived biological species can impact the composition of the atmosphere.

5.6 Acknowledgments

This study was funded through the Center for Aerosol Impacts on Chemistry of the Environment (CAICE), a National Science Foundation Center for Chemical Innovation (CHE-1305427). F.A. and F.M. were supported by Gordon and Betty Moore Foundation through grant

#2758 and 4827 to F.A. T.T. was supported by Fulbright grant (68130845) and by the Ministry of Higher Education, Science and Technology of the R Slovenia (P1-0237). Y.Z. was supported by the China Scholarship Council (from October 2013 to October 2014). N.R. would like to acknowledge NSF CAREER AGS (1254428). The authors would like to thank Tom Hill and Tim Bertram for their valuable contributions.

Chapter 5 has been submitted to ACS Central Science: Malfatti, F.,* Lee, C.,* Tinta, T., Ryder, O.S., Schiffer, J.M., Pendergraft, M.A., Celussi, M., Zhou, Y., Sultana, C.M., Rotter, A., Axson, J.L., Collins, D.B., Santander, M.V., Anides M., A.L., Aluwihare, L.I., Riemer, N., Azam, F., Prather, K.A. Sea Spray Aerosols: Tiny Biochemical Reactors in the Atmosphere. The dissertation author was the co-primary investigator and co-author of this paper. Authors with * contributed equally. F.M., C.L., F.A., and K.A.P. designed the experiment, F.M., T.T., Z.Y., M.A.P. A.M.A. performed enzyme activity measurements, C.L. performed single particle mass spectrometry measurements, N.R. performed coagulation simulations, and J.M.S. performed molecular modeling and calculations. All other coauthors participated in the experiment.

5.7 Figures

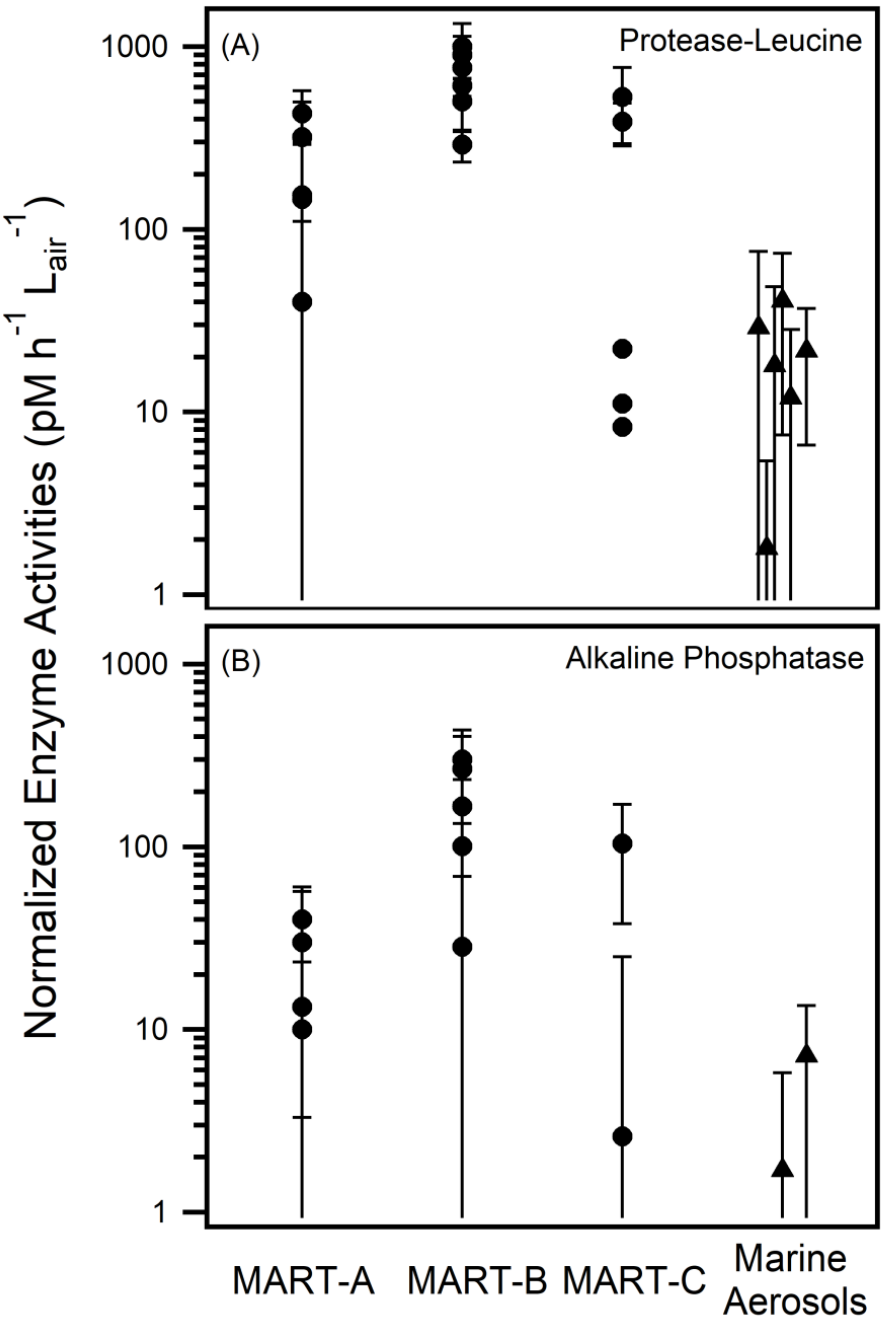

Figure 5.1. SSA hydrolytic enzyme activities for MART induced phytoplankton bloom experiments (MART-A, -B, and -C, circle) and impinged marine ambient particles from coastal Pacific Ocean (in June and July, 2017, triangle) normalized to L^{-1} of air sampled. Error bars represent 1σ. More information such as chl *a* concentration at the time of aerosol collection and temporal behavior over MART phytoplankton blooms can be found in the Section 5.8.

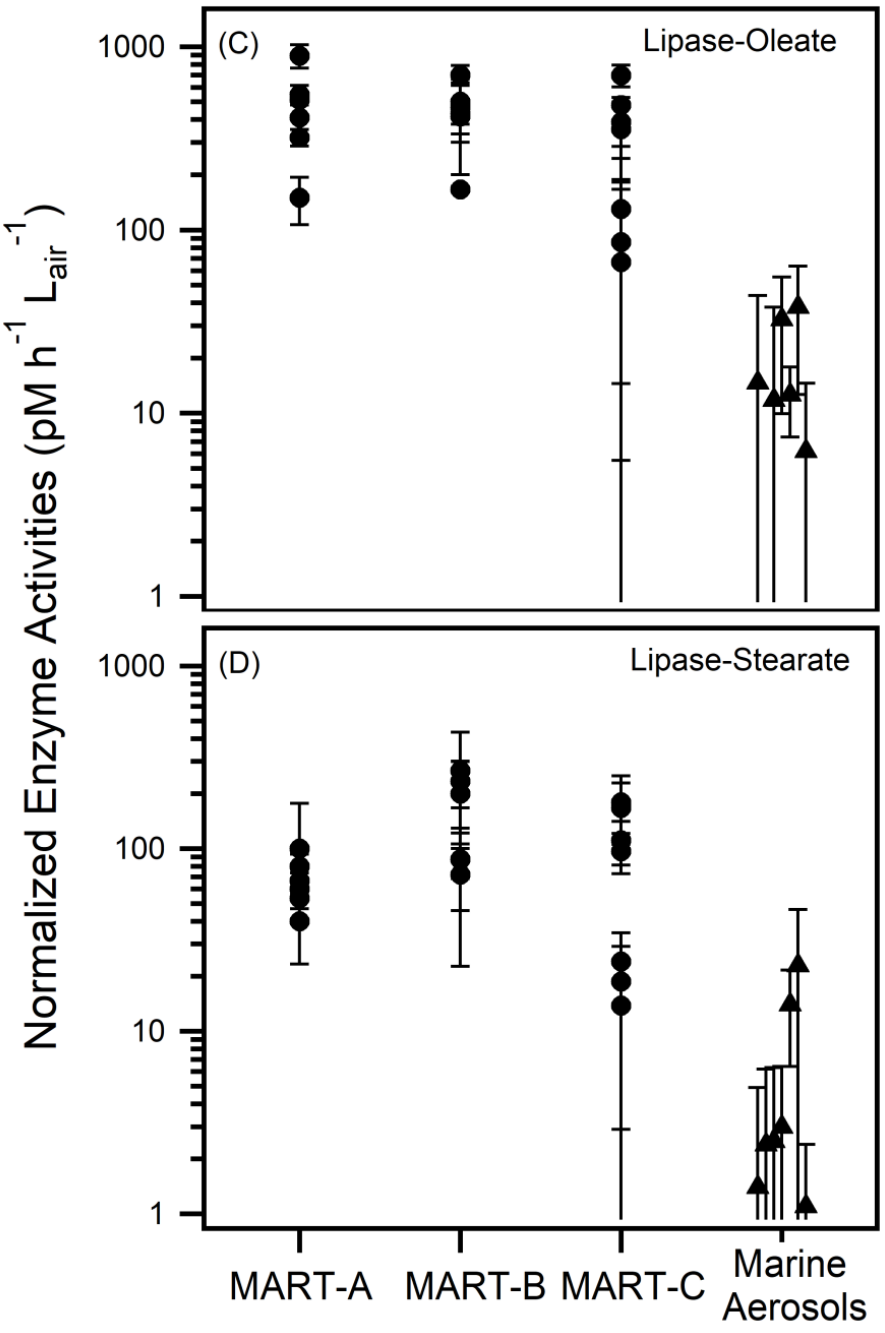

Figure 5.1. SSA hydrolytic enzyme activities for MART induced phytoplankton bloom experiments and impinged marine ambient particles from coastal Pacific Ocean continued.

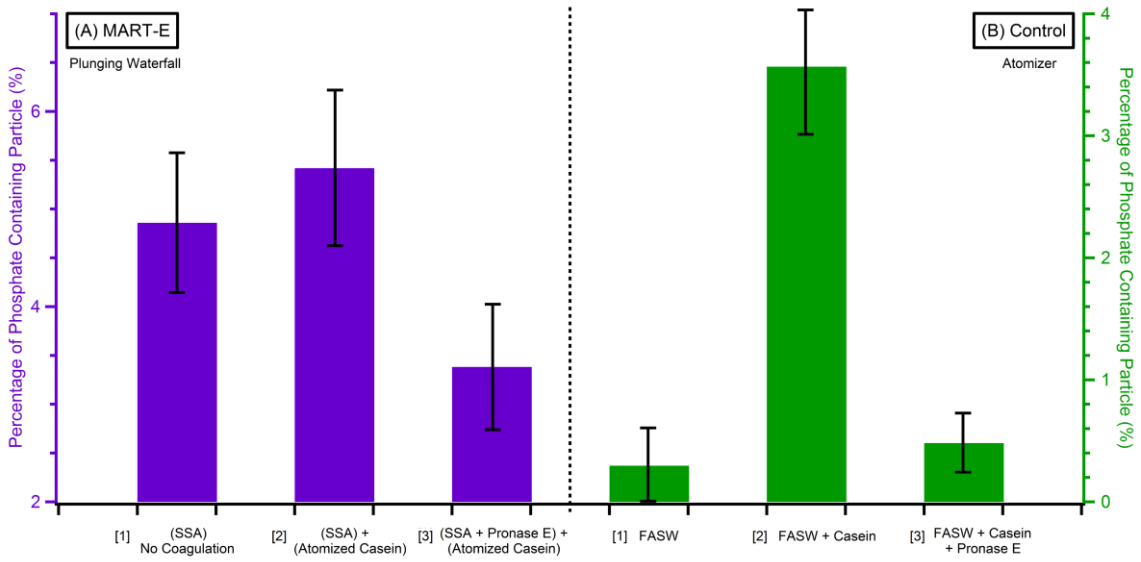

Figure 5.2. (A) Percentage of phosphate-containing particles for MART-E experiment (>2 µm D_{va}, purple) and (B) control atomizer experiment (green). FASW is filtered autoclaved seawater. Error bars represent 2σ for 95% confidence limit.

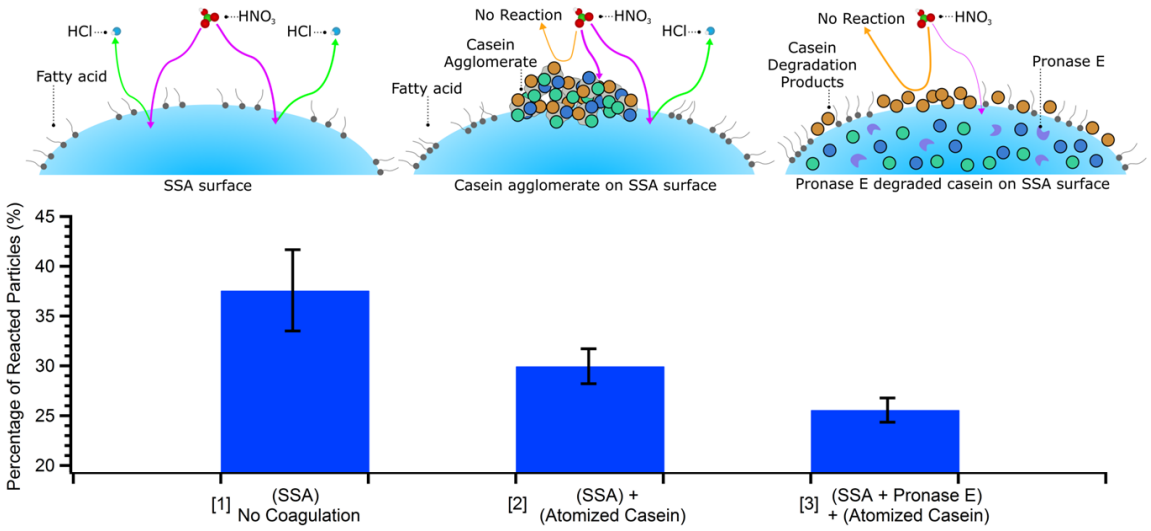

Figure 5.3. Percentage of reacted particles (>2 µm D_{va}) for MART-E experiment. Cartoon models SSA surface features based on experimental and theoretical results. Line thickness (purple and orange lines) illustrates preferred heterogeneous reaction pathway. Error bars represent 2σ for 95% confidence limit.

5.8 Supporting Information

5.8.1 Chlorophyll-a and Dissolved Organic Carbon Dynamics in MART-A, -B, and -C

During the MART experiments, intense phytoplankton blooms developed within 9 to 10 days after initiation (MART-A: 30 µg L^{-1}, MART-B: 35 µg L^{-1}, MART-C: 39 µg L^{-1}, Chl-a; Figure 5.5). In MART-C, a secondary bloom developed after 10 days (25 µg L^{-1}, Figure 5.5A). Diatoms dominated the phytoplankton community during all four blooms. DOC, sampled in seawater (SW), accumulated during the growth phase as well as during the demise of the phytoplankton blooms, and concentrations remained above pre-bloom levels through the termination of each experiment (Figure 5.5B).

5.8.2 Bacteria and Virus Dynamics in SW, SSML, and SSA of MART-A, -B, and -C

In the SW and sea surface microlayer (SSML) compartments, a bloom of heterotrophic bacteria developed following the peak in the phytoplankton bloom (Figure 5.5C, D), whereas viral abundance increased during the decaying phase of the phytoplankton bloom (Figure 5.5E, F). The SSML was enriched in bacteria and viruses relative to the bulk seawater after the collapse of the bloom, with the exception of MART-C (Figure 5.5G, H). In SSA, bacteria abundance normalized per liter of impinged air was variable in the three experiments with maximum values reaching 7.4 x 10^4, 5.4 x 10^6 and 9.3 x 10^3 cells L^{-1}, respectively, in MART-A, MART-B and MART-C. In SSA, viral abundance normalized per liter of impinged air, was the same order of magnitude in MART-A and MART-C but was one order of magnitude lower in MART-B. The observed variability in abundances reflects differences in the efficiency of the mechanisms that regulate the “ejection” of bacteria and viruses into the SSA from the SW and SSML (bacteria and virus abundance in SSA did not correlate with the relative stocks in SW and SSML). Differences

in SSA abundances of bacteria and virus could not be attributed to variability in air-flow into the MART or the impinger (Table 5.1). We plated SSA onto ZoBell solid medium to test for bacterial viability. Some bacteria formed colonies, evidencing that at least a part of the microbes were still viable once ejected into SSA.

Bacteria and virus abundances in SSA varied across the three experiments and did not directly correspond to the abundances in SW or SSML (Figure 5.5C-H). The large variability in abundance in the three experiments indicates differences in the efficiency of the SSA production mechanism in regulating the "ejection" of bacteria and viruses into SSA. Given the bacterial abundance in SSA, not all particles contained a bacterium, but most SSA particles likely contained dissolved or vesicle-associated enzymes. As shown in previously [*Patterson et al., 2016*], SSA produced during mesocosm blooms can contain vesicles which likely contain enzymes that were enriched in the SSML.

5.8.3 Ectohydrolytic Activities in SW and SSML of MART-A, -B, and -C

During the phytoplankton bloom experiments, intense protease, lipase, alkaline phosphatase, chitinase activities were measured in the SW and in the SSML (Figure 5.5A-E). In SW and SSML, protease and alkaline phosphatase trends reflected Chl-a trends ($p < 0.01$; $p = 0.05$, Table 5.5). This suggests that the bacterial enzymatic intensity likely was correlated with the phytoplankton bloom. Hydrolases activities in SSML were greater than those in SW by factors ranging from 1 to 7.7 times.

As MART phytoplankton bloom experiments are isolated systems, marine aerosols at coastal ocean were impinged to demonstrate that these marine aerosols have enzymes that stay hydrolytically active in the atmosphere (Figure 5.1 and Table 5.4). As it is known for the natural seawater, but this is the first time SSA is assayed, microbial activities in SSA are diverse and can vary on a daily and hourly base due to the diverse bacteria ecotypes present in the sea (different

gene expression) and the diverse organic matter pool present in the water that can be explored by bacteria. Overall, in natural SSA, protease-leucine, lipase-stearate, and lipase-oleate presented higher hydrolysis rates. We speculate that in freshly released SSA, the rates of hydrolysis for lipases, proteases, and alkaline phosphatases are unlikely to be diffusion limited: that is, on the order of 10^9–10^{10} $M^{-1}s^{-1}$ [*Bar-Even et al., 2011*]. When we compare natural SSA with MART rates, natural values are lower in the range of pre-bloom MART and are in agreement as natural ambient aerosols were produced during period of low biological activity. This result demonstrates that aerosols from MART and ambient marine environment remain hydrolytically active and studies of MART particles are atmospherically relevant.

5.8.4 Statistical Analysis on Enzymatic Hydrolysis Rates of MART-A, -B, and -C

Pooling the temporal patterns of enzyme activities and analyzing the three compartments (SW, SSML and SSA), we conclude that: 1) In SSA, protease, lipase, alkaline phosphatase and chitinase varied inversely to the respective SW activities (Table 5.4B, see negative coefficient sign); 2) In SW and SSML, phosphatase and lipase activities showed similar trends (Table 5.5B, see positive coefficient sign); 3) SSML activities were always >> SW, as one would expect for enzymes acting at the interface, especially lipase [*Maupetit et al., 2010*; *Reis et al., 2009*] (Table 5.4B, where SSML coefficient values compared to SW are < 1, $p < 0.01$); 4) In SSA, only protease showed inverted trends *(e.g*. anticorrelated) to DOC (sampled in SW) after the bloom's demise (Table 5.5C). These results show major contributions of SSML lipase and alkaline phosphatase to SSA in quantitative terms.

We qualitatively analyzed the composition of SSA based on the enzymatic patterns of organic matter degradation in SW, SSML (Figure 5.6F-H). We found that SSA is qualitatively unique in the enzyme composition and based on the Non-Metric Multi Dimensional Scaling

(NMDS) analysis, we hypothesized that SSA enzymes are first generated in SW, and then primed in SSML before being released in SSA.

5.8.5 MART-E Coagulation Experiment and Control Experiment

To confidently track the chemical changes occurring in a single particle level due to 1) coagulation of casein and 2) degradation of casein due to protease Pronase E, a simple control experiment was performed. Solution containing casein dissolved in ultrapure water (1 mg mL^{-1}) was atomized using atomizer to produce particles, and was dried (<10% RH) prior to sampling by ATOFMS. Figure 5.8A shows the averaged dual polarity mass spectra of the analyzed particles, with dominant ion markers of biogenically derived organic markers such as $^{26}CN^-$, $^{42}CN^-$, $^{79}PO_3^-$ observed [*Lewis and Schwartz, 2004*; *Martinez et al., 1996*]. It was empirically found that degradation of casein due to Pronase E decreased the signal of $^{79}PO_3^-$ observed in both the number of particles and the relative peak area intensity, while the other bioorganic metric of $^{26}CN^-$ and $^{42}CNO^-$ did not exhibit this behavior and increased as casein and Pronase E was subsequently added. Thus, the decrease in the $^{79}PO_3^-$ signal was used throughout the work to indicate the degradation of casein and $^{26}CN^-$ and $^{42}CNO^-$ as indicator of organic-enrichment in the coagulated SSA

We assessed the protease activity in MART-E before and after the amendment with Pronase E (Figure 5.8D) in SW and in SSA. Pronase E was successfully transferred from the SW to SSA reaching orders of 60 femptomoles/ SSA particle h^{-1} and showing a consistent rate for the subsequent 24 h.

As atomizer produced much higher concentration of particles than the MART (Figure 5.8C) it cannot be confidently said that all sizes of the SSA from the MART contained casein from coagulation due to the high background. However, the inset of Figure 5.8C shows that for all three conditions of the experiment, size distribution of particles greater than 1.5 μm D_a showed

similarity within the error of the APS. Therefore, the changes in the measured chemistry, and the reactivity of the particles greater than 2 μm D_{va} by the ATOFMS (calculated from D_a assuming cubic particles with density of 1.8 g cm^{-3}) [*DeCarlo and Slowik, 2004*; *Zelenyuk et al., 2007*] from the three different experiment conditions must be due to the coagulation of the casein containing particles with SSA particles, and not due to increased number of externally mixed background particles. In addition to the three conditions detailed above, control experiments of atomized casein solution only and MART spiked with Pronase E was analyzed by ATOFMS. Results from these two control experiments further support the observation that the changes occurring for particles 2 μm D_{va} were due to coagulation of the casein containing particles, and degradation of the casein due to Pronase present in the SSA.

It should be noted, SSA produced from seawater after a phytoplankton bloom (MART-E) frequently generated mass spectra phosphate ion signal (Figure 5.2A, [1]). The percentage of phosphate-containing particles from SSA pre- and post-Pronase E addition remained unchanged (Figure 5.8B), corroborating that MART-E results must be due to enzymatic activity in SSA.

Combining the experimental above and theoretical results described in 5.3.7 and 5.3.8, Figure 5.3 top inset depicts the surface of SSA before and after Pronase E degrades casein with the probable pathway of HNO_3 heterogeneous reaction to provide explanation on the observed particle reactivity differences. It is possible that digested casein molecules, with both water soluble and insoluble peptides, are distributed within the particles, prohibiting reactive uptake of HNO_3. Moreover, the said effect could be due to the interaction of digested casein molecules with other organic molecules in SSA, such as fatty acids [*Cochran et al., 2016*], in forming a more stable organic monolayer at the particle surface to impact heterogeneous reactivity [*Donaldson and Vaida, 2006*].

5.8.6 Molecular Modeling of Enzymes and Peptides

5.8.6.1 Hydrolase Modeling and Analysis

A model of the *Pseudomonas cepacia* lipase (PDB: 3LIP)(24) was built in a multi-component SSA-mimicking monolayer, the protein depth within the monolayer was approximately 8.3 ± 0.8 Å, with a surface accessible surface area of 4650 $Å^2$ facing out towards the outside of the monolayer (Figure 5.9A). This solvent accessible surface area suggest that lipase could contribute to surface chemistry.

Enzyme activity results presented here suggest greater transfer efficiency of proteases, phosphatases, and lipases. It is possible that these enzymes are secreted and upregulated due bacterial cell stress, as is common when marine bacteria undergo stress responses [*Antelmann et al., 2003*; *Dalbey et al., 2012*; *Eggert et al., 2003*; *Green and Mecsas, 2016*; *Willsey and Wargo, 2015*]. Additionally, chitinases are secreted by bacteria in response to physical interactions with diatoms [*Li et al., 2016*] and expressed in the presence of chitin (e.g.: copepods). Since diatoms are quite large and thus are not likely found within an aerosol particle along with bacteria, chitinases could be secreted less within the SSA particles than they are within the bulk.

5.8.6.2 Casein and Pronase E Modeling

On a molecular level, casein molecules interact with one another in a micelle structure on the order of ~100 nm in diameter with colloidal calcium phosphate embedded in the casein architecture with an ~2.5 nm diameter [*Marchin et al., 2007*]. When Pronase E cleaves casein into peptides it is likely to disrupt this micelle architecture resulting in release of colloidal calcium phosphate from the micelle. This hypothesis is supported by bioinformatics methods to predict the phase state of casein pre- and post- Pronase treatment (Figure 5.9B-D).

5.8.7 Particle Coagulation Simulations

Figures 5.2 and 5.3 illustrate that, in principle the ejected enzymes in the SSA can further transform the composition of organic aerosols in the atmosphere. The particle resolved-coagulation simulations show that for all three background concentration cases, the smaller Aitken mode particles are coagulated onto the larger SSA particles (Figure 5.10, top). Increased concentration of the background aerosol led to faster rate of coagulation, but independent of the simulated case, the coagulated particles had a number size distribution ranging from 100 nm to 2 μm, with peak of the distribution at approximately 300 nm.

The ratio of mixed particles to the sum of mixed and background ($\phi_3 = N_{mix} / (N_{mix} + N_{backg}$), where N_{backg} and N_{mix} are the total number of background aerosol and background aerosol coagulated with at least one SSA particle, respectively) quantifies the change the background particles experience by coagulating with SSA. The higher the background number concentrations, the lower ϕ_3 will be, but after 24 h of simulation, 16%, 40%, and 57% of 300-nm particles (peak of the mixed particle distribution) for high, medium, and low background cases, respectively, had coagulated with potential enzyme-containing SSA (Figure 5.10, bottom). These results demonstrate the significance of this new proposed atmospheric reaction pathway.

5.8.8 Supporting Information Figures

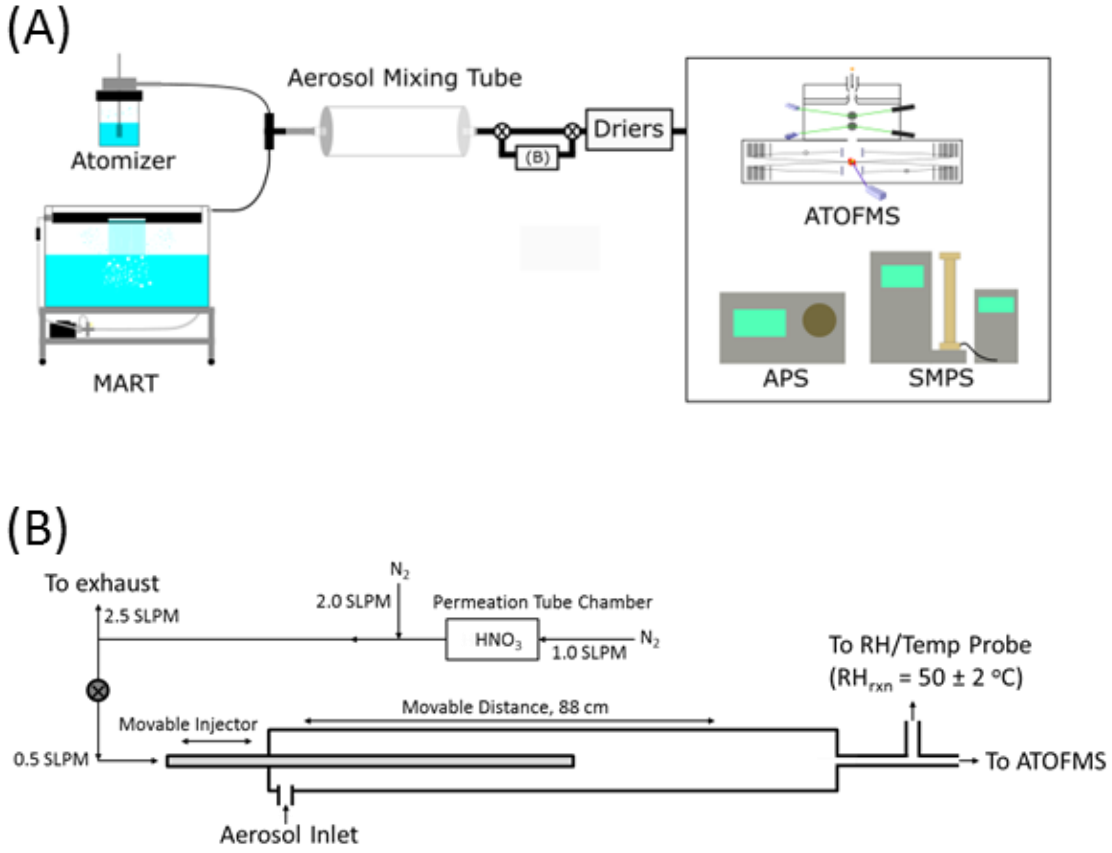

Figure 5.4. MART-E coagulation experiment setup and parameters. (A) Experimental setup investigating the role of enzyme containing SSA coagulated with particles containing the organic substrate molecule, alpha-casein. (B) Experimental setup figure of the nitric acid reaction flow tube. This apparatus with movable injector fully extended out for maximum residence time was placed in between the aerosol mixing tube and the ATOFMS in (A) to probe the heterogeneous reactivity of the particles to nitric acid. (C) Averaged Aerodynamic Particle Sizer (APS) number concentration distribution of SSA (blue), SSA coagulated with coagulated with particles containing Casein (black), and SSA spiked with Pronase E coagulated with particles containing Casein (green). Insert shows zoomed-in distribution from 1.5 µm D_a and above. (D) Leucine aminopeptidase activities in SW, and SSA during MART-E experiment. BEFORE and AFTER refer to the addition of the protease Pronase E to the SW compartment. Error bars represent 1σ.

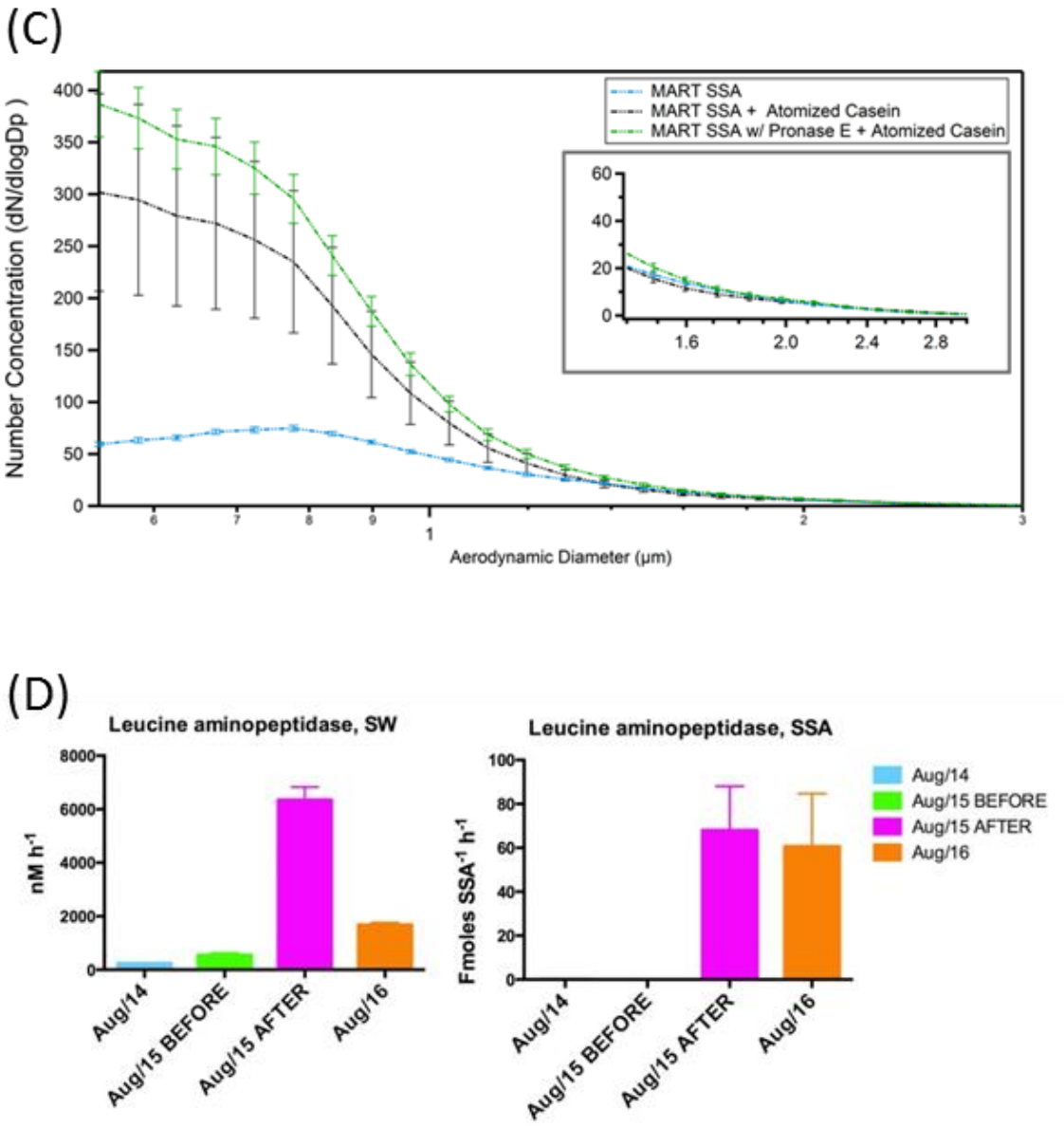

Figure 5.4. MART-E coagulation experiment setup continued.

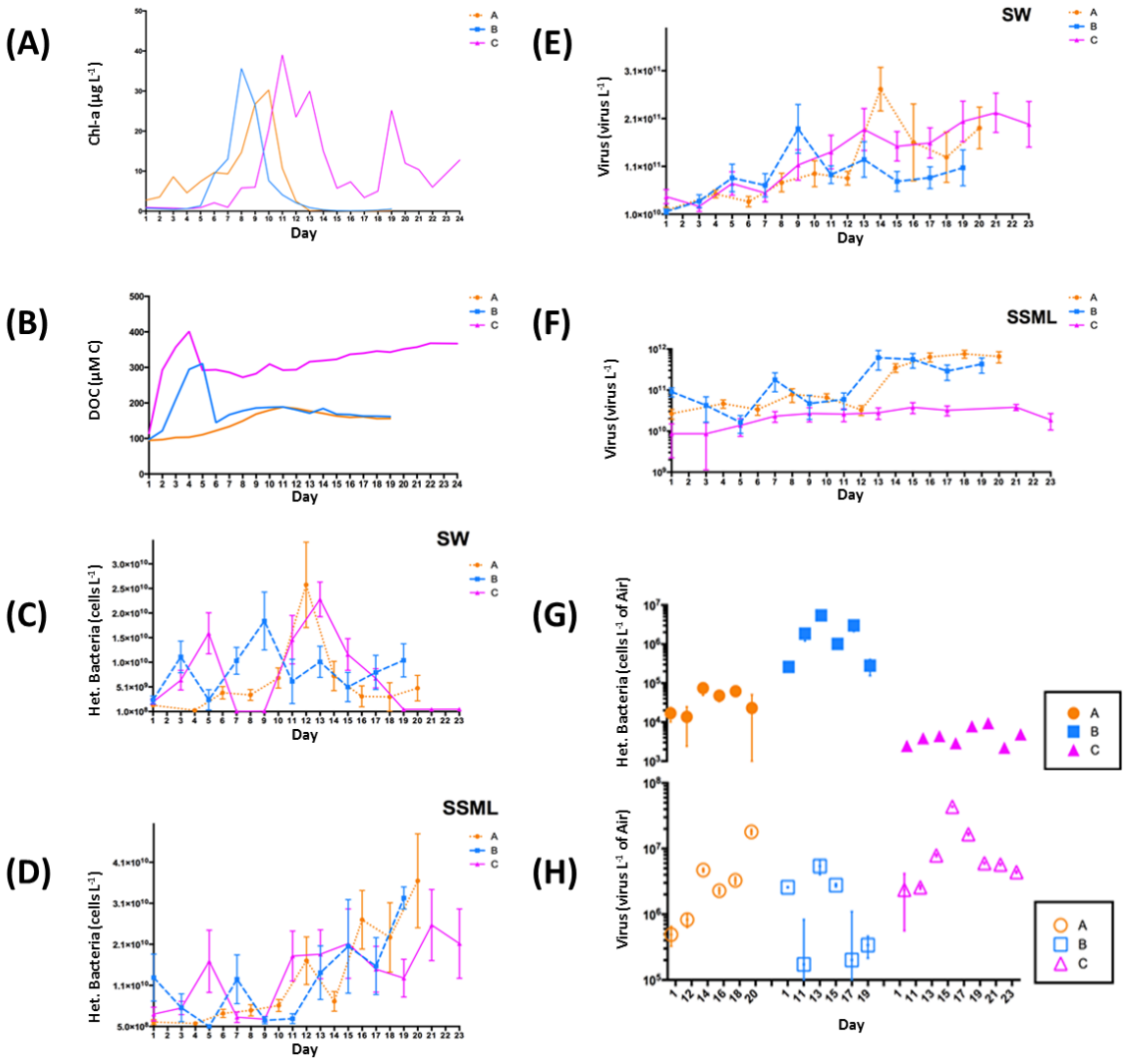

Figure 5.5. Chlorophyll-a in µg L^{-1} (A), Dissolved organic carbon (DOC) in µM C (B), heterotrophic bacteria abundance in cells L^{-1} in SW (C), in SSML (D), virus abundance (virus L^{-1}) in SW (E), and in SSML (F), bacteria (G), and virus (H) abundance in SSA per liter of air during the MART experiments. X-axis indicates the day of the experiment. MART-A in orange (circle), MART-B in blue (square), and MART-C in magenta (triangle).

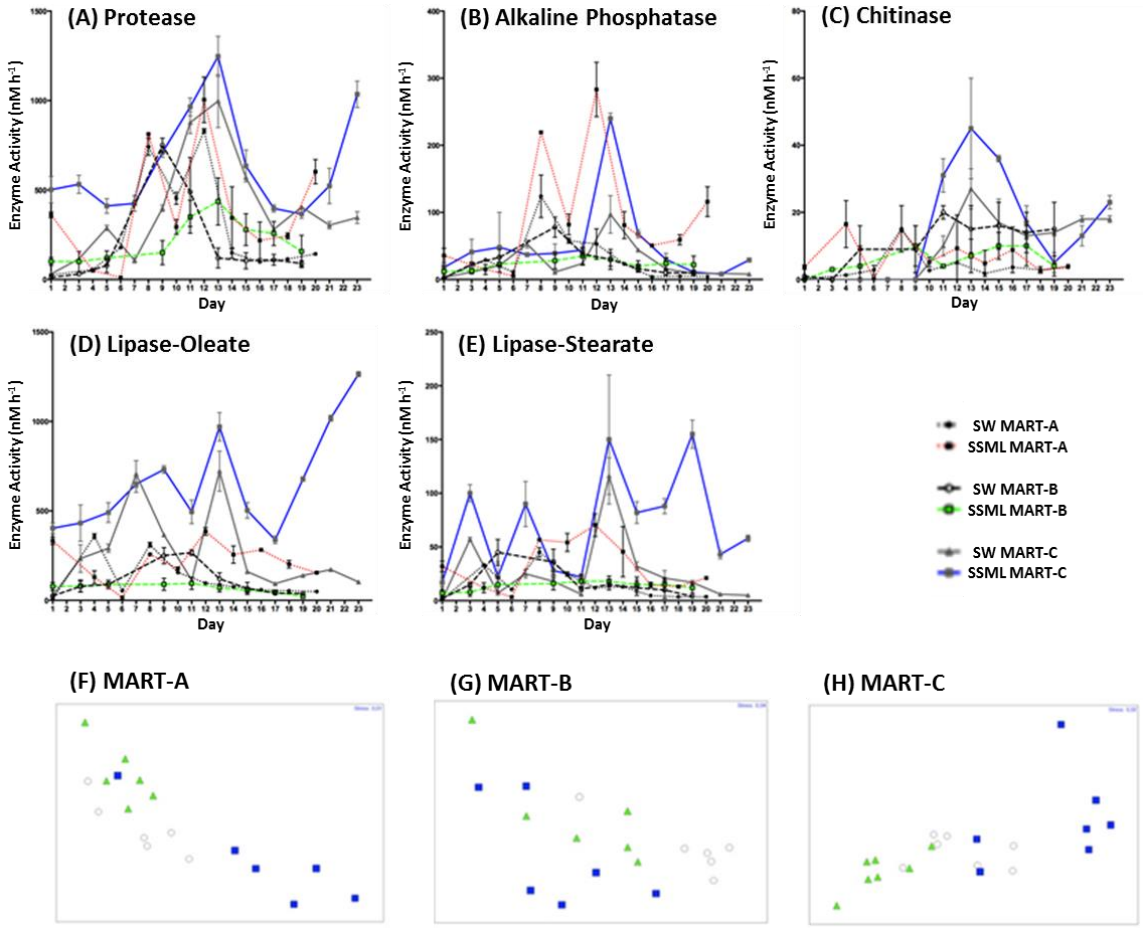

Figure 5.6. Hydrolytic enzyme activities in SW, SSML and SSA (in red) during MART experiments, expressed in nM h^{-1}. Protease (A), chitinase (B), alkaline phosphatase (C), lipase-oleate (D), and lipase-stearate (E). X-axis indicates the day of the experiment. Non-metric multidimensional scaling (NMDS) plots of enzymatic hydrolysis rates of MART-A (F), -B (G), -C (H) show qualitative enzymatic fingerprint of the SW samples (triangle), SSML samples (circle), and SSA (square). Stress level 0.01, 0.04, and 00.2 for MART-A, -B, and -C respectively.

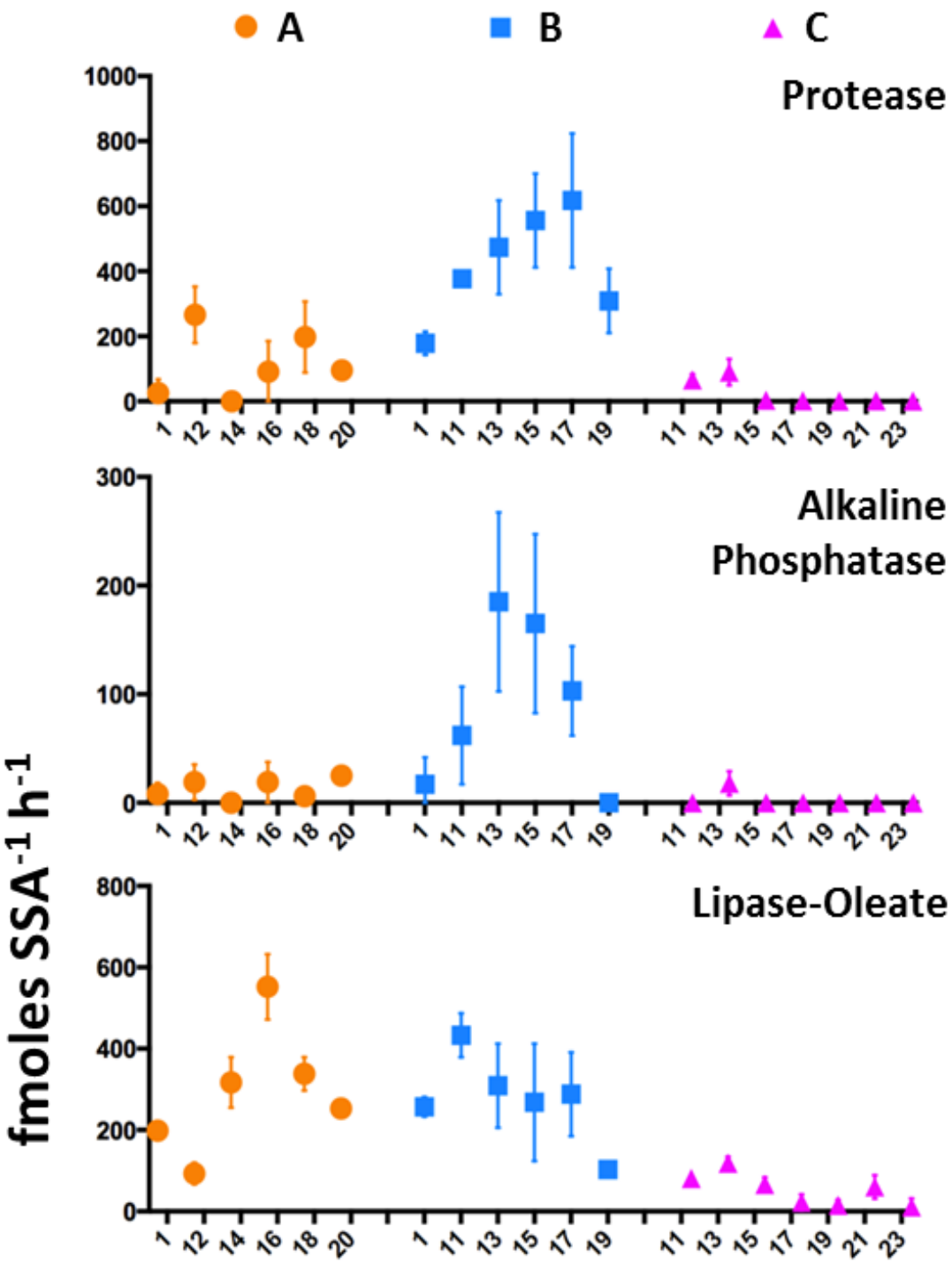

Figure 5.7. SSA hydrolytic enzyme activities over the course of three separate phytoplankton bloom microcosm experiments (x-axis, SSA production day, error bars represent 1σ). Protease, alkaline phosphatase, lipase-oleate, lipase-stearate, and chitinase normalized per total SSA volume over the course of each microcosm experiment. MART-A (orange circle), MART-B (blue square), and MART-C (magenta triangle).

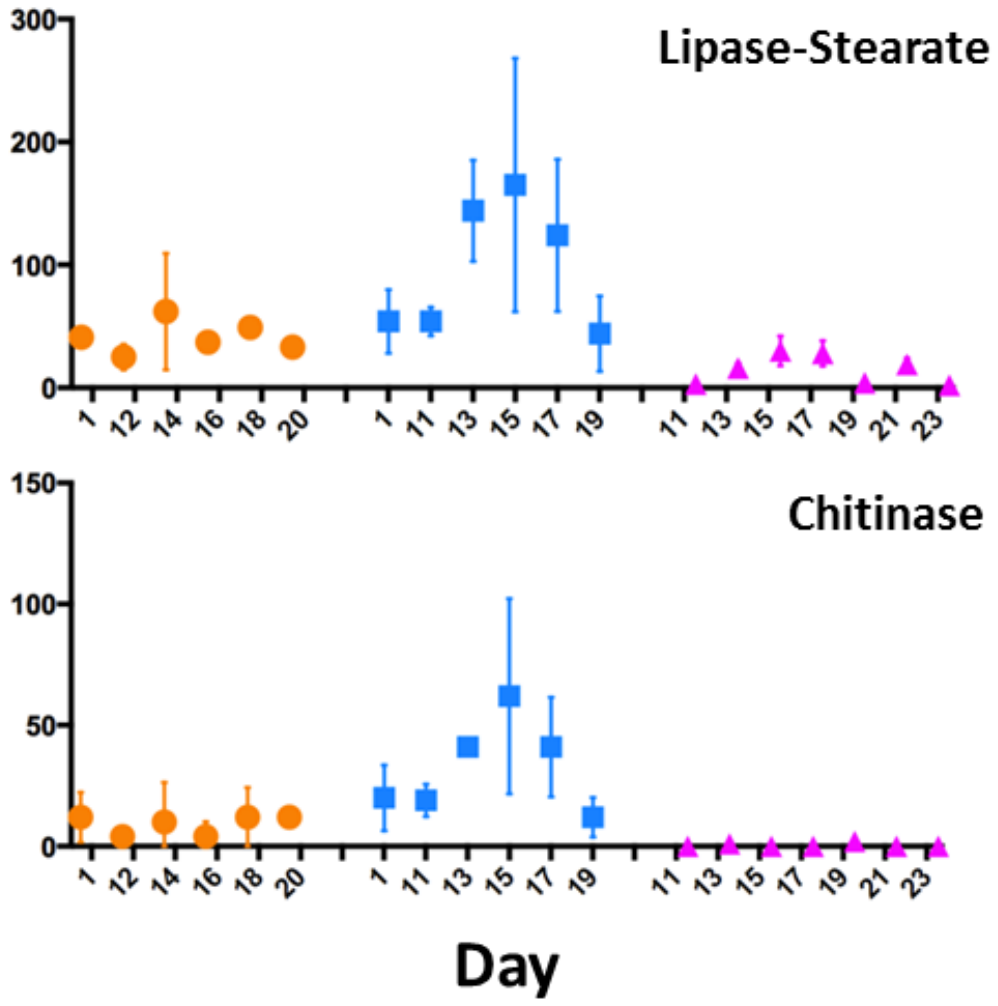

Figure 5.7. SSA hydrolytic enzyme activities over the course of three separate phytoplankton bloom microcosm experiments continued.

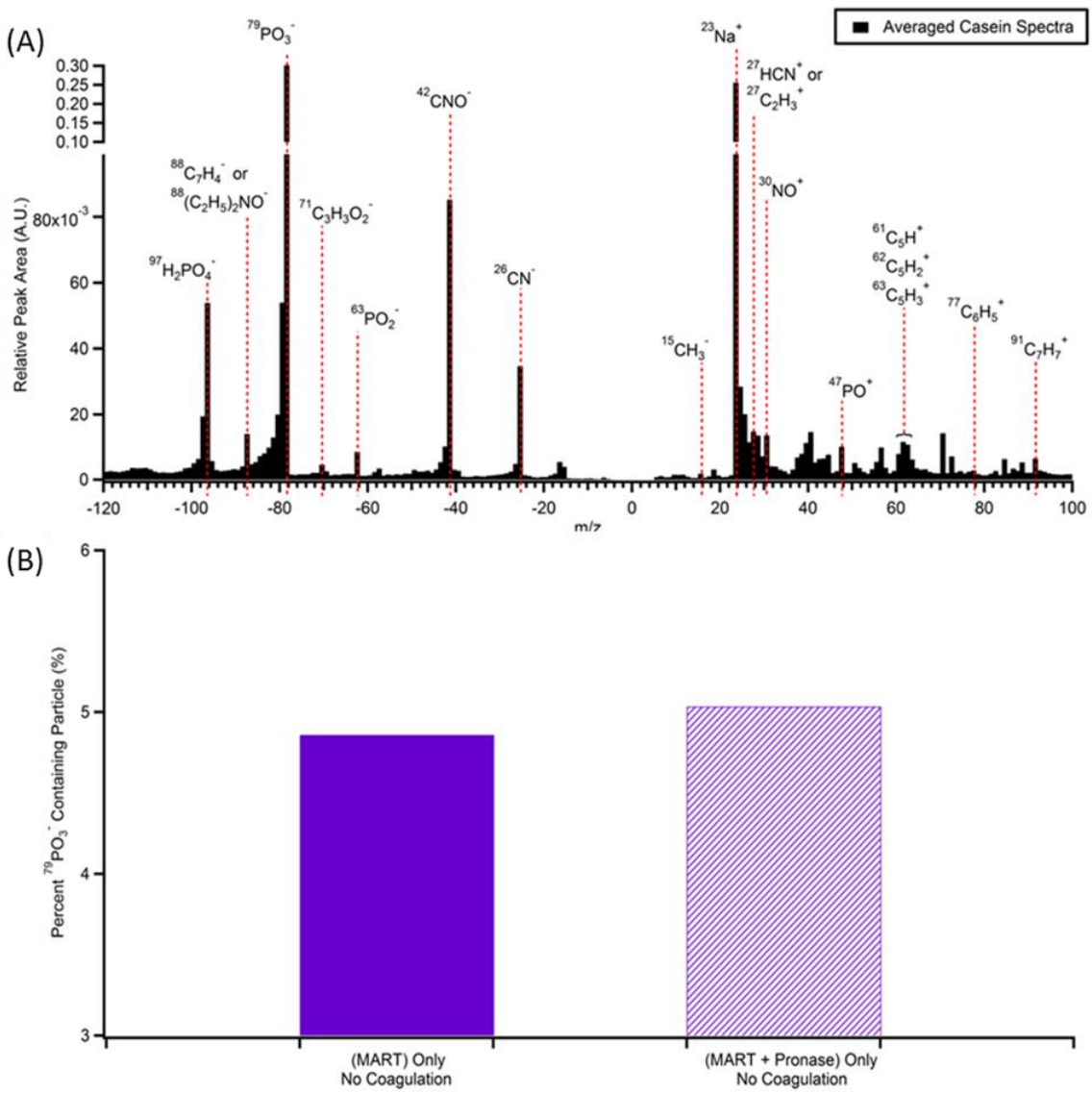

Figure 5.8. (A) Averaged single particle mass spectra of atomized casein particles dissolved in ultrapure water (1 mg mL^{-1}). Annotated ion markers provide chemical fingerprint to be used with the MART-E experiment data analysis. (B) Percentage of particles containing phosphate ($^{79}PO_3^-$) ion markers for MART-E experiment (SSA) and control experiment of MART-E with Pronase E addition, no coagulation of casein particles.. MART-E shows results from particles >2 µm D_{va}.

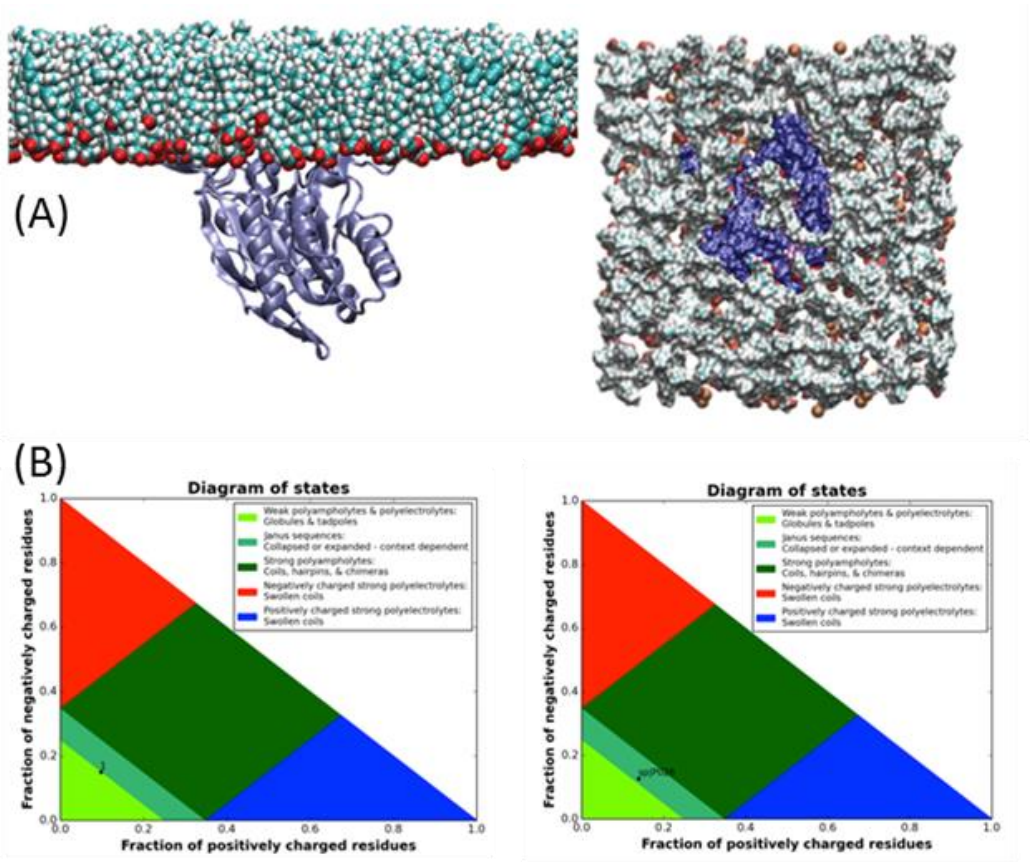

Figure 5.9. Bioinformatic analyses of the peptides produced from Pronase E degradation of Casein. (A) Atomic level model of lipase from *Pseudomonas cepacia* (PDB: 3LIP) partitions between the water and membrane interface. (left) Side view along a lipid monolayer on top and aqueous phase below showing the lipase structure in cartoon in blue. Hydrogens are colored white, carbons cyan, and oxygens red in the models for the fatty acids in the monolayer. (right) Top view from hydrophobic side of lipid monolayer showing the surface of the protein which is surface accessible in blue. (B) State Diagram of Alpha-S1-Casein (left) and Alpha-S2-Casein (right). Both casein proteins are predicted based on sequence Janus sequences. This aligns with experimental data that suggests that the colloidal state of casein changes with decrease in pH and other environmental factors. (C) Pronase E cleavage products of Alpha-S1-Casein (left) and Alpha-S2-Casein (right). Aside from being much shorter in sequence than full length casein, the cleavage products predicted of both isoforms of casein by Pronase E result in some Janus peptides, but about half of the largest cleavage products are predicted to be either weak or strong polyampholytes. (D) Example of the properties of a few of the peptides analyzed from Pronase E cleavage of alpha-S1-Casein. (top) These analyses were performed with Innovagen's Peptide calculator which demonstrate the relative sequence positions of acidic, aromatic, basic, aliphatic, polar, and cysteine residues within the amino acid sequence. (bottom) APBS calculations were performed on models of the casein peptide cleavage products. While Seq1 and Seq2 were predicted to have good water solubility and had qualitatively higher surface charge (red is negative, blue is positive, white is hydrophobic), Seq 3 was predicted to have poor water solubility as well as low surface charge.

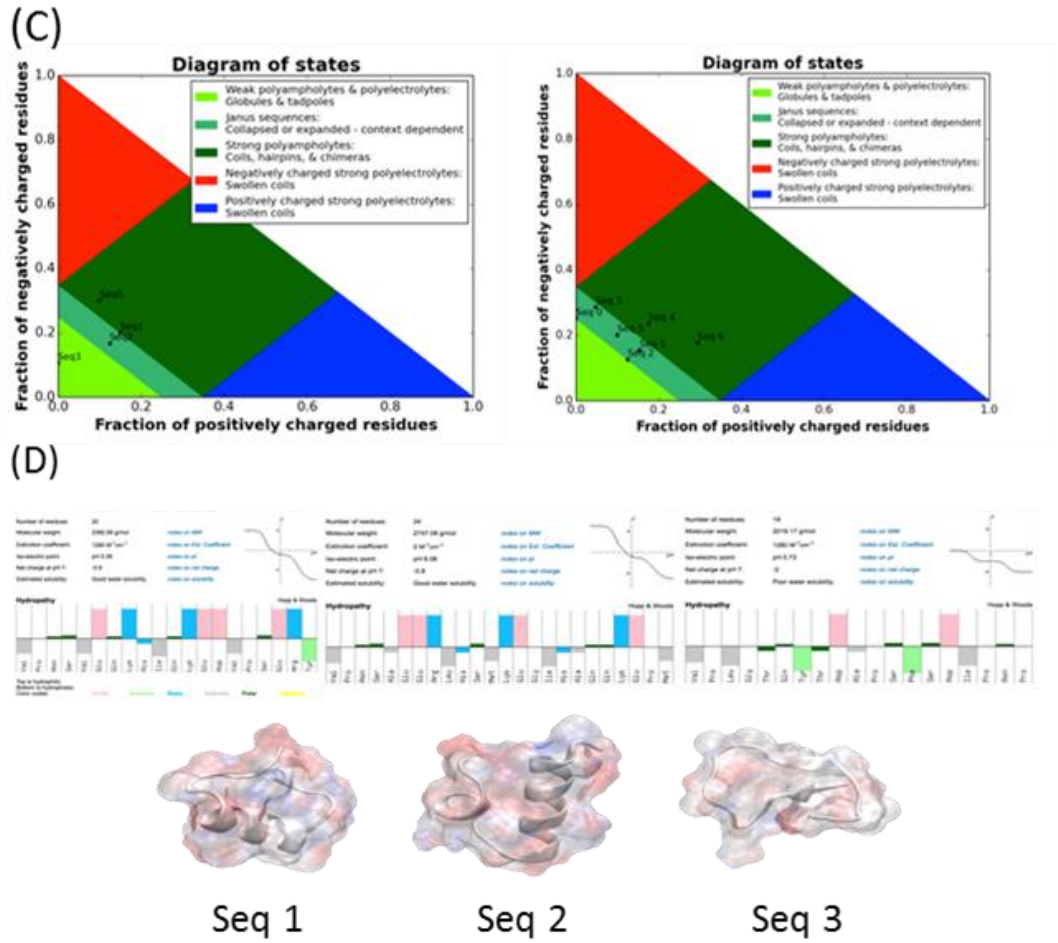

Figure 5.9. Bioinformatic analyses of the peptides produced from Pronase E degradation of Casein continued.

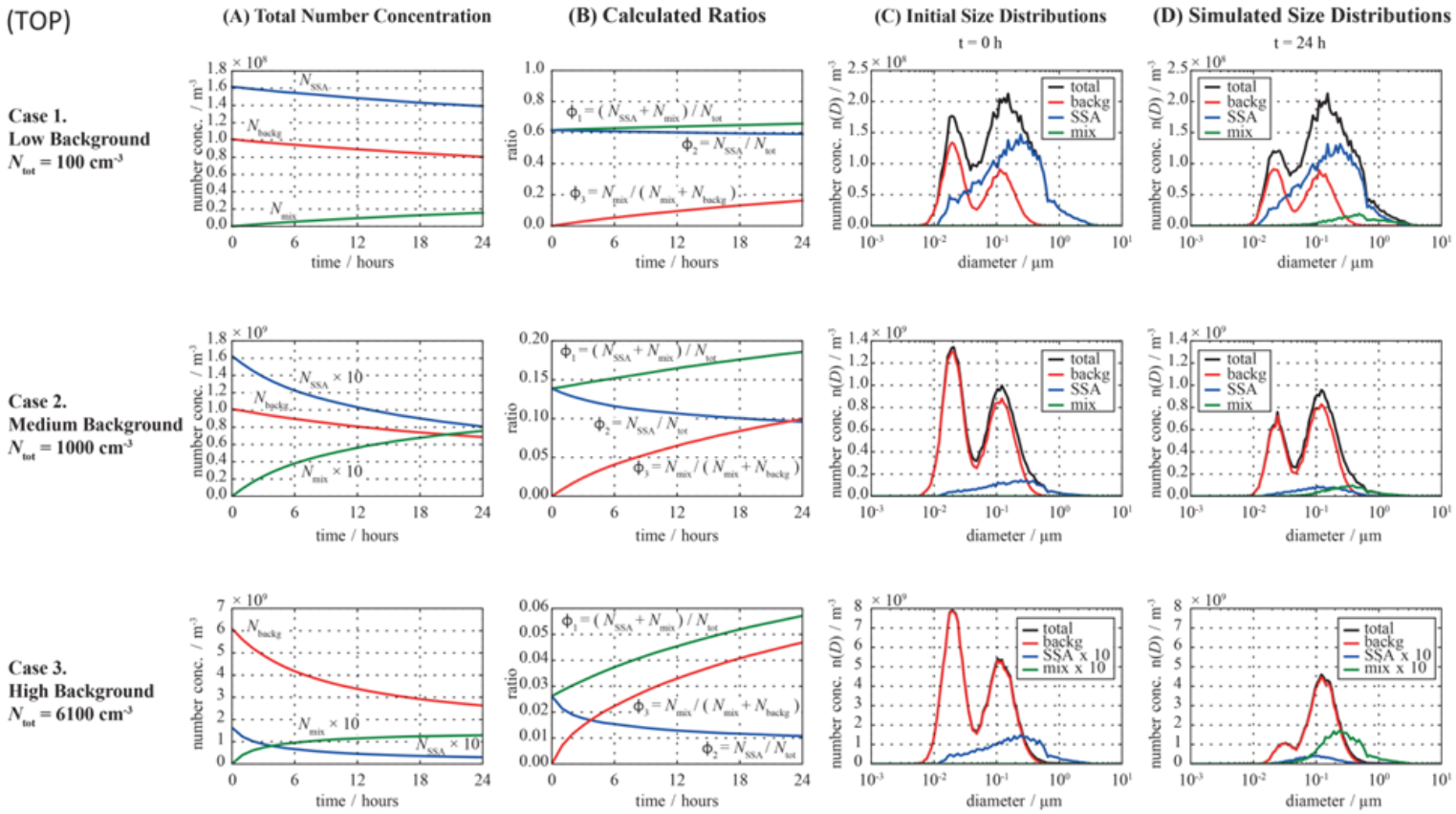

Figure 5.10. (top) Coagulation simulations of nascent SSA particles with prescribed initial background particle distributions at three background concentrations (Case 1 = 100 cm^{-3}, Case 2 = 1000 cm^{-3}, Case 3 = 6100 cm^{-3}). Panels under (A) show the evolution of total particle concentration over time, (B) shows the calculated ratios, (C) show input particle size distributions, and (D) simulated particle size distribution after 24 h. (bottom) Ratio of mixed to sum of mixed and background particles after 24 h of simulation of nascent SSA particles coagulating with prescribed background particle distributions at three background concentrations (Cases 1-3 = 100 cm^{-3}, 1000 cm^{-3}, 6100

(BOTTOM)

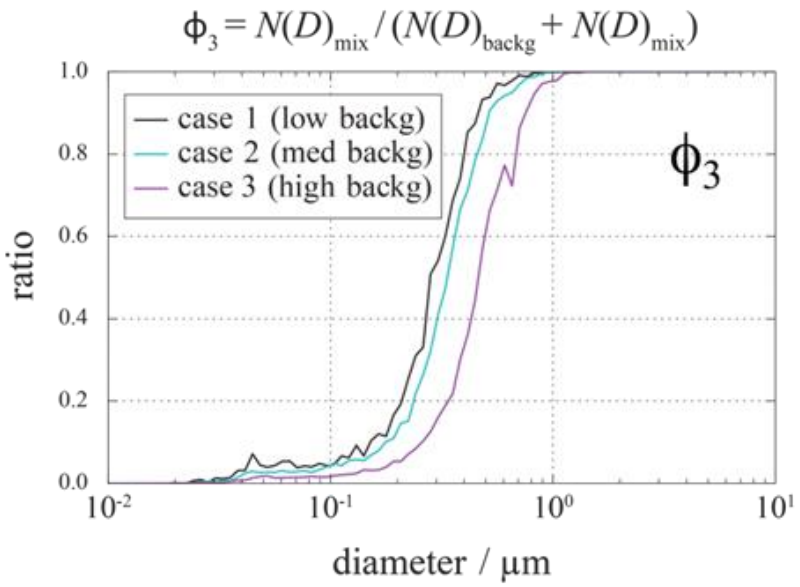

Figure 5.10. Coagulation simulations of nascent SSA particles with prescribed initial background particle distributions at three background concentrations continued.

5.8.9 Supporting Information Tables

Table 5.1. MART experiment summary. MART experiment details and SSA production day, impinging rate in (LPM), number of SSA particles and SSA particle volume estimated by APS and SMPS. SSA on first day on MART-C has not been analyzed for enzyme activities.

MART	Month	Year	# of days	Nutrients	Tank Volume (L)	Days of SSA production	Impinger Flow (LPM)	Impinging Time (min)	SSA Number Impinged average	SSA Volume average (μm^3)	Single Particle Volume average (μm^3)	Flow into MART (LPM)
A	Nov	2013	20	f/20	60	1, 12-20	1	30	4.09E+07	2.06E+07	0.50	5.8
B	Dec	2013	19	f/20	60	1,9-19	1	30	4.09E+07	2.06E+07	0.50	5.8
C	Jan	2014	23	f/2	100	1,13-23	0.3	120	4.59E+07	4.71E+06	0.10	3.1
E	Sep	2016	N/A	f/20	100	N/A	1	60	1.59E+10	2.31E+05	1.45E-05	2

Table 5.2. Parameters of prescribed idealized urban plume distribution used in the coagulations simulations where N (m^{-3}) is the number concentration, D_{gn} (μm) is the geometric mean diameter, σ_g (dimensionless) is the geometric standard deviation, and N_{total} is the sum of number concentration of Aitken and accumulation modes (adapted from Riemer et al., 2009).

	Aitken Mode			Accumulation Mode			
Case	N (m^{-3})	D_{gn} (μm)	σ_g (1)	N (m^{-3})	D_{gn} (μm)	σ_g (1)	N_{total} (m^{-3})
1	$5.25 \cdot 10^7$	0.02	1.45	$4.75 \cdot 10^7$	0.116	1.65	$1 \cdot 10^8$
2	$5.25 \cdot 10^8$	0.02	1.45	$4.75 \cdot 10^8$	0.116	1.65	$1 \cdot 10^9$
3	$3.2 \cdot 10^9$	0.02	1.45	$2.9 \cdot 10^9$	0.116	1.65	$6.1 \cdot 10^9$

Table 5.3. MART-C size-fractionated hydrolytic enzymatic activities for day 1, 11 and 23. Protease (L), chitinase (N), alkaline phosphatase (A), lipase-oleate (O) and lipase-stearate (S) were measured in SW, in SSML and in SSA. TOT, <1 µm and <0.2 µm refer respectively to the total (not filtered) sample fraction, bacterial fraction and dissolved fraction. The percentage expresses the contribution of the bacterial and dissolved fractions relative to the total activity.

	Day		TOT		<1		<0.2			
			Av	St Dev	Av	St Dev	Av	St Dev	%<1	%<0.2
SW	1	L	31.00	4.49	1.60	8.01	0.30	0.00	4	1
		N	0.00	0.00	0.00	0.00	0.00	0.00	0	0
		A	2.60	0.52	2.00	0.00	1.60	0.11	16	63
		O	26.40	0.55	19.40	1.89	10.00	3.20	36	38
		S	1.00	1.01	0.30	1.50	0.00	0.00	29	0
	11	L	877.00	61.33	800.00	31.76	2.60	0.30	91	0
		N	10.00	3.18	9.00	0.90	0.00	0.00	90	0
		A	23.70	1.03	19.10	2.30	5.00	0.51	59	21
		O	112.40	5.04	96.40	2.74	24.00	2.91	64	21
		S	5.60	0.13	4.00	0.31	0.70	0.64	59	13
	23	L	346.00	32.85	225.30	5.78	0.00	0.00	65	0
		N	18.00	0.55	6.00	0.50	0.00	0.00	33	0
		A	7.60	0.58	4.30	0.08	1.60	0.30	36	20
		O	103.00	4.85	92.50	4.30	25.00	2.59	66	24
		S	4.90	0.65	3.80	0.25	0.50	0.77	68	10
SSML	1	L	502.30	73.59	277.80	68.11	0.50	0.03	55	0
		N	0.00	0.00	0.00	0.00	0.00	0.00	0	0
		A	18.00	10.65	7.60	0.00	2.00	0.30	31	11
		O	402.90	29.63	385.50	20.51	9.00	4.00	93	2
		S	17.30	3.58	13.40	1.14	2.00	5.00	66	12
	11	L	965.30	50.39	768.00	100.16	5.00	1.00	79	1
		N	31.40	5.16	4.10	7.78	2.00	1.00	7	6
		A	43.60	8.62	14.20	7.19	7.00	8.89	17	16
		O	495.20	66.05	341.70	32.75	50.00	15.27	59	10
		S	21.50	3.24	16.50	2.81	3.00	0.90	63	14
	23	L	1035.40	74.08	375.70	3.94	0.00	0.00	36	0
		N	1201.00	1021.00	4.80	1.69	0.00	0.00	21	0
		A	28.70	2.69	12.80	2.13	4.00	1.20	31	14
		O	1264.10	14.36	1202.50	22.23	168.40	25.96	82	13
		S	57.90	3.35	55.50	6.75	2.00	1.38	92	3
SSA	1	L	Missing Sample							
		N								
		A								
		O								
		S								
	11	L	14.00	3.68	10.00	8.70	3.00	0.60	50	21
		N	0.00	0.00	0.00	0.00	0.00	0.00	0	0
		A	0.10	0.80	0.00	0.00	0.00	0.00	0	0
		O	17.30	0.63	15.00	2.37	2.00	0.30	75	12
		S	0.70	0.57	0.40	0.19	0.10	0.08	46	15
	23	L	0.30	0.00	0.30	0.00	0.00	0.00	100	0
		N	0.00	0.00	0.00	0.00	0.00	0.00	0	0
		A		0.00	0.00	0.00	0.00	0.00	0	0
		O	2.40	4.36	1.00	0.50	0.50	0.03	21	21
		S	0.50	0.55	0.00	0.00	0.00	0.00	0	0

Table 5.4. Compiled measured enzyme activities from the MART experiments and coastal marine aerosol measurements. Scripps automated shore station monitored seawater temperature and Chl-a data during the period of seawater sampling for MART experiments and coastal measurements are retrieved from Southern California Coastal Ocean Observing System (www.sccoos.org). Chl-a data with * were measured with extraction protocol described in SI M1, nm: not measured, and nd: not detected above blank.

				enzyme activities normalized to volume of air sampled, pM h^{-1} L^{-1}															
	air, L	water temp, °C	chl a, µg/L	leucine	sd	chitinase	sd	alk. phos.	sd	oleate	sd	stearate	sd	serine	sd	butyrate	sd	b-glucos.	sd
MART A																			
11/8/2013		15.9	3.7, 2.74*	40.0	70.0	20.0	16.7	13.3	16.7	320.0	33.3	66.7	10.0	-	-	-	-	-	-
11/19/2013		-	10.72*	430.0	140.0	6.7	6.7	30.0	26.7	150.0	43.3	40.0	16.7	-	-	-	-	-	-
11/21/2013	30	-	0.11*	0.0	0.0	16.7	26.7	0.0	0.0	513.3	100.0	100.0	76.7	-	-	-	-	-	-
11/23/2013		-	0.10*	146.7	153.3	6.7	10.0	30.0	30.0	893.3	130.0	60.0	13.3	-	-	-	-	-	-
11/25/2013		-	0.04*	320.0	176.7	20.0	20.0	10.0	13.3	546.7	66.7	80.0	13.3	-	-	-	-	-	-
11/27/2013		-	0.14*	153.3	0.0	20.0	0.0	40.0	0.0	410.0	3.3	53.3	6.7	-	-	-	-	-	-
MART B																			
12/2/2013		nm	nm, 1.54*	290.2	57.8	32.3	22.0	28.3	40.3	416.6	38.6	87.6	41.9	-	-	-	-	-	-
12/12/2013		-	4.07*	610.4	0.0	30.8	10.8	100.5	72.8	700.1	87.1	87.1	18.8	-	-	-	-	-	-
12/14/2013	30	-	0.86*	766.7	233.3	66.7	0.0	300.0	133.3	500.0	166.7	233.3	66.7	-	-	-	-	-	-
12/16/2013		-	0.12*	900.0	233.3	100.0	65.3	266.7	133.3	433.3	233.3	266.7	166.7	-	-	-	-	-	-
12/18/2013		-	0.12*	1000.0	333.3	66.7	33.3	166.7	66.7	466.7	166.7	200.0	100.0	-	-	-	-	-	-
12/20/2013		-	0.53*	500.0	159.7	19.5	13.3	0.0	0.0	166.7	6.2	72.0	49.4	-	-	-	-	-	-
MART C																			
1/16/2014		15.1	1.3, 0.93*	388.7	102.3	0.0	8.0	2.6	22.3	480.2	17.6	18.7	15.8	-	-	-	-	-	-
1/18/2014		-	39.02*	531.2	236.8	7.4	0.8	103.9	66.2	697.0	95.5	96.7	24.1	-	-	-	-	-	-
1/20/2014		-	29.97*	22.2	0.0	0.0	0.0	0.0	0.0	388.7	103.2	179.3	70.8	-	-	-	-	-	-
1/22/2014	36	-	3.40*	11.1	0.0	0.0	0.0	0.0	0.0	130.0	115.5	167.0	61.4	-	-	-	-	-	-
1/24/2014		-	25.17*	8.3	0.0	9.8	7.3	0.0	0.0	85.7	80.2	24.0	0.0	-	-	-	-	-	-
1/26/2014		-	10.36*	11.1	0.0	0.0	0.0	0.0	0.0	355.2	173.0	110.7	29.9	-	-	-	-	-	-
1/28/2014		-	12.78*	8.3	0.0	0.0	0.0	0.0	0.0	66.6	121.0	13.8	15.3	-	-	-	-	-	-
coastal air																			
6/8/2017	60	19.2	2.8	29.0	46.4	nm	nm	nm	nm	14.7	29.1	1.4	3.5	111.1	242.4	645.3	91.4	nm	nm
6/9/2017	113	19.1	3.5	1.8	3.6	nm	nm	nd	nd	0.0	0.0	2.4	3.8	11.0	13.3	417.6	38.1	nd	nd
6/10/2017	113	19.1	4.3	18.0	30.4	nm	nm	nd	nd	11.8	26.0	2.5	3.8	26.6	39.4	334.4	59.2	nd	nd
7/1/2017	88	17.6	6.2	40.7	33.2	nm	nm	1.7	4.1	32.5	22.6	3.0	3.4	54.3	23.1	59.5	145.9	1.0	1.4
7/7/2017	146	19.3	7.0	12.0	16.2	nm	nm	nd	nd	12.6	5.2	14.0	7.6	nd	nd	240.3	44.4	1.6	0.0
7/14/2017a	45	21.5	9.3	0.0	0.0	nm	nm	nd	nd	38.0	25.4	22.9	23.3	nd	nd	1558.9	241.9	nd	nd
7/14/2017b	170	22.1	7.9	21.7	15.1	nm	nm	7.2	6.3	6.2	8.3	1.1	1.3	32.4	17.5	nd	nd	nd	nd

Table 5.5. Linear mixed effects model estimating the relation of the hydrolytic enzyme activities depending on the location (SW, SSML, SSA). (A) Chl-a and sampling time (estimating the change in enzyme rate over time). The SSML hydrolytic enzyme activities were compared against the SW ones, represented in the model as SW vs SSML; (B) DOC and sampling time (estimating the change in enzyme rate over time) fitted for each location (SW. SSML, SSA) separately; (C) Linear nonlinear mixed effects model table among hydrolytic enzyme activities in SSA, SSML, and SW and their relationship depending on the location (SW, SSML, SSA) - SW in comparison with the other two locations and the interaction between location and sampling time. Bold indicates statistically significant relationship.

(A)

		Value	St Dev	t-value	p-value
Protease	**SW_SSML**	0.215	0.089	2.417	**0.023**
	Chl *a*	0.016	0.005	3.146	**0.005**
	Sampling Time	0.054	0.021	2.601	**0.016**
Chitinase	SW_SSML	0.065	0.108	0.597	0.557
	Chl *a*	0.01	0.006	1.726	0.101
	Sampling Time	0.066	0.025	2.642	**0.016**
Alkaline Phosphatase	**SW_SSML**	0.301	0.094	3.219	**0.003**
	Chl *a*	0.012	0.006	2.039	**0.053**
Lipase-Oleate	**SW_SSML**	0.255	0.093	2.747	**0.011**
	Chl *a*	0.003	0.005	0.538	0.0596
	Sampling Time	-0.025	0.021	-1.217	0.236
Lipase-Stearate	**SW_SSML**	0.345	0.09	3.812	**0.001**
	Chl *a*	0.008	0.006	1.398	0.176
	Sampling Time	-0.001	0.024	-0.048	0.962

(B)

			Value	St Dev	t-value	p-value
Protease	SW	**DOC**	0.002	0.001	4.891	**0.001**
		Sampling Time	-0.127	0.032	-3.872	**0.002**
	SSML	**DOC**	0.001	0.001	2.737	**0.017**
		Sampling Time	-0.051	0.035	-1.473	0.165
	SSA	**DOC**	-0.006	0.001	-5.769	**0.001**
		Sampling Time	-0.158	0.065	-2.426	**0.032**
Chitinase	SW	**DOC**	0.002	0.001	2.309	**0.038**
		Sampling Time	-0.021	0.053	-0.404	0.693
	SSML	**DOC**	0.003	0.001	3.712	**0.003**
		Sampling Time	-0.068	0.043	-1.575	0.139
	SSA	DOC	-0.002	0.002	-1.004	0.342
		Sampling Time	0.027	0.082	0.334	0.746
Alkaline Phosphatase	SW	**DOC**	0.001	0.001	2.348	**0.035**
		Sampling Time	-0.225	0.035	-6.347	**0.001**
	SSML	DOC	-0.001	0.001	-0.709	0.491
		Sampling Time	-0.139	0.062	-2.241	**0.043**
	SSA	DOC	0.001	0.005	0.123	0.906
		Sampling Time	-0.077	0.164	-0.465	0.658
Lipase-Oleate	SW	**DOC**	0.003	0.001	4.586	**0.001**
		Sampling Time	-0.133	0.031	-4.335	**0.001**
	SSML	**DOC**	0.005	0.001	4.865	**0.001**
		Sampling Time	-0.043	0.054	-0.792	0.443
	SSA	DOC	-0.001	0.001	-1.588	0.136
		Sampling Time	-0.079	0.047	-1.68	0.117
Lipase-Stearate	SW	**DOC**	0.006	0.001	4.381	**0.001**
		Sampling Time	0.049	0.091	0.539	0.56
	SSML	**DOC**	-0.001	0.001	-2.789	**0.016**
		Sampling Time	0.004	0.001	6.521	**0.001**
	SSA	**DOC**	-0.001	0.001	-0.416	**0.684**
		Sampling Time	-0.074	0.056	-1.326	0.207

(C)

		Value	St Dev	t-value	p-value
Protease	Fixed Effects: log10(EnzRate) ~ EnzLoc * Sampling Time				
	SW_SSML	0.09	0.325	0.278	0.783
	SW_SSA	-1.026	0.333	-3.086	**0.004**
	Sampling Time	-0.069	0.06	-1.149	0.271
	SW_SSML:Sampling Time	0.046	0.085	0.541	0.593
	SW_SSA:Sampling Time	-0.203	0.086	-2.362	**0.025**
Chitinase	Fixed Effects: log10(EnzRate) ~ Enz Loc				
	SW_SSML	-0.012	0.097	-0.121	0.904
	SW_SSA	-1.114	0.108	-10.285	**0.001**
Alkaline Phosphatase	Fixed Effects: log10(EnzRate) ~ EnzLoc * Sampling Time				
	SW_SSML	0.435	0.144	3.023	**0.006**
	SW_SSA	-1.077	0.171	-6.297	**0.001**
	Sampling Time	-0.111	0.041	-2.728	**0.017**
Lipase Oleate	Fixed Effects: log10(EnzRate) ~ EnzLoc * Sampling Time				
	SW_SSML	0.373	0.118	3.16	**0.003**
	SW_SSA	-0.975	0.118	-8.254	**0.001**
	Sampling Time	-0.062	0.029	-2.172	**0.049**
Lipase Stearate	Fixed Effects: log10(EnzRate) ~ Enz Loc				
	SW_SSML	0.516	0.107	4.818	**0.001**
	SW_SSA	-0.608	0.107	-5.674	**0.001**

5.9 References

Abbatt, J. P. D., A. K. Y. Lee, and J. A. Thornton, Quantifying trace gas uptake to tropospheric aerosol: recent advances and remaining challenges, Chemical Society Reviews, 41 (19), 6555, 2012.

Arrieta, J. M., and G. J. Herndl, Assessing the diversity of marine bacterial beta-glucosidases by capillary electrophoresis zymography, Applied And Environmental Microbiology, 67 (10), 4896–4900, 2001

Álvarez-Salgado, X. A., and A. E. J. Miller, Simultaneous determination of dissolved organic carbon and total dissolved nitrogen in seawater by high temperature catalytic oxidation: Conditions for precise shipboard measurements, Marine Chemistry, 62 (3–4), 325–333, 1998.

Antelmann, H., E. Darmon, D. Noone, J. W. Veening, H. Westers, S. Bron, O. P. Kuipers, K. M. Devine, M. Hecker, and J. M. Van Dijl, The extracellular proteome of Bacillus subtilis under secretion stress conditions, Molecular Microbiology, 49 (1), 143–156, 2003.

Ault, A. P., M. J. Moore, H. Furutani, and K. A. Prather, Impact of emissions from the Los Angeles Port region on San Diego air quality during regional transport events, Environmental Science and Technology, 43 (10), 3500–3506, 2009.

Ault, A. P., R. C. Moffet, J. Baltrusaitis, D. B. Collins, M. J. Ruppel, L. A. Cuadra-Rodriguez, D. Zhao, T. L. Guasco, C. J. Ebben, F. M. Geiger, T. H. Bertram, K. A. Prather, and V. H. Grassian, Size-dependent changes in sea spray aerosol composition and properties with different seawater conditions, Environ. Sci. Technol., 47, 5603–5612, 2013.

Ault, A. P., T. L. Guasco, J. Baltrusaitis, O. S. Ryder, J. V. Trueblood, D. B. Collins, M. J. Ruppel, L. A. Cuadra-Rodriguez, K. A. Prather, and V. H. Grassian, Heterogeneous reactivity of nitric acid with nascent sea spray aerosol: Large differences observed between and within individual particles, Journal of Physical Chemistry Letters, 5 (15), 2493–2500, 2014.

Azam, F., and R. E. Hodson, Size distribution and activity of marine microheterotrophs, Limnology and Oceanography, 22 (3), 492–501, 1977.

Baker, N. A., D. Sept, S. Joseph, M. J. Holst, and J. A. McCammon, Electrostatics of nanosystems: application to microtubules and the ribosome., Proceedings of the National Academy of Sciences of the United States of America, 98 (18), 10037–41, 2001.

Baltar, F., J. Arístegui, J. M. Gasol, E. Sintes, H. M. Van Aken, and G. J. Herndl, High dissolved extracellular enzymatic activity in the deep central Atlantic ocean, Aquatic Microbial Ecology, 58 (3), 287–302, 2010.

Bar-Even, A., E. Noor, Y. Savir, W. Liebermeister, D. Davidi, D. S. Tawfik, and R. Milo, The moderately efficient enzyme: Evolutionary and physicochemical trends shaping enzyme parameters, Biochemistry, 50 (21), 4402–4410, 2011.

Blanchard, D. C., and L. D. Syzdek, Concentration of bacteria in jet drops from bursting bubbles, Journal of Geophysical Research, 77 (27), 5087, 1972.

Cauwet, G., HTCO method for dissolved organic carbon analysis in seawater: influence of catalyst on blank estimation, Marine Chemistry, 47 (1), 55–64, 1994.

Clarke, K. R., and R. M. Warwick, Changes in marine communities: an approach to statistical analysis and interpretation *PRIMER-E* (260th ed.). Plymouth, U.K., 2001. Retrieved from http://www.vliz.be/imis/imis.php?refid=117939

Cochran, R. E., O. Laskina, T. Jayarathne, A. Laskin, J. Laskin, P. Lin, C. M. Sultana, C. Lee, K. A. Moore, C. D. Cappa, T. H. Bertram, K. A. Prather, V. H. Grassian, and E. A. Stone, Analysis of organic anionic surfactants in fine (PM2.5) and coarse (PM10) fractions of freshly emitted sea spray aerosol, Environmental Science and Technology, 50 (5), 2477–2486, 2016.

Collins, D. B., A. P. Ault, R. C. Moffet, M. J. Ruppel, L. A. Cuadra-Rodriguez, T. L. Guasco, C. E. Corrigan, B. E. Pedler, F. Azam, L. I. Aluwihare, T. H. Bertram, G. C. Roberts, V. H. Grassian, and K. A. Prather, Impact of marine biogeochemistry on the chemical mixing state and cloud forming ability of nascent sea spray aerosol, Journal of Geophysical Research: Atmospheres, 118 (15), 8553–8565, 2013.

Dalbey, R. E., P. Wang, and J. M. van Dijl, Membrane proteases in the bacterial protein secretion and quality control pathway, Microbiology and Molecular Biology Reviews, 76 (2), 311–330, 2012.

Danovaro, R., M. Armeni, G. M. Luna, C. Corinaldesi, A. Dell'Anno, C. R. Ferrari, C. Fiordelmondo, C. Gambi, M. Gismondi, E. Manini, M. Mecozzi, F. M. Perrone, A. Pusceddu, and M. Giani, Exo-enzymatic activities and dissolved organic pools in relation with mucilage development in the Northern Adriatic Sea, Science of the Total Environment, 353 (1–3), 189–203, 2005.

DeCarlo, P. F., and J. G. Slowik, Particle morphology and density characterization by combined mobility and aerodynamic diameter measurements. Part 1: Theory, Aerosol Science and Technology, 38 (12), 1185–1205, 2004.

Dobson, C. M., G. B. Ellison, A. F. Tuck, and V. Vaida, Atmospheric aerosols as prebiotic chemical reactors, Proceedings of the National Academy of Sciences of the United States of America, 97 (22), 11864–11868, 2000.

Dolinsky, T. J., J. E. Nielsen, J. A. McCammon, and N. A. Baker, PDB2PQR: An automated pipeline for the setup of Poisson-Boltzmann electrostatics calculations, Nucleic Acids Research, 32 (665–667), 2004.

Donaldson, D. J., and V. Vaida, The influence of organic films at the air-aqueous boundary on atmospheric processes, Chemical Reviews, 106 (4), 1445–1461, 2006.

Duce, R. A., and E. J. Hoffman, Chemical fractionation at the air/sea interface, Annual Review of Earth and Planetary Sciences, 4 (1), 187–228, 1976.

Eggert, T., U. Brockmeier, M. J. Dröge, W. J. Quax, and K. E. Jaeger, Extracellular lipases from Bacillus subtilis: Regulation of gene expression and enzyme activity by amino acid supply and external pH, FEMS Microbiology Letters, 225 (2), 319–324, 2003.

Finlayson-Pitts, B. J., and J. N. Pitts, Chemistry of the Upper and Lower Atmosphere: Theory, Experiments, and Applications, Chemistry of the Upper and Lower Atmosphere, 969, 1999.

Franze, T., M. G. Weller, R. Niessner, and U. Pöschl, Protein nitration by polluted air, Environmental Science and Technology, 39 (6), 1673–1678, 2005.

Gantt, B., and N. Meskhidze, The physical and chemical characteristics of marine primary organic aerosol: A review, Atmospheric Chemistry and Physics, 13 (8), 3979–3996, 2013.

Gard, E. E., J. E. Mayer, B. D. Morrical, T. Dienes, D. P. Fergenson, and K. A. Prather, Real-time analysis of individual atmospheric aerosol particles: Design and performance of a portable ATOFMS, Analytical Chemistry, 69 (20), 4083–4091, 1997.

Gard, E. E., M. J. Kleeman, D. S. Gross, L. S. Hughes, J. O. Allen, B. D. Morrical, D. P. Fergenson, T. Dienes, M. E. Galli, R. J. Johnson, G. R. Cass, and K. A. Prather, Direct Observation of Heterogeneous Chemistry in the Atmosphere, Science, 279 (5354), 1184–1187, 1998.

Green, E. R., and J. Mecsas, Bacterial secretion systems: An overview, Microbiology Spectrum, 4 (1), 1–19, 2016.

Guillard, R. R. L., and J. H. Ryther, Studies of marine planktonic diatoms: I. Cyclotella nana Hustedt, and Detonula confervacea (Cleve) Gran, Canadian Journal of Microbiology, 8 (2), 229–239, 1962.

Harvey, George W., Burzell, L. A., A simple microlayer method for small samples, Limnology and Oceanography, 17 (1), 156–157, 2012.

Haywood, J., and O. Boucher, Estimates of the direct and indirect radiative forcing due to tropospheric aerosols: A review, Reviews of Geophysics, 2000.

Holehouse, A. S., R. K. Das, J. N. Ahad, M. O. G. Richardson, and R. V. Pappu, CIDER: Resources to analyze sequence-ensemble relationships of intrinsically disordered proteins, Biophysical Journal, 112 (1), 16–21, 2017.

Holm-Hansen, O., C. J. Lorenzen, R. W. Holmes, and J. D. H. Strickland, Fluorometric determination of chlorophyll, J. Mar. Sci., 30 (1), 3–15, 1965.

Hoppe, H.-G., Significance of exoenzymatic activities in the ecology of brackish water: Measurements by means of methylumbelliferyl-substrates, Marine Ecology Progress Series, 11, 299–308, 1983.

Jo, S., T. Kim, V. G. Iyer, and W. Im, CHARMM-GUI: A web-based graphical user interface for

CHARMM, Journal of Computational Chemistry, 29 (11), 1859–1865, 2008.

Kim, C., Y. Nishimura, and T. Nagata, High potential activity of alkaline phosphatase in the benthic nepheloid layer of a large mesotrophic lake: Implications for phosphorus regeneration in oxygenated hypolimnion, Aquatic Microbial Ecology, 49 (3), 303–311, 2007.

Kuznetsova, M., and C. Lee, Enhanced extracellular enzymatic peptide hydrolysis in the sea-surface microlayer, Marine Chemistry, 73 (3–4), 319–332, 2001.

Lee, C., C. M. Sultana, D. B. Collins, M. V. Santander, J. L. Axson, F. Malfatti, G. C. Cornwell, J. R. Grandquist, G. B. Deane, M. D. Stokes, F. Azam, V. H. Grassian, and K. A. Prather, Advancing model systems for fundamental laboratory studies of sea spray aerosol using the microbial loop, The Journal of Physical Chemistry A, 119 (33), 8860–8870, 2015.

Lewis, E. R., and S. E. Schwartz, Sea salt aerosol production: Mechanisms, methods, measurements and models, Geophysical Monograph Series, 152, 413, 2004.

Li, Y., X. Lei, H. Zhu, H. Zhang, C. Guan, Z. Chen, W. Zheng, L. Fu, and T. Zheng, Chitinase producing bacteria with direct algicidal activity on marine diatoms., Scientific Reports, 6, 21984, 2016.

Luo, H., R. Benner, R. A. Long, and J. Hu, Subcellular localization of marine bacterial alkaline phosphatases., Proceedings of the National Academy of Sciences of the United States of America, 106 (50), 21219–21223, 2009.

Marchin, S., J. L. Putaux, F. Pignon, and J. Léonil, Effects of the environmental factors on the casein micelle structure studied by cryo transmission electron microscopy and small-angle x-ray scattering/ultrasmall-angle x-ray scattering, Journal of Chemical Physics, 126 (4), 2007.

Martinez, J., D. C. Smith, G. F. Steward, and F. Azam, Variability in ectohydrolytic enzyme activities of pelagic marine bacteria and its significance for substrate processing in the sea, Aquatic Microbial Ecology, 10 (3), 223–230, 1996.

Maupetit, J., P. Derreumaux, and P. Tufféry, A fast method for large-scale de novo peptide and miniprotein structure prediction, Journal of Computational Chemistry, 31 (4), 726–738, 2010.

May, K. R., The collison nebulizer: Description, performance and application, Journal of Aerosol Science, 4 (3), 235–243, 1973.

Mayol, E., M. A. Jiménez, G. J. Herndl, C. M. Duarte, and J. M. Arrieta, Resolving the abundance and air- sea fluxes of airborne microorganisms in the North Atlantic Ocean, Frontiers in Microbiology, 5 (OCT), 2014.

Meskhidze, N., M. D. Petters, K. Tsigaridis, T. Bates, C. O'Dowd, J. Reid, E. R. Lewis, B. Gantt, M. D. Anguelova, P. V. Bhave, J. Bird, A. H. Callaghan, D. Ceburnis, R. Chang, A. Clarke, G. de Leeuw, G. Deane, P. J. Demott, S. Elliot, M. C. Facchini, C. W. Fairall, L.

Hawkins, Y. Hu, J. G. Hudson, M. S. Johnson, K. C. Kaku, W. C. Keene, D. J. Kieber, M. S. Long, M. Mårtensson, R. L. Modini, C. L. Osburn, K.A. Prather, A. Pszenny, M. Rinaldi, L. M. Russell, M. Salter, A. M. Sayer, A. Smirnov, S. R. Suda, T. D. Toth, D. R. Worsnop, A. Wozniak, S. R. Zorn, Production mechanisms, number concentration, size distribution, chemical composition, and optical properties of sea spray aerosols, Atmospheric Science Letters, 14 (4), 207–213, 2013.

Noble, R. T., and J. A. Fuhrman, Use of SYBR Green I for rapid epifluorescence counts of marine viruses and bacteria, Aquatic Microbial Ecology, 14 (2), 113–118, 1998.

O'Dowd, C., D. Ceburnis, J. Ovadnevaite, J. Bialek, D. B. Stengel, M. Zacharias, U. Nitschke, S. Connan, M. Rinaldi, S. Fuzzi, S. Decesari, M. Cristina Facchini, S. Marullo, R. Santoleri, A. Dell'Anno, C. Corinaldesi, M. Tangherlini, and R. Danovaro, Connecting marine productivity to sea-spray via nanoscale biological processes: Phytoplankton dance or death disco?, Scientific Reports, 5, 14883, 2015.

Obayashi, Y., and S. Suzuki, Adsorption of extracellular proteases in seawater onto filters during size fractionation, Journal of Oceanography, 64 (3), 367–372, 2008.

Orellana, M. V, P. A. Matrai, C. Leck, C. D. Rauschenberg, A. M. Lee, and E. Coz, Marine microgels as a source of cloud condensation nuclei in the high Arctic., Proceedings of the National Academy of Sciences of the United States of America, 108 (33), 13612–13617, 2011.

Patterson, J. P., D. B. Collins, J. M. Michaud, J. L. Axson, C. M. Sultana, T. Moser, A. C. Dommer, J. Conner, V. H. Grassian, M. D. Stokes, G. B. Deane, J. E. Evans, M. D. Burkart, K. A. Prather, and N. C. Gianneschi, Sea spray aerosol structure and composition using cryogenic transmission electron microscopy, ACS Central Science, 2, 40–47, 2016.

Pöschl, U., Atmospheric aerosols: Composition, transformation, climate and health effects, Angewandte Chemie - International Edition, 44 (46), 7520–7540, 2005.

Prather, K. A., T. H. Bertram, V. H. Grassian, G. B. Deane, M. D. Stokes, P. J. Demott, L. I. Aluwihare, B. P. Palenik, F. Azam, J. H. Seinfeld, R. C. Moffet, M. J. Molina, C. D. Cappa, F. M. Geiger, G. C. Roberts, L. M. Russell, A. P. Ault, J. Baltrusaitis, D. B. Collins, C. E. Corrigan, L. A. Cuadra-Rodriguez, C. J. Ebben, S. D. Forestieri, T. L. Guasco, S. P. Hersey, M. J. Kim, W. F. Lambert, R. L. Modini, W. Mui, B. E. Pedler, M. J. Ruppel, O. S. Ryder, N. G. Schoepp, R. C. Sullivan, and D. Zhao, Bringing the ocean into the laboratory to probe the chemical complexity of sea spray aerosol., Proceedings of the National Academy of Sciences of the United States of America, 110 (19), 7550–5, 2013.

Quinn, P. K., D. B. Collins, V. H. Grassian, K. A. Prather, and T. S. Bates, Chemistry and related properties of freshly emitted sea spray aerosol, Chemical Reviews, 115, 4383–4399, 2015.

Rastelli, E., C. Corinaldesi, A. Dell'Anno, M. Lo Martire, S. Greco, M. C. Facchini, M. Rinaldi, C. O'Dowd, D. Ceburnis, and R. Danovaro, Transfer of labile organic matter and microbes

from the ocean surface to the marine aerosol: an experimental approach, Scientific Reports, 7 (1), 11475, 2017.

Reis, P., K. Holmberg, H. Watzke, M. E. Leser, and R. Miller, Lipases at interfaces: A review, Advances in Colloid and Interface Science, 147–148 (C), 237–250, 2009.

Riemer, N., M. West, R. A. Zaveri, and R. C. Easter, Simulating the evolution of soot mixing state with a particle-resolved aerosol model, Journal of Geophysical Research Atmospheres, 114 (9), 1–22, 2009.

Rodrigue, J., M. Ranjan, P. K. Hopke, S. Dhaniyala, M. Ranjan, and P. K. Hopke, Performance comparison of scanning electrical mobility spectrometers, Aerosol Science and Technology, 41 (4), 360–368, 2007.

Rossi, M. J., Heterogeneous reactions on salts, Chemical Reviews, 103 (12), 4823–4882, 2003.

Schrag, J. D., Y. Li, M. Cygler, D. Lang, T. Burgdorf, H.-J. Hecht, R. Schmid, D. Schomburg, T. J. Rydel, J. D. Oliver, L. C. Strickland, C. M. Dunaway, S. B. Larson, J. Day, and A. McPherson, The open conformation of a Pseudomonas lipase, Structure, 5 (2), 187–202, 1997.

Schrodinger Release 2015-3: Maestro, 2015.

Solomon, P. A., L. G. Salmon, T. Fall, and G. R. Cass, Spatial and temporal distribution of atmospheric nitric-acid and particulate nitrate concentrations in the Los-Angeles area, Environmental Science and Technology, 26 (8), 1594–1601, 1992.

Stocker, T. F., Q. Dahe, G.-K. Plattner, L. V. Alexander, S. K. Allen, N. L. Bindoff, F.-M. Bréon, J. A. Church, U. Cubash, S. Emori, P. Forster, P. Friedlingstein, L. D. Talley, D. G. Vaughan, and S.-P. Xie, Technical summary, Climate Change 2013: The physical science basis. Contribution of working group I to the fifth assessment report of the Intergovernmental Panel on Climate Change, 33–115, 2013.

Stokes, M. D., G. B. Deane, K. Prather, T. H. Bertram, M. J. Ruppel, O. S. Ryder, J. M. Brady, and D. Zhao, A Marine Aerosol Reference Tank system as a breaking wave analogue for the production of foam and sea-spray aerosols, Atmospheric Measurement Techniques, 6 (4), 1085–1094, 2013.

Sultana, C. M., G. C. Cornwell, P. Rodriguez, and K. A. Prather, FATES: A flexible analysis toolkit for the exploration of single-particle mass spectrometer data, Atmospheric Measurement Techniques, 10 (4), 1323–1334, 2017.

Trueblood, J. V., A. D. Estillore, C. Lee, J. A. Dowling, K. A. Prather, and V. H. Grassian, Heterogeneous chemistry of lipopolysaccharides with gas-phase nitric acid: Reactive sites and reaction pathways, Journal of Physical Chemistry A, 120 (32), 6444–6450, 2016.

Unanue, M., B. Ayo, M. Agis, D. Slezak, G. J. Herndl, and J. Iriberri, Ectoenzymatic activity and uptake of monomers in marine bacterioplankton described by a biphasic kinetic model, Microbial Ecology, 37 (1), 36–48, 1999.

Van Vaeck, L., H. Struyf, W. Van Roy, and F. Adams, Organic and inorganic analysis with laser microprobe mass spectrometry. Part I: Instrumentation and methodology, Mass Spectrometry Reviews, 13 (3), 189–208, 1994.

Van Vaeck, L., H. Struyf, W. Van Roy, and F. Adams, Organic and inorganic analysis with laser microprobe mass spectrometry. Part II: Applications, Mass Spectrometry Reviews, 13 (3), 209–232, 1994.

Wang, X., C. M. Sultana, J. Trueblood, T. C. J. Hill, F. Malfatti, C. Lee, O. Laskina, K. A. Moore, C. M. Beall, C. S. McCluskey, G. C. Cornwell, Y. Zhou, J. L. Cox, M. A. Pendergraft, M. V. Santander, T. H. Bertram, C. D. Cappa, F. Azam, P. J. DeMott, V. H. Grassian, and K. A. Prather, Microbial control of sea spray aerosol composition: A tale of two blooms, ACS Central Science, 1 (3), 124–131, 2015.

Willsey, G. G., and M. J. Wargo, Extracellular lipase and protease production from a model drinking water bacterial community is functionally robust to absence of individual members, PLoS ONE, 10 (11), 1–15, 2015.

Zelenyuk, A., D. Imre, L. A. Cuadra-Rodriguez, and B. Ellison, Measurements and interpretation of the effect of a soluble organic surfactant on the density, shape and water uptake of hygroscopic particles, Journal of Aerosol Science, 38 (9), 903–923, 2007.

Zobell, C. E., Studies on marine bacteria. I. The cultural requirements of heterotrophic aerobes, Journal of Marine Research, 4 (1), 42–75, 1941.

6 Calcium-Driven Lipopolysaccharide Aggregation in Sea Spray Aerosol: Impact on Nitric Acid Heterogeneous Reactivity

6.1 Synopsis

Atmospheric aerosols modify the flux of atmospheric reactive oxygen species and in turn are modified by these reactive species, with both processes impacting our climate and environment. Sea spray aerosols (SSA) ejected from oceans are composed of a heterogeneous mix of biologically derived chemicals, with each molecule participating uniquely in multiphase chemical processes. One such class of molecules, lipopolysaccharides (LPS), are ubiquitous within marine bacterial ecosystem, are readily ejected into SSA, and undergo heterogeneous reactions with atmospheric reactive gases such as HNO_3. Yet, LPS species can form a myriad of physical morphologies in a manner often dependent upon the counter ions present in solution. In this study, we investigate the role of molecular morphology on the transfer of and HNO_3 reactivity with LPS, contextualizing the organic and inorganic drivers of multiphase chemistry within LPS-containing SSA. Specifically, we elucidate the reactivity of LPS with HNO_3 in the presence of calcium and sodium counter ions, cations that are known to complex with LPS in distinct morphologies. We demonstrate that the physical sizes of LPS morphologies in solution can alter the size of aerosol particles produced, drastically in pure LPS solutions and more subtly in mesocosm experiments. We also show that HNO_3 reacts less with the calcium driven morphology of LPS than with the sodium driven morphology in both pure LPS samples and mesocosm studies. Finally, molecular simulations of LPS bilayers in the presence of sodium and calcium provide an atomic-level rationale for these observations, suggesting that calcium induced collapse of LPS stabilizes bilayer morphologies, reduces curvature of the membrane, thus creating larger morphologies, and leads to inhibited reactivity with HNO_3. Thus, for the first time,

our results provide insight into the atomic-level role of ionic interactions as drivers of morphological properties and heterogeneous reactivity of LPS-containing aerosols.

6.2 Introduction

The reaction with SSA with nitric acid gas (HNO_3) is traditionally described as a reaction between HNO_3 and inorganic salts such as NaCl, $MgCl_2$, or $CaCl_2$ [*Abbatt et al., 2012*; *Finlayson-Pitts and Hemminger, 2000*; *Rossi, 2003*]. While biogenically derived organic species present in the SSA were previously correlated with inhibition of reactive uptake of HNO_3 [*Ault et al., 2014*], some organic compounds naturally present in seawater and SSA, like lipopolysaccharides, undergo acid-base reactions with HNO_3 [*Trueblood et al., 2016*]. Thus a large range of reactivities between HNO_3 and SSA can be observed depending upon the particle type [*Ault et al., 2013, 2014*; *Prather et al., 2013*].

Lipopolysaccharides (LPS) are a major component of outer-cell membranes of the gram-negative bacteria abundant in phytoplankton growths on the ocean surface, and polysaccharides have been observed to be dominant in SSA [*Cochran et al., 2017*]. Each LPS molecule is composed of three chemical domains: (1) the lipid A tails, (2) the inner and outer core oligosaccharides, and (3) the repeating O-antigen units (Figure 6.1) [*Aurell and Wistrom, 1998*; *Wu et al., 2013*]. These molecules form micelles, inverted micelles, monolayers and bilayers [*Aurell and Wistrom, 1998; Wu et al., 2013*], due to the amphiphilic nature of LPS monomer [*Tanford and Wiley, 1980*], and are also known to form different morphological states in the presence of monovalent and divalent cations: compared to LPS salts with monovalent cations, LPS salts with divalent cations can convert the unilamellar/cubic aggregate structure to multilamellar structure of LPS [*Garidel et al., 2005*; *Snyder et al., 1999*].

Despite decades of research on LPS higher order structures, the study of LPS morphology as it relates to SSA heterogeneous chemistry is less understood. Here, we single particle chemical analysis of LPS-containing particles using aerosol time-of-flight mass spectrometry with all-atom molecular dynamics (MD) simulations to investigate the role of sodium and calcium as drivers of LPS morphology, transfer and heterogeneous reactivity.

Here we performed single particle chemical analysis of LPS-containing particles using aerosol time-of-flight mass spectrometry (ATOFMS) to better understand the impact of LPS physicochemical changes on heterogeneous reactivity of SSA with HNO_3. Molecular modeling of the LPS at the liquid surface under different cation conditions (10 mM NaCl or $CaCl_2$), mimicking SSA surfaces, was performed to provide a molecular level explanation of the observed differences in heterogeneous reactivity between non-aggregated and calcium-aggregated LPS particles. Furthermore, the experimental observations and the molecular explanation were combined and applied to a realistic nascent SSA measurement during a period of high polysaccharide enrichment.

6.3 Material and Methods

6.3.1 Studies of Lipopolysaccharide Aggregation and Impact on Reactivity

Lipopolysaccharide (LPS) powder (Sigma-Aldrich, L4130, lot #: 064M4125V, 085M4107V), $NaCl_{(s)}$ (Acros Organics, 42429-5000, lot #: B014114413), $CaCl_2 \cdot 2H_2O$ (Alfa Aesar, 33296, lot #: U13B016), reef salt (Brightwell Aquatics, NēoMarine) were purchased and used without further purification. Method of LPS aggregation was adapted from previous studies [*Aurell and Wistrom, 1998*; *Coughlin, Haug, et al., 1983*; *Li and Luo, 1998*; *Parikh and Chorover, 2007*]. Approximately 0.1 g of LPS was dissolved in 150 mL of ultrapure water (Millipore) to be analyzed as a reference standard. Three additional solutions of same LPS concentration were

prepared with NaCl added to the 1st solution (end salt concentration of 0.1 M), $CaCl_2 \cdot 2H_2O$ added to the 2nd solution (end salt concentration of 0.1 M), and 0.1 g of reef salt added to the 3rd solution. All solutions with LPS were sonicated for minimum of 30 min to ensure complete dissolution of reagents. Aliquots (75 mL) were taken out of each solution immediately after preparation to be atomized for initial analysis. Rest of the solutions were incubated for 72 hours at room temperature (24 ± 1 ^{o}C), constantly stirred using an orbital shaker. The solutions were then atomized for analysis.

A Collison atomizer [*May, 1973*] was used to atomize the solutions (1.5 SLPM). Atomized droplets were dried using two diffusion driers (RH < 10%) and sent directly into the ATOFMS. Further details on the instrument can be found elsewhere [*Gard et al., 1997*] and in Section 1.5.3. Data are imported into MATLAB (The Math-Works, Inc.) with software toolkit FATES [*Sultana et al., 2017*] for further data analysis. Equations (1) and (2) were used to calculate the uncertainty in the reported fractions of particles, where F is fraction, x is number of particles containing select ion marker, N is total number of particles, and SE stands for standard error of 1σ.

$$\mathrm{F} = \frac{x}{N} \tag{E6.1}$$

$$\mathrm{SE} = \sqrt{\frac{F(1-F)}{N}} \tag{E6.2}$$

After sampling with ATOFMS, the particle flow was sent to aerosol particle sizer (APS, TSI Model 3321, 1 SLPM sample flow), and scanning mobility particle sizer (SMPS Model 3936 and 3938, operating at 0.3/3.0 SLPM sample/sheathe flow). APS and SMPS measures particles with aerodynamic diameter (D_a) between 0.6 and 20 μm, and mobility diameters (D_m) between

0.013 and 0.7 µm, respectively. By converting both D_a and D_m to the physical diameter (D_p) [*DeCarlo and Slowik, 2004*], the average number size distributions from the two instruments were merged based on the assumption that all particles had a density of 1.8 g cm^{-3} and were spherical [*Zelenyuk et al., 2007*]. It is important to note that as the sampled particles were dried, the spherical particle assumption may not be accurate at all times.

Aerosol reaction flow tube was used to probe the reactivity of the particles. Detailed experimental setup of the flow tube can be found in Section 5.3.7. In brief, HNO_3 permeation tube (Kin-Tek, HRT-010.00-2022/60) in a temperature controlled chamber (30 ^oC) was utilized as a constant source of reactant gas. The concentration of the HNO_3 for the LPS aggregate reactivity study was approximately 10 ppb, with residence time and relative humidity (RH) of the flow tube of 1.8 min and 50 ± 2 %, respectively. The exit flow of the flow tube was split between a RH and temperature probe and ATOFMS through two diffusion driers.

6.3.2 Lipopolysaccharide Computational Simulations

6.3.2.1 Lipopolysaccharide System Preparation

CHARMMGUI [*Jo et al., 2008*] was used to build the LPS bilayer starting structure. The *E. Coli* O111 antigen and R1 core structure were chosen, with 8 repeating units of the O111 antigen. The starting box structure was determined as 70 Å for the plane of the bilayer, with a 30 Å water buffer on both sides. Each molecule of LPS was placed in the bilayer with a surface area of 190 $Å^2$ per LPS, for a total of 26 LPS molecules. The phosphates and carboxyl groups of the O111 repeats and Core domain were balanced with either Ca^{2+} or Na^+ respectively. Each phosphate maintained a net charge of -1 in the simulation to replicate a ~ pH of less than 6 environment in the context of a sea spray aerosol. Approximately 77,000 TIP3P waters [*Jorgensen et al., 1983*; *Lu et al., 2014*; *Vega and Abascal, 2011*] were placed in each system in the water buffer region as well as between the O antigens. CHARMM36 force field [*Huang and*

Mackerell, 2013] was used to parameterize the molecules and the AMBER 16 MD engine [*Case et al., 2005*; *D.A. Case, D.S. Cerutti, T.E. Cheatham, III, T.A. Darden, R.E. Duke, T.J. Giese, H. Gohlke, A.W. Goetz, D. Greene, N. Homeyer, S. Izadi, A. Kovalenko, T.S. Lee, S. LeGrand, P. Li, C. Lin, J. Liu, T. Luchko, R. Luo, D. Mermelstein, K.M. Merz, G. Monard, H., 2017*] was used to perform simulations.

6.3.2.2 Lipopolysaccharide All-Atom Molecular Dynamics Simulations

Simulations were performed with NVIDIA GK110 (GeForce GTX Titan, NVIDIA, Santa Clara, CA), and through the Amaro lab's GPU cluster with graphics processing units (GPUs) using the CUDA version of PMEMD in AMBER16 [*D.A. Case, D.S. Cerutti, T.E. Cheatham, III, T.A. Darden, R.E. Duke, T.J. Giese, H. Gohlke, A.W. Goetz, D. Greene, N. Homeyer, S. Izadi, A. Kovalenko, T.S. Lee, S. LeGrand, P. Li, C. Lin, J. Liu, T. Luchko, R. Luo, D. Mermelstein, K.M. Merz, G. Monard, H., 2017*]. The structure went through one step of minimization using the steepest descent gradient [*Ziegel et al., 1987*] algorithm and six steps of equilibration were performed. Each step of equilibration was performed for 250 ps of simulation, for a total of 1.5 ns of equilibration. GPU-enabled AMBER16 production runs were carried out as an NTP ensemble at 298.15 K, with a 2-fs time step, and particle mesh Ewald [*Darden et al., 1993*] electrostatic approximation with a nonbonding cutoff of 12 Å. Langevin dynamics [*Lamm and Szabo, 1986*] with a collision frequency of 1.0 ps^{-1}, a pressure relaxation time of 2.0 ps, and with SHAKE bond constraints on hydrogen bonds [*Ryckaert et al., 1977*].

6.3.2.3 Lipopolysaccharide Simulation Analyses

Analyses were performed using pytraj [*Roe and Cheatham III, 2013*] and numpy in the Jupyter notebook environment. The Jupyter notebooks will be provided as part of the data-sharing files. Images were taken with VMD [*Humphery Dalke and Schulten, 1996*].

6.3.3 IMPACTS 2014 Campaign Experimental Methods

Detailed experimental methods, including the phytoplankton bloom methods, on-line and off-line instrument sampling, and other sampling protocols can be found elsewhere [*Cochran et al., 2016, 2017*; *Jayarathne et al., 2016*; *Wang et al., 2015*]. Simplified schematic drawing of the wave flume, detailing the experiment setup involving the ATOFMS and the aerosol flow tube, is depicted in Figure 6.9. Filtered air using HEPA, activated carbon, and potassium permanganate filters were supplied to the headspace of the wave flume, with air flow speed of approximately 5 cm s^{-1}. Hydraulic paddle generated waves that broke off the angled beach, produced realistic sea spray aerosols (SSA) over the course of the induced phytoplankton bloom experiment. Port placed downwind of the breaking waves sampled the aerosols to the connected instruments in the study through a laminar flow manifold. Flow tube parameters for the IMPACTS 2014 campaign were: HNO_3 concentration of approximately 350 ppb, with residence time and relative humidity (RH) of the flow tube of 2 min and 60 ± 2 %, respectively.

6.4 Results and Discussion

We atomized LPS solutions with different counter cations, sodium and calcium, and with different aggregation, or cation incubation, protocols. ATOFMS provides size-resolved, dual polarity mass spectra of single particles [*Gard et al., 1997*], where Collison atomizer [*May, 1973*] produces single soluble and insoluble particles, as well as agglomerates of different particles [*Creamean et al., 2014*] across a wide size range (Figure 6.6). Select ion markers of LPS obtained from a reference mass spectrum (Figure 6.7) were used to identify particles containing LPS from the total population of the atomized particles. These atomized LPS solutions were analyzed with ATOFMS, which revealed a strong shift in the detected LPS particle size distribution depending upon which counter cation was present. Additionally, these measurements were compared with measurements of LPS-containing SSA from a previous mesocosm experiments. In brief, an

induced phytoplankton bloom within a wave flume mesocosm experiment produced realistic SSA that are representative of the ocean at varying biological activities [*Prather et al., 2013*; *Wang et al., 2015*]. Raman spectroscopic analysis of the collected SSA showed significant polysaccharide enrichment in the supermicron SSA during the second bloom of the IMPACTS 2014 campaign (Figure 6.8, red box) [*Cochran et al., 2017*]. Using LPS ion markers from the atomized LPS solutions, two types of particles were observed from the ATOFMS during the second bloom of the IMPACTS campaign, one LPS ion marker with dominant sodium signal, and the other with a dominant calcium signal. Particle size and HNO_3 reactivities are compared in these two particle types from the atomized LPS experiments and IMPACTS campaign.

The size distribution of Na^+ and Ca^{2+} containing particles were different in both atomized LPS and mesocosm experiments. In the atomized LPS experiments, the size distribution of particles shifted from predominantly submicron particles (<1 µm) to two size modes in the presence of calcium, with peaks at 0.9 and 1.5 µm (Figure 6.2A, B). Additionally, further incubation increased LPS aggregation, which led to single dominant mode at 1.5 µm (Figure 6.2C). When LPS was mixed with reef salt, and incubated for 72 hours to allow for aggregation, the resulting atomized LPS particle size distribution had two dominant modes at 0.6 and 1.7 µm (Figure 6.2D). Based on these findings, the two size modes LPS aerosol particles measured are likely due to different LPS morphologies formed in solution. Two size modes were also seen for Ca^{2+}-LPS containing SSA derived from IMPACTS 2014 during a period of high polysaccharide enrichment in the supermicron SSA (Figure 6.3A) (IMPACTS 2014). Conversely, only one mode was seen for Na^+-LPS containing SSA derived from this same mesocosm. The aerosol size distributions from this experiment are greater than the aerosol size distributions from the pure LPS studies, possibly due to greater LPS aggregation present in the heterogeneous chemical mixtures found within the mesocosm.

The heterogeneous reactivity with HNO_3 of LPS-containing aerosols was dependent upon the aerosol particle sizes, which was effected by levels of coordinating cation present, for both pure LPS particles and LPS containing particles from mesocosm experiments. From ATOFMS, submicron pure LPS aerosol particles were more associated with sodium and potassium (Figure 6.4A), whereas supermicron pure LPS aerosol particles contained a more dominant calcium signature (Figure 6.4B). Furthermore, a larger percentage of submicron particles were reactive with HNO_3 (74.6% of LPS particles reacted) than supermicron particles were (15.5% of LPS particles reacted) (Figure 6.4C). In fact, LPS-containing supermicron particles (Figure 6.4D) reacted less than NaCl supermicron particles (42.9% reacted), which served here as a reference standard for HNO_3 reactivity with particles at various size regimes [*Brink, 1998*; *Fenter et al., 1994*; *Finlayson-Pitts and Hemminger, 2000*; *Rossi, 2003*]. This difference in reactivity behavior was also observed in IMPACTS 2014 LPS containing particles, specifically Ca^{2+}-LPS containing SSA exhibiting less reactivity than Na^{+}-LPS containing SSA (Figure 6.3B).

Thus, submicron LPS particles, which had higher levels Na^{+} than Ca^{2+}, reacted more with HNO_3 than supermicron LPS particles, which had higher levels of Ca^{2+}. In Ca^{2+} or Na^{+} containing solutions, LPS particles tend to form bilayer structures [*Coughlin, Haug, et al., 1983*; *Santos et al., 2003*; *Snyder et al., 1999*]. Here, we propose that this phenomenon is guided by aqueous LPS particle morphology: Ca^{2+}-LPS containing particles form more rigid bilayer structures that are less surface active while Na^{+}-LPS containing particles form less condensed or rigid bilayer structures. These less rigid Na^{+}-LPS containing particles could be apt to disruption through bubble bursting processes, and thus have the potential to be more surface active through the formation of an inverted micelle or monolayer on particle surfaces. To study the hypothesis of cation-driven bilayer rigidity for the LPS molecules used in this study, all-atom molecular dynamics simulations were performed to understand the structural differences of these LPS

bilayers in the presence of Na^+ and Ca^{2+}, as has been studied previously [*Blasco et al., 2017*; *Schneck et al., 2009*; *Wu et al., 2013*].

All-atom molecular dynamics simulations of *E. Coli* O111 LPS bilayer were performed with either Ca^{2+} or Na^+ counter cations. We measured the distance between the most proximal sugar of the O-Antigen and the first sugar of Lipid A in the last 10 ns of simulation for all six replicates. This distance was 79.5 Å for Ca^{2+} bound LPS versus 86.6 Å for Na^+ bound LPS, suggesting that Ca^{2+} promotes collapse of the bilayer into a more compact structure (Figure 6.5). Additionally, the variance in the LPS polysaccharide distances is 13 Å for the Ca^{2+} containing system in 28.4 Å for the Na^+ containing system. Taken together, we hypothesize that the collapse of the O-antigen blocks HNO_3 reactivity, while Na^+ promotes more disordered and extended O-antigen dynamics, allowing for greater HNO_3 reactivity as well as bilayer disruption during bubble bursting processes (Figure 6.5). Future work will characterize the atomic-level mechanism that guides these different cations to mediate LPS collapse versus disorder, as well as the role of Mg^{2+} on the LPS structure and the heterogeneous reactivity of the LPS particles in the atmosphere.

6.5 Conclusions

In this study, we measured the impacts of sodium versus calcium on the size (morphology) and heterogeneous reactivity of LPS-containing aerosols. Our findings reveal that in the presence of calcium, LPS is driven to form larger aqueous particles than in the presence of sodium. The morphology of these larger Ca^{2+}-LPS particles results in lower HNO_3 reactivity as compared with Na^+-LPS particles. Finally, these morphologically differences are tied to the collapsed bilayer structure of LPS particles in the presence of Ca^{2+} as opposed to the more elongated LPS structures found in the Na^+ coordinated bilayer. While this study focused on HNO_3 reactivity, the impact of salts on LPS morphology have implications for other atmospheric

heterogeneous reactions such as oxidation or radical chemistry [*Abbatt et al., 2012*], but also in processes where surface active species would have profound effect including cloud droplet and ice nucleation processes [*Andreae and Rosenfeld, 2008*]. While SSA are known to exhibit large differences in their heterogeneous reactivity [*Ault et al., 2014*], this study provides a glimpse into the atomic-level mechanisms that are driving the difference in this chemistry for a set of biologically relevant chemical species. Future studies will aim to build up complexity through the addition of other polysaccharides to understand how other sugars could impact heterogeneous chemistry of LPS within the aerosol phase.

6.6 Acknowledgements

The authors like to thank all collaborators involved with the CAICE IMPACTS 2014 intensive campaign and the Scripps Institution of Oceanography Hydraulic Laboratory staff. The authors like to acknowledge O. Ryder, M. Santander, J. Michaud, and J. Dowling for their valuable contributions. This work is funded by Center for Aerosol Impacts on Chemistry of the Environment (CAICE), National Science Foundation Center for Chemical Innovation (CHE-1305427).

Chapter 6 is in preparation: Lee, C., Schiffer, J.M., Grassian, V.H., Prather K.A. Calcium-Driven Lipopolysaccharide Aggregation in Sea Spray Aerosol Composition and Nitric Acid Heterogeneous Reactivity. The dissertation author was the primary investigator and author of this paper. C.L., J.M.S., V.H.G., and K.A.P designed the experiment, C.L. performed LPS aggregation and single particle mass spectrometry measurements, and J.M.S. performed molecular dynamics simulations.

6.7 Figures

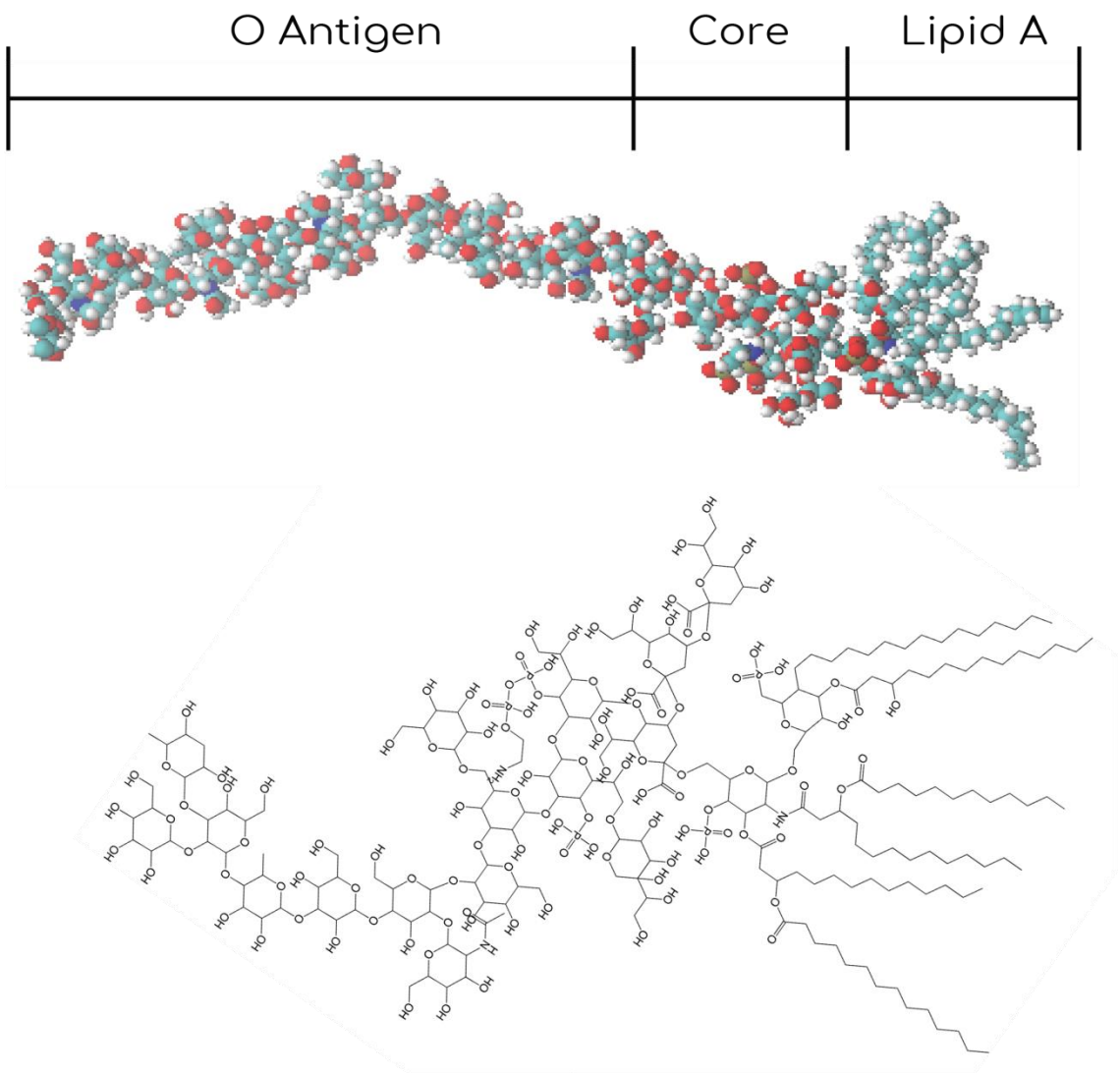

Figure 6.1. Simplified cartoon of LPS molecular structure (top) with the chemical formula (bottom). White = hydrogen; teal = carbon; red = oxygen; blue = nitrogen; and yellow = phosphorous.

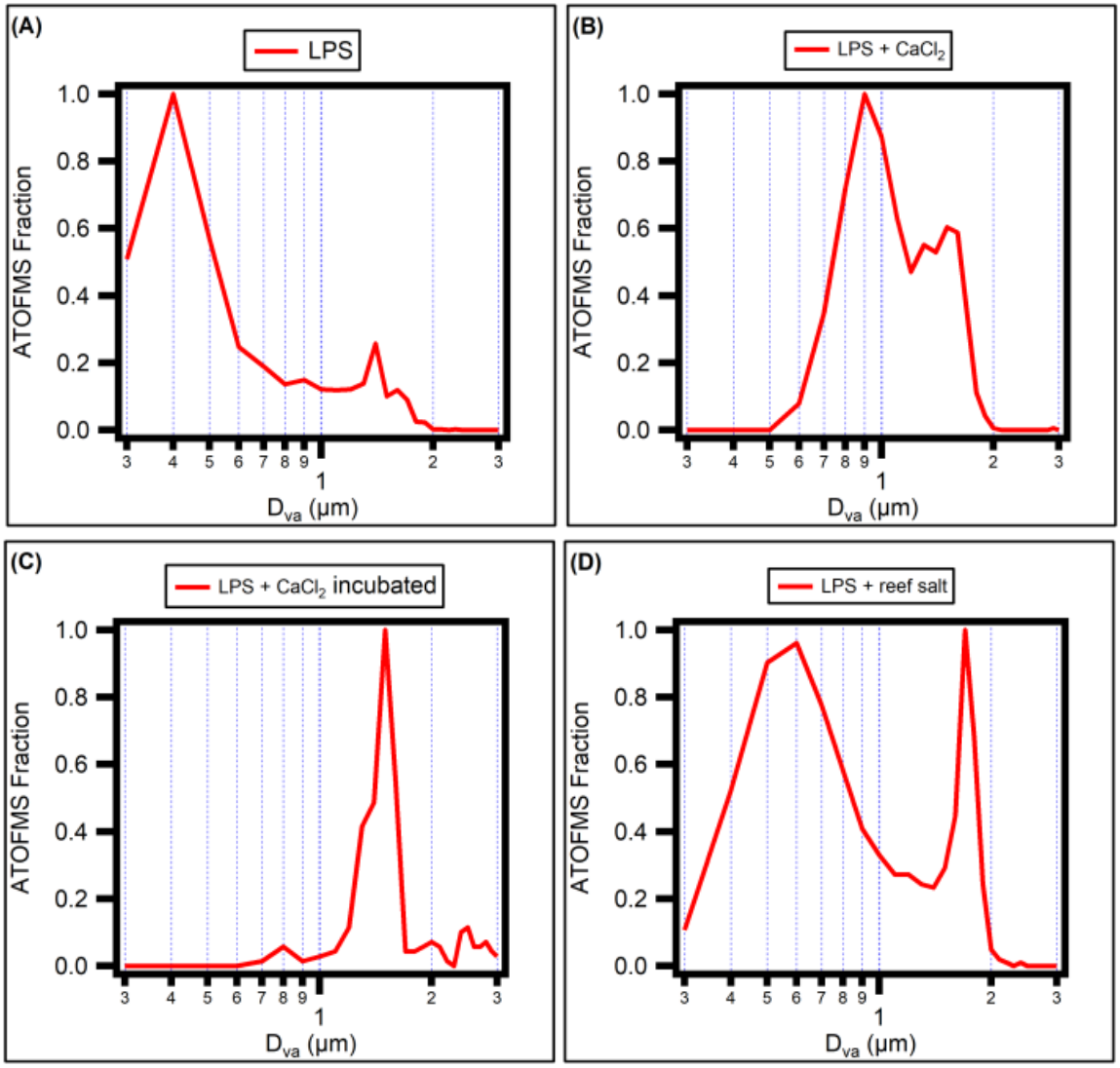

Figure 6.2. Normalized size distribution of LPS particles detected by ATOFMS for (A) LPS + NaCl salt, (B) LPS spiked with 0.010 M $CaCl_2$, (C) LPS spiked with 0.010 M $CaCl_2$ and incubated for 72 h, and (D) LPS spiked with reef salt at 1:1 ratio by mass in ultrapure water.

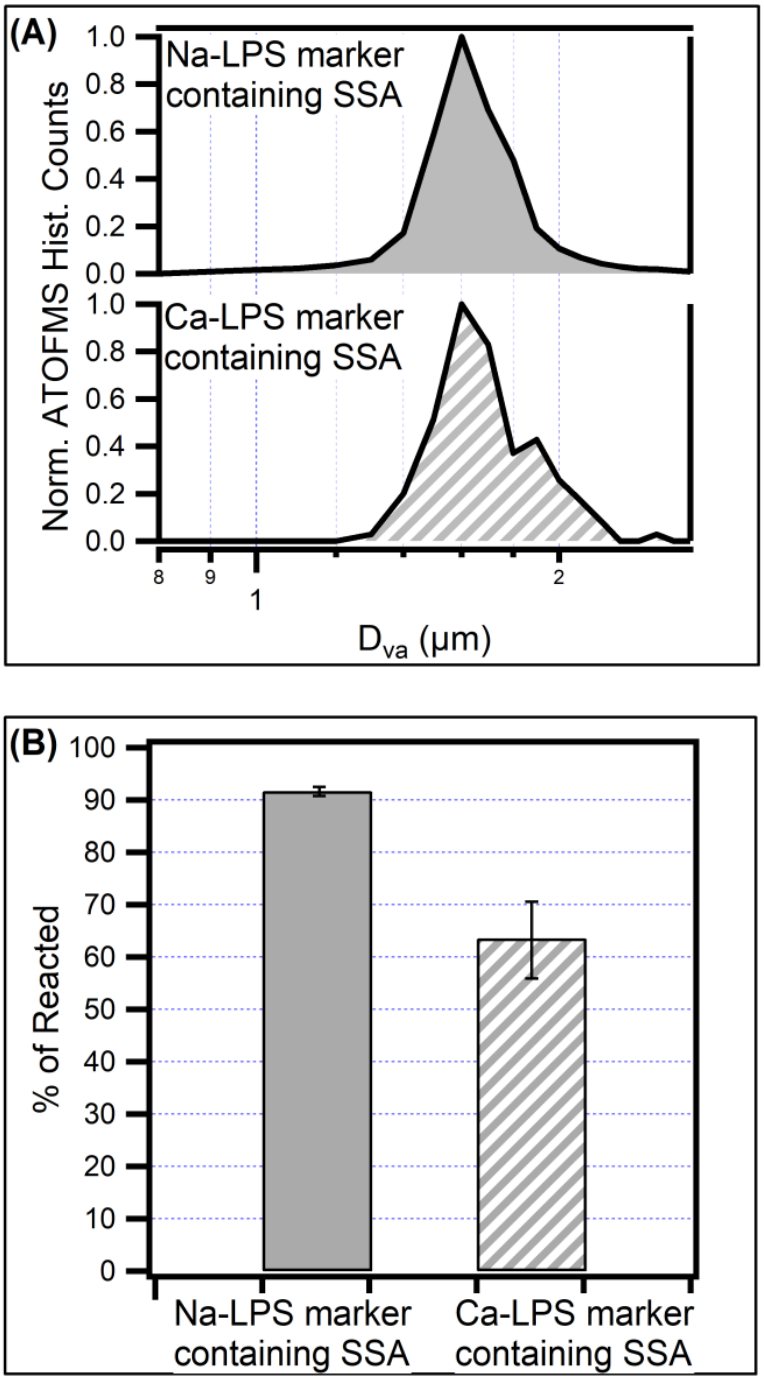

Figure 6.3. (A) ATOFMS sized histogram of Na-LPS (solid fill) and Ca-LPS (dashed fill) marker containing SSA from the IMPACTS 2014 campaign. (B) Percentage of reacted Na-LPS (solid fill) and Ca-LPS (dashed fill) ion marker containing SSA detected by ATOFMS with HNO_3 flow tube apparatus from the IMPACTS 2014 campaign. Error bars in (B) represent 2σ for 95% confidence limit.

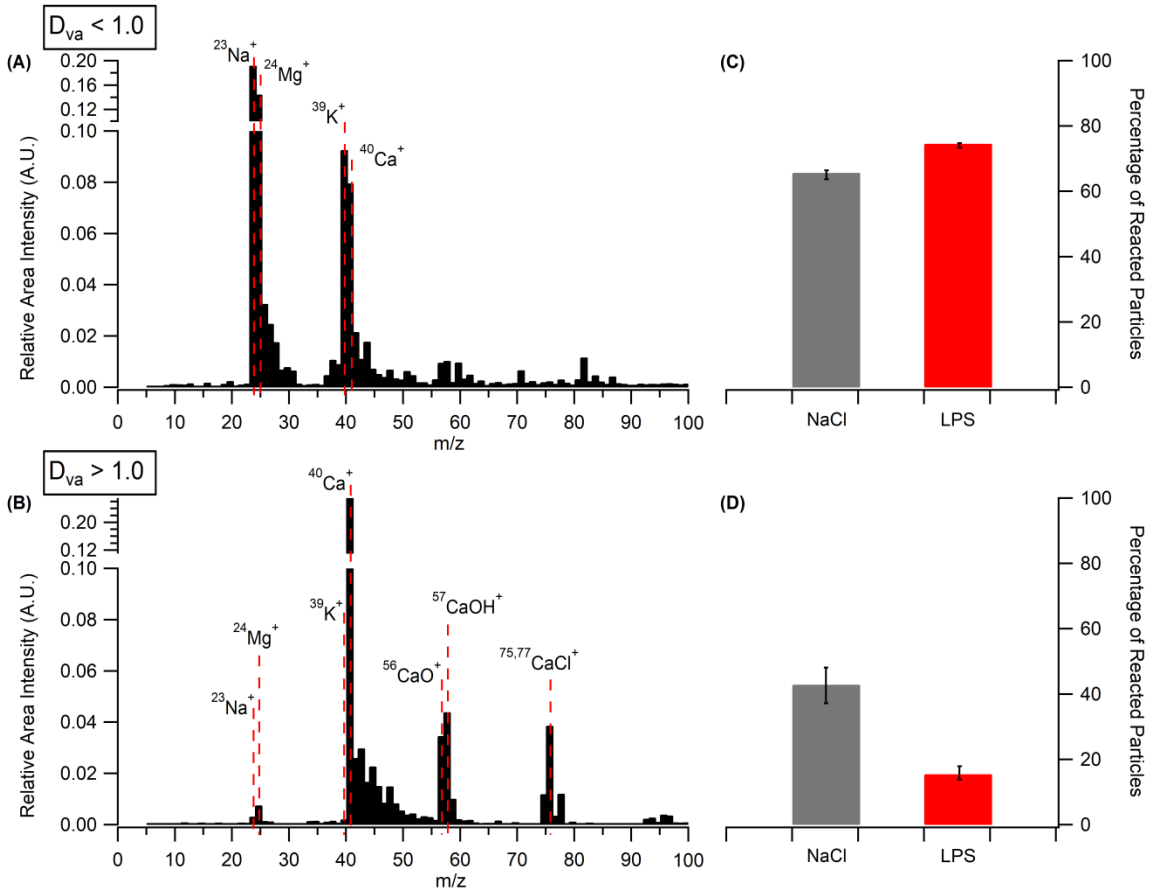

Figure 6.4. (A, B) Averaged positive ion mass spectra of identified LPS particles in NaCl and $CaCl_2$ matrix, respectively. Detailed dual polarity mass spectra can be found in SI. (C, D) percentage of reacted LPS particles that are less than or greater than 1.0 µm D_{va}, respectively, with reacted fraction of NaCl particles at the respective size ranges as a reference standard. Error bars in (C, D) represent 2σ for 95% confidence limit.

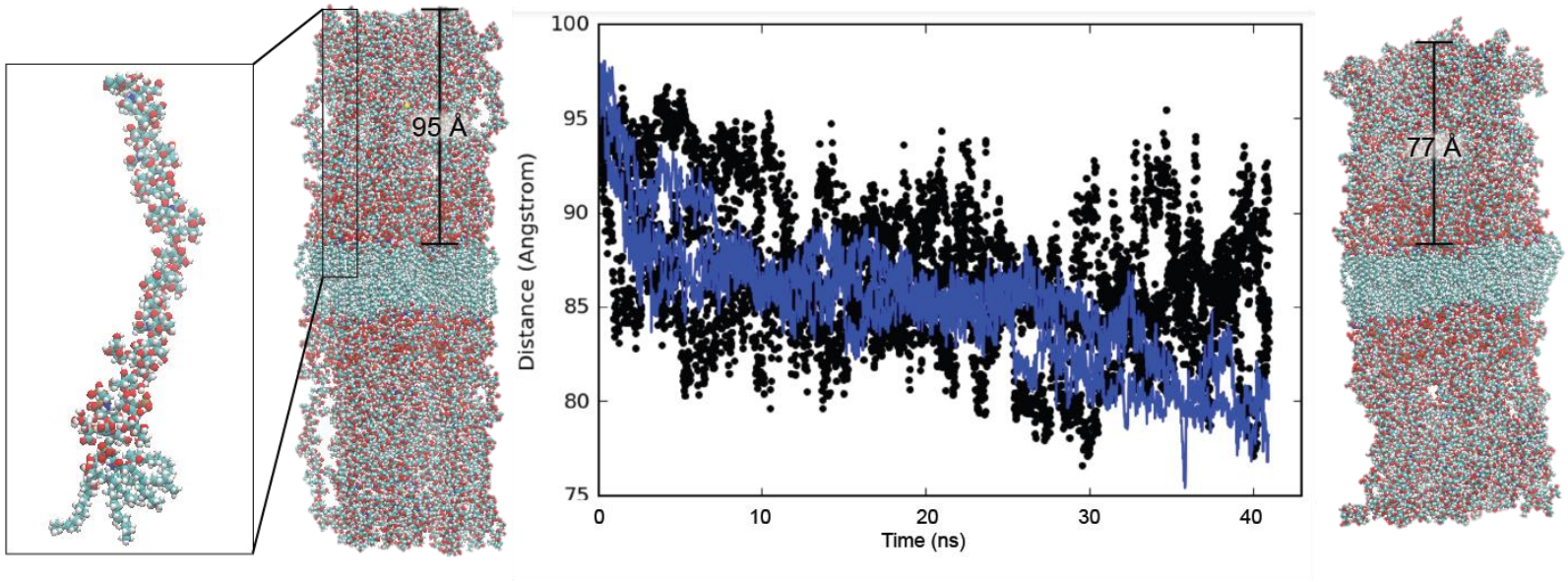

Figure 6.5. Molecular schematic of Na-LPS and Ca-LPS. Simulations of Na-LPS (black dots) demonstrated much greater variance in the distance between the most proximal ends of the O-Antigen and the Lipid A moiety than the simulations of the Ca-LPS (blue dots). On the left is the starting structure and on the right is the final frame of the Ca-LPS simulations.

6.8 Supporting Information

6.8.1 Supporting Information Figures

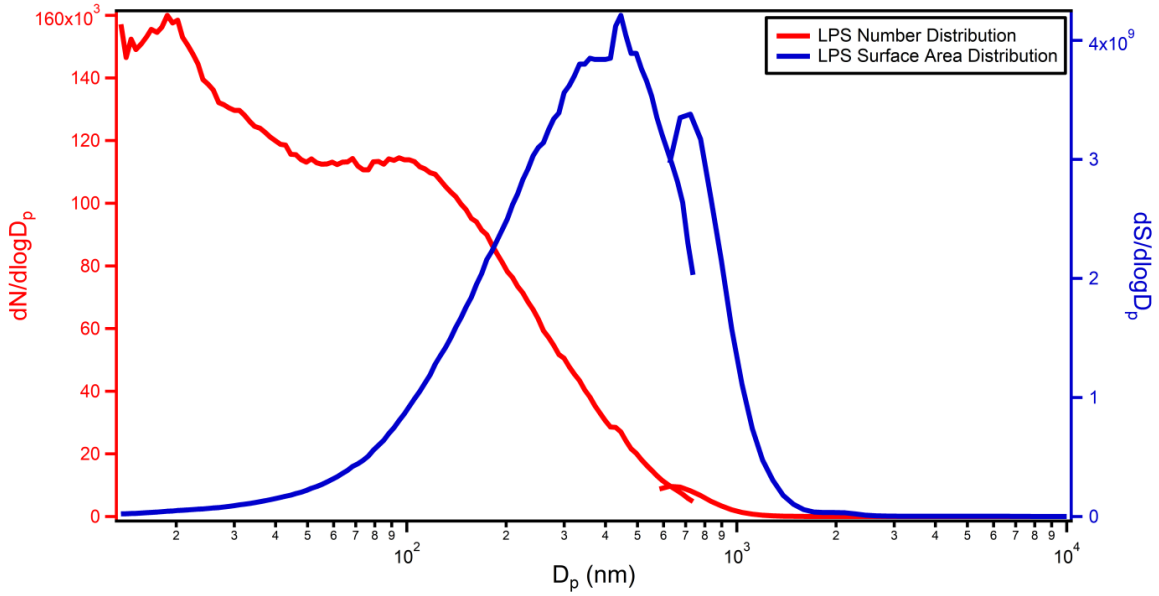

Figure 6.6. Merged APS and SMPS Number (red) and calculated surface area (blue) size distributions of atomized LPS particles.

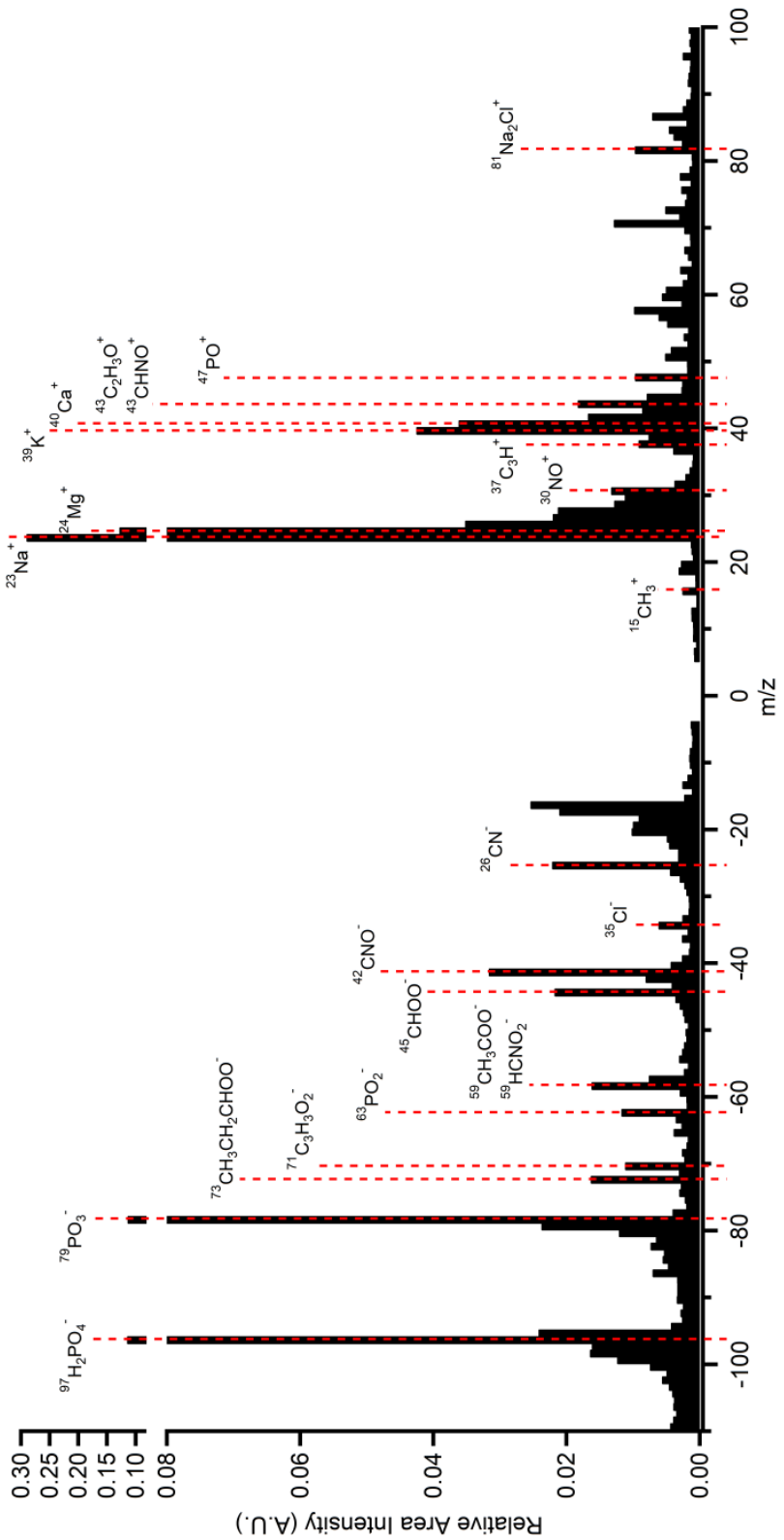

Figure 6.7. Averaged mass spectra of atomized LPS particles, with select ion markers used for identification of LPS containing particles in atomized samples of LPS salt solutions.

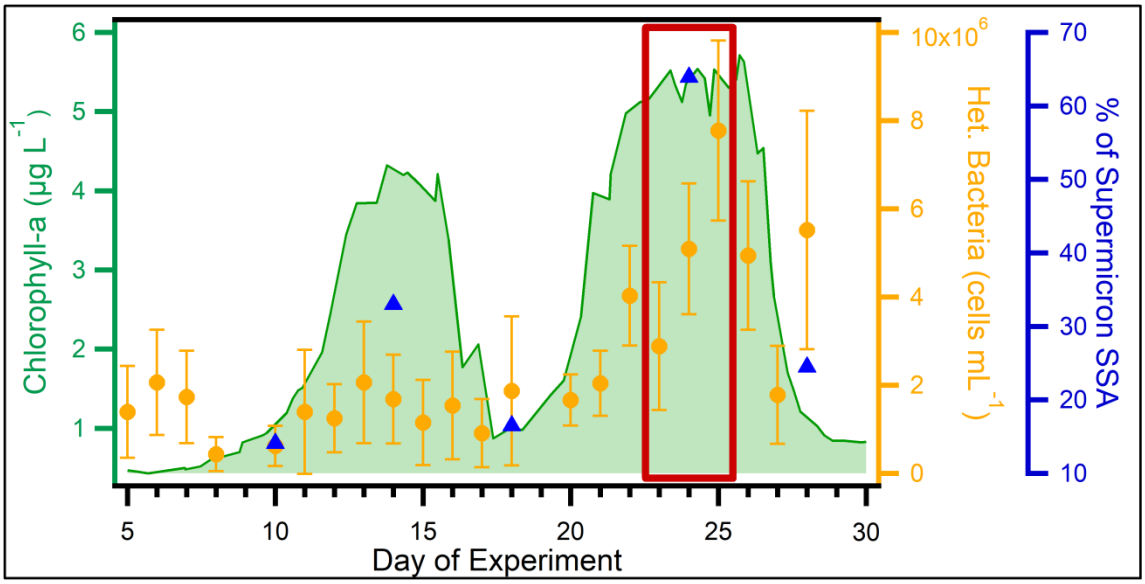

Figure 6.8. Temporal trend of polysaccharide-containing supermicron SSA during IMPACTS 2014 campaign. Seawater chlorophyll-a (green) and heterotrophic bacteria concentrations (orange) of the wave flume with the percentage of Raman spectroscopically determined polysaccharide containing supermicron SSA (blue) over the course of phytoplankton blooms from IMPACTS 2014 campaign. Period of supermicron SSA polysaccharide-enrichment for further ATOFMS data analysis is boxed in red. Raman spectroscopy determined particle type fractions are reproduced with permission from Cochran et al. 2017

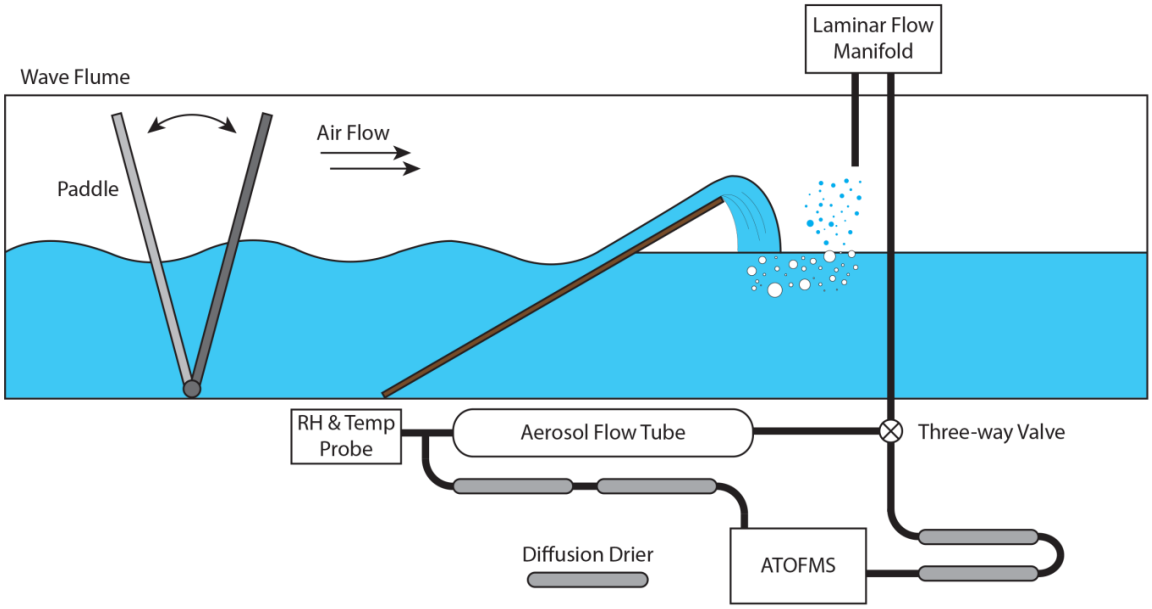

Figure 6.9. Schematic drawing of the simplified IMPACTS 2014 campaign experiment showing the wave flume and the ATOFMS with aerosol flow tube. Angled beach for breaking waves is colored brown.

6.9 References

Abbatt, J. P. D., A. K. Y. Lee, and J. A. Thornton, Quantifying trace gas uptake to tropospheric aerosol: recent advances and remaining challenges, Chemical Society Reviews, 41 (19), 6555, 2012.

Andreae, M. O., and D. Rosenfeld, Aerosol-cloud-precipitation interactions. Part 1. The nature and sources of cloud-active aerosols, Earth-Science Reviews, 89 (1–2), 13–41, 2008.

Ault, A. P., T. L. Guasco, O. S. Ryder, J. Baltrusaitis, L. A. Cuadra-Rodriguez, D. B. Collins, M. J. Ruppel, T. H. Bertram, K. A. Prather, and V. H. Grassian, Inside versus outside: Ion redistribution in nitric acid reacted sea spray aerosol particles as determined by single particle analysis, Journal of the American Chemical Society, 135 (39), 14528–14531, 2013.

Ault, A. P., T. L. Guasco, J. Baltrusaitis, O. S. Ryder, J. V. Trueblood, D. B. Collins, M. J. Ruppel, L. A. Cuadra-Rodriguez, K. A. Prather, and V. H. Grassian, Heterogeneous reactivity of nitric acid with nascent sea spray aerosol: Large differences observed between and within individual particles, Journal of Physical Chemistry Letters, 5 (15), 2493–2500, 2014.

Aurell, C. A., and A. O. Wistrom, Critical aggregation concentrations of gram-negative bacterial lipopolysaccharides (LPS), Biochemical and Biophysical Research Communications, 253 (1), 119–123, 1998.

Blasco, P., D. S. Patel, O. Engström, W. Im, and G. Widmalm, Conformational dynamics of the lipopolysaccharide from *Escherichia coli* O91 revealed by nuclear magnetic resonance spectroscopy and molecular simulations, Biochemistry, 56 (29), 3826–3839, 2017.

Brink, H. M. Ten, Reactive uptake of HNO_3 and H_2SO_4 in sea-salt (NaCl) particles, Journal of Aerosol Science, 29 (1–2), 57–64, 1998.

Case, D. A., T. E. Cheatham, T. Darden, H. Gohlke, R. Luo, K. M. Merz, A. Onufriev, C. Simmerling, B. Wang, and R. J. Woods, The Amber biomolecular simulation programs, Journal of Computational Chemistry, 26 (16), 1668–1688, 2005.

Case, D.A., D.S. Cerutti, T.E. Cheatham, III, T.A. Darden, R.E. Duke, T.J. Giese, H. Gohlke, A.W. Goetz, D. Greene, N. Homeyer, S. Izadi, A. Kovalenko, T.S. Lee, S. LeGrand, P. Li, C. Lin, J. Liu, T. Luchko, R. Luo, D. Mermelstein, K.M. Merz, G. Monard, H., D. M. Y. and P. A. K., Amber16,. University of California, San Francisco, 2017.

Cochran, R. E., O. Laskina, J. Trueblood, A. D. Estillore, H. S. Morris, T. Jayarathne, C. M. Sultana, C. Lee, P. Lin, J. Laskin, A. Laskin, J. Dowling, Z. Qin, C. D. Cappa, T. H. Bertram, A. V Tivanski, E. A. Stone, K. A. Prather, and V. H. Grassian, Molecular characterization of sea spray particles : Influence of ocean biology on particle composition and interaction with water, Chem, 2, 655–667, 2017.

Cochran, R. E., O. Laskina, T. Jayarathne, A. Laskin, J. Laskin, P. Lin, C. M. Sultana, C. Lee, K. A. Moore, C. D. Cappa, T. H. Bertram, K. A. Prather, V. H. Grassian, and E. A. Stone, Analysis of organic anionic surfactants in fine (PM2.5) and coarse (PM10) fractions of freshly emitted sea spray aerosol, Environmental Science and Technology, 50 (5), 2477–2486, 2016.

Coughlin, R. T., A. Haug, and E. J. McGroarty, Physical properties of defined lipopolysaccharide salts, Biochemistry, 22 (1978), 2007–2013, 1983.

Coughlin, R. T., S. Tonsager, and E. J. McGroarty, Quantitation of metal cations bound to membranes and extracted lipopolysaccharide of Escherichia coli., Biochemistry, 22 (8), 2002–2007, 1983.

Creamean, J. M., C. Lee, T. C. Hill, A. P. Ault, P. J. DeMott, A. B. White, F. M. Ralph, and K. A. Prather, Chemical properties of insoluble precipitation residue particles, Journal of Aerosol Science, 76, 13–27, 2014.

Darden, T., D. York, and L. Pedersen, Particle mesh Ewald: An N·log(N) method for Ewald sums in large systems, The Journal of Chemical Physics, 98 (12), 10089, 1993.

DeCarlo, P. F., and J. G. Slowik, Particle morphology and density characterization by combined mobility and aerodynamic diameter measurements. Part 1: Theory, Aerosol Science and Technology, 38 (12), 1185–1205, 2004.

Fenter, F. F., F. Caloz, and M. J. Rossi, Kinetics of Nitric Acid Uptake by Salt, The Journal of Physical Chemistry, 98 (39), 9801–9810, 1994.

Finlayson-Pitts, B. J., and J. C. Hemminger, Physical chemistry of airborne sea salt particles and their components, The Journal of Physical Chemistry A, 104 (49), 11463–11477, 2000.

Gard, E. E., J. E. Mayer, B. D. Morrical, T. Dienes, D. P. Fergenson, and K. A. Prather, Real-time analysis of individual atmospheric aerosol particles: Design and performance of a portable ATOFMS, Analytical Chemistry, 69 (20), 4083–4091, 1997.

Garidel, P., M. Rappolt, A. B. Schromm, J. Howe, K. Lohner, J. Andrä, M. H. J. Koch, and K. Brandenburg, Divalent cations affect chain mobility and aggregate structure of lipopolysaccharide from Salmonella minnesota reflected in a decrease of its biological activity, Biochimica et Biophysica Acta - Biomembranes, 1715 (2), 122–131, 2005.

Huang, J., and A. D. Mackerell, CHARMM36 all-atom additive protein force field: Validation based on comparison to NMR data, Journal of Computational Chemistry, 34 (25), 2135–2145, 2013.

Humphery Dalke, A. Schulten, K., W., VMD - Visual Molecular Dynamics, J. Molec. Graph, 14, 33–38, 1996.

Jayarathne, T., C. M. Sultana, C. Lee, F. Malfatti, J. L. Cox, M. A. Pendergraft, K. A. Moore, F. Azam, A. V. Tivanski, C. D. Cappa, T. H. Bertram, V. H. Grassian, K. A. Prather, and E. A. Stone, Enrichment of saccharides and divalent cations in sea spray aerosol during two phytoplankton blooms, Environmental Science and Technology, 50 (21), 11511–11520, 2016.

Jo, S., T. Kim, V. G. Iyer, and W. Im, CHARMM-GUI: A web-based graphical user interface for CHARMM, Journal of Computational Chemistry, 29 (11), 1859–1865, 2008.

Jorgensen, W. L., J. Chandrasekhar, J. D. Madura, R. W. Impey, and M. L. Klein, Comparison of simple potential functions for simulating liquid water, The Journal of Chemical Physics, 79 (2), 926, 1983.

Lamm, G., and A. Szabo, Langevin modes of macromolecules, The Journal of Chemical Physics, 85 (12), 7334, 1986.

Li, L., and R. G. Luo, Use of Ca+2 to re-aggregate lipopolysaccharide (LPS) in hemoglobin solutions and the subsequent removal of endotoxin by ultrafiltration, Biotechnology Techniques, 12 (2), 119–122, 1998.

Lu, J., Y. Qiu, R. Baron, and V. Molinero, Coarse-graining of TIP4P/2005, TIP4P-Ew, SPC/E, and TIP3P to monatomic anisotropic water models using relative entropy minimization, Journal of Chemical Theory and Computation, 10 (9), 4104–4120, 2014.

May, K. R., The collison nebulizer: Description, performance and application, Journal of Aerosol Science, 4 (3), 235–243, 1973.

Parikh, S. J., and J. Chorover, Infrared spectroscopy studies of cation effects on lipopolysaccharides in aqueous solution, Colloids and Surfaces B: Biointerfaces, 55 (2), 241–250, 2007.

Pomeroy, L. R., P. J. I. Williams, F. Azam, and J. E. Hobbie, The microbial loop, Oceanography, 20 (2), 28–33, 2007.

Prather, K. A., T. H. Bertram, V. H. Grassian, G. B. Deane, M. D. Stokes, P. J. Demott, L. I. Aluwihare, B. P. Palenik, F. Azam, J. H. Seinfeld, R. C. Moffet, M. J. Molina, C. D. Cappa, F. M. Geiger, G. C. Roberts, L. M. Russell, A. P. Ault, J. Baltrusaitis, D. B. Collins, C. E. Corrigan, L. A. Cuadra-Rodriguez, C. J. Ebben, S. D. Forestieri, T. L. Guasco, S. P. Hersey, M. J. Kim, W. F. Lambert, R. L. Modini, W. Mui, B. E. Pedler, M. J. Ruppel, O. S. Ryder, N. G. Schoepp, R. C. Sullivan, and D. Zhao, Bringing the ocean into the laboratory to probe the chemical complexity of sea spray aerosol., Proceedings of the National Academy of Sciences of the United States of America, 110 (19), 7550–5, 2013.

Quinn, P. K., D. B. Collins, V. H. Grassian, K. A. Prather, and T. S. Bates, Chemistry and related properties of freshly emitted sea spray aerosol, Chemical Reviews, 115, 4383–4399, 2015.

Roe, D. R., and T. E. Cheatham III, PTRAJ and CPPTRAJ: software for processing and analysis of molecular synamics trajectory data, Journal of Chemical Theory and Computation, 9 (7), 3084–3095, 2013.

Rossi, M. J., Heterogeneous reactions on salts, Chemical Reviews, 103 (12), 4823–4882, 2003.

Ryckaert, J. P., G. Ciccotti, and H. J. C. Berendsen, Numerical integration of the cartesian equations of motion of a system with constraints: molecular dynamics of n-alkanes, Journal of Computational Physics, 23 (3), 327–341, 1977.

Ryder, O. S., N. R. Campbell, H. Morris, S. Forestieri, M. J. Ruppel, C. Cappa, A. Tivanski, K. Prather, and T. H. Bertram, Role of organic coatings in regulating N_2O_5 reactive uptake to sea spray aerosol, Journal of Physical Chemistry A, 119 (48), 11683–11692, 2015.

Santos, N. C., A. C. Silva, M. A. R. B. Castanho, J. Martins-Silva, and C. Saldanha, Evaluation of lipopolysaccharide aggregation by light scattering spectroscopy, ChemBioChem, 4 (1), 96–100, 2003.

Schneck, E., E. Papp-Szabo, B. E. Quinn, O. V Konovalov, T. J. Beveridge, D. A. Pink, and M. Tanaka, Calcium ions induce collapse of charged O-side chains of lipopolysaccharides from Pseudomonas aeruginosa., Journal of the Royal Society, Interface, 6 Suppl 5 (Suppl 5), S671-8, 2009.

Snyder, S., D. Kim, and T. J. McIntosh, Lipopolysaccharide bilayer structure: Effect of chemotype, core mutations, divalent cations, and temperature, Biochemistry, 38 (33), 10758–10767, 1999.

Sultana, C. M., G. C. Cornwell, P. Rodriguez, and K. A. Prather, FATES: A flexible analysis toolkit for the exploration of single-particle mass spectrometer data, Atmospheric Measurement Techniques, 10 (4), 1323–1334, 2017.

Tanford, C., and J. Wiley, The hydrophobic effect: Formation of micelles and biological membranes., Journal of Chemical Education, 232, 1980.

Trueblood, J. V., A. D. Estillore, C. Lee, J. A. Dowling, K. A. Prather, and V. H. Grassian, Heterogeneous chemistry of lipopolysaccharides with gas-phase nitric acid: Reactive sites and reaction pathways, Journal of Physical Chemistry A, 120 (32), 6444–6450, 2016.

Vega, C., and J. L. F. Abascal, Simulating water with rigid non-polarizable models: a general perspective, Physical Chemistry Chemical Physics, 13 (44), 19663, 2011.

Wang, X., C. M. Sultana, J. Trueblood, T. C. J. Hill, F. Malfatti, C. Lee, O. Laskina, K. A. Moore, C. M. Beall, C. S. McCluskey, G. C. Cornwell, Y. Zhou, J. L. Cox, M. A. Pendergraft, M. V. Santander, T. H. Bertram, C. D. Cappa, F. Azam, P. J. DeMott, V. H. Grassian, and K. A. Prather, Microbial control of sea spray aerosol composition: A tale of two blooms, ACS Central Science, 1 (3), 124–131, 2015.

Wu, E. L., O. Engström, S. Jo, D. Stuhlsatz, M. S. Yeom, J. B. Klauda, G. Widmalm, and W. Im, Molecular dynamics and NMR spectroscopy studies of E. coli lipopolysaccharide structure and dynamics, Biophysical Journal, 105 (6), 1444–1455, 2013.

Zelenyuk, A., D. Imre, L. A. Cuadra-Rodriguez, and B. Ellison, Measurements and interpretation of the effect of a soluble organic surfactant on the density, shape and water uptake of hygroscopic particles, Journal of Aerosol Science, 38 (9), 903–923, 2007.

Ziegel, E., W. Press, B. Flannery, S. Teukolsky, and W. Vetterling, Numerical recipes: The art of scientific computing *Technometrics* (Vol. 29), 1987.

7 Conclusions and Future Work

7.1 Synopsis

This dissertation focuses on developing ways to control the SSA organic content in the laboratory in order to elucidate factors controlling heterogeneous reactivity of SSA. These fundamental physical chemistry studies of SSA take advantage of marine microbiological processes to drive SSA chemistry. Specific biogeochemical interactions of interest include the processing of organic matter via extracellular enzymes and the interaction between macromolecules and divalent cations. New findings described herein reveal that enzymes in seawater, specifically lipase, directly impact the chemical composition of SSA and their subsequent heterogeneous reactivity. Furthermore, not only do enzymes control SSA chemistry by processing organics in the seawater, but they can also get ejected into the SSA and remain active. These enzymes in SSA are able to control/transform the chemical composition of atmospheric aerosols. And finally, in addition to enzymes, other biomolecules such as bacteria-derived LPS can interact with divalent cations, and these biomolecule-cation interactions can drastically alter SSA heterogeneous reactivity. While the biogeochemical interactions in the seawater leading to organic-enriched SSA involve many processes [*Arnosti, 2011*; *Azam and Malfatti, 2007*; *O'Dowd et al., 2015, 2004*; *Pomeroy et al., 2007*; *Quinn et al., 2015*; *Rinaldi et al., 2013*], this dissertation provides new insights into SSA physics and chemistry though cross-disciplinary techniques. Section 7.2 provides a summary of the concluded work, while Section 7.3 introduces ongoing investigations and future studies arising from the research presented in this dissertation.

7.2 Conclusions

7.2.1 Replicating the Chemical Complexity of Sea Spray Aerosols in the Laboratory

The first goal of this dissertation was to develop a method that replicates the physical and chemical complexity of realistic SSA in the laboratory. A new laboratory method was necessary to provide new insights into the relationship between organic enrichment in SSA and marine biological activity [*O'Dowd et al., 2004*] and to control SSA organic content.

Chapter 2 presented a method for generating realistic SSA in the laboratory through the natural synthesis and chemical processing of organic compounds by marine microorganisms. Inducing a phytoplankton bloom forced changes in heterotrophic bacteria and virus concentrations in a MART system, promoting the formation of vast arrays of organic species mimicking those naturally formed in the ocean and controlling the organic complexity of SSA. Combined spectroscopic, microscopic, and ATOFMS results also revealed that SSA organic enrichment occurred 4 to 10 days after the peak in phytoplankton bloom. Previous studies suggest this organic enrichment likely controls its heterogeneous reactivity behavior [*Abbatt et al., 2012*; *Ault et al., 2014; Riva et al., 2016*; *Ryder et al., 2015*; *Stemmler et al., 2008*]. The method for inducing a change in SSA chemistry described here sets the stage for future studies to directly probe the marine biosphere-atmosphere link.

7.2.2 The Role of Enzymes on the SSA Physicochemical Properties

As the lipase enzyme was suggested by Wang et al., 2015 to have profound implications on SSA chemistry, Chapter 3 investigated the changes to SSA composition with seawater lipase treatment using triolein (a triacylglycerol) and a diatom lysate as simple and complex model substrates, respectively. The coupling of mass spectrometry measurements of bulk aerosol and size fractionated aerosol samples with online single particle ATOFMS measurements confirmed

the conversion of lipids to fatty acids in the bulk seawater and subsequent changes in the aerosol phase. Furthermore, supermicron SSA contained more fatty acids compared to submicron SSA, and these fatty acid-containing supermicron SSA were closely associated with calcium, consistent with previous findings that calcium has a high binding affinity to fatty acid headgroups [*Zhang et al., 2016*]. Cations and fatty acids likely alter SSA heterogeneous reactivity [*Abbatt et al., 2012; Stemmler et al., 2008*] and air-water interface chemistry [*Adams et al., 2016*; *Allen et al., 2009*; *Zhang et al., 2016*], thus influencing SSA surface sensitive climate properties such as CCN [*Moore et al., 2011; Nguyen et al., 2017*].

Extending the study of lipase-induced chemical changes in SSA, Chapter 4 demonstrates that changes in SSA chemical mixing state affect nitric acid heterogeneous reactivity. In both the triolein and lysate substrate systems, the evolution of SSA particle types behaved similarly: increase in organic-enriched SSA after substrate addition and subsequent decrease once lipase is added. However, the heterogeneous reactivity of the particles from the triolein and lysate substrate systems showed completely opposite trends: addition of triolein suppressed reactivity, while addition of lysate increased reactivity. Upon addition of lipase, degradation of the substrate molecules in the respective systems further transformed the organic component of SSA, ultimately impacting the reactivity. This study not only demonstrates the importance of replicating the ocean's natural chemical complexity in laboratory studies, but also shows specifically that lipase in seawater likely have significant impacts on SSA heterogeneous reactivity. These studies reveal a previously unidentified link between marine enzymes and heterogeneous reactivity of SSA.

Building up the complexity of the system, Chapter 5 reveals enzymes in SSA as a newly discovered atmospheric reaction pathway that alters composition and heterogeneous reactivity. Not only were active enzymes transferred from bulk seawater and the SSML to SSA during

separate induced phytoplankton bloom experiments, but also their ability to transform SSA after ejection was demonstrated in the laboratory using enzyme-substrate model systems. Furthermore, aerosol coagulation simulations predict that within hours after ejection, enzyme-containing SSA will coagulate with background aerosols. Thus SSA can act as self-contained biochemical reactors and ultimately alter aerosol composition, morphology, and properties in previously unexplored ways.

7.2.3 Cation-Driven Aggregation of Biogenically-Derived Organic Molecules in Sea Spray Aerosols

A new reaction pathway of heterogeneous chemistry that occurs between biogenically-derived organic molecules, such as lipopolysaccharides (LPS), and HNO_3 [*Trueblood et al., 2016*] was recently discovered. Delving deeper into this discovery, Chapter 6 uncovers the naturally occurring processes that control LPS heterogeneous reactivity behavior in the atmosphere. Combining single particle mass spectrometry and molecular dynamic simulations, we demonstrate for the first time how higher order structure formed from calcium-induced aggregation of LPS impact their heterogeneous reactivity, and move toward unraveling the role that composition and structure of bioaerosols has on SSA atmospheric properties.

7.3 Ongoing and Future Work

7.3.1 Marine Aerosol Composition and Phytoplankton Blooms

While this dissertation provides new insights on how biological processes influence SSA physicochemical properties, many questions still remain and are critical to uncovering aerosol impacts on the atmosphere and climate [*Carslaw et al., 2013*; *Quinn et al., 2015*] and the link between the atmosphere and the marine biosphere [*Quinn and Bates, 2011*]. The research described herein lays the foundation for future works to extend the systematic study of sea spray

aerosol transformation in the marine environment using controlled conditions in a laboratory setting. Conditions such as the concentration of other atmospheric oxidants, temperature, humidity, seawater and aerosol acidity play critical roles in transforming the atmosphere and can be controlled in the laboratory to unravel the link between the ocean and the atmosphere. Additionally, other biogenically-derived organic molecules as described in Chapter 6, including sugars [*Aller et al., 2017; Jayarathne et al., 2016*], fatty acids [*Cochran et al., 2016*], lipids [*Parrish, 2013*; *Suzumura, 2005*], and proteins [*Aller et al., 2017; Hawkins and Russell, 2010*], are known to be entrained in SSA, but atmospheric reaction pathways for these molecules remain largely unexplored. Biotransformation of these organic molecules by lipase as shown in Chapters 3 and 4 likely play a critical roles in transforming SSA organic content where a recent study has shown that these processes can directly influence cloud properties [*Nguyen et al., 2017*]. In addition, results from this study has opened up other avenues of research in biotransformation impacts on SSA chemistry, as there are multitude of marine enzymes such as protease and alkaline-phosphatase that can all efficiently transform the organic seawater and SSA organic content. Investigations into the climatic impact of enzymes on SSA will provide insight into the influence of the marine biosphere on cloud albedo, a topic that has been of interest for nearly three decades [*Charlson et al., 1987*; *Meskhidze and Nenes, 2006*; *Quinn and Bates, 2011*]. Extending the work presented in Chapter 5, it is necessary to elucidate the transfer of the multitude of marine enzymes from the ocean to air and their lifetimes in order to truly define their impact on the atmosphere.

While this dissertation focused on the primary SSA aerosols, oxidation of VOCs emitted from the marine microbiome can lead to the formation of secondary aerosols and contribute a large number of aerosols in remote marine region [*Andreae and Rosenfeld, 2008*] as detailed in Section 1.1. A change in SSA chemistry as a result of marine microbiology alone cannot account

for the changes in the SSA's CCN ability as observed in the field [*Collins et al., 2016*]. Continued characterization of SSA production flux and chemical composition under different marine biogeochemical states using realistic SSA generators (described in Section 1.5.1) is warranted to reconcile the discrepancies between observed marine aerosol CCN from laboratory and field studies. Furthermore, investigating the hygroscopicity of SSA, including the volatility of SSA constituents [*Rasmussen et al., 2017*] and impacts on hygroscopicity from heterogeneous reaction of realistic SSA and not surrogates [*Gupta et al., 2015*], in a laboratory setting will lead to more accurate estimations of SSA radiative forcing in global circulation model [*Zieger, et al., 2017*] and their influence on climate and environment.

7.3.2 Photochemical Reactions at SSA Interfaces

In the presence of sunlight and oxidants such as O_3, OH radical, and chlorine radical, SSA will undergo a multitude of transformation pathways [*Abbatt et al., 2012; Finlayson-Pitts, 1993; Finlayson-Pitts and Pitts, 1999*] that could significantly alter SSA chemistry [*Finlayson-Pitts and Hemminger, 2000*]. Based on the work presented here in, it is critical to investigate the reactivity of realistic SSA to the above mentioned oxidants, where a recent publication on bioaerosols chemistry shows that oxidation of biomolecules have important implications on the biomolecule lifetime in the atmosphere [*Estillore et al., 2016*]. Preliminary results (see Sections 4.4.3 and 5.3.7 for methods) from a MART induced phytoplankton bloom coupled with a potential aerosol mass (PAM) chamber show that photooxidation processes can affect SSA heterogeneous reactivity (Figure 7.1). It is likely that oxidation of VOCs emitted from the phytoplankton [*Nguyen et al., 1988*], either formed secondary aerosols [*Quinn and Bates, 2011*] or coated the surface of the SSA. Thus potential transformations of freshly emitted SSA via photooxidation can influence SSA physicochemical properties. Despite the advances in our knowledge of the marine microbiology-SSA heterogeneous reactivity link detailed herein, the mechanisms underlying the photooxidative impact on SSA chemistry and reactivity remain

elusive. A significant effort is needed to (1) uncover the production mechanisms contributing to the ejection of biomolecules to SSA, (2) elucidate reaction pathways of biomolecules in SSA with oxidant gases, (3) unravel the impact of photooxidation on SSA enzyme lifetime and transforming potential, and (4) directly link the interaction of bioaerosols with oxidant gases to human health and climate.

To conclude, the results and future work discussed throughout this dissertation provide insight into factors controlling the heterogeneous reactivity of SSA. In order to fully define the link between the ocean and the atmosphere, the complex biophysical processes driving SSA chemistry must be unraveled. The ultimate goal is to uncover the key atmospheric transformations of SSA in order to predict the impact of SSA on climate

7.4 Acknowledgements

Mitchell V. Santander is acknowledged for assisting in the editing of this chapter.

7.5 Figures

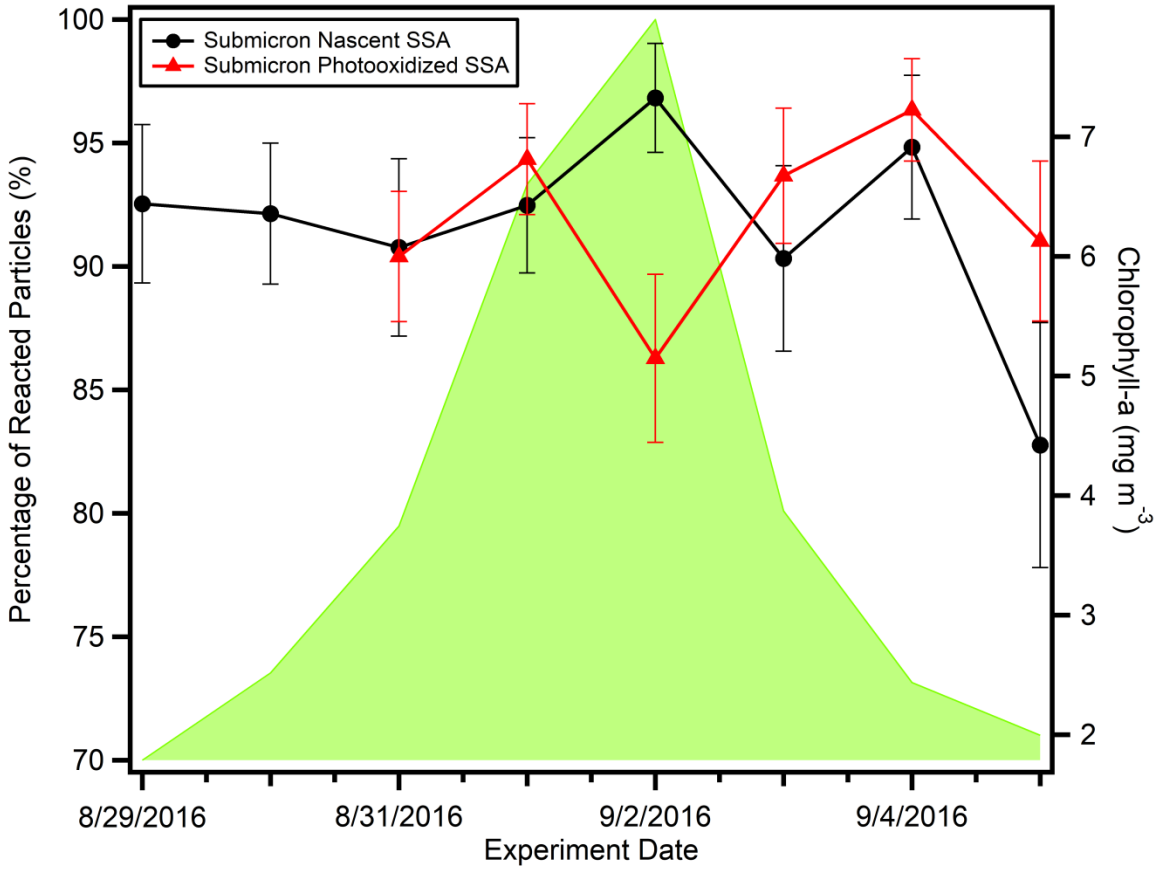

Figure 7.1. Percentage of reacted submicron SSA over the course of the induced phytoplankton bloom MART experiment. Black line represents the percentage of reacted for freshly emitted SSA, and the red line represents the percentage of reacted for PAM aged SSA (equivalent of 7 days of photooxidation aging). Green shade represents the Chl-a level. Error bars represent 1σ.

7.6 References

Abbatt, J. P. D., A. K. Y. Lee, and J. A. Thornton, Quantifying trace gas uptake to tropospheric aerosol: recent advances and remaining challenges, Chemical Society Reviews, 41 (19), 6555, 2012.

Adams, E. M., C. B. Casper, and H. C. Allen, Effect of cation enrichment on dipalmitoylphosphatidylcholine (DPPC) monolayers at the air-water interface, Journal of Colloid and Interface Science, 478, 353–364, 2016.

Allen, H. C., N. N. Casillas-Ituarte, M. R. Sierra-Hernández, X. Chen, and C. Y. Tang, Shedding light on water structure at air-aqueous interfaces: ions, lipids, and hydration., Physical Chemistry Chemical Physics : PCCP, 11 (27), 5538–5549, 2009.

Aller, J. Y., J. C. Radway, W. P. Kilthau, D. W. Bothe, T. W. Wilson, R. D. Vaillancourt, P. K Quinn, D. J. Coffman, B. J. Murray, and D. A. Knopf, Size-resolved characterization of the polysaccharidic and proteinaceous components of sea spray aerosol, Atmospheric Environment, 154, 331-347, 2017.

Andreae, M. O., and D. Rosenfeld, Aerosol-cloud-precipitation interactions. Part 1. The nature and sources of cloud-active aerosols, Earth-Science Reviews, 89 (1–2), 13–41, 2008.

Arnosti, C., Microbial extracellular enzymes and the marine carbon cycle, Annual Review of Marine Science, 3 (1), 401–425, 2011.

Ault, A. P., T. L. Guasco, J. Baltrusaitis, O. S. Ryder, J. V. Trueblood, D. B. Collins, M. J. Ruppel, L. A. Cuadra-Rodriguez, K. A. Prather, and V. H. Grassian, Heterogeneous reactivity of nitric acid with nascent sea spray aerosol: Large differences observed between and within individual particles, Journal of Physical Chemistry Letters, 5 (15), 2493–2500, 2014.

Azam, F., and F. Malfatti, Microbial structuring of marine ecosystems., Nature Reviews. Microbiology, 5 (10), 782–791, 2007.

Carslaw, K. S., L. A. Lee, C. L. Reddington, K. J. Pringle, A. Rap, P. M. Forster, G. W. Mann, D. V Spracklen, M. T. Woodhouse, L. A. Regayre, and J. R. Pierce, Large contribution of natural aerosols to uncertainty in indirect forcing., Nature, 503 (7474), 67–71, 2013.

Charlson, R. J., J. E. Lovelock, M. O. Andreae, and S. G. Warren, Oceanic phytoplankton, atmospheric sulphur, cloud albedo and climate, Nature, 326 (6114), 655–661, 1987.

Cochran, R. E., O. Laskina, T. Jayarathne, A. Laskin, J. Lasking, P. Lin, C. M. Sultana, C. Lee, K. A. Moore, C. D. Cappa, T. H. Bertram, K. A. Prather, V. H. Grassian, and E. A. Stone, Analysis of organic anionic surfactants in fine and coarse fractions of freshly emitted sea spray aerosol, Environmental Science and Technology, 50 (5), 2477-2486, 2016.

Collins, D. B., T. H. Bertram, C. M. Sultana, C. Lee, J. L. Axson, and K. A. Prather, Phytoplankton blooms weakly influence the cloud forming ability of sea spray aerosol, Geophysical Research Letters, 43 (18), 9975–9983, 2016.

Estillore, A. D., J. V. Trueblood, and V. H. Grassian, Atmospheric chemistry of bioaerosols: Heterogeneous and multiphase reactions with atmospheric oxidants and other trace gases, Chemical Science, 7 (11), 6604-6616, 2016.

Finlayson-Pitts, B. J., Chlorine atoms as a potential tropospheric oxidant in the marine boundary layer, Research on Chemical Intermediates, 19 (3), 235-249, 1993.

Finlayson-Pitts, B. J., and J. N. Pitts, Chemistry of the upper and lower atmosphere: Theory, experiments, and applications, 969, 1999.

Finlayson-Pitts, B. J., and J. Hemminger, Physical chemistry of airborne sea salt particles and their components, Journal of Physical Chemistry A, 104 (49), 11463-11477, 2000.

Gupta, D., H. Kim, G. Park, X. Li, H. J. Eon, and C. U. Ro, Hygroscopic properties of NaCl and $NaNO_3$ mixture particles as reacted inorganic sea-salt aerosol surrogates, Atmospheric Chemical Physics, 15 (6), 3379-3393, 2015.

Hawkins, L. N., and L. M. Rusell, Polysaccharides, proteins, and phytoplankton fragments: Four chemically distinct types of marine primary organic aerosol classified by single particle spectromicroscopy, Advances in Meteorology, 1-14, 2010.

Jayarathne, T., C. M. Sultana, C. Lee, F. Malfatti, J. L. Cox, M. A. Pendergraft, K. A. Moore, F. Azam, A. V. Tivanski, C. D. Cappa, T. H. Bertram, V. H. Grassian, K. A. Prather, and E. A. Stone, Enrichment of saccharides and divalent cations in sea spray aerosol during two phytoplankton blooms, Environmental Science and Technology, 50 (21), 11511-11520, 2016.

Kieber, R. J., L. H. Hydro, and P. J. Seaton, Photooxidation of triglycerides and fatty acids in seawater: Implication toward the formation of marine humic substances, Limnology and Oceanography, 42 (6), 1454–1462, 1997.

Meskhidze, N., and A. Nenes, Phytoplankton and cloudiness in the Southern Ocean, Science, 314 (5804), 1419–1423, 2006.

Moore, M. J. K., H. Furutani, G. C. Roberts, R. C. Moffet, M. K. Gilles, B. Palenik, and K. a. Prather, Effect of organic compounds on cloud condensation nuclei (CCN) activity of sea spray aerosol produced by bubble bursting, Atmospheric Environment, 45 (39), 7462–7469, 2011.

Nguyen, B. C., S. Belviso, N. Mihalopoulos, J. Gostan, and P. Nival, Dimethyl sulfide production during natural phytoplanktonic blooms, Marine Chemistry, 24 (2), 133–141, 1988.

Nguyen, Q. T., K. H. Kjær, K. I. Kling, and T. Boesen, Impact of fatty acid coating on the CCN activity of sea salt particles, Tellus B: Chemical and Physical Meteorology, 889, 1–15, 2017.

O'Dowd, C. D., M. C. Facchini, F. Cavalli, D. Ceburnis, M. Mircea, S. Decesari, S. Fuzzi, Y. J. Yoon, and J.-P. Putaud, Biogenically driven organic contribution to marine aerosol., Nature, 431 (7009), 676–680, 2004.

O'Dowd, C., D. Ceburnis, J. Ovadnevaite, J. Bialek, D. B. Stengel, M. Zacharias, U. Nitschke, S. Connan, M. Rinaldi, S. Fuzzi, S. Decesari, M. Cristina Facchini, S. Marullo, R. Santoleri, A. Dell'Anno, C. Corinaldesi, M. Tangherlini, and R. Danovaro, Connecting marine productivity to sea-spray via nanoscale biological processes: Phytoplankton dance or death disco?, Scientific Reports, 5, 14883, 2015.

Parrish, C., Lipids in Marine Ecosystems, ISRN Oceanography, 1-16, 2013.

Pomeroy, L. R., P. J. I. Williams, F. Azam, and J. E. Hobbie, The microbial loop, Oceanography, 20 (2), 28–33, 2007.

Quinn, P. K., and T. S. Bates, The case against climate regulation via oceanic phytoplankton sulphur emissions, Nature, 480 (7375), 51–56, 2011.

Quinn, P. K., D. B. Collins, V. H. Grassian, K. A. Prather, and T. S. Bates, Chemistry and related properties of freshly emitted sea spray aerosol, Chemical Reviews, 115, 4383–4399, 2015.

Rasmussen, B. B., Q. T. Nguyen, K. Kristensen, L. S. Neilsen, and M. Bilde, What controls volatility of sea spray aerosol? Results from laboratory studies using artificial and real seawater samples, Jounal of Aerosol Science, 107, 134-141, 2017.

Riva, M., D. M. Bell, A. K. Hansen, G. T. Drozd, and H. Allen, Effect of organic coatings, humidity and aerosol acidity on multiphase chemistry of isoprene epoxydiols, (509), 2016.

Ryder, O. S., N. R. Campbell, H. Morris, S. Forestieri, M. J. Ruppel, C. Cappa, A. Tivanski, K. Prather, and T. H. Bertram, Role of organic coatings in regulating N_2O_5 reactive uptake to sea spray aerosol, Journal of Physical Chemistry A, 119 (48), 11683–11692, 2015.

Stemmler, K., A. Vlasenko, C. Guimbaud, and M. Ammann, The effect of fatty acid surfactants on the uptake of nitric acid to deliquesced NaCl aerosol, Atmospheric Chemistry and Physics, 8, 5127–5141, 2008.

Suzumura, M., Phospholipids in marine environments: A review, Talanta, 66, 422-434, 2005.

Trueblood, J. V., A. D. Estillore, C. Lee, J. A. Dowling, K. A. Prather, and V. H. Grassian, Heterogeneous chemistry of lipopolysaccharides with gas-phase nitric acid: Reactive sites and reaction pathways, Journal of Physical Chemistry A, 120 (32), 6444–6450, 2016.

Wang, X., C. M. Sultana, J. Trueblood, T. C. J. Hill, F. Malfatti, C. Lee, O. Laskina, K. A. Moore, C. M. Beall, C. S. McCluskey, G. C. Cornwell, Y. Zhou, J. L. Cox, M. A. Pendergraft, M. V. Santander, T. H. Bertram, C. D. Cappa, F. Azam, P. J. DeMott, V. H. Grassian, and K. A. Prather, Microbial control of sea spray aerosol composition: A tale of two blooms, ACS Central Science, 1 (3), 124–131, 2015.

Zeiger, P., O. Vaisanen, J. C. Corbon, D. G. Partridge, S. Bastelberger, M. Mousavi-Fard, B. Rosati, M. Gysel, U. K. Krieger, C. Leck, A. Nenes, I. Riipinen, A. Virtanen, and M. E. Slater, Revising the hygroscopicity of inorganic sea salt particles, Nature Communications, 8, 1-10, 2017.

Zhang, T., M. G. Cathcart, A. S. Vidalis, and H. C. Allen, Cation effects on phosphatidic acid monolayers at various pH conditions, Chemistry and Physics of Lipids, 200, 24–31, 2016.